GENERAL ATOMIC

DIVISION OF

GENERAL DYNAMICS

JOHN JAY HOPKINS LABORATORY FOR PURE AND APPLIED SCIENCE

P.O. BOX 608, SAN DIEGO, CALIFORNIA 92112

GA-5009, Vol. IV

NUCLEAR PULSE SPACE VEHICLE STUDY

Vol. IV--MISSION VELOCITY REQUIREMENTS AND SYSTEM COMPARISONS

George C. Marshall Space Flight Center
Future Projects Office
National Aeronautics and Space Administration
Huntsville, Alabama

Contract NAS 8-11053

Issued February 28, 1966 [redacted]

FOREWORD

The technical report on the Nuclear Pulse Vehicle Study performed under National Aeronautics and Space Administration Contract NAS8-11053 consists of four volumes.

Volume I	Summary Report (Secret)
Volume II	Vehicle Systems Performance and Costs (Secret)
Volume III	Conceptual Vehicle Designs and Operational Systems (Secret/Restricted Data)
Volume IV	Mission Velocity Requirements and System Comparisons (Unclassified), prepared by General Dynamics/Convair.

In addition to the technical report, a condensed summary of the study has been published as General Atomic Report GA-4891 (Secret).

The work reported in the present volume (Vol. IV) was performed primarily by K. A. Ehricke, Director, Advanced Studies, B. Brown, P. Horio, and B. Oman of the General Dynamics/Convair Advanced Studies Department. The work was performed in cooperation with P. B. Shipps Study Project Engineer, and under the overall project direction of J. C. Nance, Project Manager, Nuclear Pulse Propulsion Project.

In addition to Vol. IV a Supplement Volume IV has been furnished by GD/C Advanced Studies, containing mission velocity and mass ratio charts. This supplement has been published as General Atomic Report GA 5009, Vol. IV (Suppl.), as a separate volume.

TABLE OF CONTENTS

TABLE OF CONTENTS (concluded)

LIST OF FIGURES

LIST OF FIGURES (continued)

LIST OF FIGURES (continued)

LIST OF FIGURES (continued)

LIST OF FIGURES (continued)

LIST OF FIGURES (continued)

LIST OF TABLES

LIST OF TABLES (continued)

0. INTRODUCTION AND SUMMARY

0.1 Task Break-Down

The Mission Velocity Requirements and System Comparisons portion of the Nuclear Pulse Space Vehicle Study Consists of four parts: Definition of mission requirements; Vehicle analysis; Economic requirements analysis; and Evaluation. The general approach is outlined in Sect. 1.

The Mission Requirements Analysis in Sect. 2 covers mono-elliptic round-trip missions to Mercury, Venus, Mars, and Jupiter. Geocentric missions (Earth-Moon and orbit launch missions), missions involving return from Mars and Jupiter using perihelion brake maneuvers, bi-elliptic transfer profiles involving planetary fly-by (swing-by) enroute and bi-planet capture missions. The supplement, Vol. IVA contains mission charts and graphs to determine gravitational losses at medium-low thrust to weight ratios for planetary departure and arrival. A break-down of the charts of Vol. IVA is listed subsequently for the convenience of the reader of this volume:

Ea - Me; Me-Ea: 1980, 81, 82, 83, 84, 85, 86, 87

Mercury Capture : Δv vs v_∞ ; $r^* =$ 1.1, 1.5, 2.0

Mercury - centric: Apoapsis impulse for ell.-to-circ. orbit change

Ea - Ve; Ve - Ea: 1975, 77, 78, 80, 81

Venus: Atmospheric entry velocity vs. v_∞

Venus capture: Δv vs. v_∞: $r^* = 1.1$, 1.3, 1.5, 2.0, 3.0, 5.0

Venus - centric: Apoapsis impulse for ell.-to-circ. orbit change

Earth: Earth departure mass ratio and burning time vs. v_∞ for $1000 \leq I_{sp} \leq$ 10,000 sec and initial thrust accelerations of: 0.001, 0.005, 0.01, 0.05, 0.1 g.

Earth arrival mass ratio and burning time vs. v_∞ for $1000 \leq I_{sp} \leq$ 10,000 sec and terminal thrust acceleration of 0.05 g.

Mars: Mars arrival mass ratio and burning time vs v_∞ for $1000 \leq I_{sp} \leq$ 10,000 sec and terminal thrust accelerations of 0.001, 0.005, 0.01 0.05 Earth-g.

Ea - Ju; Ju - Ea: 1980, 81, 82, 84, 85, 86, 87, 88, 89

Jupiter capture: $\frac{\Delta v}{v_\infty}$ vs. v_∞ ; $r^* = 1.1, 2, 4, 6, 8, 10, 15, 20, 25, 30, 50, 100$

Jupiter capture: Δv vs v_∞; $r^* = 1.1, 2.4$

Joviocentric: Periapsis and apoapsis velocities; apoapsis impulses.

Ea - Sa; Sa - Ea: 1985, 86, 87, 88.

Saturn capture: $\frac{\Delta v}{v_\infty}$ vs. v_∞ ; $r^* = 1.1, 2, 4, 6, 8, 10, 15, 20, 25, 30, 50$.

Δv vs. v_∞ ; $r^* = 1.1, 2, 4, 6, 8, 10, 15, 20, 25, 30, 50, 70, 100$

The Vehicle Analysis consists of an explanation of the transportation methodology applied (Sect. 3), vehicle propulsion module analysis (Sect. 4), and general vehicle/mission integration (Sect. 5). The transportation methodology defines the vehicles involved in overall transportation systems. In particular, the close interrelation between Earth launch vehicle (ELV) and interorbital space vehicle (ISV) is recognized. The vehicle propulsion module analysis concerns itself with the definition and specification of scaling coefficients for propellant dependent and thrust dependent hardware and with the specification of mass fractions. The propulsion modules treated in this manner are:

- Chemical propulsion modules, independently of any particular ELV.
- Solar Heat Exchanger (SHE) propulsion modules, independently of any particular ELV.
- Solid Core Reactor propulsion modules, divided into:
  - Graphite moderated systems (SCR/G), Saturn V[1] compatible, modified (40 ft. diameter payload section) Saturn V[1] compatible, and post-Saturn[1] compatible.
  - Non-moderated systems (SCR/N) referred to as "-23 configuration"; primarily post-Saturn compatible, but could also be assembled in orbit from parts carried aloft in Saturn V type ELV's.
- Gaseous Core Reactor (GCR) propulsion modules.
- Nuclear Pulse (NP) propulsion modules.

The general vehicle/mission integration combines the scaling coefficients or mass fractions and specific impulses which characterize the propulsion module with the mission performance requirement to determine propellant fraction and gross payload fraction (GPF) per maneuver. A mission consists of a series of discrete maneuvers. By combining the results of the computations for each maneuver, the (Earth) orbital departure weight (ODW) and the mission gross payload fraction (MGPF) are obtained.

The third part, Evaluation, consists of six sections. In Sect. 6 a general transportation cost analysis is presented, based on the GPF and distinguishing between reconnaissance missions, shuttle missions with

[1] For definition of ELV models used in this study cf. Tab. 1-1.

one-way destination payload and shuttle missions with two-way destination payload. A payload analysis follows in Sect. 7, to the extent to which such analysis is required for the present study. Two types of GPF analysis are explained; the general analysis in Sect. 8, the special analysis, including associated cost analysis in Sect. 9. The special analysis is applied in Sect. 10 over a broad range of missions. The resulting GPF's and ODW's are presented in charts. Sect. 11 presents the overall comparison and evaluation of the propulsion systems on the basis of the results of the preceding sections. The nuclear-electric system is included although it was not treated in detail in the preceeding parts of the report. The attributes and evaluation criteria are discussed. The propulsion systems are graded relative to each other by their attributes and subsequently rated relative to a specific set of evaluation criteria.

0.2 Ground Rules and Limitations

In the course of this work, the following ground rules and limitations were observed:

1. The systems comparison was carried out with respect to inter-orbital space vehicles (ISV's) only. Earth launch vehicles (ELV's) and destination space vehicles (DSV's) were not considered.

2. The mission velocities were taken as the sum of the impulsive maneuvers which constitute the mission. The difference between the individual propulsion system types is sufficiently pronounced so that consideration of gravitational losses would not alter the trends. Vol. IVA provides charts which permit the consideration of such losses if this detail is warranted in specific cases.

3. Three ELV's were used as reference models in the Earth-to-orbit logistic systems which entered into the cost comparison. These are Saturn V, a modified Saturn V, and a nominal post-Saturn ELV. Their characteristics are given in Tab. 1-1.

4. In the vehicle/mission integration and subsequent evaluation, three classes of ISV's were considered,

   - Reusable orbit launch vehicles (OLV's) injecting a (pay-) load at near-parabolic velocity and returning into a near-Earth circular orbit.

- Reusable cislunar vehicles (CISV's) on shuttle missions between an Earth satellite orbit and a Moon satellite orbit. In connection with the nuclear pulse system, free fall delivery was considered also (Fig. 2-19).

- Helio-centric vehicles (HISV's) on exploration missions to Mercury, Venus, Mars, and Jupiter.

5. In the SCR propulsion systems the thrust levels for the SCR/G systems were set at 63 k and 250 k per engine. The 63 k engines can be clustered to up to 4 engines, the 250 k engines up to 2 engines. Except for the reusable OLV missions, the operating life of the SCR/G engines was assumed to be for one maneuver only.

   For the SCR/N engines 50 k thrust was assumed, unconstrained engine clustering (actually, clusters up to 8 engines used) and unconstrained operating life, resulting in the repeated use of some engines throughout a mission.

   For thrust values from 75 k to 150 k the SCR/N and the NASA Lewis R C concept of the water moderated (SCR/W) engine were expected to be comparable in weight and lighter than the SCR/G engine. A relation for the scaling coefficient of the SCR/N and SCR/W engine types in the above thrust range is given in Eq. (4-81).

6. The weight data of the GCR engines are uncertain. The NASA Lewis R C coaxial flow engine was used as a general model. A relation for the engine scaling coefficient in the 1000 to 4000 k thrust range is given in Eq. 4-87. Specific engine thrust values used in the numerical analysis are 750 k, 1000 k, 1500 k, and 3000 k.

7. Parametric nuclear pulse module mass fractions were worked out for Saturn V, Saturn V M, and post-Saturn conpatible systems (NP-1, NP-2, and NP-3, respectively). Because of the large number of variables in the vehicle/mission integration and systems evaluation, only the NP-1 was used in the analysis and applied to the three reference ELV's.

8. Scaling coefficients and mass fractions for nuclear-electric (NE) propulsion systems could not be worked out within the limits of this study. However, on the basis of its general characteristics, the NE system (ion propulsion) was included in the final evaluation.

9. Approximate development cost data are presented for the individual systems. For a variety of reasons, outlined in Sect. 11-2, they were not included in the comparison proper.

10. Direct operating cost figures were entered into the evaluation on a comparative basis. Therefore, they should not be taken as absolute figures. Cost items which are comparable for all systems, and cost items for which an insufficient foundation for estimates exists, were excluded. The following cost items were included:

    Manufacturing cost and Earth-to-orbit (ETO) transportation cost of propellants

    Manufacturing cost and ETO transportation cost of propulsion hardware; for the exploration missions only, not for the shuttle missions.

    Earth-to-orbit transportation cost of the payload.

    It was shown that these cost items should account for 70 and 90 percent of the direct cperating cost for LH_2 and NP vehicles, respectively.

11. With the exception of the ELV requirement curves in Sect. 9, all ELV requirements and cost data are based on one vehicle in Earth orbit.

12. ELV launch requirements and ELV procurement requirements (i.e., launch requirements plus redundancies) were determined and are presented in Tables. The comparative cost analysis, however, was based on the launch requirements only.

0.3 Summary of Comparison

Systems comparison and evaluation was carried out with the use of 16 propulsion system attributes and 6 evaluation criteria. Of the 16 attributes, 6 can be regarded as elementary attributes,

Specific impulse
Mass fraction
Propellant density
Propellant state
Propellant cost
Hardware cost

Ten can be regarded as complex attributes, containing the elementary attributes at varying degrees of importance,

Propellant consumption factor
Orbital departure weight
Mean packaging density (as ELV payload)
Vehicular ruggedness
Mission capability: Inner solar system
Mission capability: Outer solar system
Growth capability
Pre-mission shake-down capability
Vehicular mission reliability

The evaluation criteria use attributes of both groups in varying degrees of importance. They are management oriented,

Cost effectiveness	Development Cost[2)]
Operating effectiveness	Availability[2)]
Gross payload fraction	Present Confidence Level of Development Success[2)]
Mission versatility	Present Acceptance of Operational Characteristics of System[2)]
Orbital operations Ability	

They are described in Para. 1.4. The principal propulsion systems to which they were applied are C, SCR/G, SCR/N, GCR, NP, and NE.

---

2) These criteria are recognized as playing a role in high-level management decisions. However, insufficient agreement exists presently on the first three, whereas the fourth is rather affected by personal opinions and probably will be subject to changes. For these reasons, these four were not used as primary criteria.

NE and NP lead in specific impulse, both being well above 2000 sec initial operational capability. GCR around 1800 sec, the SCR engines 800 to 900 sec and the C engines 430 to 450 sec.

Conversely, C modules have the highest mass fractions, followed by the SCR/N and SCR/G modules. Following a gap, the low mass fraction systems are GCR, NP, and NE, in that order.

In terms of propellant density NP and NE have the lead, using dense metallic propellants, followed by C systems and by the LH_2 carrying SCR and GCR systems.

Solid state propellants are more desirable, for a number of reasons, than those in a liquid state. In matters of propellant state NP leads, NE may use solid (cesium) or heavy liquid (mercury) propellants; the rest use liquids.

In terms of propellant manufacturing cost, NP appears to be least favorable.

In terms of propulsion (thrust dependent and propellant dependent) hardware manufacturing cost, the systems are much more comparable, except for the NEV, which has costs/lb estimated to be approximately 10 times that of the others.

Propellant consumption factor (PCF) is primarily affected by specific impulse, but can be boosted at low mission velocities, if the mass fraction is low. High gross payload fraction (GPF) is always accompanied by low PCF. A low GPF may indicate low or high PCF, depending upon whether the mean fraction is high or low. The cost effectiveness of shuttle vehicles is affected more by the PCF and propellant manufacturing cost than by orbital departure weight (ODW). See also "Cost Effectiveness" below. Generally, NE and NP have the lowest PCF, but in the low energy mission classes the difference may not be large enough to overcome the large difference in propellant cost.

Low orbital departure weight (ODW) for given mission and payload conditions is a highly important advantage. It may assure extended use of Saturn V. For comparable missions and payloads, only NP and NE have ODW's low enough to assure considerably extended use of Saturn V.

Mean packaging density should be high. This requires high propellant density and compact design characteristics. High packaging density, if combined with low ODW improve the possibility of orbital delivery in one piece; i. e. fully assembled and readied out of the ground, though not necessarily fully fueled. This, in turn simplifies and economizes orbital operations. The NP leads in meeting the requirements for high mean packaging density. The NE system is of far less compact design.

Vehicular ruggedness is determined by the degree of insensitivity to a variety of hostile environments, ranging from the vibrational environment in the ELV payload section to the conditions in space, at various heliocentric distances, to the conditions in the atmospheres of Venus or Jupiter. The NP design indicates by far the highest degree of vehicular ruggedness.

In terms of mission capability, the NP leads in terms of fast transfers across the inner solar system. Only the NE and NP have an extensive outer solar system capability, with the NE possibly superior to the NP due to its large I_{sp}-growth potential at very low thrust accelerations, and due to the fact that very low thrust accelerations are a comparatively lesser disadvantage for missions into the outer solar system.

In terms of growth capability, referring here essentially to I_{sp}-growth, both, NP and NE have a decisive lead over all other systems, since their initial capability exceeds even the growth potential of the other systems. I_{sp}-growth potential as offered by these two systems assures continued low ODW even as mission energy requirements increase. Therefore, a post-Saturn ELV can be smaller than otherwise required and has a reduced rate of obsolescence.

Pre-mission shake-down capability is superior if the vehicle uses one engine or one set of engines throughout the entire mission. For orbital injection missions and lunar missions, this capability includes potentially all systems considered. For planetary missions, it applies unconditionally to NP and NE systems and conditionally to SCR/N and GCR missions. The reason for the inclusion of the GCR in the latter group is that the heavy weight of the GCR engine tends to reduce severely the mission GPF if applied to terminal Earth capture, since its I_{sp} is not quite large enough to overcome the effect of the poor mass fraction for the last maneuver. Therefore, the transportation quality of the GCR is, in most cases, improved considerably by using an SCR/N or a chemical stage for the terminal maneuver.

Vehicular mission reliability (VMR) represents the inherent reliability of the vehicle, as determined by its design characteristics and degree of operational complexity. The lower the VMR, the more tasks for the crew to make up the difference and the more potential risks are involved for the crew. No across-the-board VMR comparison was conducted for all systems in this study. VMR comparisons between C, SCR/G and NP vehicles as part of another study, showed a definite superiority of the NP system.

Cost effectiveness comparisons are influenced so strongly by the ELV used in the ETO logistic system, that they must be approached from the standpoint of ELV-ISV combinations, rather than treatment of the ISV alone. For Saturn V-ISV combinations, the NP system always was found to be more economical. Fig. 0-1 summarizes the results of a systems comparison for near-parabolic injection of loads by reusable OLV's. The systems are compared on the basis of injected loads of 220,000 lb except for the GCR and NP systems for which 880,000 lb load packages were used (i.e. 1 mission for every 4 missions of the other systems). Three levels of transportation volume are applied to the 1971-1990 period, shown as Plans 1, 2 and 3. Operational availabilities were assumed as follows: C-1971, SCR/G-1977, SCR/N-1980, GCR-1984, NP-1984. Where relevant, the use of a given system was discontinued when the next system became available. This must be kept in mind when considering the results shown; in other words, the advanced systems would show an even greater superiority over the chemical system if they were available from 1971 on. The lead of the NP system would be even stronger, were it not for the high propellant cost of this system.

On the basis of cost effectiveness per mission, that is including the manufacturing cost and ETO transportation cost of the propulsion hardware (not included in Fig. 0-1), the NP is no longer the most economical drive, but rather the SCR/N system with 375 $/lb versus 397 $/lb.
This is caused by the large mass plus the high propellant cost of the NP system, whose combined effect negates the I_{sp} advantage (2500 sec). Not much I_{sp}-growth is needed to reverse the situation. This result illustrates the potential sensitivity of high performance systems of large mass and high propellant cost at low energy missions. For shuttle service, the lower PCF assures the NP economic superiority over all other systems (Fig. 0-1).

Aside from the high specific impulse of NP, an important reason for its lead is the relatively poor cost effectiveness of Saturn V, compared to a larger and/or reusable post-Saturn. The cost effectiveness of all other systems is extremely poor, because of the high cost of ETO transportation. The results

Fig. 0-1 COMPARISON OF PROPULSION SYSTEMS
REUSABLE OLV
NEAR PARABOLIC INJECTION OF LOADS

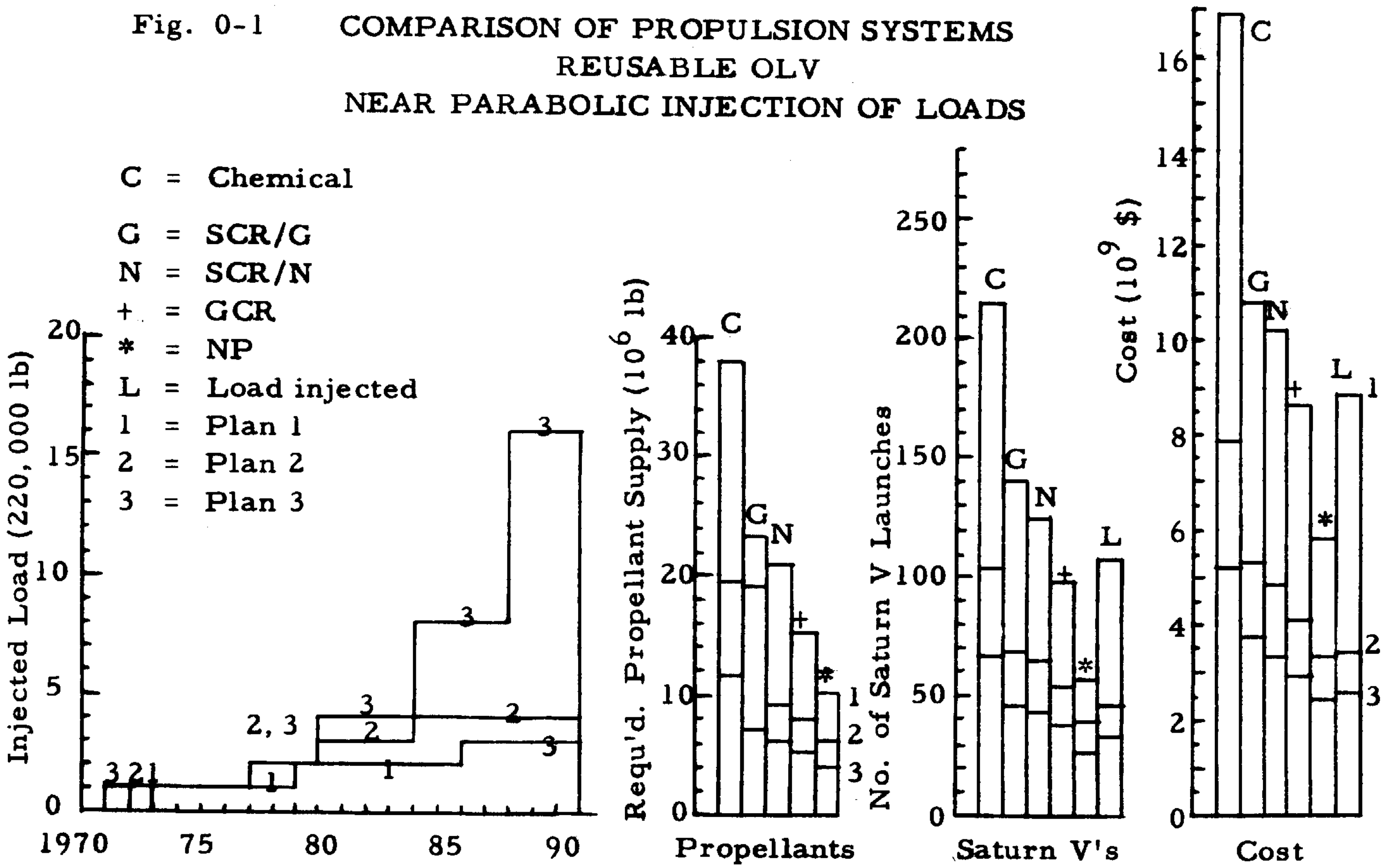

Data Refer to Propell't & Pld. Supply Only. No Hardware; Propell's Res. Incl.; No Redundancies of the many cost analyses conducted make it quite apparent that, if Saturn V is considered for extended use over the next 10 to 20 years, only the NP and possibly the NE system offer a low-cost approach to space flight over a wide range of lunar and planetary missions. This is on the basis of 2500 sec specific impulse for the NP. In the lower mission energy region (orbital injection, lunar, certain Venus and Mars missions) the SCR/N shows up a good second. If a post-Saturn of high cost effectiveness (50 to 100 $/lb payload in orbit) is developed, the missions operations costs are improved vastly for all systems. SCR/G and even chemical systems with post-Saturn drop to the cost level of the Saturn V-NP combination. Post-Saturn-NP combinations are still superior, though by a smaller margin. The lowest cost is obtained in this case with post-Saturn-SCR/N combinations. If the I_{sp}-growth potential of the NP is brought to bear, the situation changes once more, and NP with post-Saturn leads in cost effectiveness. In order to illustrate the strength of the cost effectiveness trends, Fig. 0-2 compares the cost effectiveness of various ISV propulsion systems with Saturn V and post-Saturn and for four different I_{sp}-values of the NP system with post-Saturn, using a relatively high-energy Mercury mission as example. Fig. 0-3 compares cost data of various drives for a reusable CISV and illustrates the fact that the cost effectiveness of a system as powerful as the NP may depend very much upon its deployment. Its greater payload capability demands fewer shuttle missions with larger payloads for best cost effectiveness than less energetic systems which can commute effectively more frequently and with smaller payloads at a time. The chart compares the C, SCR/N and NP systems in terms of propellant requirement, Saturn V launchings required for ETO transportation of propellants and load and cost (propellant manufacturing and ETO transportation; pld. transportation only) for three cislunar transportation levels (Plans 1, 2, 3). For the NP system (Saturn V compatible) three alternatives are shown:

a: Free fall delivery of load.

b: Delivery of load into lunar satellite orbit in packages of 220, 000 lb as with the C and SCR/N systems.

c: Delivery of load into lunar satellite orbit. In Plan I: 1 package of 880, 000 lb. In Plan II: 2 packages, one @ 880, 000 lb, 1 @ 440, 000 lb. In Plan 3: 2 packages, one @ 880, 000 lb, one @ 1, 100, 000 lb.

Fig.0-4, finally, compares the cumulative costs if all fast (about 450 day) mission opportunities to Mars (mono-elliptic transfers both ways) were utilized in the 1980-90 time period. The relatively high energy requirement of fast Mars missionsquickly brings out the economic advantage associated with the use of the NP system. The cost advantage, however, becomes small when post-Saturn is introduced.

Fig. 0-2 COMPARISON OF PROPULSION SYSTEMS
MERCURY MISSION 85-5
COST EFFECTIVENESS

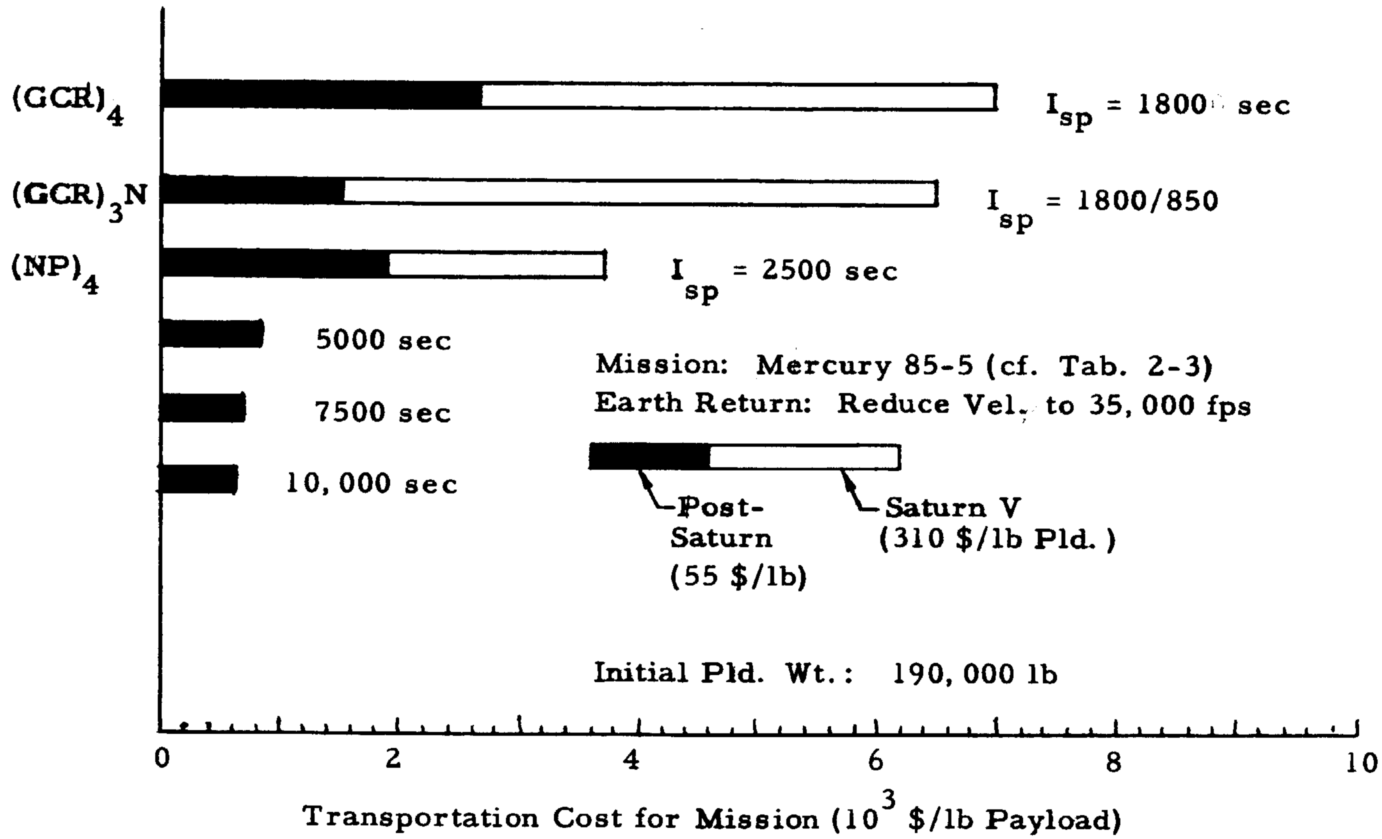

Fig. 0-3 COMPARISON OF PROPULSION SYSTEMS
REUSABLE CISV
DELIVERY OF LOADS INTO CIRCUMLUNAR ORBIT

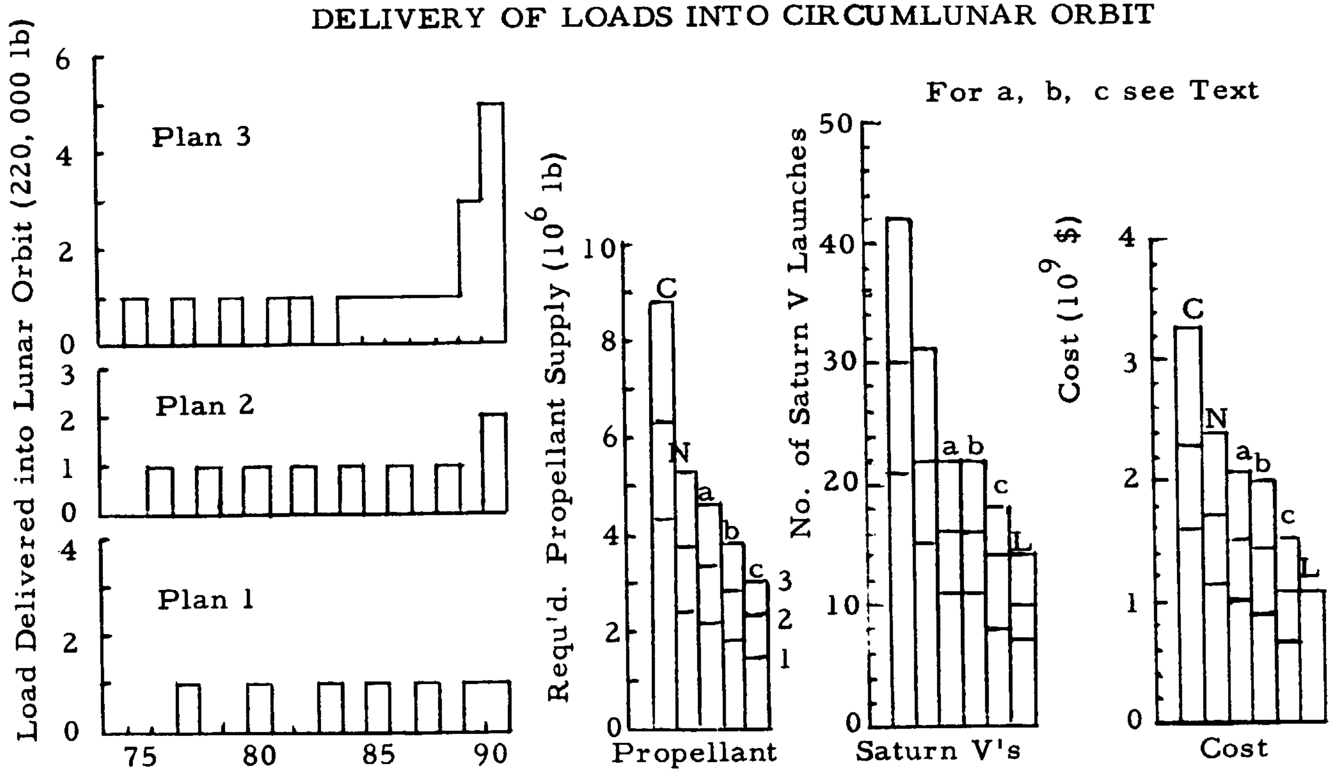

Data Refer to Propellant & Pld. Supply Only. No Hardware; No Propellant Reserve; No Redundancies

Fig. 0-4 COMPARISON OF PROPULSION SYSTEMS
EXPLORATION MISSIONS TO MARS
FAST "STANDARD" MONO-ELLIPTIC ROUND-TRIP CAPTURE MISSIONS

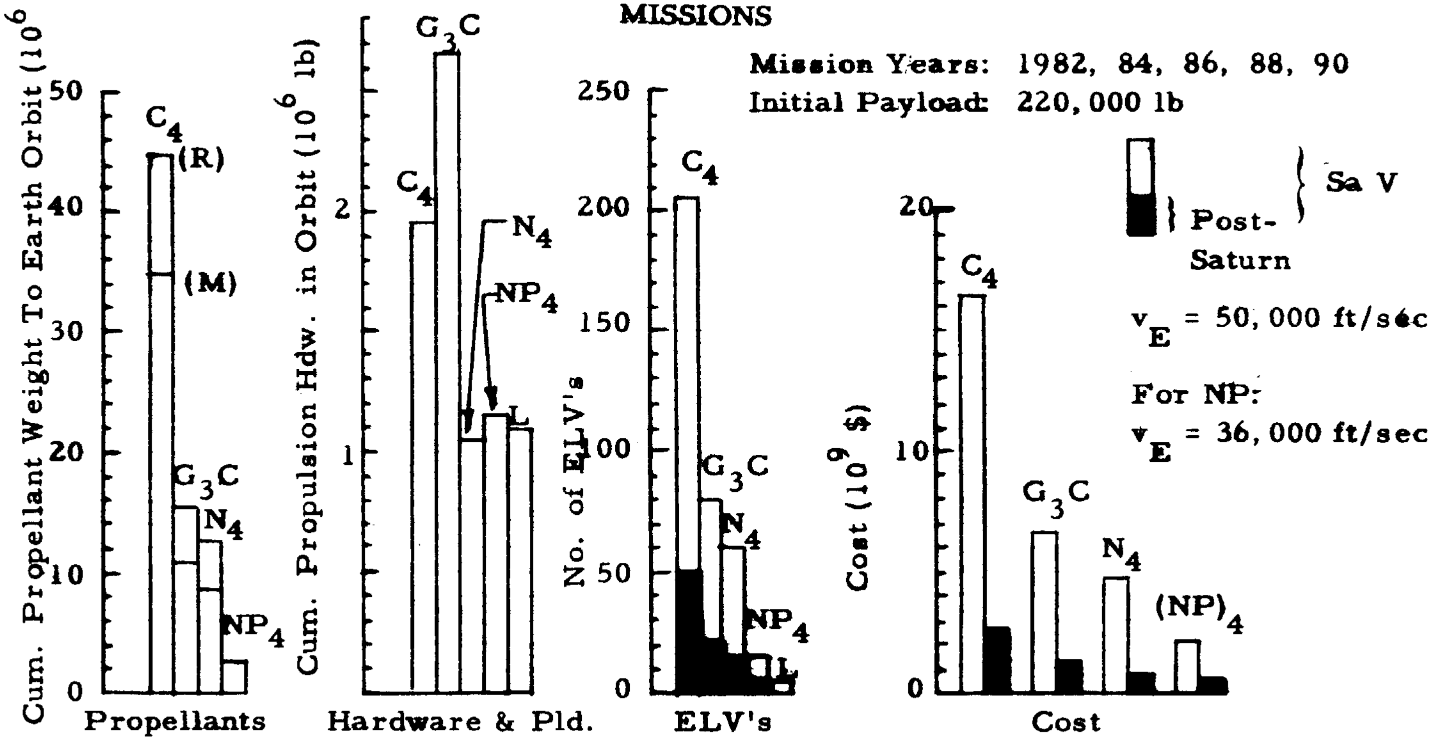

Data Refer to 1 HISV in Orbit. & Propellant Reserves Included. No Redundancies

The operating effectiveness is a measure for the degree to which a low theoretical cost effectiveness can be translated into operational practice. The operating effectiveness, therefore, is essentially a function of reliabilities and of the capability to perform operations which improve the mission success probability, so that fewer redundancies are required. Factors which improve the operating effectiveness are:

Small number of matings and fuelings in orbit. Based on Saturn V as ETO logistic vehicle, the propulsion systems rank in the order: NP, NE, GCR, SCR/N, SCR/G, C. Based on post-Saturn, the ranking more likely is: (NP, NE, GCR), SCR/N, SCR/G, C where the parenthesis means essentially equal ranking.

Pre-mission shake-down capability. This is best accomplished with 1-stage or tankage modularized vehicles and the ranking here is: NE, NP, GCR, SCR/N, (SCR/G, C).

Vehicular mission reliability (VMR) the system ranking is: NP, (SCR/N, SCR/G, C), NE. The ability of the crew to improve the mission reliability depends primarily upon vehicle simplicity (NP, (GCR, SCR/N), (SCR/G, C), NE); diagnostic methods and procedures (all rank about equal); accessibility and interchangeability of parts (NP, (GCR, SCR/N, SCR/G, C), NE); repairability (ranking not feasible at this time) and spare carrying capability (NE, NP, SCR/N, SCR/G, C).

The gross payload fraction (GPF) is a function of I_{sp} and propulsion system weight which strongly influences the mass fraction. The SCR/N system, in the medium to low energy portion of the mission spectrum, often showed a higher GPF than the GCR or even the NP systen, because the weakness of a relatively low I_{sp} was overcompensated by the advantage of a much higher mass fraction. The GCR suffers from very heavy engine weight which often cannot be balanced by its I_{sp} in the range of 1800 to 2000 sec. The NP system too suffers from a heavy "engine" weight, but its higher I_{sp} more readily overcomes the effect of low mass fraction. The NE, finally, has a comparatively still far heavier engine weight, but its specific impulse is high enough to overcompensate for the very low mass fraction even on low-energy missions, if given long transfer times. A high GPF means low propellant consumption and low ODW for given payload; or greater payload carrying capability at a given ODW. The NE, NP and SCR/N systems are the leading contenders for high GPF values.

Mission versatility can contribute importantly to cost effectiveness and can speed up the amortization of development cost. Important qualifications for attaining high mission versatility are :

High I_{sp}, yielding 1-stage or tankage modularized vehicles over a wide range of mission energies, yielding, in turn, improved simplicity and reliability, as well as better prospects for reusability.

High propellant density, yielding small areas to be meteoroid shielded and thermo-controlled; reducing sensitivity. In the case of the NE, this effect is overcompensated in the other direction by the radiation coolers.

Solid propellants with similar effects as high propellant density.

High thrust/weight ratio increases the mission versatility in specific respects which are not always relevant.

Superior ruggedness and high thrust/weight combined, add further to mission versatility.

Reusability (a special kind of mission versatility) requires 1-stage or tankage modularized configuration; requires capability of returning its operational payload into the terminal Earth orbit (i.e., high I_{sp}); and requires low propellant consumption and/or low propellant cost.

In every one of these points, except specific impulse, the NP system ranks highest.

Orbital operations are determined by the amount of matings and fuelings in orbit and the number of supply flights required of the ETO logistic system. Factors which minimize orbital operations are, therefore, low ODW, high propellant density, and solid state of propellant. High density and low ODW improve the possibility of transporting the ISV into orbit in one piece, though not necessarily fully fueled. The NP clearly leads in all attributes which minimize orbital operations.

Ability designates the general quality of the system and includes its operating effectiveness, capability of shorter transfer times than other systems and mission safety which, in turn, is a function of vehicular ruggedness, performance reserves for emergency maneuvers and vehicular mission reliability. In every one of these aspects, the NP shows the highest rating.

0.4 Principal Conclusions

In studying this report, it must be kept in mind that systems are compared which do not yet exist. One can, therefore, replace freely one by the other. Most of present long-range operational planning is based on the ground rule that it must be attainable with what is available or that it must fit presently committed development programs in the propulsion field. Therefore, if necessary, very long planetary mission periods, low-yield manned planetary missions, very high Earth entry velocities, a paucity of emergency options to raise crew survival probability on advanced missions and other performance-dependent operational characteristics are justified as acceptable. It is obvious that all these constraints can be accepted. It is evident that operational progress under some of these constraints is better than no progress at all. It is also long apparent that the development of SCR/G systems does constitute a very significant improvement over what can be accomplished with chemical HISV's in alleviating the above mentioned constraints and still remain compatible with the capability of a Saturn V based ETO logistics system.

However, after all this is granted and done, one still has not progressed beyond the point of an (from the standpoint of advanced space operations) expensive ETO logistics system, and an ISV propulsion system whose capability deteriorates rapidly in the face of rapidly increasing energy requirements beyond lunar and modest Venus or Mars round-trip missions.

Therefore, it is justified and, indeed, necessary, to give attention to the "other side" of long-range planning; that is to the question of what constitutes a desirable capability, in addition to what constitutes a feasible capability with the means now available or development committed. Every now feasible capability once was a desirable capability and as such outside the frame of reference of most of the then realistic planners.

The question probably should be asked as follows: Assuming man wants to reach and, where desirable, utilize for scientific or economic purposes, the immediate vicinity or surface of the bodies of this solar system; which is the most desirable and potent transportation system that could be available by, say, no later than the middle eighties:

Missions, operations and associated economy studies suggest the following specifications for such a system

1. ISV: Initial specific impulse well over 1000 sec with growth potential to no less than 7500 sec

2. ISV: Chemically stable mono-propellant

3. ISV: Propellant in solid state over a wide range of environmental temperatures likely to be encountered.

4. ISV: Propellant manufacturing cost not more than 50 $/lb

5. ISV: Mean cost of manufacturing of propulsion hardware not more than 100 $/lb.

6. ISV & DSV: Long operating life and multi-mission reusability of thrust systems.

7. ISV: High propulsion system thrust/weight ratio keeping mass fractions from falling below 0.5 in terminal maneuvers.

8. ISV & DSV: High vehicular ruggedness.

9. ISV & DSV: High vehicular mission reliability.

10. ISV: Compact design for high packaging density in the ELV payload section.

11. ISV & DSV: Wide range of vehicular thrust acceleration feasible for high mission versatility.

12. ELV & ISV: Compatible with a reusable low-cost ELV of payload capability into near-Earth orbit of about 300 tons (660, 000 lb) at very low obsolescence rate of the ELV due to insufficient size, as missions are extended over the solar system, taking ISV growth potential (specif. No. 1) into account.

Tab. 0-1 compares the various systems treated in this report, and those treated incompletely or not at all, against these ideal specifications. The points were added, because on the basis of yes/no counts, some systems appear comparable which obviously are not comparable. It is also realized that the SCR/G system is far more superior to the chemical system than the points indicate, because, if measured against these ideal specifications the advantages of the superior I_{sp} of the SCR/G over the chemical system are not recognized. This table is not meant to compare the individual systems relative to each other (for this cf. Sect. 11.5), but to compare them against the ideal systems specification, in order to provide a perspective in the before mentioned "other side" of long-range planning.

The table reflects several principal conclusions of this study, namely,

1. None of the systems evaluated meets completely the ideal system specifications.

2. Only two of the systems evaluated come significantly close to meeting the specifications, namely, the nuclear pulse and the nuclear electric systems.

Tab. 0-1 COMPARISON OF SYSTEMS AGAINST AN IDEAL SYSTEM SPECIFICATION

Spec. No.	Plus-Points for "Yes"; Minus-Points for "No"	Specification Met? Yes/No							
		C	SCR/G[1)]	SCR/N	GCR	NP	NE	Advanced MHD System	Controlled Thermonuclear Reactor System
1	+10/-10	No	No	No	No	Yes	Yes	Yes	Yes
2	+8/-7	No	Yes	Yes	Yes	Yes	Yes	Yes	Yes
3	+4/-2	No	No	No	No	Yes	Yes	No	No
4	+8/-8	Yes	Yes	Yes	Yes	No	Yes	Yes	Yes
5	+6/-4	Yes	Yes	Yes	Yes	Yes	No	No	No
6	+5/-4	Yes	No	Yes	Yes	Yes	Yes	Yes	Yes
7	+3/-1	Yes	Yes	Yes	No	No	No	?	No
8	+5/-3	No	No	No	No	Yes	No	?	?
9	+9/-4[2)]	No	No	Yes	Yes	Yes	No	?	?
10	+2/-2	Yes	No	No	No	Yes	No	No	No
11	+2/-1	Yes	Yes	Yes	Yes	Yes	No	?	?
12	+10/-10	No	No	No	No	Yes	Yes	Yes	Yes
Yes/No/?		6/6	5/7	7/5	6/6	10/2	6/6	5/3/4	5/4/3
Points		-10	-8	+14	+10	+52	+30	(+33)	(+32)
Remarks		System characteristics & dev. requirements fairly well understood. Potential availability 1985 or sooner.						System characteristics & dev. requirements less well understood. Potential availability later than 1985	
		Included in mass fraction & pld. fraction on analysis and in evaluation					Included in evaluation	Not included	

1) On the basis of limited engine operating life as tentatively specified by the National Aeronautics and Space Administration. For operating life comparable to that assumed for the SCR/N type, specifications No. 6 and 9 would be met and the number of points would be equal to that of the SCR/N.

2) The relatively small penalty is valid for manned ISV's only.

3. Between these two, the nuclear pulse systems meets these specifications far more comprehensively. The nuclear pulse clearly appears to be the most promising long-range advanced propulsion system which could be available in the middle eighties or sooner.

Other principal conclusions are:

4. High propellant cost is a major (technological) weakness of the NP system.

5. The economic superiority of the NP is particularly striking in combination with Saturn V which is comparatively expensive and has low payload capability as far as orbital departure weights (ODW) for many planetary missions are concerned. Because Saturn V is expensive, the high cost of NP propellant is less of a factor; and because of payload weight limitations of Saturn V, the low ODW of the NP is of special importance.

6. Consequently, the economic superiority of the NP system with 2500 sec specific impulse is reduced sharply, or eliminated altogether (usually by the SCR/N system, in the latter case), as more economical ELV's (larger than Saturn V and/or reusable) become available.

7. The potential I_{sp}-growth capability of the NP system, however, can reverse the situation again in favor of the NP system. Even limited realization of this growth potential to, say, 5000 sec renders this system economically unbeatable.

8. Only the selection of either the NP or the NE system eliminates the need for operational availability of a post-Saturn or even an improved Saturn V prior to the period around 1990 and still does not restrict HISV mission capability to Venus and Mars during that period. If, on the other hand the ISV development is limited to SCR/G and SCR/N systems, it is fairly apparent that either restriction to Venus and Mars must be accepted; or the ELV capability of the ETO logistic system must be improved.

9. It is realized that above considerations are not the only incentive for improving the ELV. An even stronger incentive is likely to be provided by the eventual need to improve the cost effectiveness of ETO transportation. This becomes very apparent from the results of cost analyses presented in Sect. 10. In spite of the fact that Saturn V represents a tremendous step forward, its low cost effectiveness, if compared with the probable requirements of the late seventies and the eighties, may impose an effective constraint on the manned planetary exploration much beyond Venus and Mars, even if an NP or NE system is available.

10. However, even if cost effectiveness improvement were the only reason for developing a post-Saturn, the NP or NE systems would still constitute the two most desirable choices, because they would reduce the size of the post-Saturn ELV; and the inherent performance growth potential of the NP and NE systems would practically eliminate obsolescence of the post-Saturn on account of its size. A smaller post-Saturn (say, about 300 tons or 660,000 lb payload capability into Earth orbit) will be used more frequently than one $\geq$ 450 tons ($\geq 10^6$ lb) payload. Therewith reusability will become effective more rapidly in yielding high economic payoff. This particular aspect merits considerable thought and study in the future, because it is a key issue in the decision complex concerning the entire ELV-ISV combination. In fact, a well-founded decision on the future development of either ELV or ISV can be made only if both are considered simultaneously as complementary parts of one integral space transportation system.

1. CONCEPTUAL AND ANALYTICAL METHODOLOGY

The primary objective of a comparison of various vehicle systems is to arrive at an engineering solution to the problem of space transportation which is satisfactory from the standpoint of feasibility, timely availability, reliability, cost and mission versatility. The last mentioned criterion is of particular significance for a program of manned missions to explore the planets of this solar system, because of the cost and reliability implications in general and because of the multitude of problems other than transportation per se, which demand attention and efforts and which make it desirable to solve the problem of interplanetary transportation in as few development cycles as possible.

1.1 PLANNING AND EVALUATION

Planning means to set up models of future courses of action and eventually select one of these for actual realization. A model is an idealized set of conditions, of sequence of events, or a combination of both. A model can be made of an important sub-vehicular system, such as a propulsion system, of a vehicle of a transportation system (i.e. a combination of vehicles, e.g. Earth launch vehicle, interorbital space vehicle and destination landing vehicle), of an operational technique (e.g. readying an interplanetary convoy in Earth orbit by module mating and/or fueling), of a mission, a project or of an entire program. A model is described by attributes. Attributes are defined as a set of parameters, or of figures of merit, characterizing and distinguishing the models from each other. The models are evaluated by their parameters or figures of merit.

Evaluation is the process of establishing the (relative) value of each model by applying criteria to the attributes. Criteria are standards of measurement which are derived from the objectives of the model. The "value" is a quantitative result of evaluating the particular model. The value measures the degree to which a given model conforms with the standards of measurement. Hence, it determines its rank in a system of classifications; i.e. its relative intrinsic worth or utility. If the attributes cannot be expressed in fixed and "hard" numbers, but are subject to uncertainties, a range must be selected, the probability distribution established over the range and these so defined bands used to determine the probability that the utility of one plan is lower, equal or higher than the utility of another plan.

1.2 LEVELS OF ACTIVITY

A plan may refer to various levels of activity. Relevant activity levels are defined in Fig. 1-1. The General Space Plan (GSP) is broken down into three program categories. Each of these represents a combination of projects, some of which are clustered together to form sub-programs. In the operations oriented programs, a project consists of a number of missions. For example:

Program:	C.	Planetary Exploration
Sub-Programs:	C-1	ISP[1] Inner Solar System
	C-2	ISP/Outer Solar System
	C-3	Manned/Inner Solar System
	C-4	Manned/Outer Solar System
Projects:	C-3.1	Mars Exploration (up to a suitable capability plateau, such as capture, landing, synodic base or long-term base)
Missions:	C-3.1.1	Mars Powered Fly-By
	.2	Capture
	.3	Orbital Reconnaissance Station (ORS)
	.4	Surface Excursion (SE)
	.5	Synodic Base (SB)
	.6	Long-Term Base (LTB)

A mission, therefore, is defined by limited achievements and specific characteristics. A project is defined by one or several capability plateaus, based on a particular transportation system and their product improvement versions, or on a sequence of different transportation systems. A sub-program is defined by a series of capability plateaus, achieved by a single transportation system or by a family of transportation systems and payloads. A program, finally, is defined by a progressing sequence of capability plateaus of families of sub-programs.

The programs and projects of each of the three categories shown in Fig. 1-1 are detailed further in Fig. 1-2. Ten technology-oriented programs can be defined. Three development-oriented programs (SOP-1, 2, 3) are indicated, each consisting of numerous development projects, involving

---

1) ISP = Instrumented Space Probe

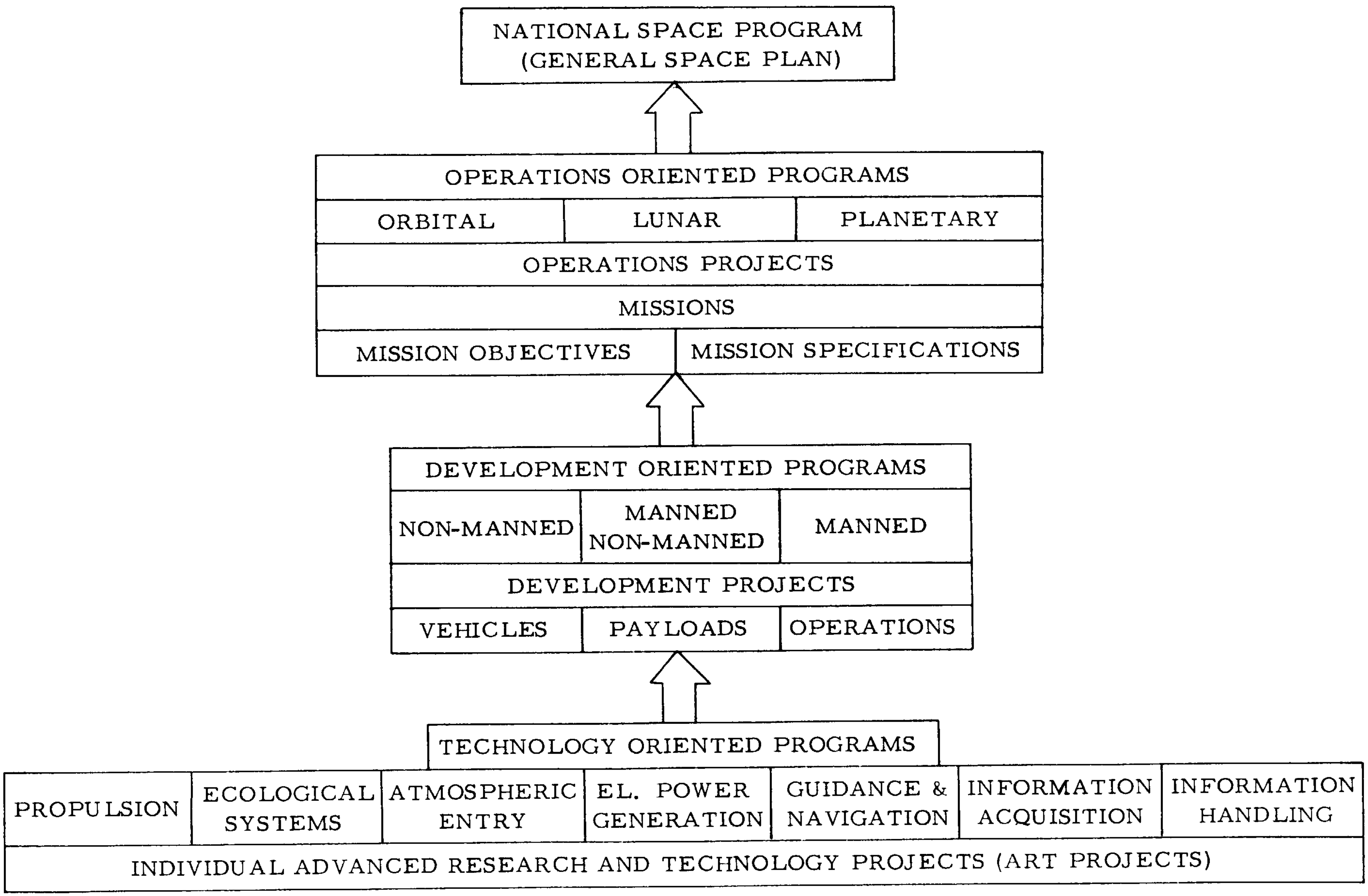

Fig. 1-1 DEFINITION OF PROGRAMS

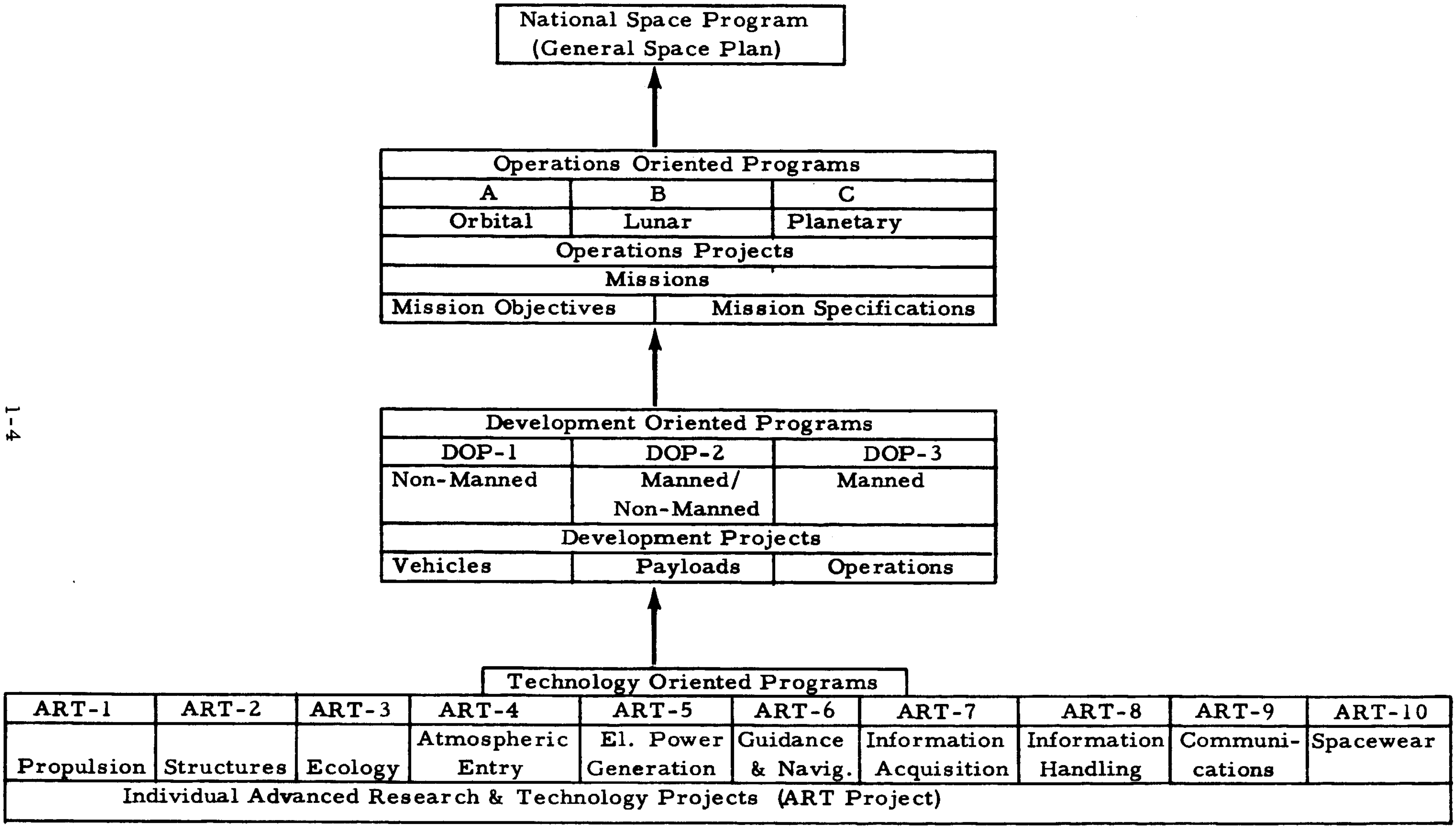

Fig. 1-2 DEFINITION OF PROGRAMS

either vehicles, or payloads or space operations, or a combination of these. The non-manned program is based on instrumented space probes; the manned program on manned transportation all the way to the destination. The manned/non-manned program is one in which both types of vehicles are extensively employed; such as, for instance, in a Mars or Venus orbital reconnaissance station (ORS) project, where manned flight is extended into a circumplanetary capture orbit and instrumented probes are used from the station as a substantial portion of the planet exploration activity.

1.3 SCOPE OF REPORT REGARDING LEVELS OF ACTIVITY

Within the framework of the before described reference system, the scope of this report covers primarily the operations oriented levels of activity and secondarily the development aspects of the propulsion systems under consideration.

1.4 EVALUATION CRITERIA

The evaluation of plans for given level of activity is carried out in two respects, namely, relative to the objective or objectives and relative to the quality of the approach. Only the latter is of interest here; i.e. the quality of systems, especially propulsion systems, is evaluated with respect to a variety of projects and missions. The evaluation of the objectives justifying these missions is not of concern in this report.

The propulsion systems are evaluated on the basis of four fundamental quality parameters which pervade all levels of activity:

$$\text{Cost Effectiveness (CE)} = \frac{\text{Cost}}{\text{Unit of Parameter}} \tag{1}$$

$$\text{Operating Effectiveness (OE)} = \frac{\text{Ideal CE}}{\text{Actual CE}} \tag{2}$$

$$\text{Ability (AY)} = \frac{\text{Quality of Transportation}}{\text{System}} \tag{3}$$

$$\text{Growth Rate (GR)} = \frac{\text{Ability Increase}}{\text{Unit Time}} \tag{4}$$

Fig. 1-3 shows the interrelation between mission, vehicle and cost. The abbreviations in this figure have the following significance:

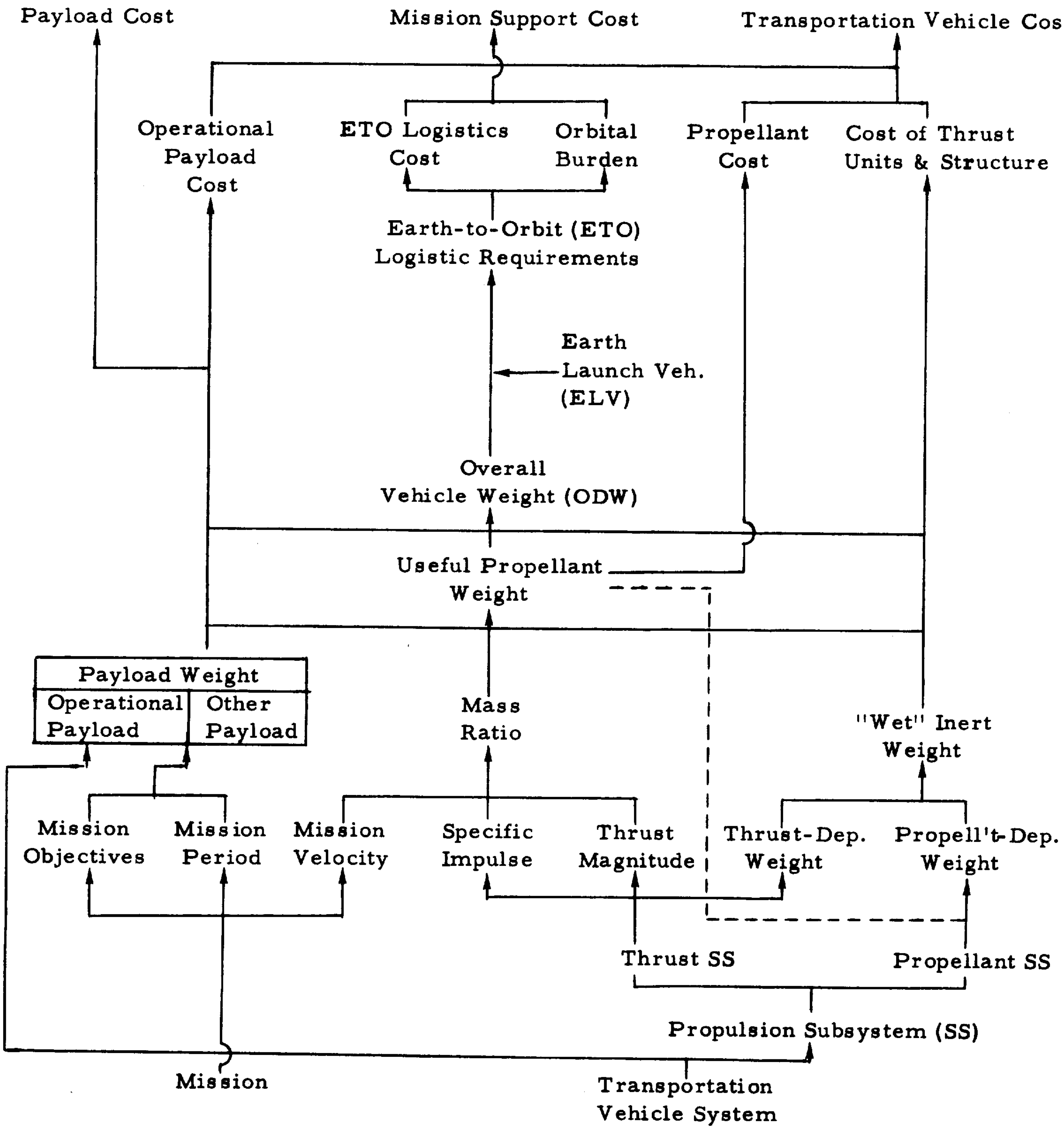

Fig. 1-3 MISSION-VEHICLE INTERRELATION PATTERN
Dep. = Dependent

SS = subsystem

ODW = orbital departure weight

The term "wet inert weight" designates the weight including residual fluids, which is left after all payload and the usefully expended propellant have been subtracted. Based on this interrelation, Fig. 1-4 shows the interrelation of important vehicle performance parameters. For a multi-stage vehicle, Fig. 1-4 applies to one stage (i), with other stages (j, k) preceding or following. At the same time, Fig. 1-4 defines the quantities which play an important role in the comparison of systems. They are building blocks which, together with others named below, represent the structure of the more complex quality parameters defined above.

Fig. 1-5 describes this build-up. The payload fraction is a function of specific impulse and mass fraction.

The orbital departure weight of a given ISV[2)] for a given mission, is a function of specific impulse, mass fraction and thrust level. In the case of the gaseous core reactor (GCR), the engine thrust is very high (at least 10^6 lb) as a condition for its operational feasibility, thereby forcing the ODW up, by upping the payload, in order to avoid unduly high thrust accelerations. This is an example for thrust constraint on the lower ODW limit. Thrust limitation of the individual solid core reactor (SCR), and possible limitation of the number of engines in a cluster, together with a limited specific impulse (800 - 900 sec) impose certain limitations on the upper limit of the ODW of ISV's with SCR drives.

The Earth-to-orbit (ETO) logistic requirements, that is, the number of Earth launch vehicles (ELV's) required to ready an ISV or a convoy of ISV's in orbit is, for a given mission and convoy size, a function of ODW and propellant density. For hydrogen-carriers the mean vehicle density is low, causing the volume of a payload section such as that of Saturn V to be an equal or greater constraint than its payload weight carrying capability.

The orbital operations requirements are expressed by the number of matings of vehicle modules and the number of fuelings which have to take place in orbit before mission readiness of the ISV or of the convoy is achieved. They are, for a given ELV, a function of the same parameters as the logistics requirements.

The mission versatility, defined by how well the ISV can carry out a more or less large variety of missions and explained in greater detail

---

2) ISV = Interorbital Space Vehicle (Manned)

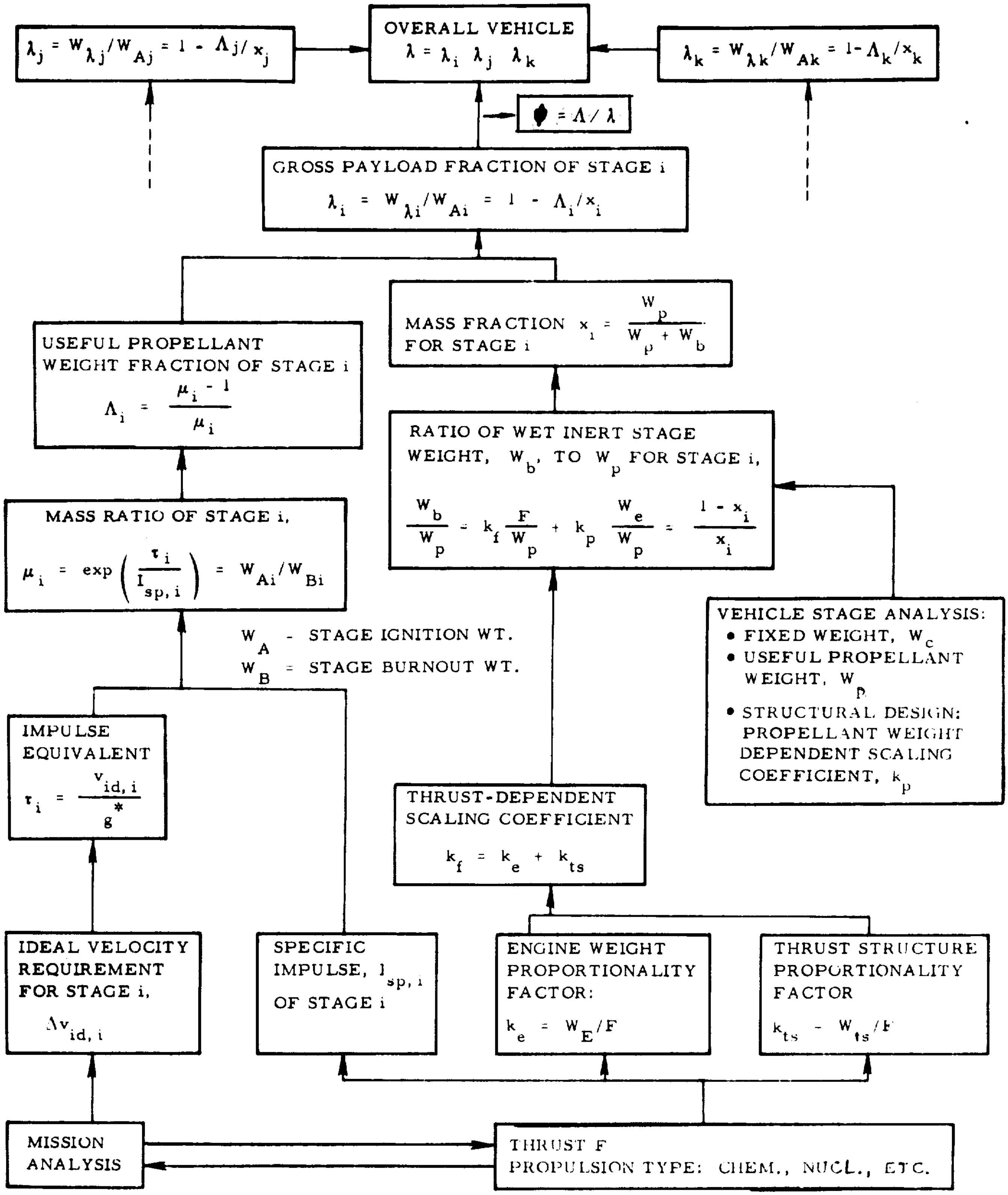

Fig. 1-4 INTERRELATION OF IMPORTANT VEHICLE PERFORMANCE PARAMETERS

- Payload Fraction $= f(I_{sp}, x)$

- Propellant Consumption Factor, $\psi = \Lambda / \lambda = W_p / W_\lambda$

- Orbital Departure Weight (ODW) $= f(I_{sp}, x, F, W_\lambda)$

- ETO Logistic Requirements = f (ODW, Propellant Density)

- Orbital Operations Requirements = f (ODW, Propellant Density)

- Mission Versatility = f (I_{sp}, Propellant Density, F, Reusability)

- Cost Effectiveness = f (ISV Dev. Cost, ISV Manuf. Cost, ISV Propellant Cost, ETO Logistic Requirements Cost, Payload Fraction, Mission Versatility)

- Operating Effectiveness = f (DSV Reliability, ISV Reliability, ELV Reliability, Orb. Operations Reliability)

- Ability = f (Operating Effectiveness, Mission Period, Mission Safety)

- Growth Rate = f (Propulsion System)

Fig. 1-5 EVALUATION CRITERIA

below, is a function of specific impulse, propellant density, thrust and, in some cases, reusability. Fig. 1-5 shows that the above mentioned criteria play an important role in determining the four quality parameters. Additional criteria are the ISV development cost, the ISV manufacturing and propellant cost, the reliability of the destination space vehicle (DSV), if any, the ISV, the ELV, the orbital operations, the mission period and the mission safety, i.e. the number of options in the face of emergencies en route. The ability parameter is seen to be expressed here primarily in terms of reliabilities, duration of the mission (of particular importance for interplanetary transfers) and safety for the human participants. The growth rate, finally, must be evaluated on the basis of specific characteristics of the propulsion system.

- The propulsion systems which are involved in the evaluation are
- Chemical (C)
- Chemical/Solar Heat Exchanger (C/SHE)
- Solid Core Reactor (SCR) with graphite (SCR/G) or water (SCR/W) as moderator or non-moderated (SCR/N)
- SCR/SHE
- Gaseous Core Reactor (GCR)
- Nuclear Pulse (NP)

SHE is a low-thrust drive, using solar energy, in focused form, to heat hydrogen which subsequently is expelled at high specific impulse ($600 \leq I_{sp} \leq 800$ sec).

The missions which are considered in the evaluation are:

- Mono-Elliptic Round-Trip Capture Missions to Mercury
- Mono-Elliptic Round-Trip Capture Missions to Venus; fast (about 400 d) and very fast (200 - 250 d)
- Round-Trip Capture Missions to Mars; fast (about 450 d) and very fast (200 - 250 d); synodic (slow-slow and fast-slow transfers).
- Mono-Elliptic Round-Trip Capture Missions to Jupiter with various capture conditions, incl. visit of J IV.

- Lunar Round-Trip Missions, involving Capture only, Surface Landing and Disorbiting to Free Fall Delivery

- Reusable Orbit Launch Vehicle Missions

The capability of any of the propulsion systems to carry out any of the missions must be rated in the light of certain characteristics, because a "yes" or "no" relative to a given capability is not sufficient. These characteristics are:

- the ELV needed
- for missions no. 1 and 2: Manned Interorbital Space Vehicle (ISV) (for lunar or planetary mission) or deep space probe (DS) as payload

Three ELV models are used in the comparison. They are defined in Tab. 1-1. The trend set by rating figures must be to penalize those ISV propulsion systems which require a modified Saturn V or even a post-Saturn for mission capabili y, based on the desirability to broaden the usefulness of Saturn V as the principal ETO logistics vehicle for lunar and planetary missions. The reason for this is the high cost and the long lead time required for the development of a post-Saturn ELV. Once developed, the cost effectiveness of ETO logistic transportation will be improved. But this improvement is of practical significance only if the mission frequency is sufficiently large and this, in turn, requires an acceptably high cost effectiveness of the interorbital mission proper, as one of the necessary prerequisites.

1.5 ANALYTICAL METHODOLOGY

The basis of the analytical methodology is the concept of the close interrelation of Mission, Vehicle, Operations and Economy (MOVE). The analysis proceeds in the following major steps:

		Output:
1.	Mission Analysis	Maneuvers Mission Velocity Mission Period
2.	Propulsion Module Analysis	Scaling Coefficients Mass Fractions
3.	General Vehicle/Mission Integration	Payload Fractions
4.	General Transportation Cost Analysis	Transportation Cost Effectiveness Index (TCEI)

ELV	Saturn V (Apollo)	Saturn V Mod. *	Post Saturn
Payload (Module Carrier)(10^3 lb)	250	350	1000
Payload Section Diameter (ft)	33	40	70
Payload Section Length (ft)	155	155	450
Payload Section Volume (10^3 ft^3)	115	169	1500
Mean Payload Density (lb/ft^3)	2.17	1.24	0.6
Liquid Propellant Weight when used as Tanker Carrier (10^3 lb)	225	315	900

*Saturn V Mod. is a hypothetical growth version designed to illustrate the potential probable capability of the Saturn V ELV. It is a hammer-head configuration, with a 40 foot payload section diameter and a 33 foot tank diameter. Saturn V Mod. is not planned by NASA at this time.

Tab. 1-1 ELV MODEL CONFIGURATIONS

		Transportation Cost Effectiveness (TCE)
5.	Payload Analysis	Payload Requirements Analysis Payload Weight Analysis Payload Cost Analysis
6.	Special Cost Analysis	Special Payload Fractions Special Transportation Cost Effectivness Overall Cost

The first step determines the mission requirements.

The second step determines the scaling coefficients and the associate mass fractions. These are functions of engine thrust and/or propellant weight and as such are not general. However, average values can be derived from them which represent conditions with acceptable accuracy over specified ranges of thrust and propellant weight.

The third step combines the results of the first and second steps in the form of a general vehicle/mission integration, in order to obtain the payload fractions (ratio of payload to initial vehicle weight) from mission velocity requirements and mass fractions. The general vehicle/mission integration procedure uses average mass fractions and thereby avoids the iteration process required in the special vehicle/mission analysis where propellant-dependent mass fractions or scaling coefficients are used to determine the required propellant weight and overall vehicle weight.

The fourth step which is part of the generalized analysis, deals with transportation cost (since no specific payload is defined in the general analysis, hence payload cost cannot be determined). This step is the last of the general analysis.

The subsequent two steps deal with what is referred to, briefly, as special analysis.

Step 5, payload analysis, yields absolute payload weights and defines the payload. Therewith a size parameter is introduced which leads to specific vehicle weights; and payload cost analysis becomes possible.

Step 6 computes size dependent payload fractions and transportation cost effectiveness coefficients. With these and with the payload cost data, the overall cost of a specific mission or a specific supply operation can be determined.

2. MISSION REQUIREMENTS

2.1 DEFINITION AND METHODOLOGY

A mission is something very specific, indivisible and, therefore, the basic unit of operations planning. A mission is a closely integrated sequence of events with a clearly defined beginning and ending. A mission involves only the operation, but not the development, of equipment, components, subsystems and systems. A mission (orbital, lunar or planetary) is defined by

- Objectives
- Mission Profile
- Payload
- Transportation System

The mission mode, chosen from a variety of operational alternatives, follows from mission profile and transportation system. A definition of the above four mission parameters is presented in Fig. 2-1.

In lunar and planetary missions, the main mission consists of the cislunar or heliocentric transfer either way and of the intermediate selenocentric or planetocentric operations of the HISV. Sub-missions consist of excursions by means of destination space vehicles (DSV) either to other orbits (orbital excursion) or to the surface (surface excursions), or to a planet moon (planet moon excursion).

The mission velocity is the sum of all principal maneuvers (velocity changes) carried out during the mission. Their sequence and magnitude is part of the mission profile definition; so is the mission period, consisting of cislunar or heliocentric transfer periods T_1, T_2 etc., plus the capture period (T_{cpt}). The mission phases are defined and described in Tab. 2-1 for planetary missions. They are applied analogously to lunar missions. Environmental conditions during the main mission are defined by heliocentric distance, meteoroid flux density and solar corpuscular radiation.

The payload is divided into four weight groups:

- Operational Payload = All weight items required to operate the manned ISV

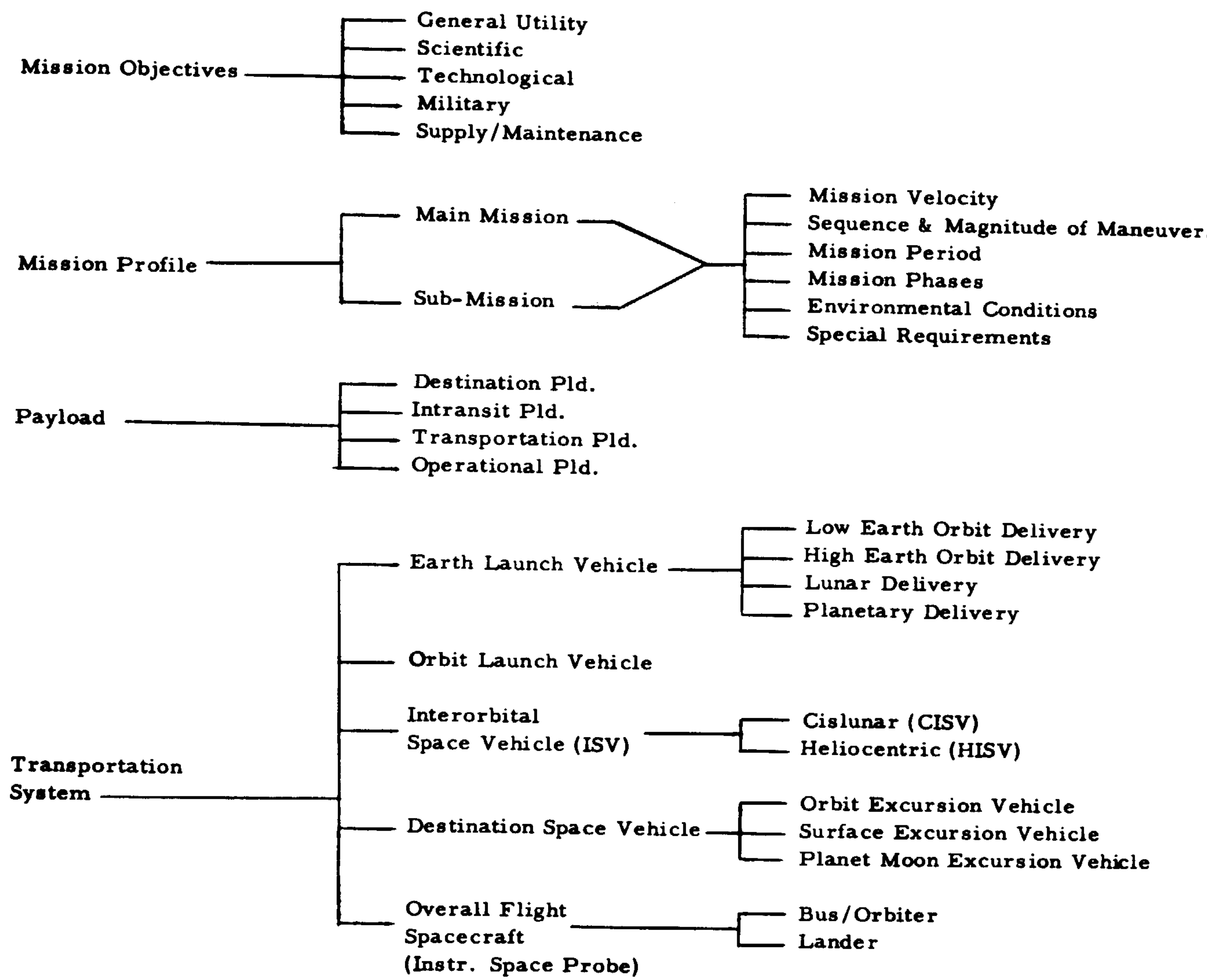

Fig. 2-1 MISSION DEFINITION PARAMETERS

Tab. 2-1 DEFINITION OF SEQUENCE OF EVENTS

A. BY PHASES

Phase No.	Designation	Description
0	Orbital Pre-Launch	From launch of first ELV to complete assembly and fueling of I/Vs.
1	Orbit Launch Preparations	From I/V checkout through completion of mission readiness test and stacking in mission departure flight formation.
2	Earth Departure	From engine ignition in Earth orbit to termination of geocentric flight phase (nominal beginning of heliocentric coast phase).
3	Heliocentric Transfer Phase	From nominal termination of geocentric flight to nominal beginning of target planetocentric flight phase.
4	Target Planet Arrival	Planetocentric approach up to periapsis of approach hyperbola including any capture of PFB maneuver that might be carried out according to mission plan.
5	Target Planet Capture	From capture orbit trimming to departure readiness (i. e., including orbit launch preparations).
6	Target Planet Orbit Launch	Powered injection maneuver into departure hyperbola.
7	Target Planet Departure	Analogous to 2, except that powered injection is not included (the separation of what is covered under 2 for Earth into 6 and 7 for target planet is done to facilitate accounting for differences between PFB and capture.
8	Heliocentric Transfer Phase	From termination of planetocentric flight phase to beginning of next planetocentric flight phase.
9	Target Planet Arrival	Analogous to 4.
10	Target Planet Capture	Analogous to 5.
11	Target Planet Orbit Launch	Analogous to 6.
12	Target Planet Departure	Analogous to 7.
13	Heliocentric Transfer Phase	Analogous to 8.
14	Target Planet Arrival	Analogous to 4.
15	Target Planet Capture	Analogous to 5.
16	Target Planet Orbit Launch	Analogous to 6.
17	Target Planet Departure	Analogous to 7.
18	Heliocentric Transfer Phase	From termination of planetocentric flight phase beginning of geocentric flight phase.
19	Earth Arrival	From beginning of geocentric flight phase to a point just prior to beginning of re-capture phase (in electric HISVs, this point is taken nominally as the beginning of negative orbital energy condition). Retro-thrust phase for the purpose of reducing hyperbolic entry speed belongs in this phase.
20	Earth Terminal Phase	From beginning of atmospheric entry to touch-down; or from beginning of capture maneuver (or first maneuver of a multi-maneuver operation) to pick-up from a terminal capture orbit (or descent from a terminal capture orbit by means of a terminal vehicle which was part of the HISVs payload) to a re-conditioning space station or to Earth surface.

- Intransit Payload = All weight items required to maintain and protect Transport Payload or Destination Payload during cislunar or heliocentric transfer.

- Transport Payload = All weight items needed for sub-missions at the destination, primarily the destination space vehicles.

- Destination Payload = All weight items needed at the final destination.

The transportation system, finally consists of Earth launch vehicle (ELV), cislunar or heliocentric interorbital space vehicle (CISV or HISV) and destination space vehicle (DSV). The principal correlation affecting selections is between mission, ELV and ISV propulsion system.

The missions are arranged according to target planets, assigning a number to each planet, beginning with Mercury as No. 1. Earth-Moon missions are, therefore, associated with No. 3.

2.2 MONO-ELLIPTIC ONE-PLANET MISSION PROFILES

The mission profiles are arranged according to target planets in the order of increasing distance from the target planet. Earth-Moon missions are, therefore, associated with the third planet.

For the purpose of orientation, Figures 2-1 through 2-4 show the position of the planets Mercury through Neptune at various years. Tab. 2-2 presents planetary constants.

As reference, Hohmann transfer missions between coplanar orbits at mean distance are used. The mission data are listed in Tab. 2-3.

Subsequently, many data are given in EMOS. A conversion chart from EMOS to km/sec and ft/sec is presented in Fig. 2-5. Fig. 2-6 correlates the Earth atmospheric entry velocity

$$v_E^* = \sqrt{(v_\infty^*)^2 + \frac{2\,K_{Ea}}{\bar{U}_{Ea}\,(r_{oo} + y)}} \qquad (2\text{-}1)$$

where the asterisk indicates that EMOS is the unit of velocity; $r_{oo} + y = r$, the

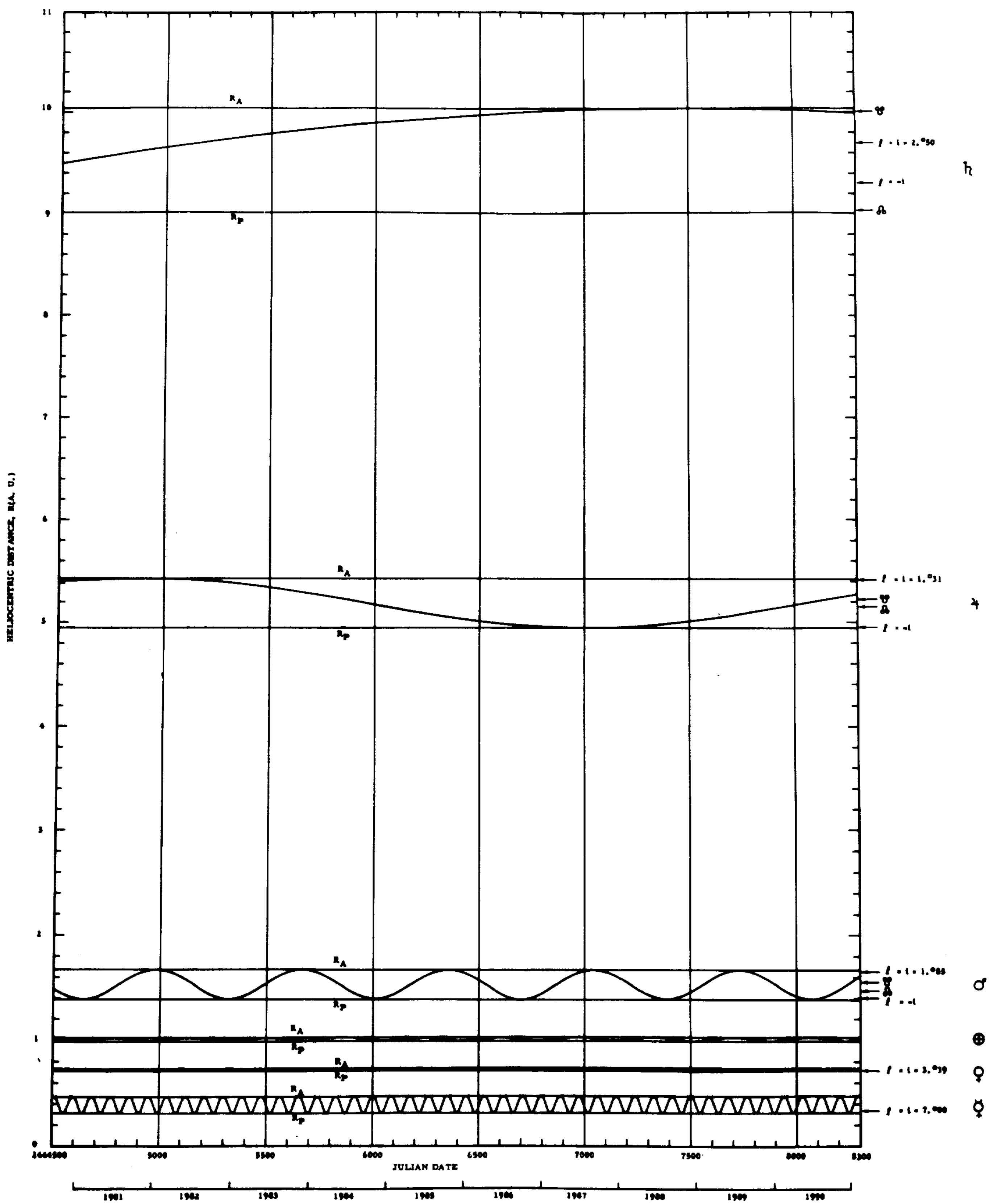

FIG. 2-2 HELIOCENTRIC DISTANCES AND POSITIONS OF PLANETS MERCURY THROUGH SATURN 1981-1990

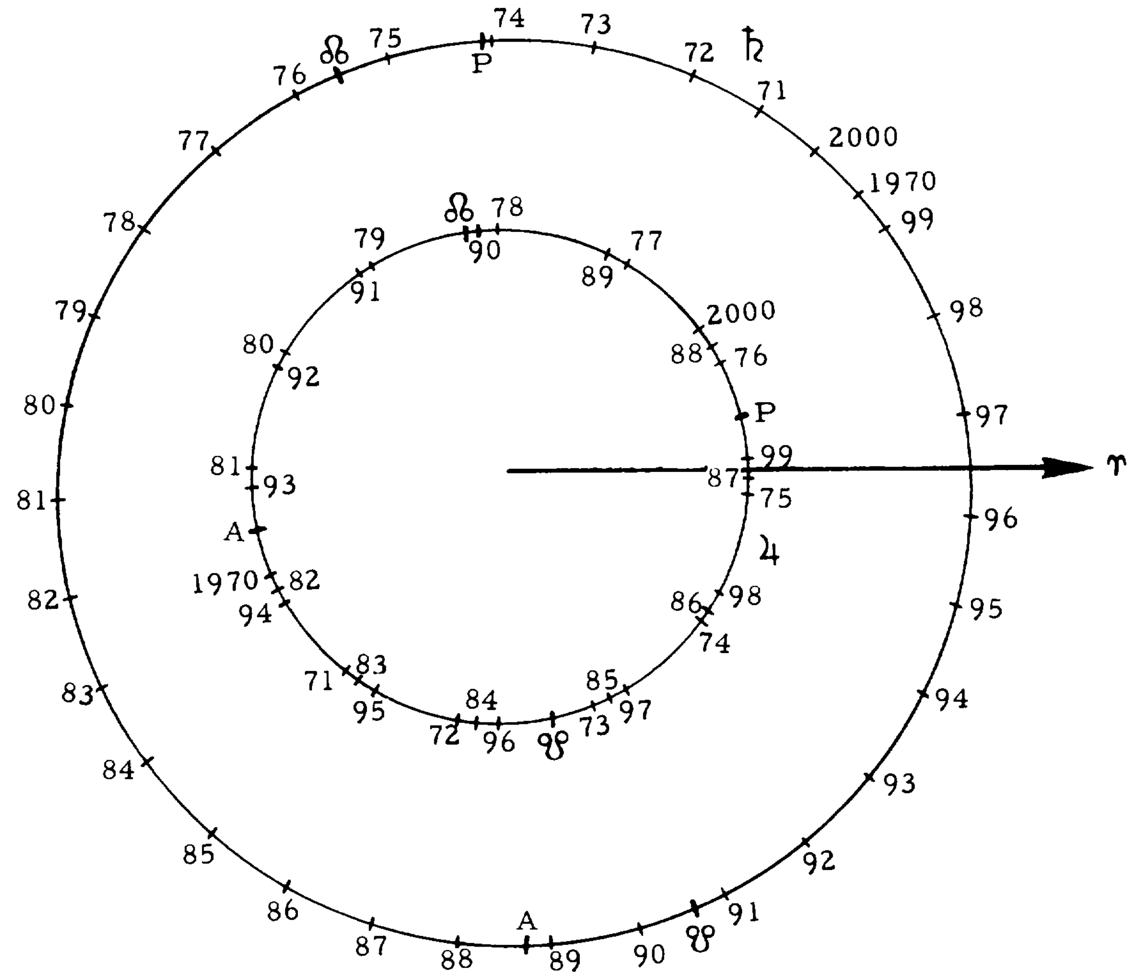

Fig. 2-3 POSITIONS OF JUPITER AND SATURN 1970 - 2000
Positions refer to the beginning of the year indicated (first days of January)

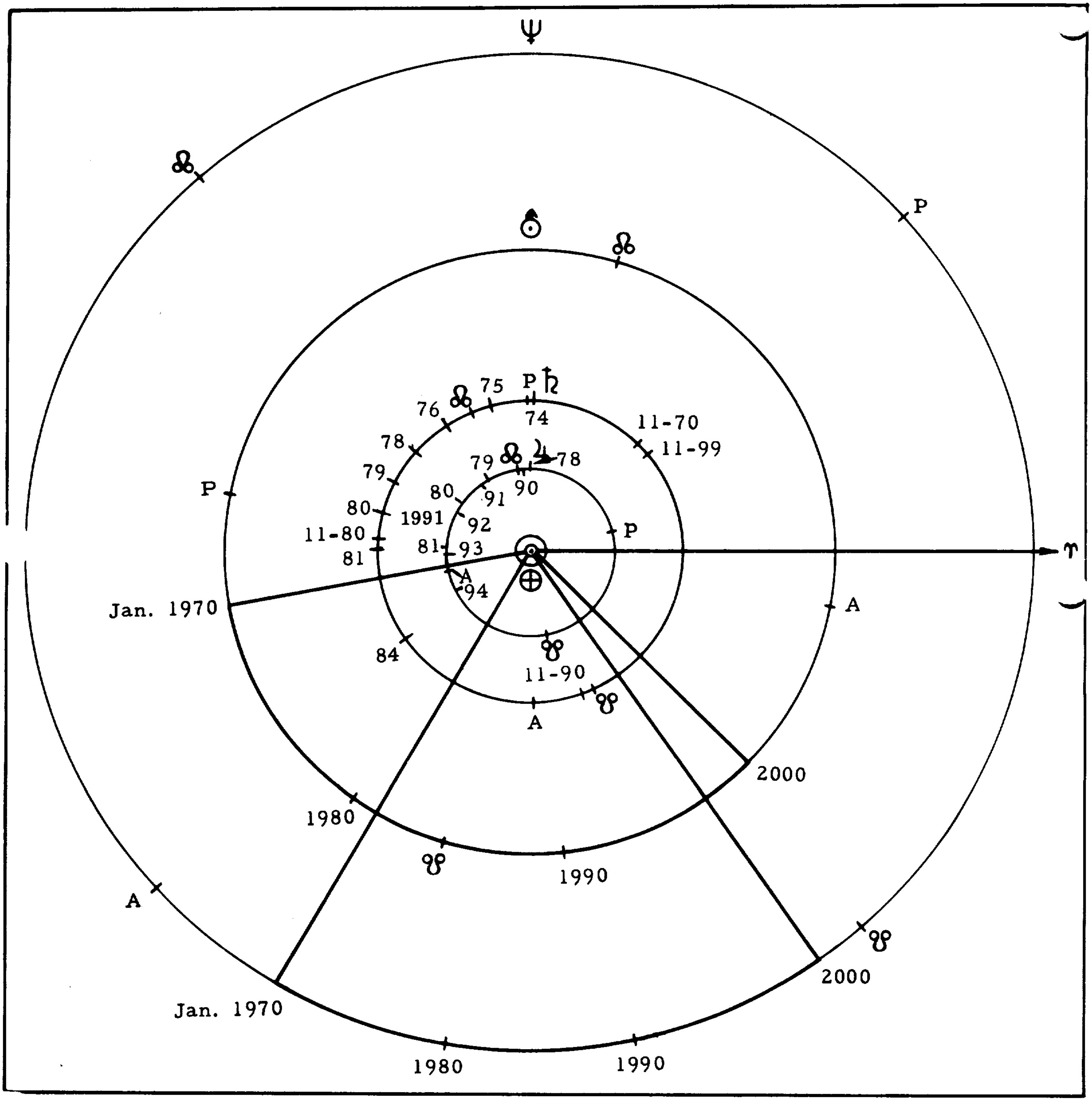

Fig. 2-4 POSITIONS OF JOVIAN PLANETS 1970 - 1990
Positions refer to the beginning of the year indicated (first days of January)

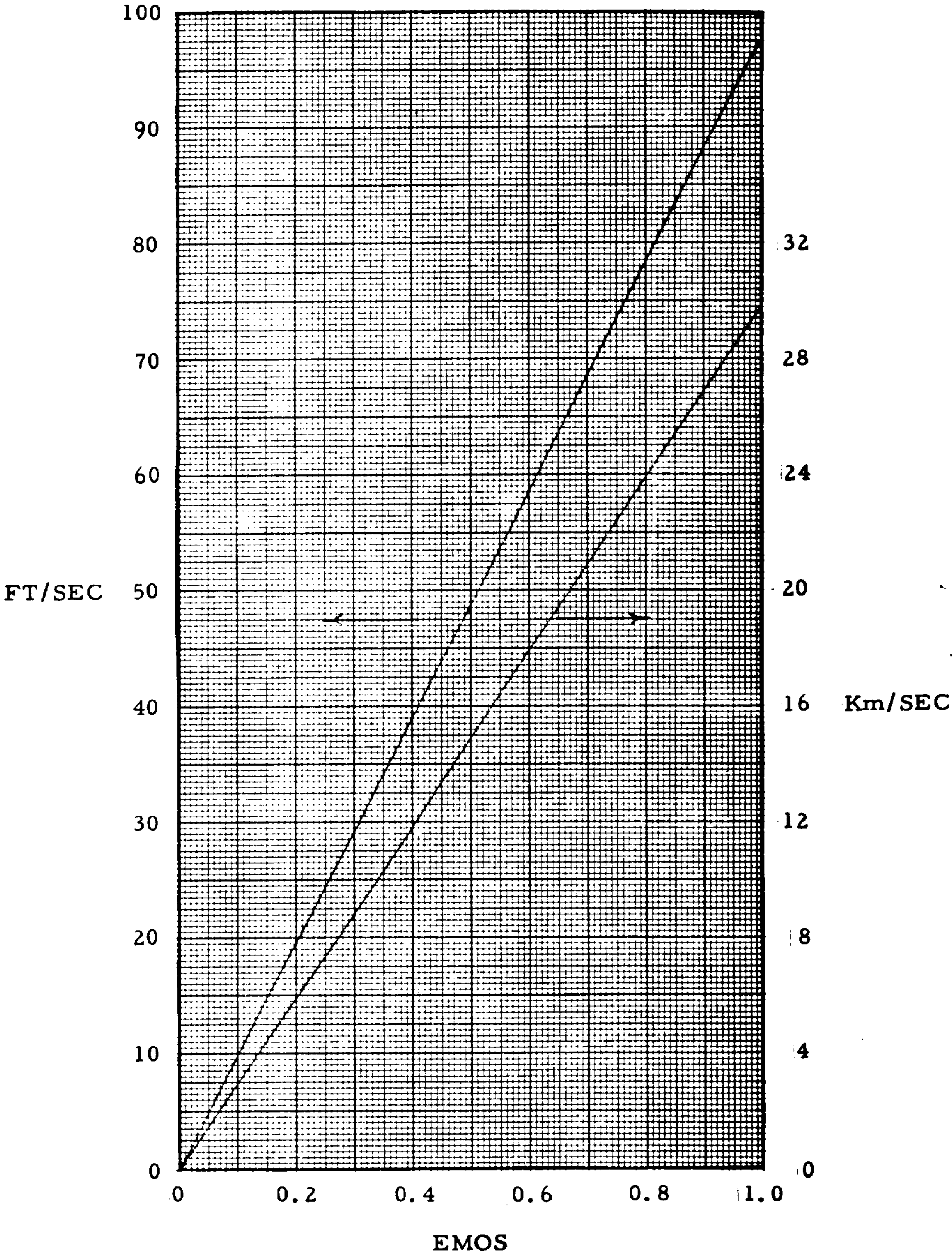

FIG. 2-5 CONVERSION FROM EARTH MEAN ORBITAL SPEED (EMOS) TO Km/SEC AND FT/SEC

Target Planet	$\Delta v_1^* = \Delta v_4$ n = 1 $r^* = 1.1$ (EMOS)	$\Delta v_2 = \Delta v_3$ n = 1 $r^* = 1.1$ (EMOS)	$T_1 = T_2$ (Days)	Years	T_{cpt} (Synodic Capture) (Days)	UHE[1)] (Earth) (EMOS)	Mission Period T		Mission Velocity (EMOS)	
							Days	Years	$\sum_1^3 \Delta v$	$\sum_1^4 \Delta v$
Mercury	0.1849	0.2525	105.5	0.2887	67	0.418	278	0.772	0.6899	0.8748
Venus	0.1150	0.1860	146	0.3999	468	0.392	760	2.08	0.4870	0.6020
Mars	0.1184	0.0730	258.8	0.7086	455	0.3925	972.6	2.66	0.2644	0.3774
Jupiter	0.2109	0.5730	997.3	2.731	214	0.429	2208	6.05	1.3569	1.5678
Saturn	0.2432	0.3515	2208.7	6.05	341	0.446	-	13.03	0.9462	1.1894
Uranus	0.2703	0.2215	5853.3	16.03	346	0.463	-	32.998	0.7133	0.9836
Neptune	0.2779	0.2489	11,174	30.6	292	0.467	-	61.98	0.7757	1.0536
Pluto	0.282	0.1622	16,650	45.6	291	0.468	-	91.97	0.6064	0.8884

1) UHE = Unretarded Hyperbolic Entry

Tab. 2-2 HOHMANN REFERENCE MISSION DATA

Tab. 2-3 IMPULSIVE MANEUVER ON MONO-ELLIPTIC MISSIONS TO MERCURY WITH DEPARTURE FROM CIRCULAR EARTH ORBIT ($r^* = 1.1$) AND CIRCULAR CAPTURE ORBIT ($r^* = 1.1$) AT MERCURY

No.	Mission 1)	EaDD 2) (CD)	EaDD 2) (JD)	Longitude 3) (Deg) Ea	Longitude 3) (Deg) Me	Lat. 3) (Deg) Me	T_1 (days)	$v_{\infty 1}^*$ (EMOS)	Δv_1 (ft/sec)	Δv_1 (km/sec)	$v_{\infty 2}^*$ (EMOS)	Δv_2 (ft/sec)	Δv_2 (km/sec)	MeAD 2) (JD)	Mercury Long. 3) (Deg)	Mercury Lat. 3) (Deg)	T_{cpt} (days)	MeDD 2) (CD)	Longitude 3) (Deg) Me	Longitude 3) (Deg) Ea	Lat. 3) (Deg) Me	T_2 (days)	$v_{\infty 3}^*$ (EMOS)	Δv_3 (ft/sec)	Δv_3 (km/sec)	$v_{\infty 4}^*$ (EMOS)	v_E 10^3 ft/sec	T
1	Me80-5	5/1-5/16	4360.5-4375.5	230	38	-1.2	80-85	0.375	24,600	7.5	0.4	32,000	9.75	4440.5-4460.5														
2	Me81-4	4/20-5/5	4714.5-4729.5	215	27	-2.4	80	0.4	27,300	8.32	0.4	32,000	9.75	4794.5-4809.5	348	-6.1	~ 80	9/25-10/5	316	9	-7.0	180	0.45	38,600	11.77	0.46	58.4	340
3	Me81-7	7/22-8/2	4807.5-4818.5	306	69	+2.6	110	0.35	24,200	7.39	0.5	41,400	12.6	4917.5-4928.5	165	+6.2	~267	1/3-1/18	7	110	-4.6	110	0.4	32,000	9.75	0.35	50	487
4	Me81-11	11/10-11/21	4918.5 4929.5	49	165	+6.2	110	0.27	19,100	5.82	0.5	41,400	12.6	5028.5-5039.5	240	-1.5	~ 60	5/8-5/18	182	230	+5.0	90	0.5	41,400	12.6	0.32	48.2	260
5	Me82-4	4/3-4/12	5063.5-5071.5	200	17	-3.6	80	0.37	25,600	7.8	0.4	32,000	9.75	5143.5-5151.5	320	-7	~ 75	9/6-9/18	310	354	-6.9	180	0.5	41,400	12.6	0.44	56.7	335
6	Me82-10	10/23-11/5	5265.5-5278.5	34	157	+6.6	110	0.25	17,300	5.27	0.5	41,400	12.6	5375.5-5388.5	235	-0.8	~ 70	4/20-5/1	175	215	+5.6	90	0.5	41,400	12.6	0.37	51.6	270
7a	Me83-3	3/12-3/28	5405.5 5421.5	175	324	-6.9	80	0.4	27,300	8.32	0.5	41,400	12.6	5485.5-5501.5	314	-7	~ 75	8/12-8/22	260	325	-3.7	90	0.45	38,600	11.77	0.375	52	245
7b																	~200	12/14-12/24	13	84	-4	180	0.45	38,600	11.77	0.515	61.8	
8	Me84-2	2/23-3/5	5753.5-5764.5	160	317	-7.0	80	0.37	25,600	7.8	0.5	41,400	12.6	5833.5-5844.5	291	-6.3	~ 70	7/26-8/5	241	306	-1.6	90	0.45	38,600	11.77	0.28	45.3	240
9	Me84-5	5/17-5/29	5837.5-5849.5	244	307	-6.9	110	0.4	27,300	8.32	0.5	41,400	12.6	5947.5-5959.5	47	-5.3	~ 80	11/27-12/7	4	69	-4.9	180	0.40	32,000	9.75	0.515	61.8	370
10	Me85-5	5/3-5/19	6188.5-6204.5	229	301	-6.7	110	0.36	24,100	7.35	0.4	32,000	9.75	6298.5-6314.5	36	-1.4	~ 80	11/8-11/20	355	53	-5.6	180	0.40	32,000	9.75	0.50	60.6	370
11	Me86-4	4/15-4/24	6535.5-6544.5	209	280	-5.6	110	0.39	26,700	8.15	0.4	32,000	9.75	6645.5-6654.5	360	-5.2	~ 73	10/27-11/3	346	38	-6.2	180	0.40	32,000	9.75	0.50	60.6	363
12	Me86-5	5/18-5/28	6568.5-6578.5	243	73	+3.0	80	0.39	26,700	8.15	0.4	32,000	9.75	6648.5-6658.5	25	-2.6	~170	1/29-2/9	20	134	-3.2	90	0.40	32,000	9.75	0.40	52.8	340
13	Me87-3	3/25-4/6	6879.5-6891.5	189	261	-3.8	110	0.4	27,300	8.32	0.5	41,400	12.6	6989.5-7081.5	330	-6.8	~ 90	10/5-10/16	18	319	-7.0	180	0.45	36,700	11.2	0.47	58	380

1) Mission designation by target planet, year, and month of beginning of Ea departure window.

2) EaDD = Earth departure date; MeAD = Mercury arrival date; MeDD = Mercury departure date.

3) Heliocentric ecliptic system, data pertain to a date within the Ea departure or Me departure window for which the Mercurocentric maneuver (Δv_2, Δv_3) is close to minimum.

radial distance, where y is the altitude; $\overline{U}_{Ea}$ is the Earth mean orbital speed.

The hyperbolic excess speed with respect to a planet can conveniently be converted into the impulse required for departure from, or arrival in, a circular orbit at radial distance r* (Earth radii), or at the periapsis r_P^* of an elliptic orbit, by means of the equation

$$\Delta v = v_\infty^* \overline{U}_{Ea} \left(1 - \sqrt{\frac{2+\epsilon}{2 \times z}}\right) \sqrt{1 + \frac{2}{z}} \tag{2-2}$$

where $Z = Q r^* (v_\infty^*)^2$, or r_P^* instead of r*; Q is listed in Tab. 2-2; ϵ in the relative orbital energy ($\epsilon = -1.$ for any circular orbit),

$$\epsilon = - \frac{2}{n+1} \tag{2-3}$$

$$n = r_A / r_P \tag{2-4}$$

which is related to the ratio of apoapsis to periapsis (ellipticity) by the relation given. The ratio $\Delta v^* / v_\infty^*$ for Earth is plotted in Fig. 2-6 for n = 1, r* = 1.0, 1.1, 1.2. By using this graph, Δv is obtained, for the given conditions, from

$$\Delta v = \frac{\Delta v^*}{v_\infty^*} \cdot v_\infty^* \cdot \overline{U}_{Ea} \tag{2-5}$$

If the HISV is captured in an elliptic rather than a circular orbit, the capture maneuver requires a smaller impulse, provided the maneuver is carried out at the periapsis of the ellipse. Its magnitude is $\Delta v_{P,2}$ coinciding with the periapsis of the h perbola. In order not to lose this gain when departing, the departure maneuver must also take place at or near the periapsis of the ellipse; that is, the major axis of the ellipse must coincide closely with that of the departure hyperbola. In order to ascertain this, it may be necessary to rotate the major axis of the ellipse[3]. This is accomplished comparatively most economically by entering a circular orbit at the apoapsis and, after having passed through the required turning angle,

---

3) The underlying assumption is that the capture orbit has been placed into a plane which coincides, or with the aid of precision, will coincide with the place of the departure hyperbola.

re-enters the elliptic orbit by a reverse maneuver. The magnitude of the impulsive maneuver is Δv_A. The departure maneuver consists, in this case, of 3 maneuvers and has the magnitude $2\Delta v_A + \Delta v_P$, 3. The value of Δv_A is given for the individual planets in the subsequent paragraphs.

Intermediate dates in 20 to 30 day Earth departure windows are shown in Fig. 2-7, based on the determination of favorable mono-elliptic transfer corridors from Earth to the target planets.

Fig. 2-8 surveys the mission velocity capability required for 1-way missions (with capture at target) to Mercury and to Jupiter and for round-trip missions to the planets Mercury through Jupiter. These velocities are shown in bands. For the two Jupiter bands, the upper limit is based on an elliptic capture orbit of $n = r_A/r_P = 3$ with $r^*_P = 1.1$ planet radii; the lower limit is based on a highly elliptic capture orbit, $n = 30$, $r^*_P = 1.1$. For Mars, the upper limit is based on unfavorable mission year conditions with circular capture (CC) at Earth return ($r^* = 1.1$); the lower limit is based on a hyperbolic Earth entry velocity limit of $v_E = 50,000$ ft/sec (50k) for favorable mission year conditions. In the case of Venus, the upper limit represents circular orbit capture ($r^* = 1.1$) at Venus and return into a circular capture orbit about Earth ($r^* = 1.1$); the lower limit represents elliptic capture at Venus ($n = 8$; $r^*_P = 1.1$) and unretarded hyperbolic entry (UHE) at Earth return. For the Mercury round-trip mission, the lower limit represents the minimum coplanar case (nodel transfers), the upper line is based on more frequently recurring mission opportunities; capture at Mercury is in circular orbit ($n = 1$; $r^* = 1.1$) and return to Earth is limited to a 50k entry velocity.

2.2.1 Mercury Missions

Fig. 2-1 shows the positions of Mercury at inferior conjunctions during the 1975/83 period. Conjunctions which occur during a particular month of the Earth year tend to cluster together in the manner shown. The sidereal period of Mercury is 88 days. Transfer times around 90 days correspond to medium-fast transfers from Earth to Mercury (transfer angles 130 to 150 degrees), so that Mercury completes about one revolution during such a transfer. It is seen[3] that the same constellation of Earth and Mercury recurs every 7 years, approximately 7 to 8 days earlier every time around. A cycle of Mercury missions is, therefore, 7 years long.

For one such cycle, ranging from April 1980 through April 1987, Ea-Me and Me-Ea missions were computed for transfer between inclined,

[3] cf. No. 47 & 69; No. 48 & 70; No. 49 & 71

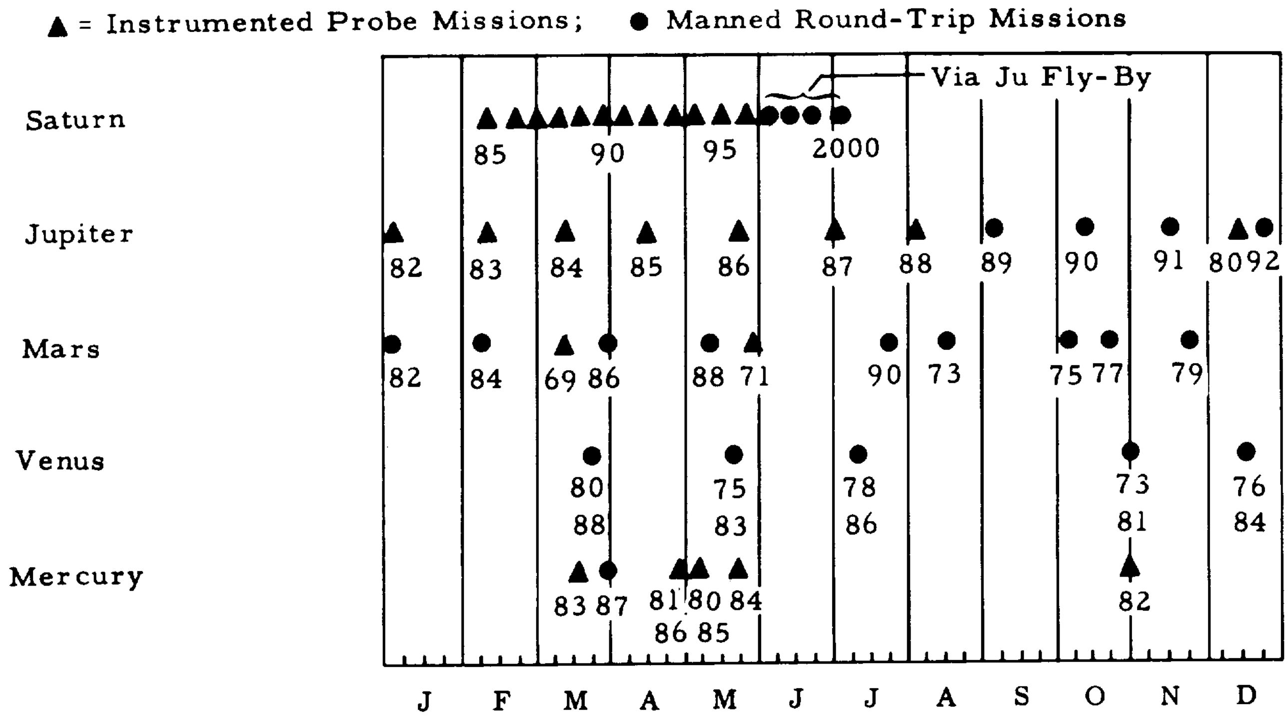

Fig. 2-7a EARTH DEPARTURE DATES FOR MONO-ELLIPTIC PLANETARY MISSIONS

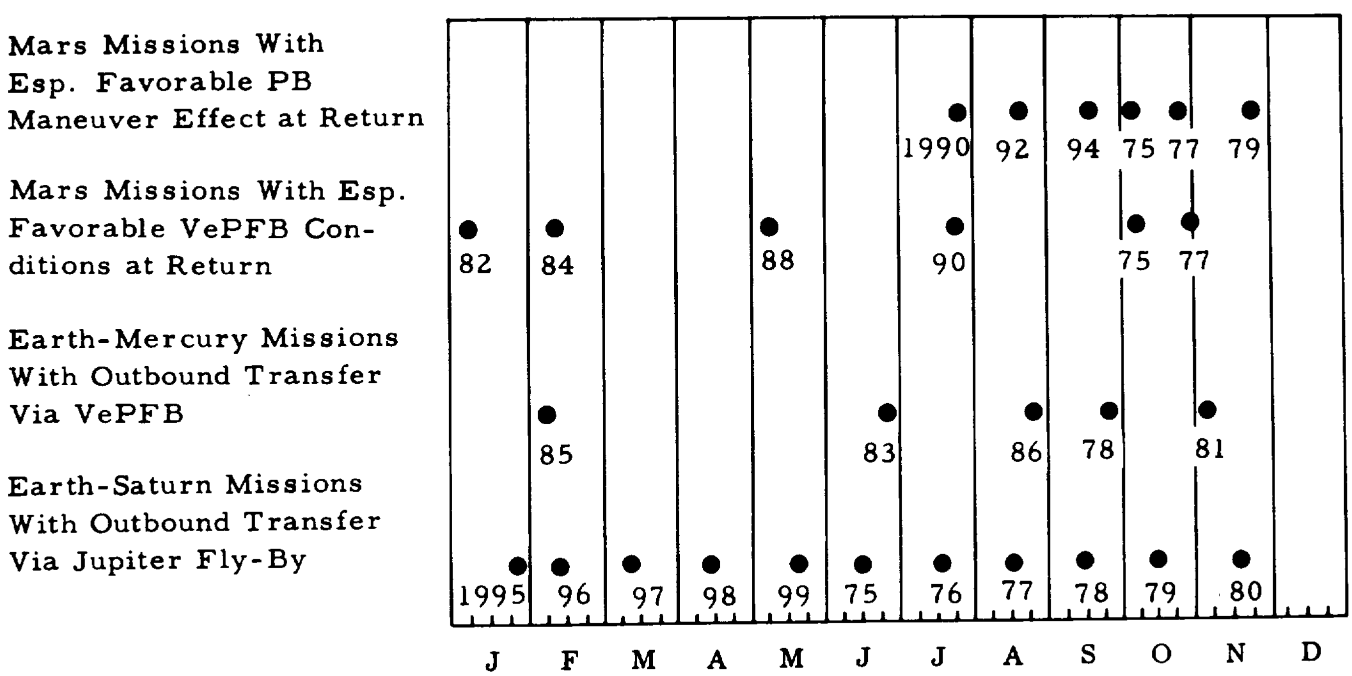

Fig. 2-7b EARTH DEPARTURE DATES FOR PLANETARY MISSIONS INVOLVING PERIHELION BRAKE OR FLY-BY EN ROUTE TO OR FROM TARGET PLANET

Fig. 2-8 OVERALL MISSION VELOCITY ENVELOPES TO VARIOUS TARGET PLANETS

----- = 1 Way with Capture; ——— Round-Trip

v_E = 50k = Earth Entry Velocity limited to 50,000 ft/sec

UHE = Unretarded Hyperbolic Entry into Earth Atmosphere

EaCC = Circular Capture ($r^* = 1.1$) at Earth Return

● = Hohmann Transfer

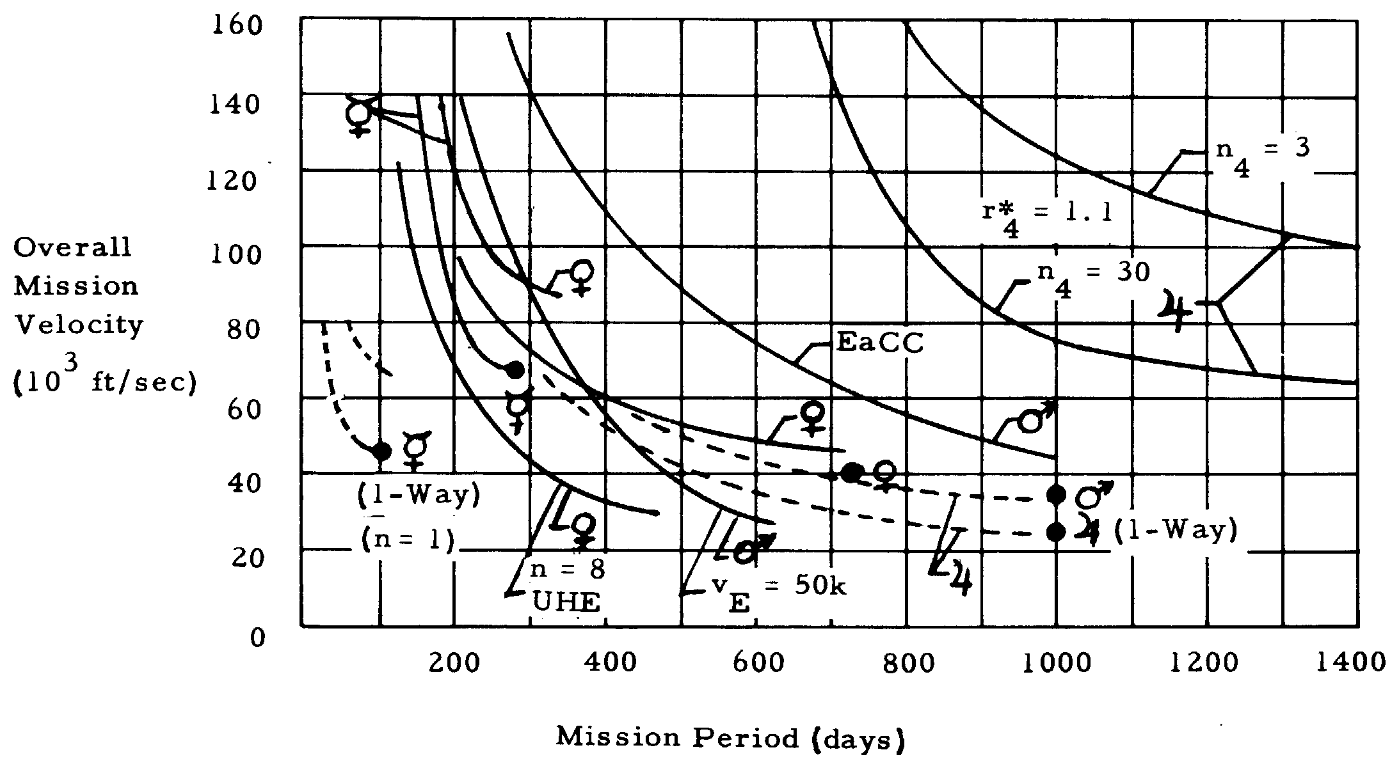

elliptic orbits (Gauss-Lambert Method). The results are plotted in six Figures in the Appendix in the back of this report for Ea-Ma transfer times of 80, 85 (1980 only), 90, 110 (Hohmann transfer is 105.5 days) and 180 days. For the same time span, Me-Ea transfer orbits were computed. These are plotted for the cases of 90 and 180 days transfer time in six Figures shown also in the Supplement of this report. The plots show the hyperbolic excess velocity as function of launch date (either way), the solid lines referring to Earth, the dashed lines referring to Mercury. Three conversion charts v_{∞}^{*} to Δv (ft/sec) at $1 \leq n \geq 30$ capture orbits for r^{*} or r_{p}^{*} of 1.1, 1.5 and 2 planet radii are added; and finally a chart from which Δv_{A} for elliptic circum-Mercurian orbits can be read. Therewith the data are provided for the construction of a larger variety of Mercury missions, either 1-way without capture, or 1-way with capture or round-trip.

Inspection of the v_{∞}^{*} -charts shows that the high speed of Mercury causes the local minima of the Mercury arrival velocities to be quite narrow. In fact, their narrowness determines the values of $v_{\infty 1}^{*}$ and $v_{\infty 2}^{*}$ and raises them quickly with increasing width of the Earth departure window.

Tab. 2-3 shows a set of impulsive maneuvers Δv for Earth departure windows of 1 to 2 weeks. The departure dates from Earth and from Mercury are determined primarily by the Mercury arrival and departure impulses. Therefore, the data shown in Tab. 2-3 are oriented toward keeping these impulses low. Fortunately, this can be done most of the time without excessive penalty in Earth departure impulse or in Earth entry velocity.

The impulses and the Earth entry velocities listed in Tab. 2-3 are plotted in Fig. 2-9 and 2-10, for purposes of comparison. Although round-trip missions are shown in all years, except 1980, the presentation permits also comparison of one-way missions with or without capture. For one-way missions, the years 1980, 1981, 1982, 1985 and 1986 are more favorable than the other mission years. For these more favorable years, a fairly invariant Mercury capture maneuver capability of 32,000 ft/sec is required. The Earth departure maneuver varies a little more, but mostly lies between 24,000 and 28,000 ft/sec. Unretarded hyperbolic entry (UHE) velocities can readily be kept between 50,000 and 60,000 ft/sec. They vary less than for Mars mission returns. The mission periods vary between 270 and 380 days.

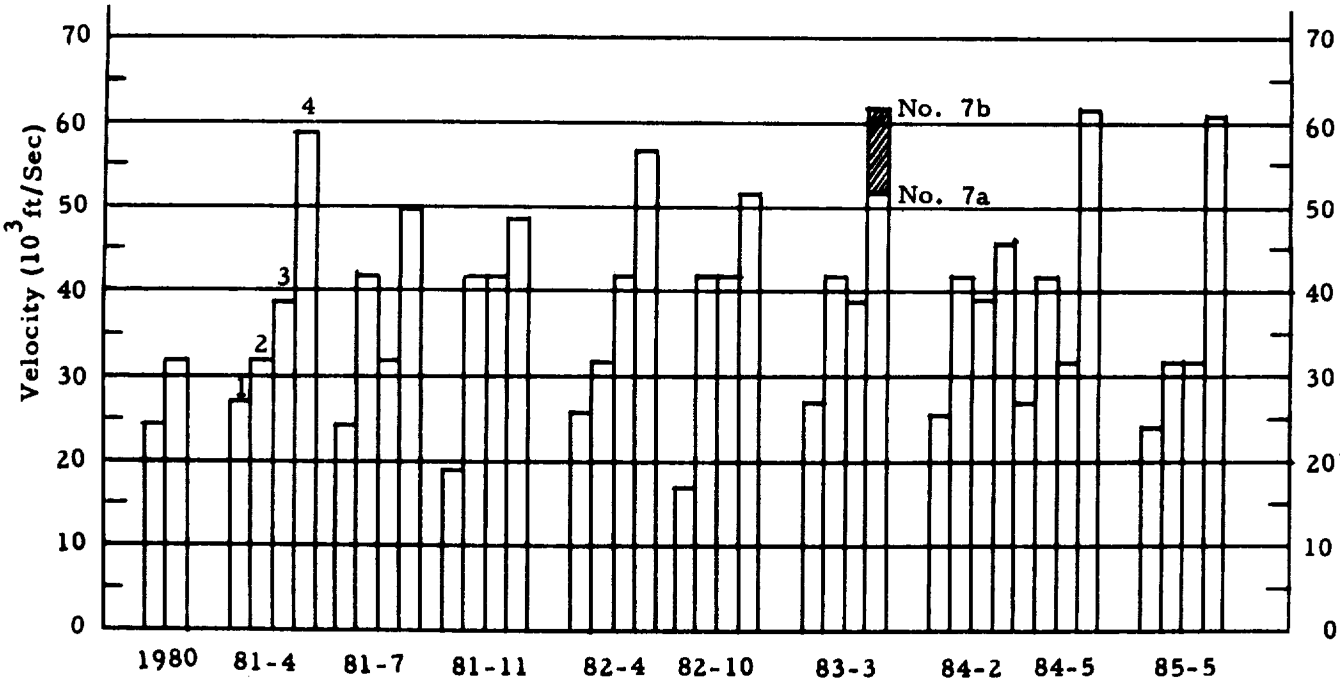

Fig. 2-9 MONO-ELLIPTIC MERCURY MISSION PROFILES 1980-85
(cf. Tab. 2-3)
$1 = \Delta v_1$; $2 = \Delta v_2$; $3 = \Delta v_3$; $4 = v_E$

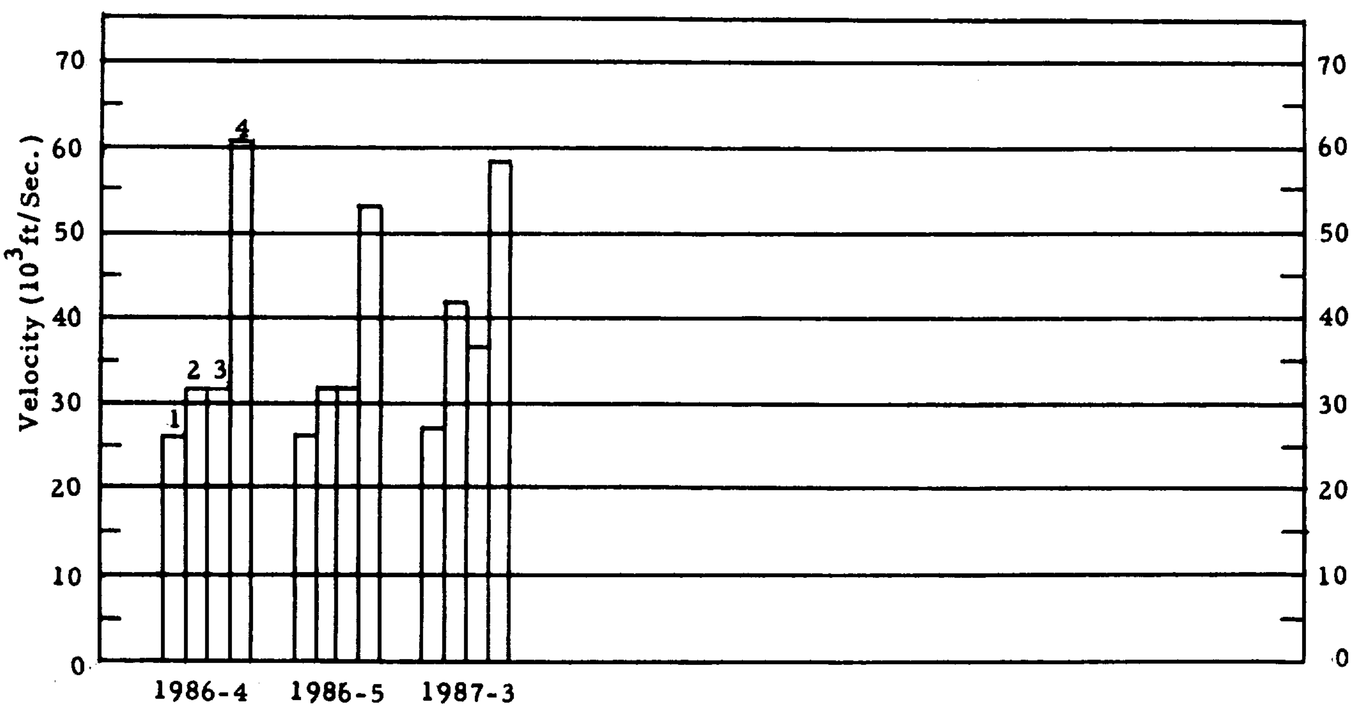

Fig. 2-10 MONO-ELLIPTIC MERCURY MISSION PROFILES, 1986-87
(cf. Tab. 2-3)
$1 = v_1$; $2 = v_2$; $3 = v_3$; $4 = v_E$

2.2.2 Venus Missions

Fig. 2-2 shows that a given Venus position is repeated almost exactly every 8 years. Venus mission conditions, therefore, recur rather precisely in 8-year cycles. Within a given cycle, the mission velocity requirement varies little, due to the near-circularity of the Venus orbit. Tab. 2-4 and 2-5 list, for one cycle, the impulse maneuvers involved in medium-fast Venus capture missions of 400 to 420 days duration for capture in a circular orbit at $r^* = 1.1$ and for capture in an elliptic orbit, $n = 8$, $r_p^* = 1.1$. The corresponding velocity distributions are plotted in Figs. 2-11 and 2-12, for comparison purposes. In the case of elliptic capture, Tab. 2-5 lists the dual apoapsis maneuver, $2\Delta v_A$. Fig. 2-12 shows that elliptic capture reduces the overall mission energy requirement in the case of Venus, even if the dual apoapsis maneuver is accounted for; and even more so, if no apoapsis maneuver is required; which is often the case when the capture period is short. Fig. 2-11 shows that an HISV is easily standardized for Venus missions, because the individual impulses vary little. The Earth entry velocities lie under 50,000 ft/sec for the mission periods in question. Fig, 2-12 shows the variation of the mission velocity over a full cycle of recurring nearly identical mission conditions and for various mission modes, using a mission period of 400 to 420 days with 20 days capture. The six bars at the left refer to capture in a circular orbit ($n = 1$; $r^* = 1.1$) with circular capture at Earth return (1); or with Earth entry limited to 40,000 ft/sec (2); or with UHE at Earth return; or for 1-way missions (4) with circular capture at $r^* = 1.1$. The second group of 6 bars refers to the same return modes, but for elliptic capture ($n = 8$; $r_p^* = 1.1$) at Venus, including the previously described double apoapsis maneuver. The third group of bars refers to the same conditions as the second, but without the two apoapsis maneuvers.

Fig. 2-13 through 2-16 show the variation of hyperbolic excess velocity versus departure date for fast ($\geq$ 60 days) and very fast ($<$ 60 days) mono-elliptic transfers between Earth and Venus and between Venus and Earth for the mission years 1977 and 1983. On the right hand ordinate of Fig. 2-14 and on the top abscessa of Fig. 2-16 is shown the unretarded hypberolic entry (UHE) velocity so that for the solid lines the entry velocity can readily be assessed which corresponds to a given value of $v_{\infty 4}^*$. Since the conditions for a given transfer to or from Venus are very nearly the same every 2920 days, the graphs can also be applied readily to the other mission years listed. Moreover, as in the case of the medium-fast missions before, the mission velocity varies little over a full 8-year mission cycle. This fact is illustrated in Tab. 2-6, where the impulse maneuvers (not hyperbolic excess velocities) for Earth departure and Venus arrival (circular and elliptic) are listed for four transfer periods throughout one mission cycle. The impulse maneuvers represent the approximate minima; the associated Julian dates show that the Earth departure dates for minimum

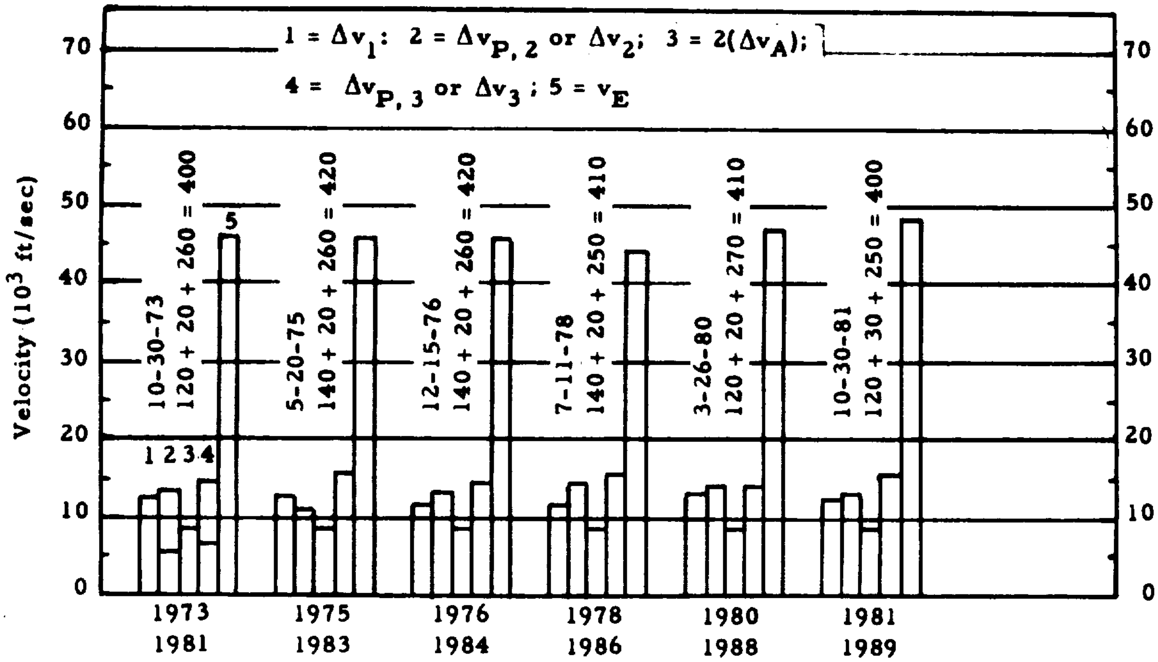

Fig. 2-11 MONO-ELLIPTIC VENUS ROUND-TRIP MISSION VELOCITY PROFILE THROUGH ONE CYCLE OF RECURRING MISSION CONDITIONS

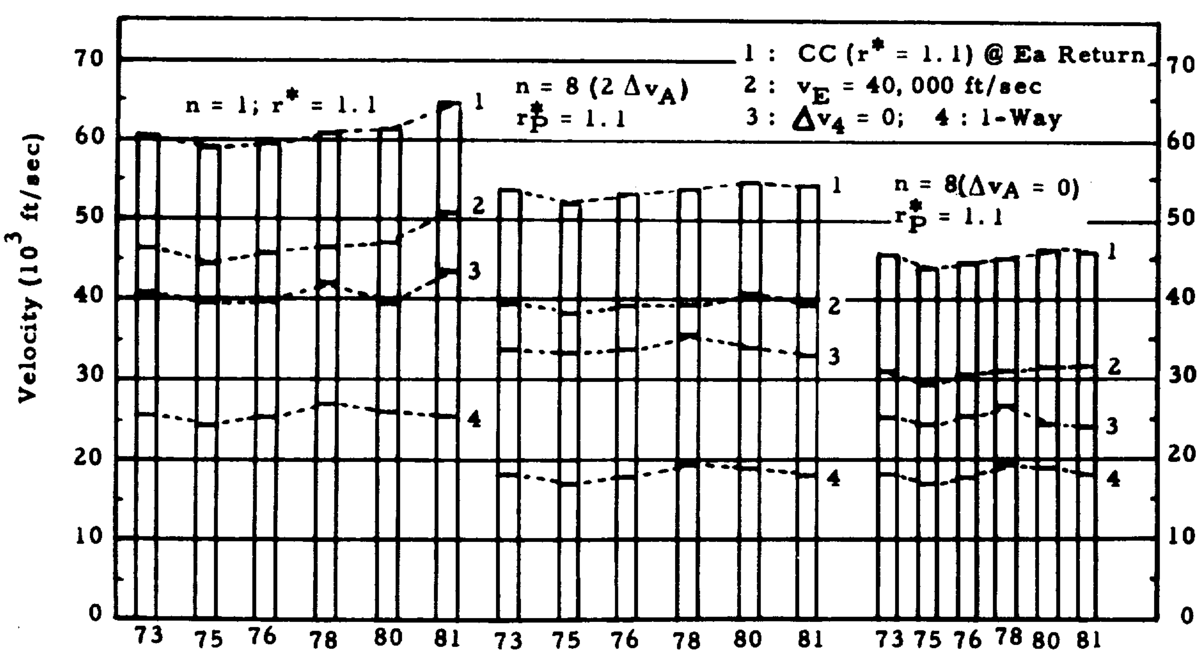

Fig. 2-12 MONO-ELLIPTIC VENUS MISSION VELOCITY PROFILES FOR ONE-WAY AND ROUND-TRIP MISSIONS WITH VARIOUS EARTH RETURN CONDITIONS

v_E = Earth Entry Vel.; Δv_4 = Earth Return Retro-Maneur Maneuver
CC = Circular Capture; $n = r_A/r_P$

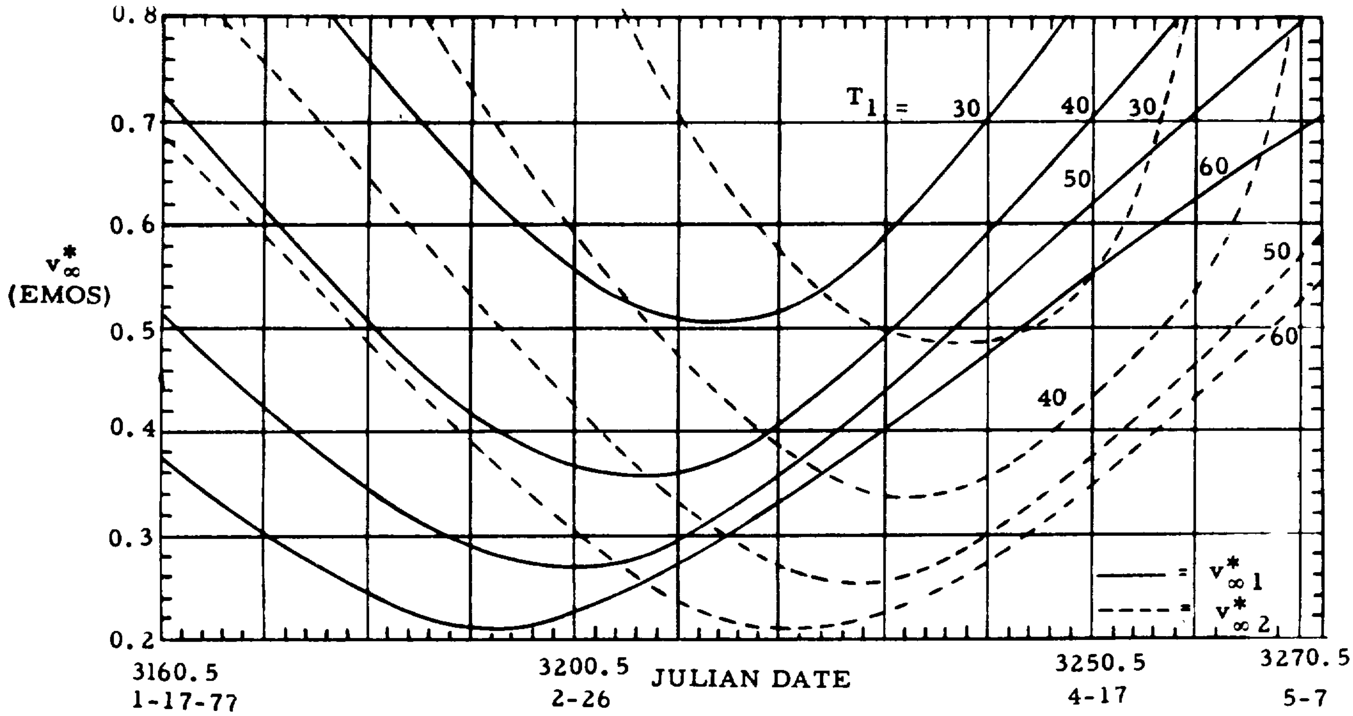

Fig. 2-13 VERY FAST EARTH-VENUS TRANSFERS, 1977, 1985, 1993
HYPERBOLIC EXCESS VELOCITIES
(T_2 = Transfer Time (Days))

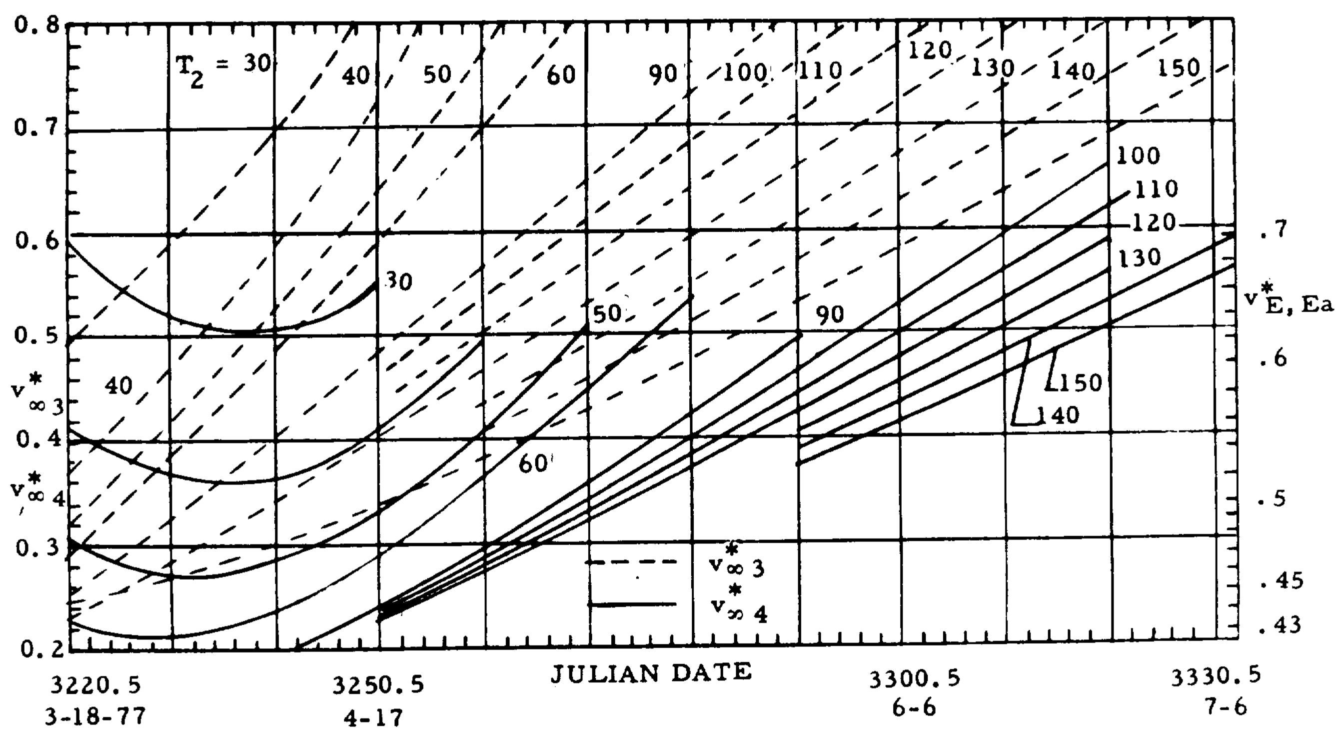

Fig. 2-14 VERY FAST VENUS-EARTH TRANSFERS, 1977, 1985, 1993
HYPERBOLIC EXCESS VELOCITIES AND EARTH ENTRY VELOCITIES
(T_2 = Transfer Time (Days))

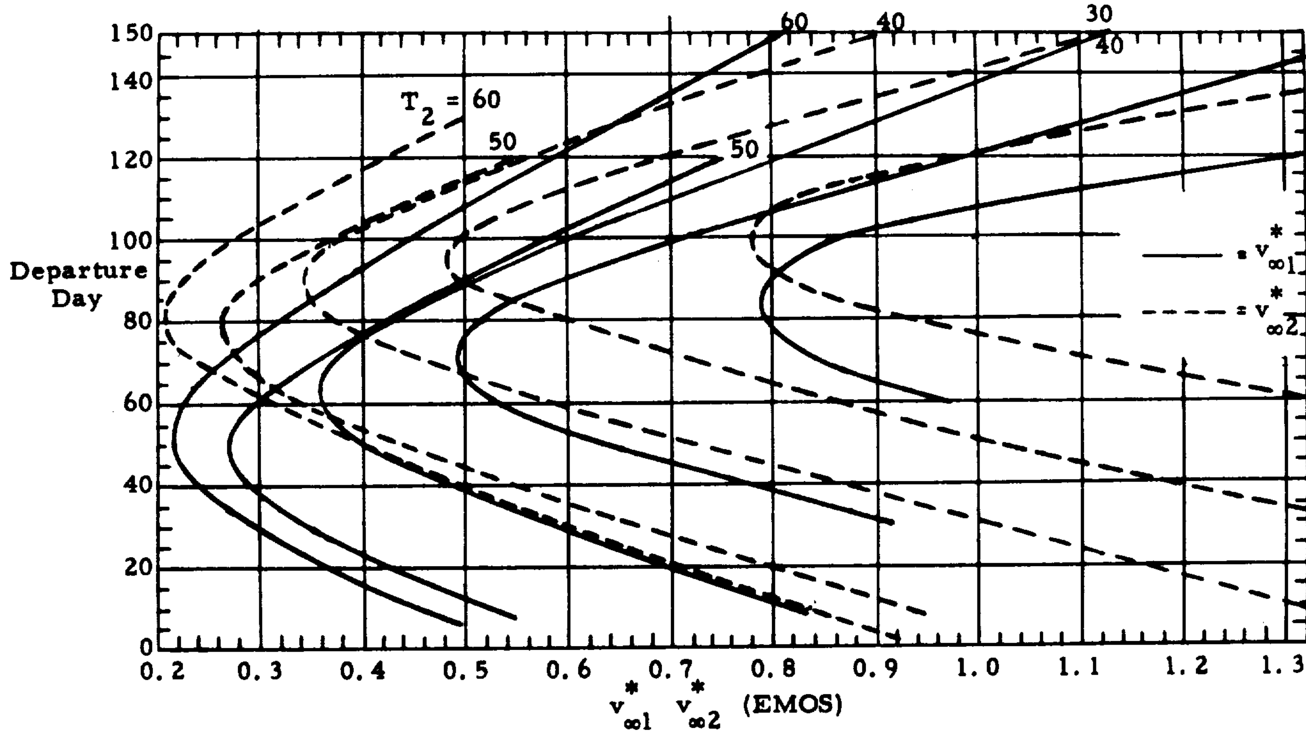

Fig. 2-15 VERY FAST EARTH-VENUS TRANSFERS, 1975, 1983, 1991
Day 0 = 2445472.5 = 5/18/83; Day 150 = 2445622.5 = 10/15/63

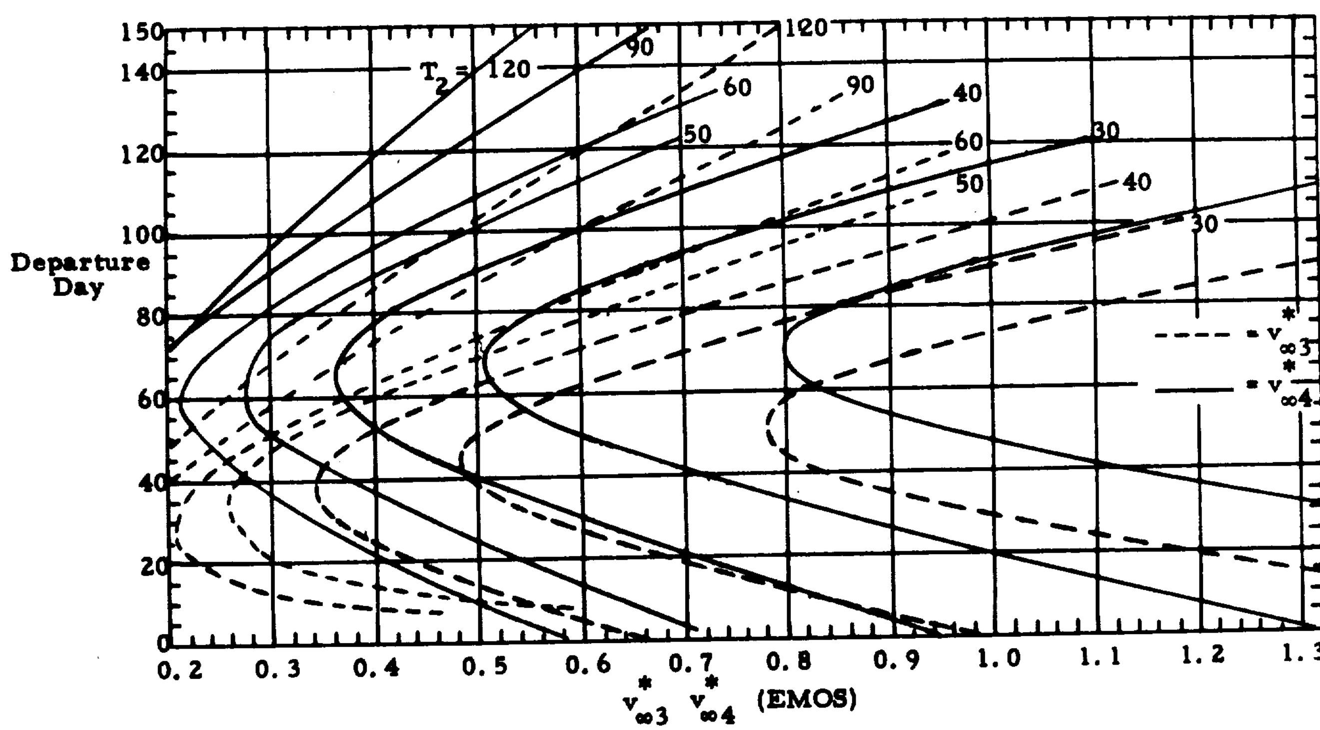

Fig. 2-16 VERY FAST VENUS-EARTH TRANSFERS, 1975, 1983, 1991
Day 0 = 2445502.5 = 6/17/83; Day 150 = 2445652.5 = 11/14/83

Tab. 2-4 **VENUS CAPTURE REFERENCE MISSIONS (n = 1)**

EaDD Y M D	Julian	T_1 T_{cpt} T_2 = ΣT Days	Δv_1, $r^* = 1.1$ ft/sec	Δv_1 (EMOS)	Δv_2, $r^* = 1.1$ ft/sec	Δv_2 (EMOS)	Δv_3, $r^* = 1.1$ ft/sec	Δv_3 (EMOS)	v_E, y = 100 km ft/sec	v_E (EMOS)	VeDD Y M D	Julian	EaAD Y M D	Julian
1973 10 30	1985.5	120 20 260 400	12,512	.1281	12,947	.1325	14,735	.151	45,845	.469	1974 3 19	2525.5	1974 12 4	2385.5
1975 5 20	2552.5	140 20 260 420	12,565	.1286	12,170	.1246	15,230	.156	44,800	.459	1975 10 27	2712.5	1976 7 13	2972.5
1976 12 15	3127.5	140 20 260 420	12,289	.1258	12,858	.1316	14,850	.152	45,400	.464	1977 5 24	3287.5	1978 2 7	3547.5
1978 7 11	3700.5	140 20 250 410	12,240	.1253	14,885	.1524	15,076	.154	43,858	.449	1978 12 18	3860.5	1979 8 25	4110.5
1980 3 26	4324.5	120 20 270 410	12,300	.1259	13,709	.1403	13,780	.141	47,174	.483	1980 8 13	4464.5	1981 5 10	4734.5
1981 10 30	4907.5	120 30 250 400	12,527	.1282	12,683	.1298	17,973	.184	47,310	.484	1982 3 29	5057.5	1982 12 4	5307.5

EaDD = Earth Departure Date
T_1 = Earth-Venus Transfer Time
T_{cpt} = Venus Capture Period
T_2 = Venus-Earth Transfer Time

ΣT = Mission Period

Δv_1 = Earth Departure Impulse (ideal)
r^* = Distance in Planet Radii

Δv_2 = Venus Capture Impulse (ideal)
Δv_3 = Venus Departure Impulse (ideal)
v_E = Earth Entry Velocity (unretarded)
y = Altitude
VeDD = Venus Departure Date
EaAD = Earth Arrival Date

Tab. 2-5 VENUS CAPTURE REFERENCE MISSIONS (n = 8)

EaDD				T_1 T_{cpt} T_2	Δv_1 $r^* = 1.1; n = 8$		Δv_{P2} $r_P^* = 1.1; n = 8$		$2\Delta v_A$		Δv_{P3} $r_P^* = 1.1; n = 8$		v_E $y = 100$ km		VeDD				EaAD			
Y	M	D	Julian	Days	ft/sec	(EMOS)	ft/sec	(EMOS)	ft/sec	(EMOS)	ft/sec	(EMOS)	ft/sec	(EMOS)	Y	M	D	Julian	Y	M	D	Julian
1973	10	30	1985.5	120 20 260	12,512	.1281	5,483	.0561	8,480	.0868	7,179	.0735	45,845	.469	1974	3	19	2525	1974	12	4	2385.5
1975	5	20	2552.5	140 20 260	12,567	.1286	4,731	.0484	8,480	.0868	7,540	.077	45,666	.467	1975	10	27	2712	1976	7	13	2972.5
1976	12	15	3127.5	140 20 260	12,289	.1258	5,402	.0553	8,480	.0868	7,500	.0765	45,643	.467	1977	5	24	3287	1978	2	7	3547.5
1978	7	11	3700.5	140 20 250	12,240	.1253	7,325	.0750	8,480	.0868	7,501	.0768	43,858	.449	1978	12	18	3850	1979	8	25	4110.5
1980	3	26	4324.5	120 20 270	12,300	.1259	6,219	.0636	8,480	.0868	6,250	.064	47,174	.483	1980	8	13	4464	1981	5	10	4734.5
1981	10	30	4907.5	120 30 250	12,527	.1282	5,227	.0535	8,480	.0868	6,547	.0670	47,310	.484	1982	3	29	5057	1982	12	4	5307.5

Tab. 2-6 VARIATION OF EARTH DEPARTURE AND VENUS ARRIVAL IMPULSES FOR VERY FAST TRANSFERS THROUGHOUT ONE MISSION CYCLE

Transfer Time T_1 (Days)		30	40	50	60
Years					
1973	Δv_1 (ft/sec)(n = 1; r^* = 1.1)	34,900	24,600	19,300	16,400
1981	EaDD (1973)	2040.5	2040.5	2030.5	2020.5
1989	Δv_2 (ft/sec) (n = 1; r^* = 1.5)	32,800	22,100	16,600	13,600
	(n = 8; r_p^* = 1.5)	26,500	15,700	10,100	7,200
	EaDD (1973)	2070.5	2060.5	2060.5	2050.5
	Δv_1 (ft/sec) (n = 1; r^* = 1.1)	37,200	25,900	20,300	17,300
1975	EaDD (1975)	2630.5	2620.5	2610.5	2600.5
1983	Δv_2 (ft/sec) (n = 1; r^* = 1.5)	35,600	24,400	18,000	14,900
1991	(n = 8; r_p^* = 1.5)	29,300	18,000	11,500	8,400
	EaDD (1975)	2650.5	2640.5	2640.5	2630.5
	Δv_1 (ft/sec) (n = 1; r^* = 1.1)	37,200	25,900	20,000	16,700
1977	EaDD (1977)	3215.5	3205.5	3200.5	3190.5
1985	Δv_2 (ft/sec) (n = 1; r^* = 1.5)	35,600	23,600	17,700	14,900
1993	(n = 8; r_p^* = 1.5)	29,300	17,100	11,200	8,400
	EaDD (1977)	3240.5	3230.5	3225.5	3220.5
	Δv_1 (ft/sec) (n = 1; r^* = 1.1)	34,400	24,200	19,000	16,200
1979	EaDD (1979)	3790.5	3790.5	3780.5	3770.5
1987	Δv_2 (ft/sec) (n = 1; r^* = 1.5)	32,800	22,400	16,800	14,100
1995	(n = 8; r_p^* = 1.5)	26,500	16,000	10,300	7,600
	EaDD (1979)	3820.5	3810.5	3810.5	3800.5

Venus arrival velocity are 20 to 30 days later than those for minimum Earth departure velocity. The Earth departure impulses for transfer times around 40 days are seen to be comparable to those for 80-day transfers to Mercury. The corresponding Venus circular capture impulses are lower than those for the 80-day Mercury transfers. For Earth departure at a compromise date between lowest Earth departure and lowest Venus arrival impulse, such as at JD 3225 for a 30-day transfer in 1977, and for a short capture period of 10 - 20 days, the HISV can still depart inside the minimum velocity corridor for long return transfer periods (220 - 270 days) to Earth; the minimum velocity corridor representing that time span during which the impulses on both ends of the transfer path are particularly low. However, as Figs. 2-14 and 2-16 show, the minimum velocity corridor for faster return transfers is already passed at the time the HISV arrives along a fast outbound transfer. For a return transfer of 80 to 50 days duration, the impulses increase rapidly with time. If the departure impulse from a Venus circular capture orbit (CCO) is to be comparable to that from a Mercury CCO (90 - 180 day transfer orbit), then return transfer times of 90 days and higher must be accepted. An example of two missions involving very fast Earth-Venus transfer is presented in Tab. 2-7. One is referred to as exploration mission, the other as shuttle mission. The distinction between the two lies in the capture period and in the Earth return conditions. A shuttle mission should require a much shorter capture period (eventually perhaps as brief as 1 - 2 days). The earlier departure permits a smaller departure impulse, or injection into a faster return transfer orbit. An added advantage is the lower Earth approach velocity. These two advantages are overcompensated by the high Earth departure impulse. In the exploration mission, this departure impulse is exchanged for a longer capture period resulting in higher impulses at Venus departure and Earth arrival, if the mission is to terminate in a circular Earth capture orbit. While this may be desirable in the case of shuttle operations where reusability is an economy factor, it may not be required in the case of an exploration mission.

Additional charts pertaining to Venus missions of 350 to 450 days mission period, conversion charts from hyperbolic excess velocity to impulse maneuvers and hyperbolic entry velocity and a chart for reading apogee maneuver impulses are included in the Appendix. The mission charts show the impulse maneuvers. Capture at Venus is shown at $r^* = 1.1$ for circular or for circular and elliptic ($n = 8$; $r_p = 1.1$) capture orbits.

2.2.3 Geocentric Missions

2.2.3.1 Earth-Moon Missions

Fig. 2-17 shows the correlation between cislunar transfer time and Earth departure velocity for an initial parking orbit altitude of

Tab. 2-7 EXAMPLES OF EXPLORATION AND SHUTTLE ROUND-TRIP MISSION TO VENUS INVOLVING VERY FAST EARTH TO VENUS TRANSFERS

	Exploration Mission	Shuttle Mission
Ea-Ve Transfer Time, T_1 (d)	60	40
EaDD (1977)	3205	3220
$v^*_{\infty 1}$ (EMOS)	0. 26	0. 41
Δv_1 ($n = 1$; $r^* = 1.1$)(ft/sec)	19, 500	29, 200
$v^*_{\infty 2}$ (EMOS)	0. 26	0. 385
Δv_2 ($n = 8$; $r^*_P = 1.5$)(ft/sec)	11, 500	20, 700
VeAD (1977)	3265	3260
VeDD (1977)	3295	3265
Ve-Ea Transfer Time, T_2 (d)	150	120
$v^*_{\infty 3}$	0. 555	0. 5
Δv_3 ($n = 8$; $v^*_P = 1.5$)(ft/sec)	34, 800 + 2 x 3600 ($2\Delta v_A$)	30, 200 + 2 x 3600
$v^*_{\infty 4}$	0. 39	0. 3
Δv_4 ($n = 1$; $r^* = 1.1$)(ft/sec)	28, 000	21, 600
Δv_4 (v_E = 40, 000 ft/sec)	13, 600	N/A
Mission Velocity (ft/sec)	101, 000/86, 600 (v_E = 40 k)	108, 900
Mission Period (days)	240	165

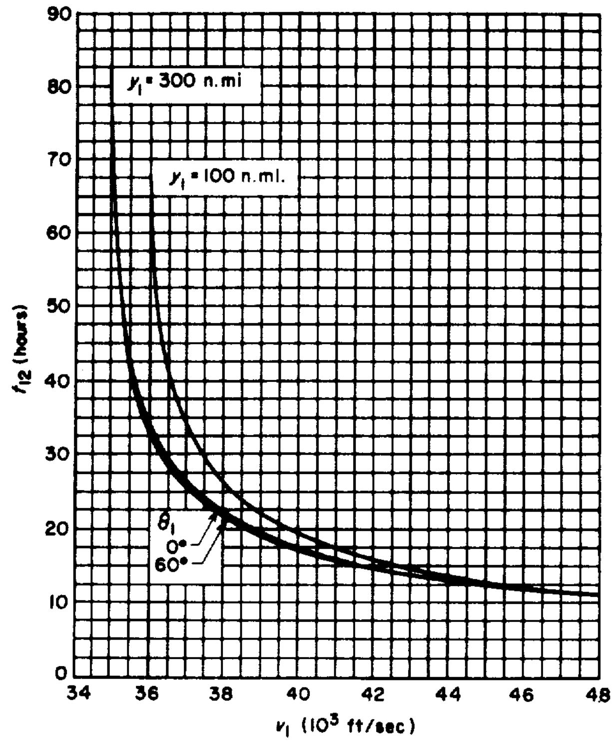

Fig. 2-17 VARIATION OF TRANSFER TIME AS FUNCTION OF DEPARTURE VELOCITY AND DEPARTURE ANGLE FOR TWO DEPARTURE ALTITUDES (CO-PLANER TRANSFER, CIRCULAR LUNAR ORBIT)

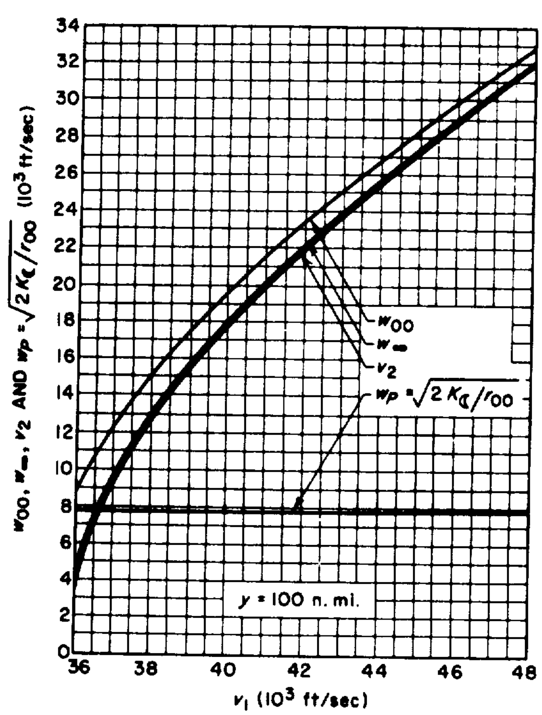

Fig. 2-18 VELOCITY ω_{00} AT 100,000 FT LUNAR ALTITUDE, SELENOCENTRIC HYPERBOLIC EXCESS, ω_∞, AND GEOCENTRIC ARRIVAL VELOCITY, v_2, AS FUNCTION OF GEOCENTRIC DEPARTURE VELOCITY

of 100 and 300 n. miles. In the latter parking orbit, the difference between tangential departure ($\theta_1 = 0$) and departure at a path angle of 60^o with respect to the direction of circular flight is seen to be negligible as far as the transfer time is concerned. The circular and parabolic velocities at 100, 150, 200 and 300 n. mi. are

y	=	100 n. mi.	v_c = 25, 583 ft/sec = 7.79 km/sec v_p = 36, 180 ft/sec = 11.0 km/sec
y	=	150 n. mi.	v_c = 25, 404 ft/sec = 7.77 km/sec v_p = 35, 927 ft/sec = 10.95 km/sec
y	=	200 n. mi.	v_c = 25, 229 ft/sec = 7.7 km/sec v_p = 35, 679 ft/sec = 10.9 km/sec
y	=	300 n. mi.	v_c = 24, 890 ft/sec = 7.6 km/sec v_p = 35, 199 ft/sec = 10.7 km/sec

Using the circular velocity at 100 or 300 n. mi. and reading the departure velocity v_1 from Fig. 2-17, the departure impulse for a given departure angle θ_1 and plane change α_1 follows from

$$\Delta v_1 = \sqrt{v_1^2 + v_c^2 - 2 v_1 v_c \cos \theta_1 \cos \alpha_1}$$

Fig. 2-18 shows the velocity w_{oo} at 100, 000 ft lunar altitude, the selecocentric hyperbolic excess velocity w_{oo} and geocentric arrival velocity v_2 at lunar distance, as function of the geocentric departure velocity. The hyperbolic velocity at lunar periapsis is

$$W_{P,h} - \sqrt{\frac{K_☾}{\rho} + W_\infty^2}$$

where $K_☾ = 4890 \text{ km}^3/\text{sec}^2 = 1.7270 \cdot 10^{14} \text{ ft}^3/\text{sec}^2$ and ρ is the distance from the lunar center. The lunar radius is 1738 km or 939 n. miles. The capture impulse is, therefore, for circular orbit capture,

$$\Delta W = W_{P,h} - \sqrt{\frac{K_☾}{\rho}}$$

Like the interplanetary missions, lunar missions can be divided into a number of mission phases which are separated by maneuvers.

These phases are listed in Tab. 2-8. Phases 1 and 8 are the outbound and return transfers across cislunar space, during which transfer correction maneuvers are carried out. Phases 2, 3 and 4 are alternates. If the powered maneuver at the perilune becomes negligible or zero, this phase becomes simply a fly-by phase. The third phase assumes a cislunar transfer orbit which is on collision course with the Moon. The vehicle carries out the lunar landing maneuver directly out of the hyperbolic approach orbit. The fourth, or lunar orbit phase can be of arbitrary duration, considering that it may be a terminal condition in its own right.

Between landing and orbiting lies an intermediate phase, referred to as hovering or free fall. This phase is initiated by what is referred to as disorbit maneuver, in distinction from the de-orbit maneuver which is the initial part of a descent and landing maneuver. The disorbit maneuver essentially reduces the orbital velocity to zero relative to the surface so that the vehicle remains over the particular area of the Moon. The vehicle can now be supported by a small amount of thrust which presents, or at least reduces in a controlled manner, the free fall to the surface. This requires a continuous-thrust non-nuclear (i.e. chemical) propulsion system, if personnel transfer to and from the surface takes place during this phase. If merely cargo is "dropped" (with their own small thrust system for braking the free fall velocity and land), also nuclear engines could be employed, if they are of the continuous-thrust variety. If a nuclear pulse system is involved, either a separate, small continuous-thrust drive must be provided; or disorbiting must occur at an altitude which permits a free fall of adequate duration with subsequent re-orbiting before the surface or a critically low altitude is reached (Fig. 2-19). This method of delivery is designed to bring to bear the advantage of very high I_{sp} ISV's equipped with destination space vehicles (DSV's) of lower I_{sp}. The energy requirement for eliminating the orbital velocity is absorbed in this case by the ISV, reducing greatly the propellant weight of the DSV needed if delivery occurred from orbiting condition. Compared to ISV landing, the hovering or free fall method has the advantage of avoiding potential conflicts with the characteristics of the propulsion system (e.g. surface contamination). Moreover, the need for carrying heavy landing gear and for subjecting the vehicle to the strains and uncertainties of touchdown are avoided. This increases particularly the reliability and reusability of shuttle vehicles, hence the safety and economy of the operation.

For ascent from the lunar surface, Fig. 2-20 correlates the orbital altitude achieved with the lunar thrust/weight ratio yielding the lowest mass ratio, with the specific impulse of the lunar ascent vehicle. For reasons of convenience, the reciprocal of the mass ratio ($1/\mu$) is shown on the abscissa. These curves are based on the assumption of vertical initial

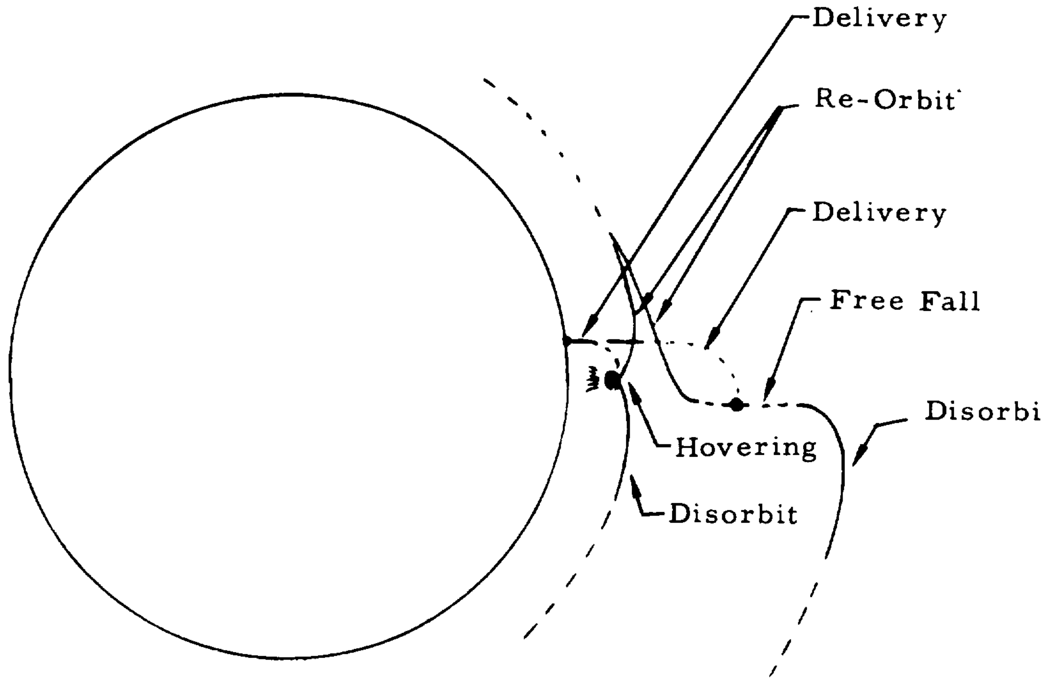

Fig. 2-19 HOVERING AND FREE FALL DELIVERY

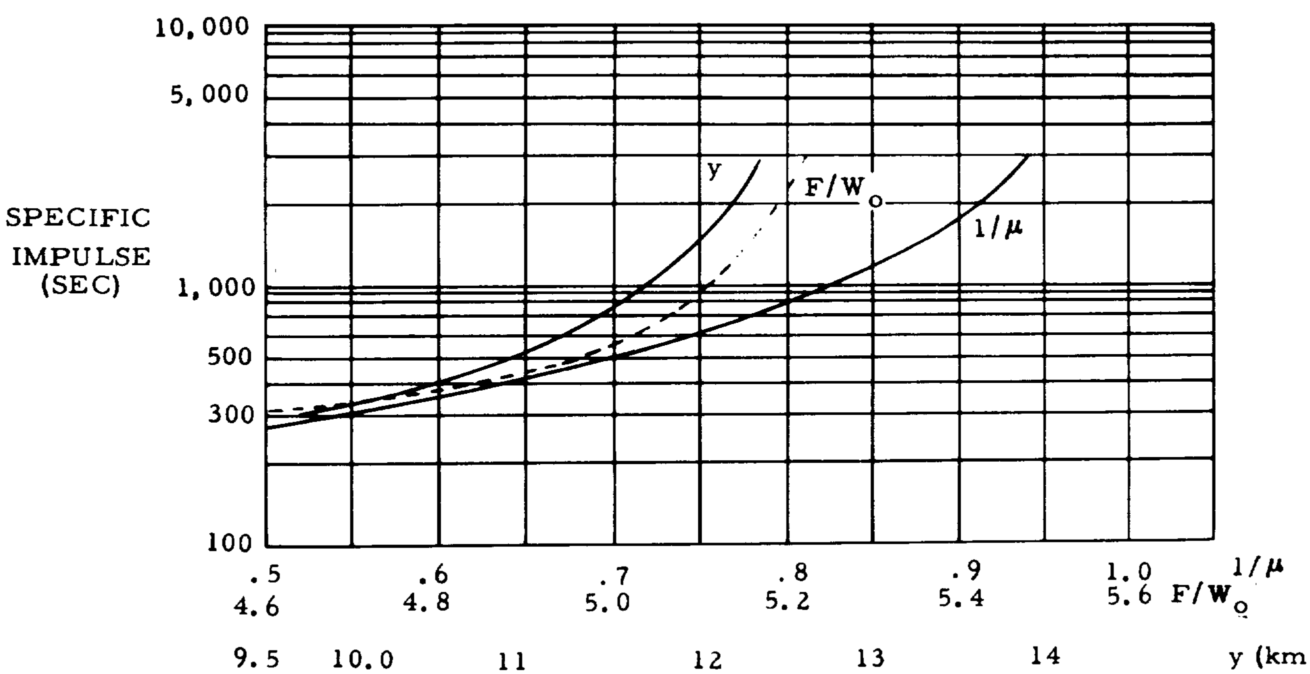

Fig. 2-20 VARIATION OF ORBITAL ALTITUDE OPTIMUM THRUST/ WEIGHT RATIO AND RECIPROCAL OF MASS RATIO WITH SPECIFIC IMPULSE FOR ASCENT FROM LUNAR SURFACE INTO LUNAR ORBIT

Tab. 2-8 LUNAR MISSION PHASES

Phase No.	Description	Maneuver	
		At Beginning of Phase	At Termination of Phase
1	Cislunar transfer to Moon	Earth injection maneuver	Near-lunar maneuver depending on mission
2	Lunar powered fly-by. Vehicle enters lunar activity sphere, follows an essentially selenocentric hyperbolic orbit around the Moon. As the perilune of this hyperbola a powered maneuver is carried out, designed to re-inject the vehicle into a cislunar transfer orbit which leads close to Earth	--	--
3	Lunar surface phase without preceding lunar orbiting phase	Direct lunar landing maneuver	Re-ascent into a lunar orbit
4	Lunar orbit phase of arbitrary duration	Lunar capture maneuver	Either landing maneuver or re-injection into cislunar transfer orbit
5	Lunar hovering phase or lunar free fall phase	Disorbit maneuver followed by near-vertical free fall or by hovering	Re-orbiting maneuver
6	Lunar surface phase with preceding lunar orbiting phase	Lunar descent maneuver	Lunar ascent maneuver
7	Lunar orbit phase lasting from a fraction of one revolution to several revolutions	Lunar ascent maneuver	Moon injection maneuver into cislunar transfer orbit to Earth
8	Cislunar transfer to Earth	Moon injection maneuver	Earth terminal maneuver

thrust direction and horizontal terminal thrust direction as well as flight direction; and on the assumption of continuous thrust. However, the results should closely represent also pulse thrust at sufficiently rapid sequence of detonations.

Tab. 2-9 summarizes the impulse maneuvers involved in lunar missions as function of cislunar transfer time. From this table "symmetrical" (outbound transfer time equal to return transfer time) mission profiles as well as unsymmetrical mission profiles can be constructed. For example, a lunar capture mission with a 60-hour outbound transfer time from a 150 n. mi. Earth orbit, a circular orbit at 152.5 km and a 24-hour return transfer into a 150 n. mi. Earth orbit has the mission impulse velocity: 10,466 + 3400 + 9900 + 12,521 = 36,267 ft/sec. In an analogous manner, the mission impulse velocity for departure from a 100 n. mi. Earth orbit and return into a 300 n. mi. Earth orbit can be computed, if first the Earth injection maneuver from 100 and 300 n. mi. high orbits is determined from their respective circular velocities and the Earth injection velocity shown in Tab. 2-9. The above example shows that medium-fast lunar round-trip missions with lunar capture and return into an Earth orbit are comparable to Venus round-trip missions with elliptic capture ($n = 8$) and unretarded hyperbolic entry (UHE) speed (cf. Fig. 2-12). If, in addition lunar disorbit and re-orbit, or lunar descent and ascent are involved, the lunar mission impulse velocity requirements become comparable to, or exceed, those required for a Venus round-trip mission with circular capture and restricted hyperbolic entry of 40k. The orbital departure, however, can still be smaller for the lunar mission, even at equal destination payload, because less operational payload and fewer losses are involved in view of the brief mission period.

2.2.3.2 Orbit Launch Missions

The other group of geocentric missions refers to parabolic and hyperbolic injection of payloads with reusable orbit launch vehicles. Typical mission profiles are shown in Fig. 2-21. In this mission model a fixed initial Earth orbit is postulated in which the OLV are "stationed". From this orbit the reusable OLV injects payload into a parabolic or hyperbolic orbit and then breaks away via a return maneuver into a return path which leads more or less tangentially back into the initial Earth orbit which is entered in a final re-arrival maneuver.

Parabolic velocities for impulse injection maneuvers and cislunar injection maneuvers are presented in Par. 2.2.3.1. Hyperbolic injection velocities for planetary missions are listed in the Sections for the respective target planets.

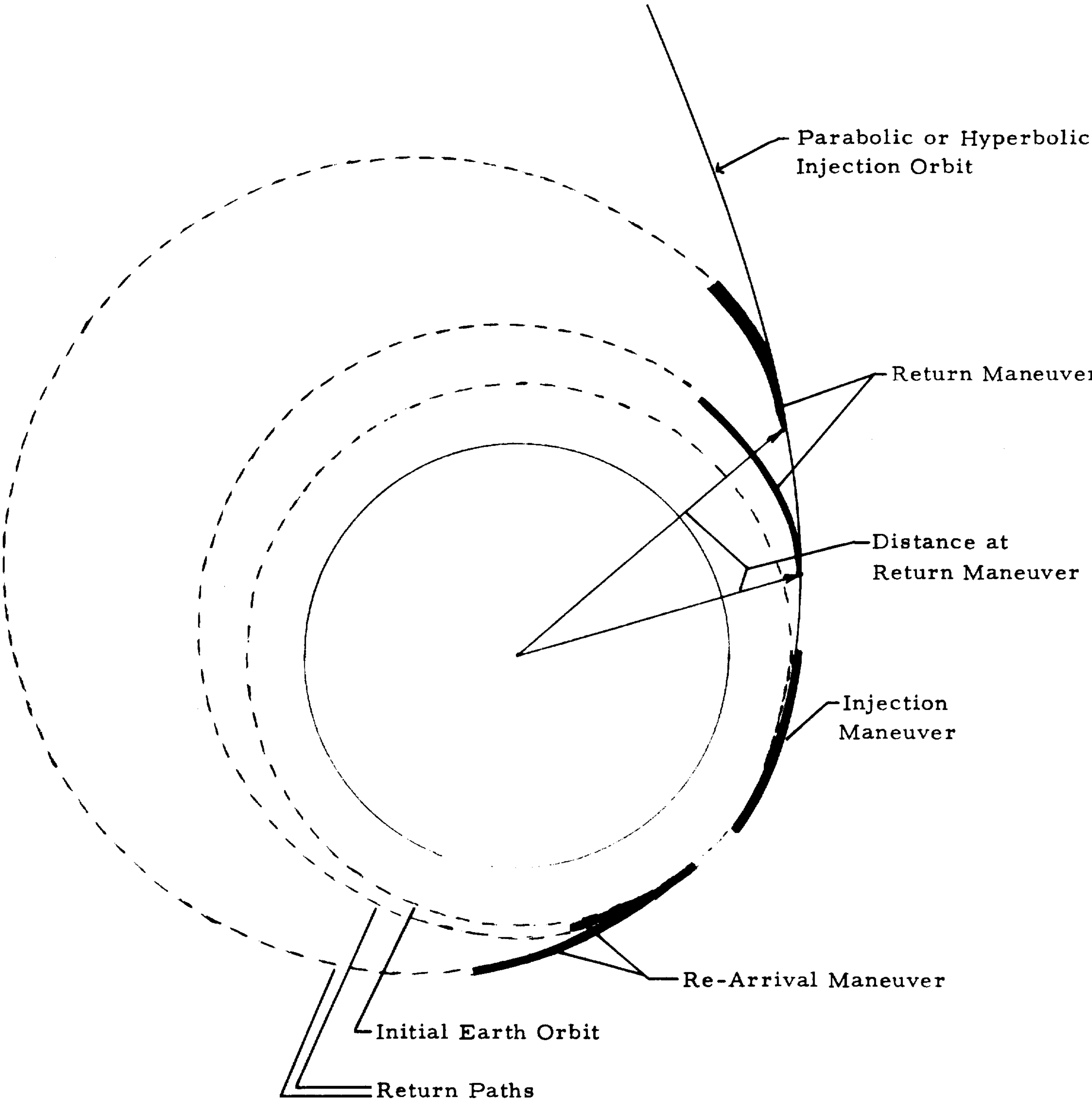

Fig. 2-21 MISSION PROFILES OF REUSABLE ORBIT LAUNCH VEHICLES FOR PARABOLIC AND HYPERBOLIC INJECTION OF PAYLOADS

Tab. 2-9 SURVEY OF IMPULSE MANEUVERS FOR LUNAR MISSIONS

Cislunar Transfer Time (hours)	72	60	48	36	24	12
Earth injection velocity (ft/sec)						
from 100 n. mi. orbit	35,950	36,020	36,250	36,700	38,300	45,300
from 150 n. mi. orbit	35,790	35,850	36,025	36,525	37,925	45,200
from 300 n. mi. orbit	35,040	35,125	35,325	35,825	37,200	45,000
Earth injection maneuver (ft/sec) from 150 n. mi. orbit	10,386	10,446	10,621	11,121	12,521	19,796
Lunar orbit capture maneuver (y = 500,000 ft = 152.5 km) (ft/sec) from 150 n. mi. Earth orbit	3,100	3,400	4,000	5,700	9,850	23,500
De-orbit and landing maneuver (ft/sec) (Hohmann transfer from 152.5 to 10-14 km altitude; then continuous thrust descent)			7,000			
Ascent into lunar orbit (ft/sec) (10-14 km altitude)			6,000			
Moon injection maneuver (from 10-14 km orbit) (ft/sec)	3,300	3,550	3,900	5,700	9,900	23,500
Fly-by round-trip mission duration (hrs)	138-140	N/A	N/A	N/A	N/A	N/A

The return maneuver is shown in Fig. 2-21 to occur relatively close to Earth. In the extreme case, the OLV, following injection, immediately separates from its payload and initiates a retro-maneuver. In that case, the magnitude of the return maneuver is approximately equal to the injection maneuver. In cases where immediate payload separation is not practical, or where low thrust extends the injection process over one or more Earth radii, the return maneuver must necessarily occur at greater distance. Finally, for reasons of minimizing exposure of the OLV crew to radiation belt irradiation, it may be desirable to traverse quickly the belt zones at parabolic or hyperbolic speed and to initiate the return maneuver in cislunar space outside the belt (i.e. at 10 radii or beyond).

A brief analysis of the impulsive return maneuver follows which is based on the following ground rules:

(1) Analysis is based on a central force field.

(2) Orbits are coplanar unless stated otherwise.

(3) The return maneuver is designed to establish a return orbit which leads tangentially back into the initial Earth orbit, as shown in Fig. 2-21, without additional intermediate maneuvers.

(4) No time constraints, for purposes of rendezvousing with a fixed point (orbit launch facility) in the initial Earth orbit, are imposed in computing the return maneuver.

It is convenient to use in the analysis the concept of the relative orbital energy constant

$$\epsilon = \frac{v^2}{K/r} - 2 \quad \text{(for any conic)}$$

The geocentric distance is r (in Earth radii), apogee and perigee are designated by the subscripts A and P and the Earth's gravitational parameter is K. Elliptic, parabolic and hyperbolic orbits are indicated by the subscripts ell, p and h. Then, for the parabola, $\epsilon_p = 0$; for the hyperbola, for given values of v_∞ and r_P,

$$\epsilon_h = v_\infty^2 / (K/r_P)$$

and for the elliptic return orbit, defined by r_P (the same as for the hyperbola) and r_A,

$$\epsilon_{ell} = -2/(n+1)$$

$$n = r_A / r_P$$

Let the distance at which the (impulsive) return maneuver be r. Then the path velocities are

$$v_h = \left(K(2 + \epsilon_h)/r\right)^{1/2}$$

$$v_p = \left(2\ K/r\right)^{1/2}$$

$$v_{ell} = \left(K\ (2 + \epsilon_{ell})/r\right)^{1/2}$$

The instantaneous flight path angle (angle between velocity vector and local horizon) is, for either orbit,

$$\tan\theta = \frac{(1+\epsilon)\sin\eta}{1 + (1+\epsilon)\cos\eta}$$

where the true annomaly η is, for the hyperbolic orbit

$$\cos\eta_h = \frac{(r_P/r)\ (2 + \epsilon_h) - 1}{1 + \epsilon_h}$$

$$\cos\eta_p = \frac{2\ r_P}{r} - 1$$

For the elliptic orbit a more convenient expression for the flight path angle, in view of the known values of r_A and r_P, is

$$\cos\theta_{ell} = \sqrt{\frac{r_P}{r}}\ \sqrt{\frac{r_A}{2a - r}}$$

where the semi-major axis is

$$a = (r_A + r_P)/2$$

With these equations the flight path angle at r can be established and the return impulse velocity vector determined from

$$\Delta v(r) = \sqrt{v_h^2 + v_{ell}^2 - 2\, v_h v_{ell} \cos(\theta_h - \theta_{ell})}$$

for return from a hyperbolic injection orbit; and, correspondingly, for return from a parabolic injection orbit.

The flight time from periapsis to the return maneuver point at r is, in the hyperbolic injection orbit

$$t_{Pr,h} = \sqrt{r_P^3/\epsilon_e^3 K} \left[(1 + \epsilon_h) \tan H - \ln \tan (45^\circ + H/2)\right]$$

$$\cos H = \left(1 + \epsilon_h\right)/\left(1 + \epsilon_h r/r_P\right),$$

for the parabolic injection orbit,

$$t_{Pr,p} = \frac{4}{3}\left(2\, r_P^3/K\right)^{1/2}\left(\frac{1}{2}\,\frac{r}{r_P}\right)^{1/2}\left(1 + \frac{1}{2}\,\frac{r}{r_P}\right)$$

and for an elliptic injection orbit

$$t_{Pr,ell} = \left(-\, r_P^3/\epsilon_{ell}^3 K\right)^{1/2}\left(E - (1 + \epsilon_{ell}) \sin E\right)$$

$$\cos E = \frac{1 + \epsilon_{ell} r/r_P}{1 + \epsilon_{ell}} \qquad (r > r_P)$$

Let an additional condition for the elliptic return orbit be that $r_A \geq r$; i.e. the path angle following the return maneuver is either positive ($r_A > r$) or zero ($r_A = r$), but not negative (in which case it would hold $r_A < r$ and the OLV would not pass through the apogee on its return flight). Then, the flight time in the return ellipse (from r to r_P) can be expressed by the relation

$$t_{rP,\,ell} = T_{ell} - t_{Pr,\,ell}$$

where t_{Pr} is given above and the period of the return ellipse follows from

$$T_{ell} = 2\pi\left(-r_P^3/\epsilon^3 K\right)^{1/2}$$

It might be added that for a plane change α at the return maneuver, the equation for the impulse velocity vector is modified in that the last term under the square root sign must be multiplied by cos α .

Instead of computing the impulse vector, the scalar velocity difference can be formed between hyperbolic or parabolic velocity on the one hand and elliptic velocity on the other. This corresponds to a tangential retro-maneuver. In terms of the circular velocity at r_P, this difference becomes

$$\frac{\Delta v}{\sqrt{K/r_P}} = \sqrt{\frac{r_P}{r}}\left[\sqrt{2+\epsilon_h} - \sqrt{2+\epsilon_{ell}}\right]$$

or

$$\frac{\Delta v}{\sqrt{K/r_P}} = \sqrt{\frac{r_P}{r}}\left[\sqrt{2} - \sqrt{2+\epsilon_{ell}}\right]$$

In that case, however, one would not know whether condition (3) above has been met, because ϵ_{ell} depends on n and not on r_A. In order to check the resulting return orbit in that respect, it is necessary to determine, by an independent set of equations, the perigee distance of the elliptic return orbit, entered by this tangential return impulse. The post-impulse elliptic velocity v_{ell}, distance r and flight path angle $\theta_{ell} = \theta_h$ or $\theta_{ell} = \theta_p$ are known. Therewith the Kepler constant of the return orbit can be determined

$$C = r\ v_{ell}\ \cos\theta_{ell}$$

from it the semi-latus rectum

$$p = C^2/K$$

and, thence, the perigee distance,

$$r_P = p(2 + \epsilon_{ell})$$

The resulting values of r_A and t_{rP} follow then from the previously given equations.

Fig. 2-22 shows, for a cislunar injection mission (transfer orbit eccentricity $e = 0.967$), the variation of a tangential return impulse (for a perigee alttitude $y_P \gtrsim 100$ km) with return time to Earth (flight time from the break-away point to return into the initial Earth orbit) for four values of Earth distance at initiation of the return maneuver. Fig. 2-23 shows the variation of the return impulse versus the eccentricity of the return orbit for the case of a parabolic injection for several distances at the return impulse maneuver. The dashed line applies to the case where the distance at the retromaneuver r_R^* is equal to the apoapsis distance r_A^* of the return flight path, resulting in the minimal eccentricity among all the return orbits with given periapsis distance. The flight path angles θ after the return impulse are positive for the curves to the left of the limiting line and negative for the curves to the right of that line. Fig. 2-24 correlates eccentricity and flight time in the return flight path, just as the preceding chart correlates eccentricity and return impulse maneuver. For a given distance at Earth return maneuver and given return time (Fig. 2-24); the return impulse for the parabolic orbit can be read from Fig. 2-23. Knowing the eccentricity and the perigee distance ($r_P = 1.07$), the relative orbital energy and the major axis follow from

$$\epsilon_{ell} = e - 1$$

$$a = - r_P/\epsilon_{ell}$$

the apogee from

$$r_A = - r_P (2 + \epsilon_{ell})/\epsilon_{ell}$$

and the perigee velocity from

$$v_{P,ell} = \left(K \ (2 + \epsilon_{ell})/r_P\right)^{1/2}$$

Fig. 2-22 RETURN IMPULSE MANEUVER vs. RETURN TIME INTO INITIAL EARTH ORBIT FOR VARIOUS DISTANCES AT THE RETURN MANEUVER

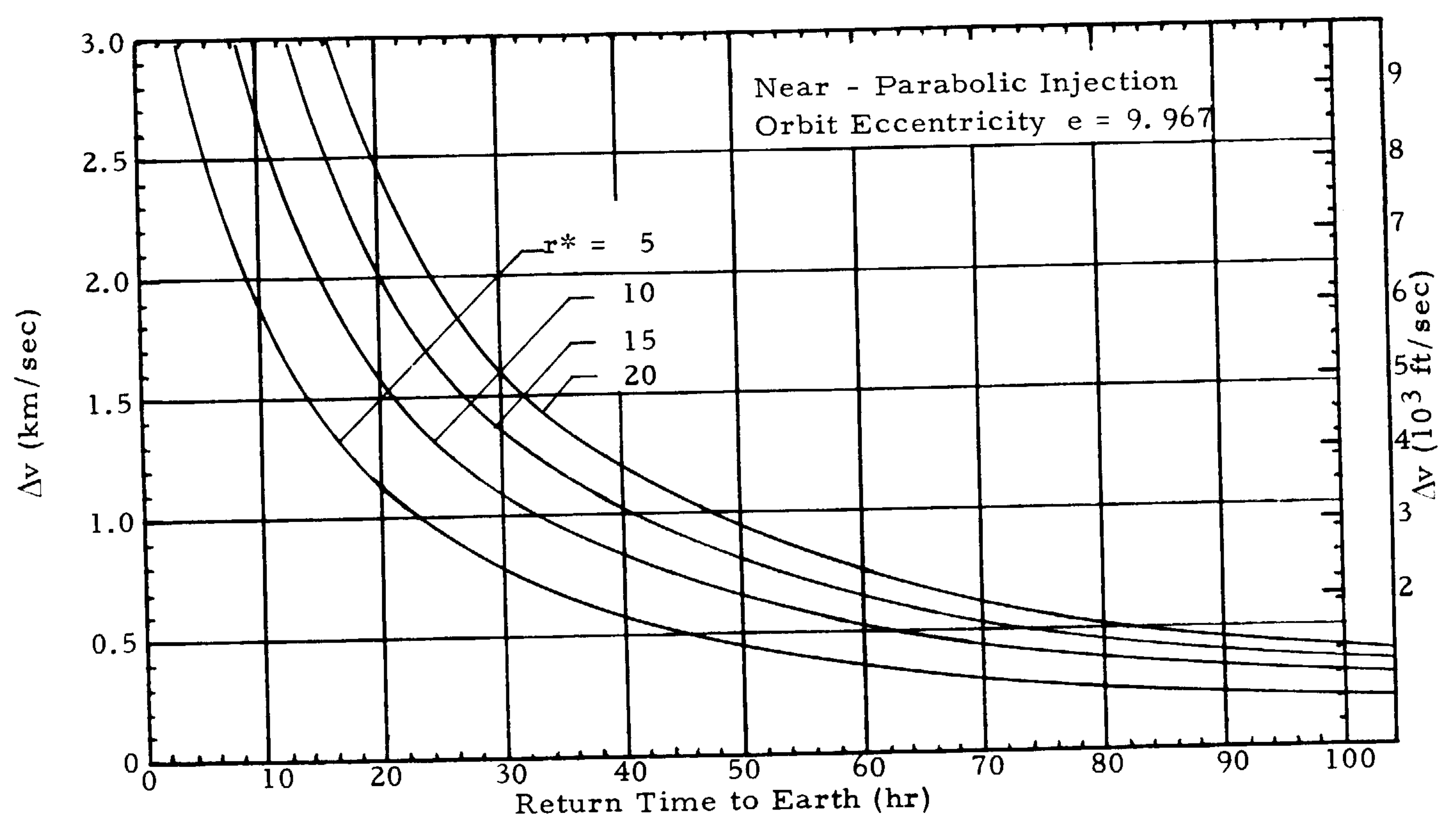

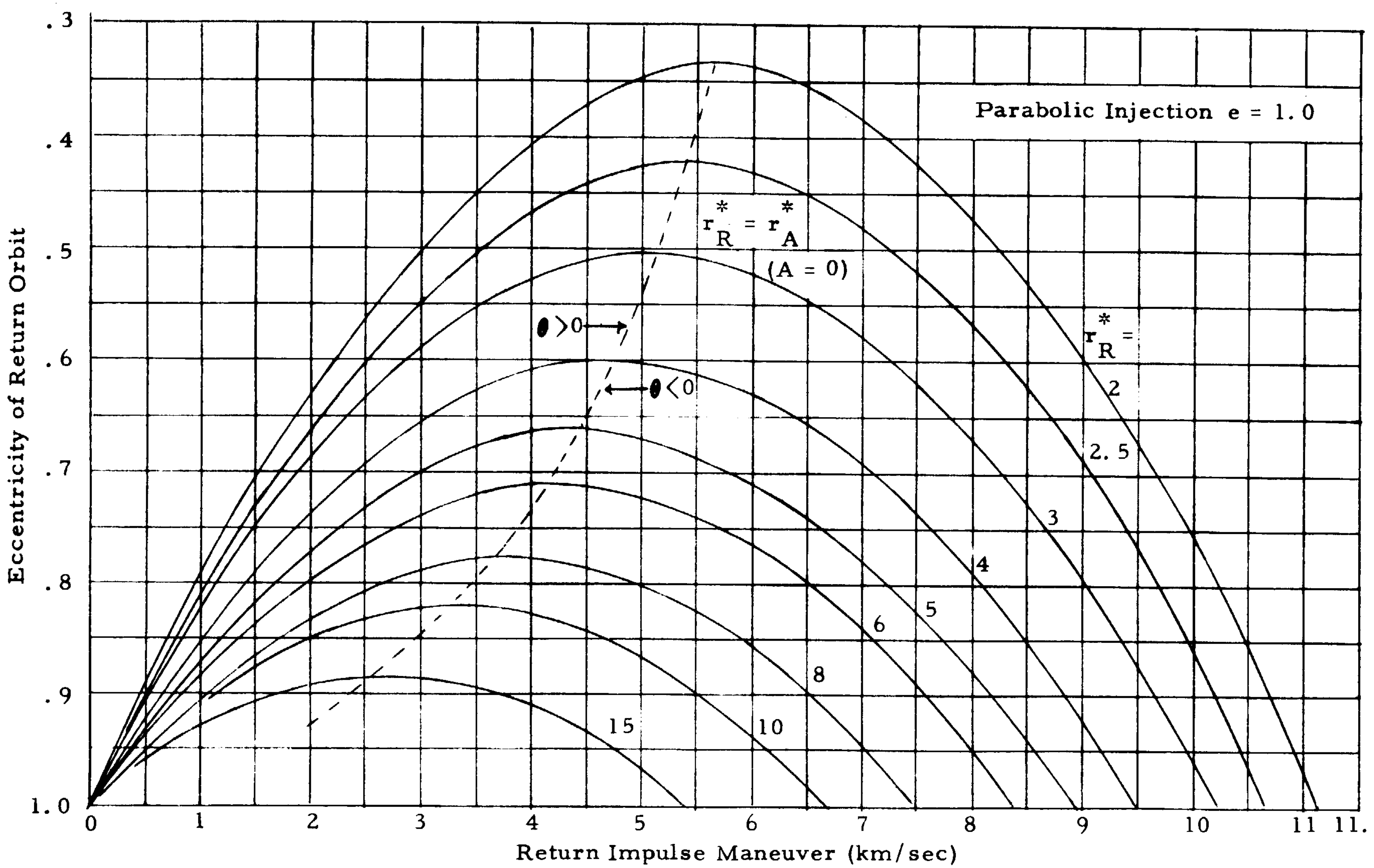

Fig. 2-23 RETURN IMPULSE vs. ECCENTRICITY OF RETURN ORBIT FOR VARIOUS DISTANCES AT EARTH RETURN MANEUVER

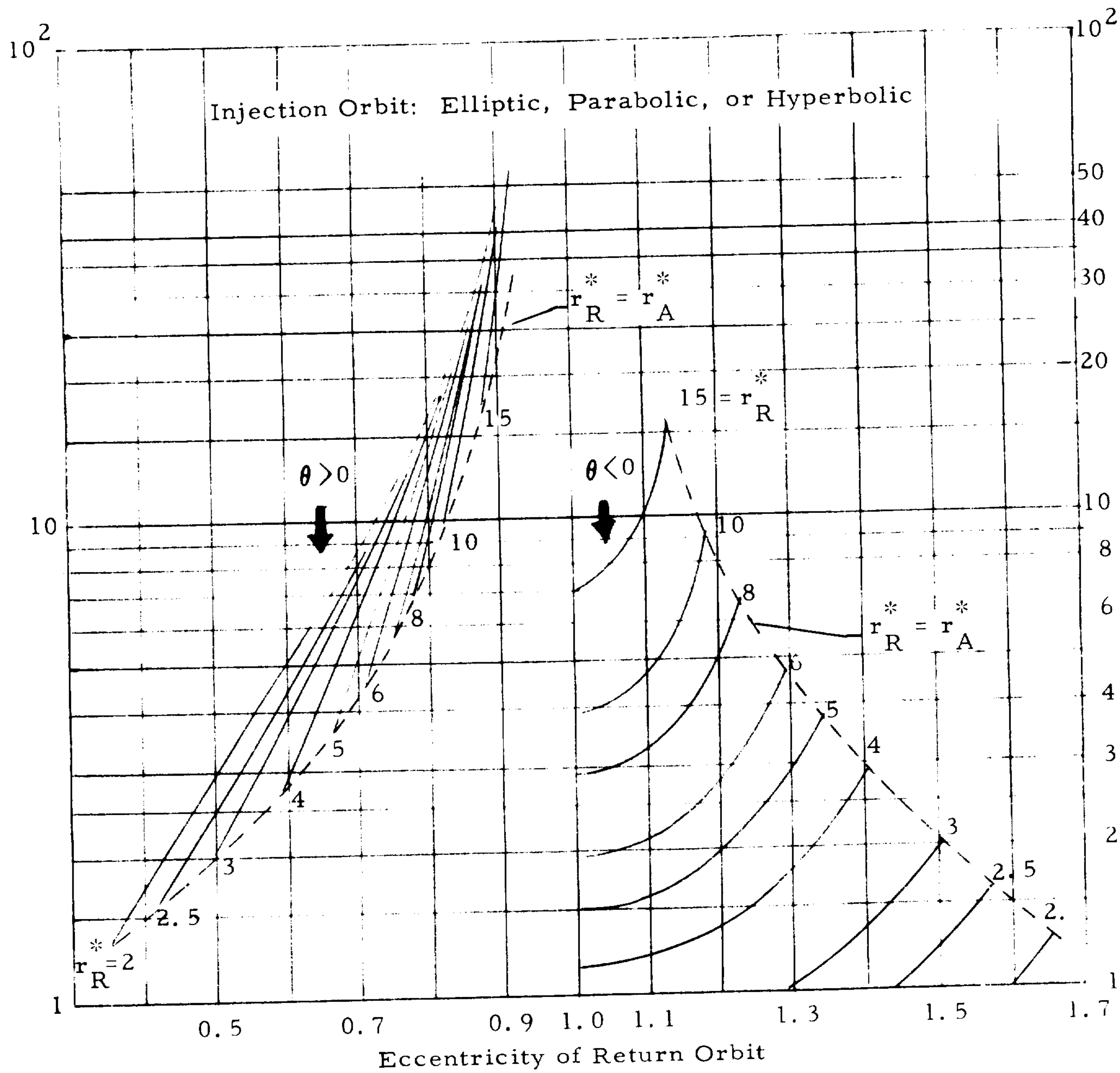

Fig. 2-24 ECCENTRICITY OF RETURN PATH AFTER vs.. RETURN TIME FOR SEVERAL DISTANCES AT RETURN MANEUVER

It should be noted that Fig. 2-24 is valid for any conic, while Fig. 2-23 applies to the parabolic orbit only. Charts similar to that of Fig. 2-23 must be constructed for the hyperbolic orbits of interest, using the before given equations. Considering the rapid increase in velocity requirement, it is apparent to be advantageous to trade higher economy for shorter return flight times and restrict oneself essentially to conditions of $r < r_A$.

Fig. 2-25 shows the variation of the return impulse maneuver as function of v_∞^* for the conditions defined. Since the distance Υ for the return maneuver has been set as $r = 15\ r_{oo}$ in this example, the required impulse increases faster with increasing hyperbolic excess velocity than if the return maneuver were given in the immediate vicinity of Earth.

2.2.4 Mars Missions

Fig. 2-26 and Tab. 2-10 show the variation of the principal maneuvers involved in a mono-elliptic Mars round-trip mission: Earth departure (1), Mars arrival (2), Mars departure (3) and the unretarded Earth entry velocity v_E (4). The data are for medium-fast missions of 420 to 450 day mission period. It is seen that the difference between "favorable" and "unfavorable" mission years (FMY and UMY) is due primarily to the variation in v_E. The numbers in Fig. 2-26 represent transfer time, capture period and return transfer time.

For Mars, the difference between FMY and UMY is more pronounced than for the other planets, unless, unretarded hyperbolic entry (UHE; $\Delta v_4 = 0$) is used, or perihelion braking or Venus powered fly-by (VePFB) is applied. Fig. 2-27 shows that the more limited the Earth entry velocity, the larger is the variation in overall mission velocity, if Earth approach retro-maneuvers are applied.

Faster mono-elliptic round-trip missions to Mars are listed in Tab. 2-11 and shown in Fig. 2-28 through 2-32. In Tab. 2-11, the first column shows the year, the headings for the hyperbolic excess velocity and the impulsive velocity changes for maneuvers 1 and 2, as well as the hyperbolic excess velocities for maneuver 3 and Earth approach, the maneuver 3 impulse and the unretarded hyperbolic entry (UHE) speed for capture periods (T_{cpt}) of 10 and 30 days. The second and third columns give the departure dates (calendar and Julian) and the associated velocities involved in maneuvers 1 and 2, for transfer periods (T_1) of 60 and 90 days. The subsequent four columns show the velocities pertaining to Mars departure and Earth arrival resulting from a combination of 60 day outbound and 90, 120 & 150 day return transfers for capture periods of 10 and 30 days. The last 3 columns show the return conditions associated with 90 day outbound and 90, 120, 150 day return transfers.

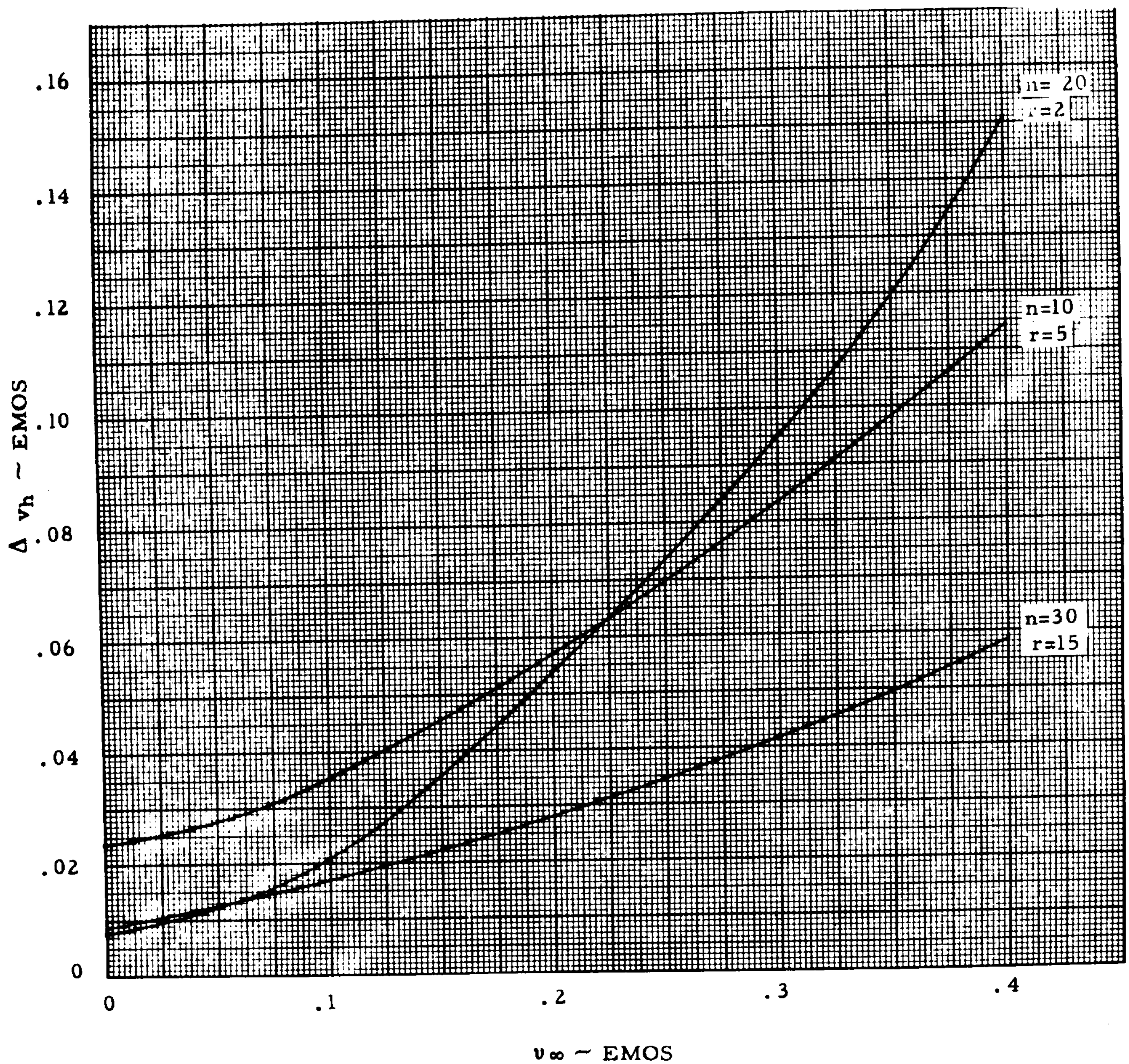

Fig. 2-25 VARIATION OF RETURN IMPULSE MANEUVER AS A FUNCTION OF v^*_∞

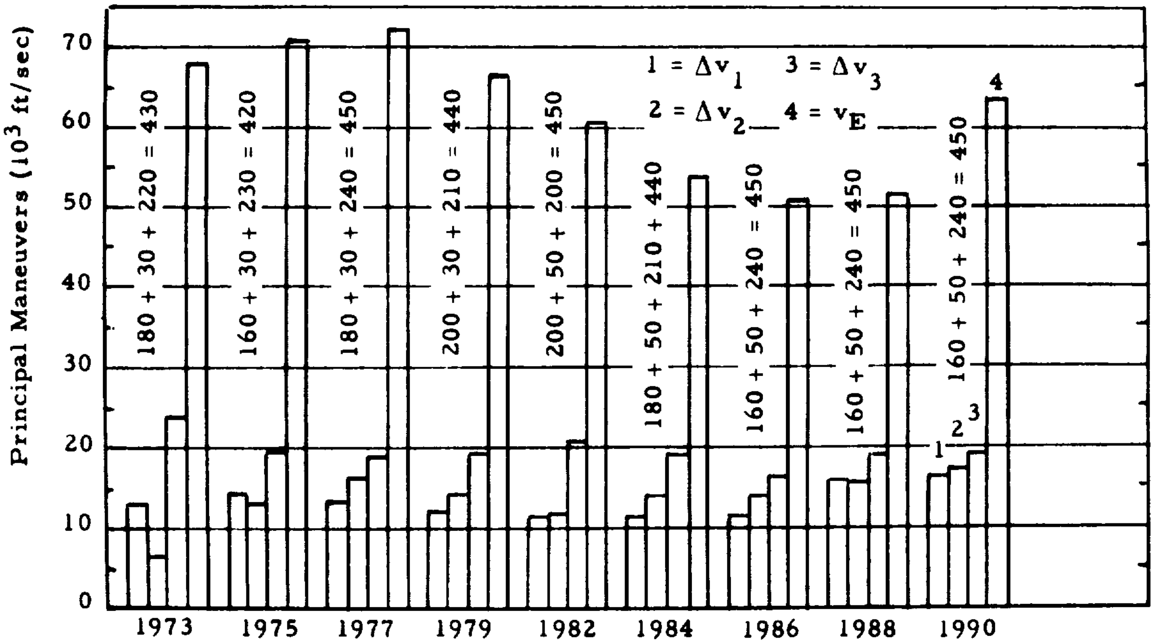

Fig. 2-26 MONO-ELLIPTIC MARS ROUND-TRIP MISSION VELOCITY PROFILE, 1973 THROUGH 1990

Ea Dep: $r^* = 1.1$; $n = 1$; Ma Capture: $r^* = 1.3$; $n = 1$
Numbers Give $T_1 + T_{cpt} + T_2 = T$ = Mission Period (Days)

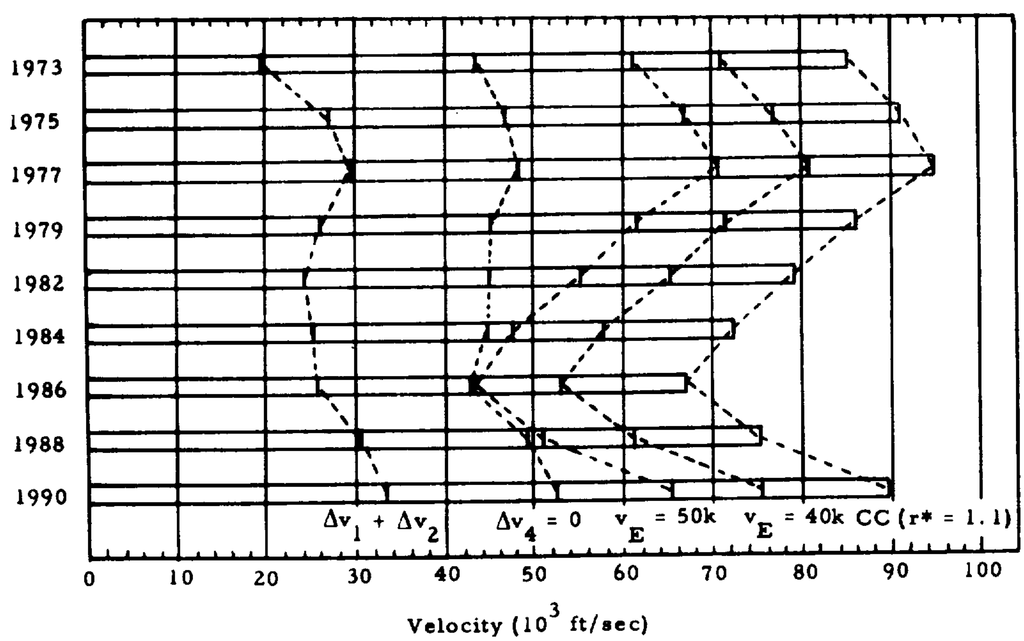

Fig. 2-27 MONO-ELLIPTIC MARS MISSION VELOCITY PROFILES FOR ONE-WAY AND ROUND-TRIP MISSIONS WITH VARIOUS EARTH RETURN CONDITIONS 1973 - 1990

v_E = Earth Entry Vel.; Δv_4 = Earth Return Retro-Maneuver
Δv_1 = Earth Departure Maneuver; Δv_2 = Mars Capture Maneuver
CC - Circular Capture

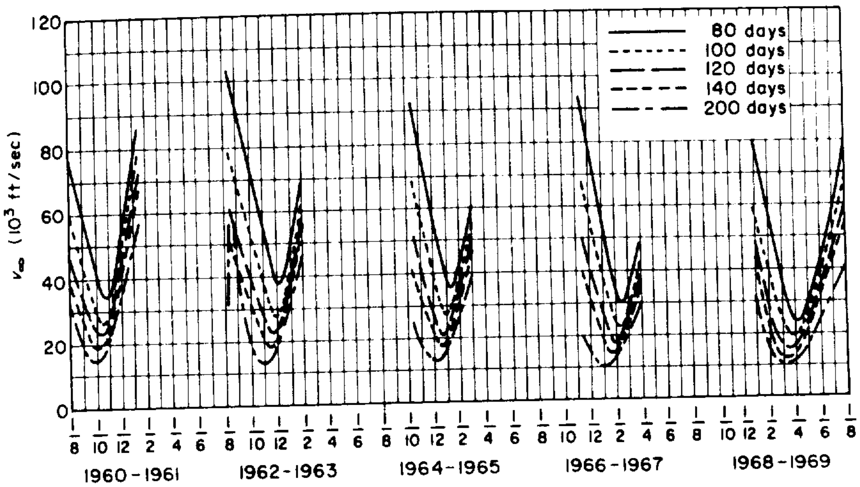

Fig. 2-28 THREE-DIMENSIONAL TRANSFER ORBIT TO MARS: HYPERBOLIC EXCESS VELOCITY VS. DEPARTURE DATE

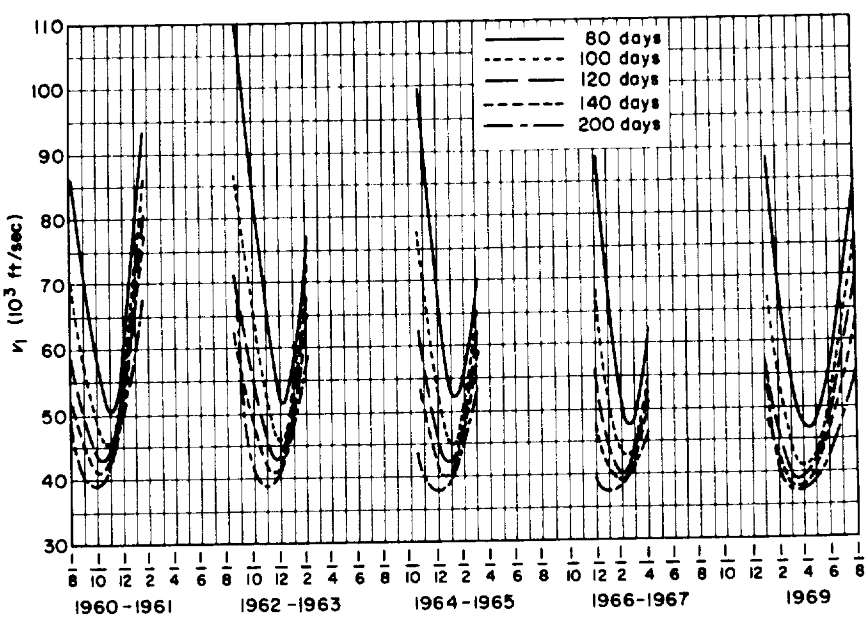

Fig. 2-29 THREE-DIMENSIONAL TRANSFER ORBIT TO MARS: GEOCENTRIC DEPARTURE VELOCITY FROM A 100 N.MI. SATELLITE ORBIT VS. DEPARTURE DATE

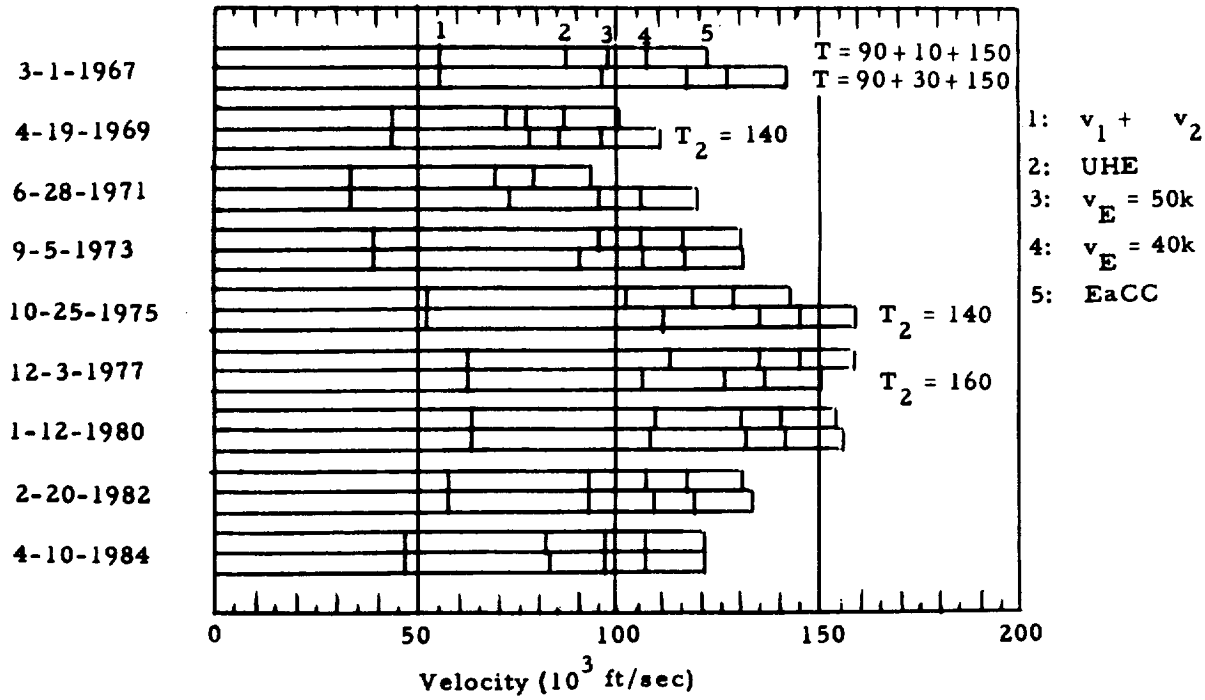

Fig. 2-30 MONO-ELLIPTIC MARS MISSION VELOCITY PROFILES FOR 1-WAY AND ROUND-TRIP MISSIONS WITH VARIOUS EARTH RETURN CONDITIONS, 1967 - 1984 (T = 250 and 270 d, unless noted otherwise)

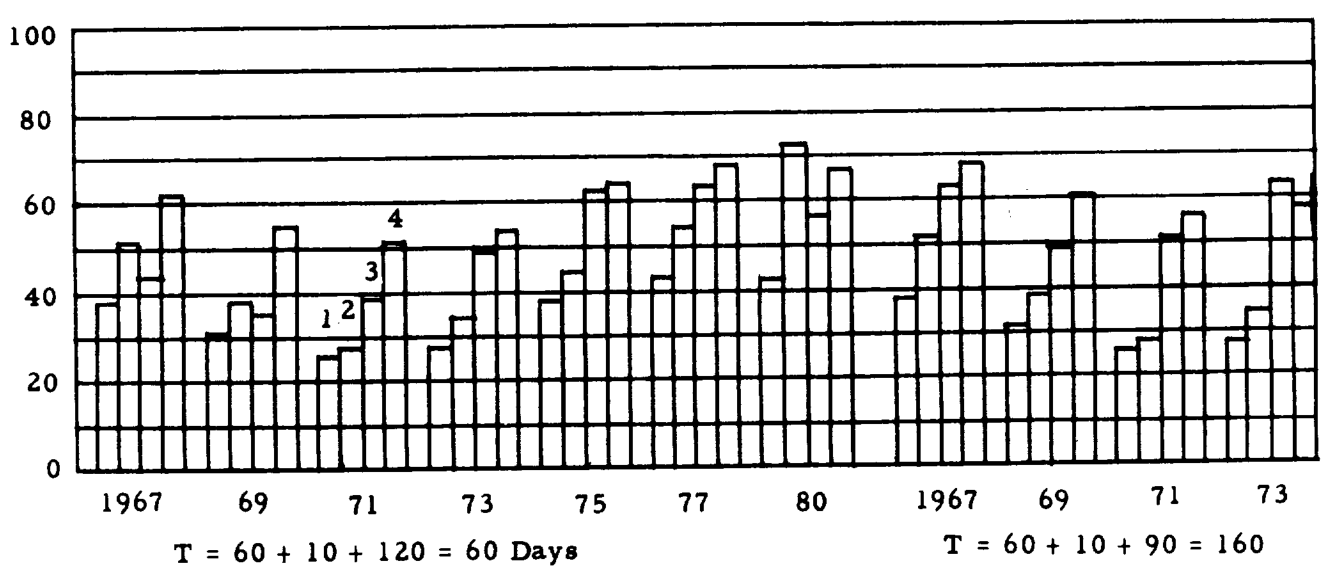

Fig. 2-31 MONO-ELLIPTIC MARS ROUND-TRIP VELOCITY PROFILE FOR FAST AND VERY FAST MISSIONS, 1967 THROUGH 1973

Ea Dep.: n = 1; r* = 1.1; Ma Capture: n = 1; r* = 1.3
1 = Δv_1; 2 = Δv_2; 3 = Δv_3; 4 = v_E; all in 10^3 ft/sec.

Fig. 2-32 MONO-ELLIPTIC MARS MISSION VELOCITY PROFILES FOR 1-WAY AND ROUND-TRIP MISSIONS WITH VARIOUS EARTH RETURN CONDITIONS, 1967 - 1979 (T = 190 Days)

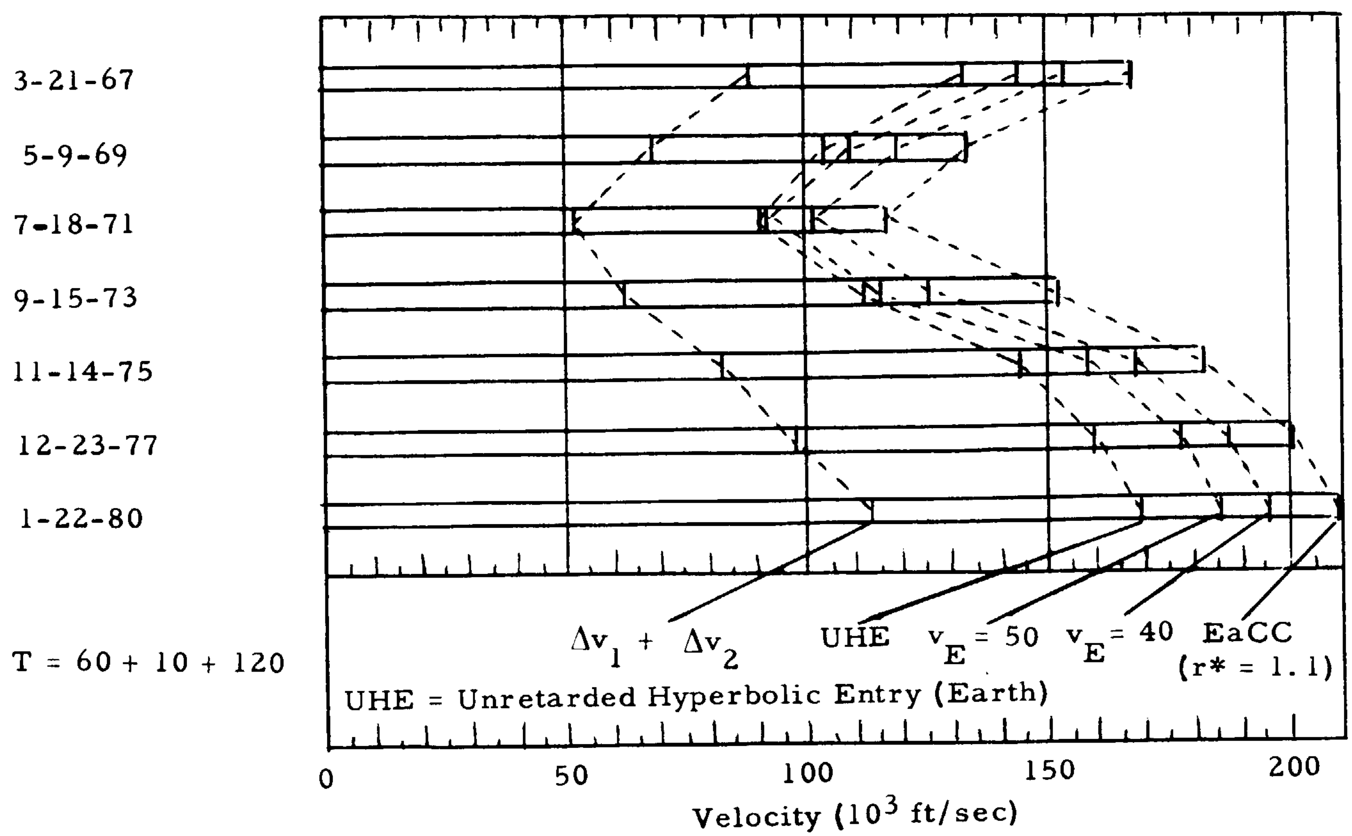

Tab. 2-10 MARS REFERENCE MISSIONS (n = 1)

IMPULSE MANEUVERS

EaDD Y	M	D	Julian	ΔV_1 r* = 1.1 ft/sec	ΔV_1 r* = 1.1 KM/sec	ΔV_2 r* = 1.3 ft/sec	ΔV_2 r* = 1.3 KM/sec	ΔV_3 r* = 1.3 ft/sec	ΔV_3 r* = 1.3 KM/sec	V_E y = 100 KM ft/sec	V_E KM/sec	$\sum_1^3 \Delta V$ ft/sec	$\sum_1^3 \Delta V$ KM/sec
1973	8	16	1910.5	12,915	3.936	6,802	2.073	23,767	7.244	67,714	20.639	43,484	13.254
1975	10	5	2690.5	14,288	4.355	12,737	3.882	19,859	6.053	70,245	21.411	46,883	14.290
1977	10	20	3436.5	13,315	4.058	16,309	4.971	18,905	5.762	72,251	22.022	48,529	14.792
1979	11	25	4202.5	12,405	3.781	13,606	4.147	19,341	5.895	66,556	20.286	45,352	13.823
1982	1	2	4971.5	11,971	3.649	12,397	3.779	20,746	6.323	60,345	18.393	45,114	13.751
	1	17	4986.5	13,088	3.989	12,725	3.879	18,798	5.730	59,253	18.060	44,612	13.598
1984	2	10	5740.5	11,611	3.539	13,814	4.211	19,180	5.846	53.331	16.255	44,605	13.596
1986	3	31	6520.5	11,980	3.651	13,919	4.243	16,820	5.127	50,293	15.329	42,719	13.021
1988	5	9	7290.5	15,386	4.690	15,106	4.604	18,939	5.773	51,791	15.786	49,431	15.067
1990	7	28	8100.5	16,113	4.911	17,472	5.325	18,945	5.774	63,219	19.269	52,530	16.011

Tab. 2-11 COMPARISON OF IMPULSE MANEUVER REQUIREMENTS FOR FAST AND VERY FAST MARS ROUND-TRIP MISSIONS FOR 10 AND 30 DAY CAPTIVE PERIODS IN A CIRCULAR ORBIT AT 1.3 RADII. (Δv_1, Δv_2, Δv_3, and v_E in 10^3 ft/sec)

T_1 and T_1/T_2	·60	90	60/60	60/60	60/120	60/150	90/90	90/120	90/150
1967 $v^*_{\infty 1}/v^*_{\infty 2}$ $\Delta v_1/\Delta v_2$ T_{cpt} = 10; $v^*_{\infty 3}/v^*_{\infty 4}$ $\Delta v_3/v_E$ 30	3-21/9570 .524/.610 38/51	3-1/9550 .338/.393 24.4/30.7		.718/.593 62.2/68.5	.536/.501 44/61.4 .565/.567 46.8/66.6	.410/.492 32.4/60.6		.551/.538 45.5/64.3 .577/.593 47.8/68.5	.405/.471 32/60.1 .503/.621 41/70.9
1969 $v^*_{\infty 1}/v^*_{\infty 2}$ $\Delta v_1/\Delta v_2$ T_{cpt} = 10; $v^*_{\infty 3}/v^*_{\infty 4}$ $\Delta v_3/v_E$ 30	5-9/0350 .421/.478 30.3/38.8	4-19/0330 .238/.341 18/26		.587/.483 49/60	.441/.414 35.3/54.9		.619/.523 52/63 .685/.598 58.2/69.2	.462/.440 37.3/58.5 .504/.488 41.1/60.5	.362/.414 27.8/54.7 .426/.459[1)] 33.8/58[1)]
1971 $v^*_{\infty 1}/v^*_{\infty 2}$ $\Delta v_1/\Delta v_2$ T_{cpt} = 10; $v^*_{\infty 3}/v^*_{\infty 4}$ $\Delta v_3/v_E$ 30	7-18/1150 .349/.349 25.2/26.7	6-28/1130 .201/.240 16.2/17.4	.793/.536 69.2/64.1	.603/.421 50.4/55.4 .753/.563 65.2/66.4	.480/.364 38.9/51 .583/.462 48.5/58.4		.653/.467 55.2/58.7 .753/.563 65.2/66.3	.514/.396 42/53.5 .583/.462 48.5/58.4	.397/.346 35.8/49.5 .478/.650 38.6/73.1
1973 $v^*_{\infty 1}/v^*_{\infty 2}$ $\Delta v_1/\Delta v_2$ T_{cpt} = 10; $v^*_{\infty 3}/v^*_{\infty 4}$ $\Delta v_3/v_E$ 30	9-15/1940 .382/.435 27.2/34.8	9-5/1930 .248/.275 18.8/20.2	.937/.569 83.2/66.7	.733/.451 63.4/57.5 .851/.580 74.8/67.5	.595/.398 49.7/53.5 .671/.491 57/60.6		.851/.580 74.8/67.6	.671/.491 57/56.9 .740/.583 64.1/67.5	.564/.489 56.3/60.5 .613/.557 51.4/65.9
1975 $v^*_{\infty 1}/v^*_{\infty 2}$ $\Delta v_1/\Delta v_2$ T_{cpt} = 10; $v^*_{\infty 3}/v^*_{\infty 4}$ $\Delta v_3/v_E$ 30	11-14/2730 .527/.541 38.2/44.6	10-25/2710 .309/.380 22.3/29.6		.912/.628 80.4/71.4	.717/.538 62/63.3 .778/.640 67.8/.721	.574/.498 47.6/61 .742/.845 64.4/90.4		.750/.591 65/68.5 .804/.687 70.2/76.5	.603/.563 50.4/66.1 .691/.663[1)] 58.8/74.3[1)]
1977 $v^*_{\infty 1}/v^*_{\infty 2}$ $\Delta v_1/\Delta v_2$ T_{cpt} = 10; $v^*_{\infty 3}/v^*_{\infty 4}$ $\Delta v_3/v_E$ 30	12-23/3500 .594/.641 43.4/54.2	12-3/3480 .344/.457 25/36.8			.724/.588 62.6/67.9	.572/.545 47.9/64.8			.604/.622 50.4/72.9 .540/.608[2)] 44.5/69.7[2)]
1980 $v^*_{\infty 1}/v^*_{\infty 2}$ $\Delta v_1/\Delta v_2$ T_{cpt} = 10; $v^*_{\infty 3}/v^*_{\infty 4}$ $\Delta v_3/v_E$ 30	1-22/4260 .574/.714 41.9/71.6	1-12/4250 .361/.467 25.9/37.6			.660/.560 56/66.1	.513/.514 42/62.4 .556/.621 46/70.7			.556/.621 46/70.7 .545/.651 44.9/73.1
1982 $v^*_{\infty 1}/v^*_{\infty 2}$ $\Delta v_1/\Delta v_2$ T_{cpt} = 10; $v^*_{\infty 3}/v^*_{\infty 4}$ $\Delta v_3/v_E$ 30		2-20/5020 .346/.427 23.8/34							.448/.522 .35.9/62.9 .448/54.9 35.9/64.1
1984 $v^*_{\infty 1}/v^*_{\infty 2}$ $\Delta v_1/\Delta v_2$ T_{cpt} = 10; $v^*_{\infty 3}/v^*_{\infty 4}$ $\Delta v_3/\Delta v_4$ 30		4-10/5800 .467/.291 21.4/24.9							.440/.553 35.2/65 .451/.535 36.2/63.9

1) T_2 = 140d, because of a discontinuity at 150d.

2) T_2 = 160d, because of a discontinuity at 140 and 150d.

The capture orbit at Mars is circular at $r^* = 1.3$. In the 90/150 day column it was necessary in some of the mission years to change the return transfer period to 140 or 160 days, in order to avoid excessively large impulse values associated with highly inclined return transfer orbits at 150 days. Fig. 2-28 and 2-29 show the hyperbolic excess velocity and the Earth departure velocity (not the departure impulse) for Earth-Mars transfer periods down to 80 days. They show that 1969 is a comparatively favorable year, so far as orbit launches are concerned. Fig. 2-30 shows mono-elliptic mission velocity profiles (for Earth departure dates in favorable transfer corridors) for 1-way and round-trip missions of 90 + 10 + 150 and 90 + 30 + 150 day mission periods, based on the data of Tab. 2-11. The time period (1967/84) presented includes FMY's (1969, '71, '84) and UMY's (1975, '77, '80). From Fig. 2-3 it is seen that the 1967 position of Mars is similar to that in 1999, 1969 similar to 1984, 1971 to 1986, 1973 to 1988, 1975 to 1990, 1977 to 1993 and 1979 to 1995. But caution must be exercised in comparing these mission pairs, because they are not nearly as similar as a pair of Venus missions one cycle apart. However, rough comparisons are justified, in the sense that a 1986 mission, for example will resemble more closely a 1971 or 1969 mission than a 1975 or 1977 mission velocity profile. Fig. 2-31 shows the variation of the individual impulse maneuvers for fast (60 + 10 + 120 days) missions (1967 - 1980 time period) and for very fast (60 + 10 + 90 days) missions (1969 - 1973), also based on the data listed in Tab. 2-11. The summary mission velocity profiles for the fast missions are shown in Fig. 2-32. This figure shows 1980 to be the least favorable mission year for this very fast mission profile, rather than 1977 as for the fast and medium-fast missions. The very high overall mission velocities even for a 190-day mission period show clearly the enormous requirements on the HISV propulsion technology for such or even still shorter mission periods.

Compared with the medium-fast missions shown in Fig. 2-26 and 2-27, the pronounced dominance of the unretarded Earth entry velocity (v_E) has disappeared, mainly because the impulse maneuvers 1 through 3 have increased. The entry velocity has not increased, but, in some instances, has rather been decreased. This indicates that development of entry technology to the 50 - 65 $\cdot$ 10^3 ft/sec level for medium-fast missions also would meet most of the entry requirements for much faster missions. By the same token, however, fast and very fast missions do not derive anywhere near the energy relief from UHE or high hyperbolic entry that is obtained for medium-fast missions. In other words, the trade-off between high hyperbolic entry and relief of propulsion development requirements is far smaller for the fast and the very fast missions than for the medium-fast missions. If, then, very advanced, high-I_{sp} propulsion systems are required for the fast and very fast missions as is obvious from the preceding data), the capability of UHE or high hyperbolic velocity entry is comparatively less important, or of no importance at all, because of the possible requirement to reuse these HISV's. Comparing, then mono-elliptic round-trip mission velocity profiles involving return into a near-Earth capture orbit (EaCC), as shown in Figs. 2-27, 2-30 and 2-32 and considering the time period 1980 - 1990 (using the above described mission pair techniques for Figs. 2-30 and 2-32) it follows that a mission velocity capability is required which lies between 80,000 and 90,000 ft/sec (24.5 and 27.5 km/sec) for medium-fast missions (T = 420 - 450 days); between 110,000 and 150,000 ft/sec (33.5 and 46.5 km/sec) for fast missions (T = 250 - 270 days); and between 130,000 and 180,000 ft/sec (40 and 55 km/sec) for very fast missions (190 days). The resulting trend is indicated in Fig. 2-33a, b which show mono-elliptic Mars round-trip mission velocity profiles involving EaCC as function of mission period for favorable and unfavorable mission years. The charts show that the difference between FMY and UMY increases with decreasing mission period. For the other extreme, namely synodic missions (900 - 1000 days mission period) with long ($> 180^{\circ}$) outbound and return transfer periods, the difference between mission years becomes very small.

2.2.5 Jupiter Missions

A number of mission velocity charts showing the hyperbolic excess velocities for Jupiter missions in the years 1982 through 1991 is presented in the Supplement together with circular and elliptic capture impulse charts for $1.1 \leq r^* \leq 100$ and $1 \leq n \leq 30$ and a chart for reading apoapsis maneuvers (to rotate the elliptic capture orbit prior to departure). With their aid, the user of this report can construct a wide variety of 1-way or round-trip Jupiter missions. They form the basis for the specific missions discussed below. Fig. 2-4 shows the positions of Jupiter which is seen to be in the vicinity of its perihelion in 1987/88 and 1999/2000. At that time (i.e. for Earth departure dates of 350 to 450 days earlier) the mission velocity requirements are slightly more favorable than when Jupiter is in the vicinity of the aphelion (1981/82; 1993/94), although the difference is much smaller than in the case of Mars.

Tab. 2-12 shows the impulse velocities for a number of 1-way and round-trip missions with elliptic capture (n = 3 and n = 30 for $r_P^* = 1.1$) at the planet. These data are compared in Fig. 2-34. For an outbound transfer time of 460 days, the Earth departure maneuvers are of comparative magnitude relative to Mercury missions; so are the capture maneuvers (n = 3; $r_P^* = 1.1$) which vary less than those for

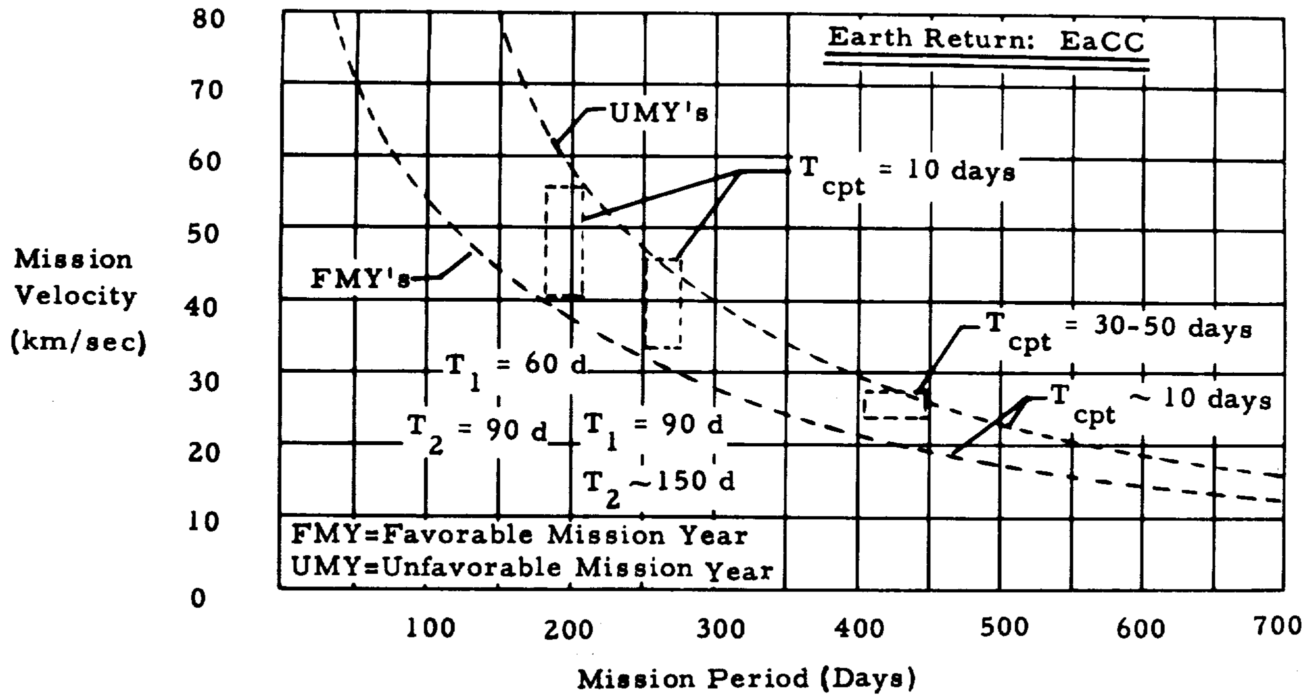

Fig. 2-33a TREND IN VARIATION OF MARS ROUND-TRIP MISSION VELOCITY WITH MISSION PERIOD (Velocity in km/sec)

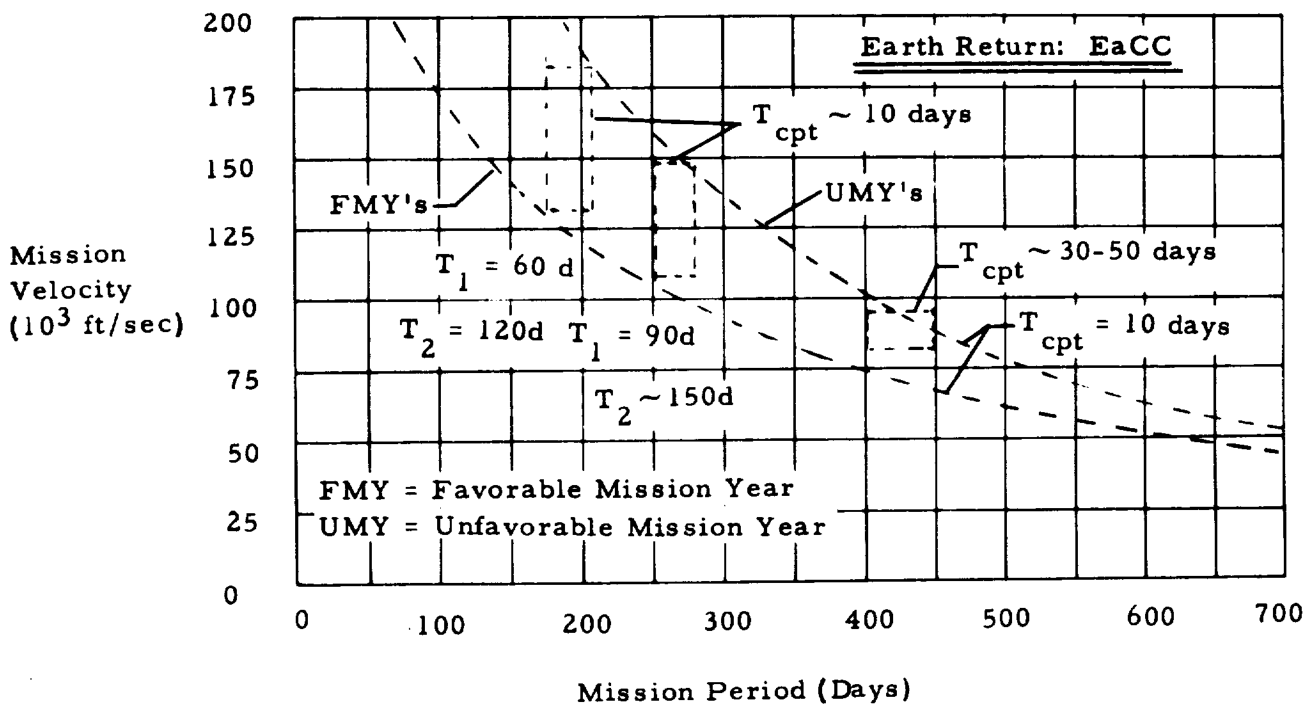

Fig. 2-33b TREND IN VARIATION OF MARS ROUND-TRIP MISSION VELOCITY WITH MISSION PERIOD (Velocity in ft/sec)

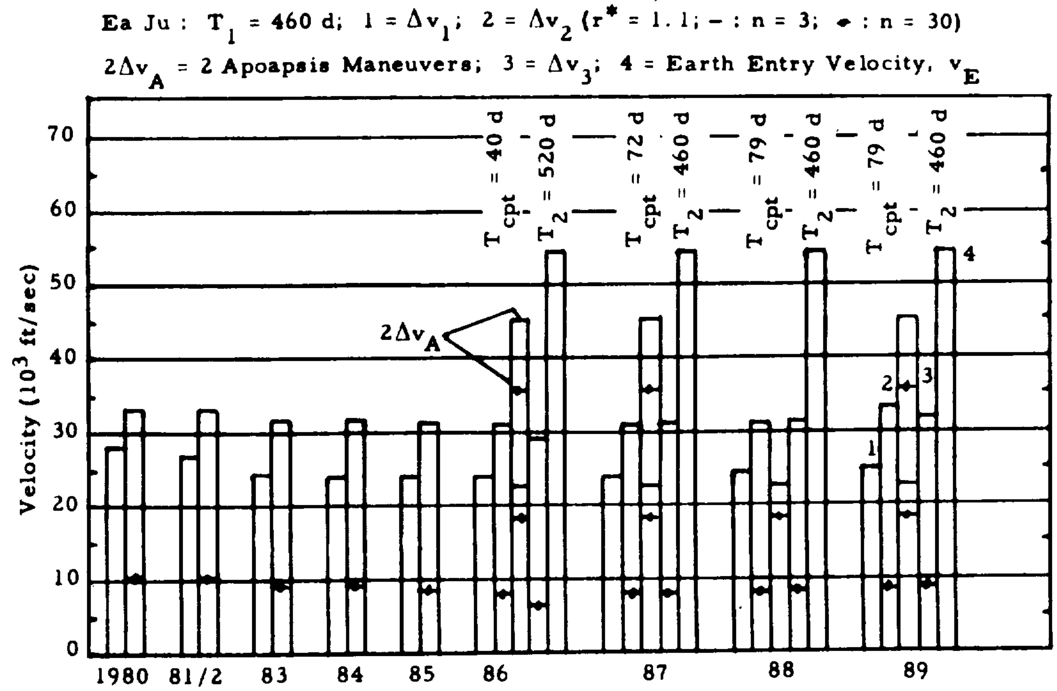

Fig. 2-34 MONO-ELLIPTIC JUPITER MISSION PROFILES

Tab. 2-12 JUPITER MISSION DATA

Planet	EaDD	T_1 (days)	$V^*_{\infty 1}$ (EMOS)	ΔV_1 (ft/sec)	$V^*_{\infty 2}$ (EMOS)	ΔV_2 (n=3; r*=1.1) (ft/sec)	T_{cpt} (days)	JuDD	T_2 (days)	$V^*_{\infty 3}$ (EMOS)	ΔV_3 (ft/sec)	$V^*_{\infty 4}$ (EMOS)	V_E (10^3 ft/sec)
Ju	12/3-12/21, 1980	460	–	28,000	–	33,000 10,000 (n=30)	-	-	-	-	-	-	-
Ju	12/29, 1981-1/22, 1982	460	0.4	27,300	0.53	33,000 10,000 (n=30)	-	-	-	-	-	-	-
Ju	2/3-2/17, 1983	460	0.38	24,700	0.513	32,000 9,600 (n=30)	-	-	-	-	-	-	-
Ju	3/8-3/21, 1984	460	0.37	24,400	0.492	32,000 9,600 (n=30)	-	-	-	-	-	-	-
Ju	4/10-4/28, 1985	460	0.37	24,400	0.472	31,500 8,600 (n=30)	-	-	-	-	-	-	-
Ju	5/18-6/6, 1986	460	0.37	24,400	0.456	30,000 8,200 (n=30)	40	10/15, 1987	520	0.39	29,500 6,900 (n=30)	0.40	54,000
Ju	6/24-7/9, 1987	460	0.36	24,100	0.452	31,000 8,200 (n=30)	72	12/22, 1988	460	0.462	31,200 8,200 (n=30)	0.40	54,000
Ju	8/2-8/17, 1988	460	0.38	24,700	0.46	31,200 8,300 (n=30)	79	1/28, 1990	460	0.478	31,500 8,700 (n=30)	0.40	54,000
Ju	9/6-9/21, 1989	460	0.39	25,000	0.48	33,000 8,800 (n=30)	79	–	460	0.498	32,000 9,100 (n=30)	0.40	54,000

Mercury. The Jupiter departure impulses are likewise fairly constant. The UHE velocity at Earth return is kept constant at 54, 000 ft/sec. Since the capture orbits are elliptic, their major axis in many cases will have to be rotated prior to re-departure in order to have their periapsis coincide with that of the departure hyperbola, namely, when precession about the highly oblate planet does not satisfy the turning rate during the capture period. In this case the vehicle enters a circular orbit at the apoapsis, passes through the required arc and subsequently reverts back into the elliptic orbit. This results in 2 apoapsis maneuvers. In the case of n = 3 each maneuver requires 22, 500 ft/sec; in the case of n = 30, it requires 18, 000 ft/sec. In spite of these velocity requirements, a net velocity saving is obtained, compared to capture in circular orbit. The extent of velocity saving is inversely proportional to the strength of the planetary g-field. It pays off for Jupiter and also for Venus. It is hardly worthwhile for Mars and of negligible advantage for Mercury.

The mono-elliptic mission velocity profiles for 1-way and round-trip missions to Mercury and Jupiter are compared in Fig. 2-35. The three bars at the left pertain to Mercury for capture in a circular orbit ($r^* = 1.1$) and T_1, T_{cpt}, T_2 represent the periods of outbound transfer, capture and return transfer. Velocity level 1 refers to 50, 000 ft/sec return into the Earth atmosphere. The shaded portions refer to variations in velocity due to slight variations in capture and/or return transfer period. Velocity level 2 represents unretarded hyperbolic entry. For Jupiter, case A refers to capture in an elliptic orbit of n = 3, case B to an elliptic capture orbit of n = 30, $r^*_P = 1.1$ in both cases.

Inspection of the hyperbolic excess velocity charts in the Supplement show that, while the outbound transfer period can be decreased below 460 days without resulting immediately in a sharp rise in outbound transfer energy, it is the return transfer which is subject to rigid constraints, especially so far as the Earth approach velocity is concerned. This velocity shows a definite minimum for a given return transfer time and a given Jupiter departure date (JuDD); and longer or shorter transfer times sharply increase the Earth return velocity for that particular JuDD. This condition is distinctly different from that for Venus or Mars and results in a pronounced coupling of departure date (hence, capture period) and return transfer time. In contrast to Venus or Mars missions, an extension of the capture period beyond 30 to 60 days may result in a faster return flight at reduced overall velocity requirement, but it does not reduce materially, if at all, the overall mission period. This fact can also be derived readily from the Tables below.

Tab. 2-13 lists the principal data of Jupiter's satellites. The Galilean moons J I through J IV are included in the subsequent mission

Fig. 2-35 MONO-ELLIPTIC MISSION VELOCITY PROFILES FOR ONE-WAY AND ROUND-TRIP MISSIONS TO MERCURY AND JUPITER

UHE = Unretarded Hyperbolic Entry

Mercury: T_1 : 80 - 110 d; T_{cpt} : 70 - 170 d; T_2 : 180-90

Jupiter: T_1 = 460 d; T_{cpt} : 40 - 80 d; T_2 : 460 - 520 d

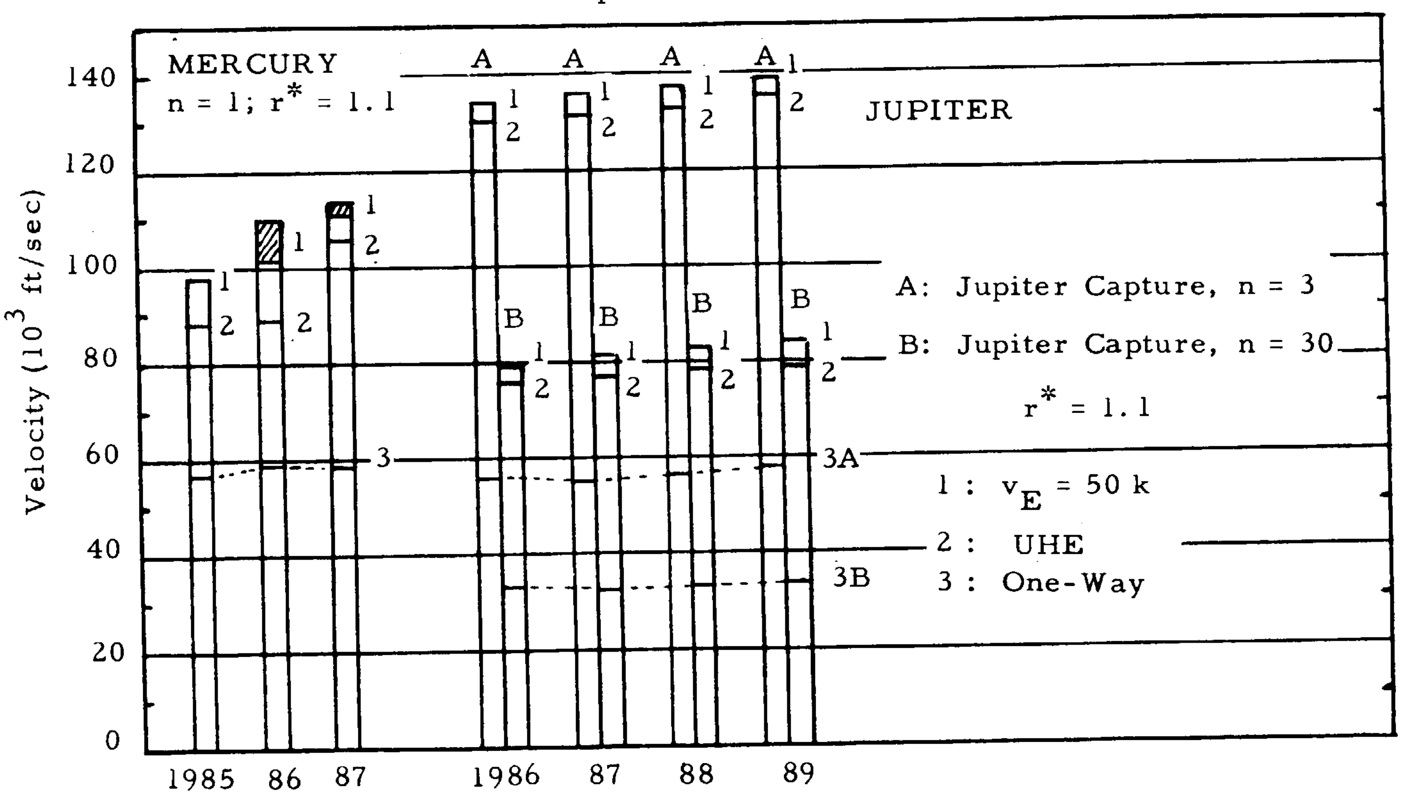

Tab. 2-13 DATA ON JUPITER SATELLITES

MOON	Distance from Planet (Radii)	Distance from Planet (km)	Period of Revolution (Days)	Incl. to Planet's Equator (Deg.)	Direction of Rotation	Diameter (km)	Gravitation Parameter K (km^3/sec^2)	Gravitation Parameter K (ft^3/sec^2)	Parabolic Velocity (km/sec)	Parabolic Velocity (ft/sec)	Surface Gravitation (Earth-g)	Eccentricity of Moon Orbit
Jupiter V	2.54	181,500	0.498	27.3	Direct	75-100						0.0028
Jupiter I (Jo)	5.905	422,000	1.769	1.6	Direct	3730	4,841	$1.71 \cdot 10^{14}$	2.279	7476	0.1337	0.0
II (Europa)	9.401	671,400	3.552	28.1	Direct	3150	3,130	$1.10 \cdot 10^{14}$	1.994	6541	0.1286	0.0003
III (Ganymede)	14.995	1,071,000	7.154	11.0	Direct	5150	10,319	$3.64 \cdot 10^{14}$	2.831	9288	0.1586	0.0015
IV (Callisto)	26.379	1,884,000	16.689	15.2	Direct	5180	6,455	$2.28 \cdot 10^{14}$	2.2333	7325	0.0981	0.0075
VI	161	11,500,000	250.7		Direct	120?						0.155
VII	165	11,750,000	260		Direct	50?						0.207
X	165	11,750,000	260		Direct	20?						0.08
XI	315	22,500,000	692		Retrograde	25?						0.21
VIII	330	23,500,000	713-768		Retrograde	50?						0.29-0.45
IX	332	23,700,000	758		Retrograde	22?						0.1 -0.4

data. Tab. 2-14 shows the impulse velocity requirements for Jupiter capture in orbits equal to those of the Galilean moons for the case of a fixed hyperbolic excess velocity. The HISV approaches Jupiter to a periapsis distance which is less than the distance of the target moon and enters an elliptic capture orbit whose apoapsis lies at the distance of the target moon. Two periapsis distances, $r_p^* = 1.1$ and 2.0 are used in Tab. 2-14. The operation is assumed to be coplanar. The difference in orbital period of the HISV in its elliptic orbit and of the moon in its practically circular orbit can bring about eventual rendezvous at the apoapsis of the intermediate ellipse.[1)] At that point the HISV enters the moon's orbit. In the examples in Tab. 2-14, the gravitational potential of the Galilean moons, which is not negligible, has been disregarded. Tab. 2-15 shows that consideration of their g-field, reduces the velocity requirement by 3000 to 4000 ft/sec; a relatively small amount if compared with the overall Jupiter mission velocity.

Using 1988 as reference year for Earth departure on a Jupiter mission, the effect of Earth-Jupiter transfer time, of various capture conditions and departure conditions and the effect of various Earth return conditions are listed, on a broad, comprehensive scope, in Tabs. 2-16 through 2-18. With the aid of these tables, the mission impulse velocities can quickly be determined and the effect of transfer times both ways, of Jupiter capture orbits, of Jupiter capture periods and of Earth return conditions, be assessed. The velocities given are such that the worst conditions within the respective Earth departure windows and the Jupiter departure windows can be met. The Jupiter departure windows, in particular, are determined primarily by limiting the Earth approach velocity. The hyperbolic excess velocity charts in the Supplement show that, outside these departure windows, the Earth approach velocity increases far more rapidly than the Jupiter departure velocity. Tab. 2-19 compares the effect of the ratio of outbound to return transfer time and the effect of capture period together with the associated variation of outbound transfer time for a fixed return transfer time. The comparison, which is based on the data of Tabs. 2-16 through 2-18, is carried out for capture in two elliptic capture orbits ($r_p^* = 1.1$, $n = 3$ and 30) and for capture in the orbit of J IV (Callisto).

---

1) It is realized that, in order for this to happen within an acceptable time period, an overshoot or undershoot maneuver above or below the moon's orbit may have to be carried out which requires additional velocity.

Tab. 2-14 IMPULSE VELOCITY REQUIREMENT FOR JUPITER CAPTURE IN ORBITS EQUAL TO THOSE OF JUPITER MOONS I THROUGH IV (MOON'S MASSES NEGLECTED)

Moon	J I	J II	J III	J IV
Capture Distance, r^*_P (Jupiter)	1.1	1.1	1.1	1.1
$v^*_{\infty 2}$ (EMOS)	0.46	0.46	0.46	0.46
Δv (n = 1) (10^3 ft/sec)	60	60	60	60
v_c (r^*_P = 1.1) (10^3 ft/sec)	133	133	133	133
$n = r^*_{Sat}/r^*_P$	5.37	8.55	13.1	21.5
Arrival Vel. v_2 (10^3 ft/sec)	193	193	193	193
Capt. Maneuver, $\Delta v_{P,2}$ (10^3 ft/sec)	21	15.5	12.5	9.4
Capt. Orbit, v_P (10^3 ft/sec)	172	177.5	180.5	183.6
Moon Velocity, $v_{c,Sat}$ (10^3 ft/sec)	57.5	45.5	36.2	27.3
Capt. Orbit, $v_A = v_P/n$ (10^3 ft/sec)	32	20.5	13.8	8.5
Apoapsis Maneuver, Δv_A (10^3 ft/sec)	25.5	25.0	22.4	18.8
(Disregarding Moon g - Field)				
Total, $\Delta v_{P,2} + \Delta v_A$ (10^3 ft/sec)	46.5	40.5	34.9	28.2
Capture Distance, r^*_P (Jupiter)	2.0	2.0	2.0	2.0
$v^*_{\infty 2}$ (EMOS)	0.46	0.46	0.46	0.46
Δv (n = 1) (10^3 ft/sec)	48	48	48	48
v_c (r^*_P = 2.0) (10^3 ft/sec)	99	99	99	99
$n = r^*_{Sat}/r^*_P$	2.95	4.7	7.5	13.19
Arrival Vel. v_2 (10^3 ft/sec)	147	147	147	147
Capt. Maneuver, $\Delta v_{P,2}$ (10^3 ft/sec)	27	20	16	12.4
Capt. Orbit, v_P (10^3 ft/sec)	120	127	131	134.6
Moon Velocity, $v_{c,Sat}$ (10^3 ft/sec)	57.5	45.5	36.2	27.3
Capt. Orbit, v_A (10^3 ft/sec)	40.7	27	17.5	10.2
Apoapsis Maneuver, Δv_A (10^3 ft/sec)	16.8	18.5	18.7	17.1
(Disregarding Moon g - Field)				
Total, $\Delta v_{P,2} + \Delta v_A$ (10^3 ft/sec)	43.8	38.5	34.7	29.5

Tab. 2-15 JUPITER MOONS (GANYMEDE AND CALLISTO) CAPTURE, DESCENT AND RE-ASCENT

Moon	J III	J IV
Jupiter Capt. Dist. r^*_P	2.0	2.0
Jupiter Moon Capt. Dist.	1.05	11.05
Local Parab. Vel. at Ju Moon (10^3 ft/sec)	9100	7200
Hyp. Approach Vel. to Ju Moon (10^3 ft/sec)	18.7	17.1
Ju Moon Arrival Vel. (10^3 ft/sec)	20.9	18.6
Ju Moon Circ. Vel. at Capt. Dist. (10^3 ft/sec)	6.3	4.9
Capt. Orbit about Ju Moon	n = 1	n = 1
Ju Moon Capt. Maneuver, Δv_{arr} (10^3 ft/sec)	14.6	13.7
Reduction in Vel. for Capt. Manuever, Compared to Apoapsis Maneuver, Disregarding Moon's g - Field (10^3 ft/sec)	18.7-14.6=4.1	17.1-13.7=3.4
Hence, Total, $\Delta v_2 + \Delta v_{arr}$ (10^3 ft/sec)	30.6	26.1
De-orbit of Landing on Moon (10^3 ft/sec)	7.0	5.5
Ascent and Injection into Moon Satellite Orbit (10^3 ft/sec)	6.7	5.2

Tab. 2-16 OUTBOUND IMPULSE VELOCITY REQUIREMENTS FOR JUPITER CAPTURE MISSIONS WITH VARIOUS CAPTURE CONDITIONS

EaDD 1988	T_1 (D)	$v^*_{\infty 1}$ (EMOS)	Δv_1 (10^3 ft/sec) n = 1, r* = 1.1	$v^*_{\infty 2}$ (EMOS)	$\Delta v_{P,2}$ (10^3 ft/sec)									JuAD (JD) (Approx.)
					n = 3, r^*_P = 1.1	n = 30, r^*_P = 1.1	J I n = 2.95, r^*_P = 2.0	J II n = 4.7, r^*_P = 2.0	J III n = 13.1, r^*_P = 1.1	J IV n = 21.5, r^*_P = 1.1	n = 2, r^*_P = 50	Circ. Orb. @ r* = 100 via n = 2, r^*_P = 50	n = 1, r* = 50	
8/2-8/17	460	0.38	24.7	0.46	31	8.3	27	20	12.5	9.4	30.1	30.1	33.1	7840
8/3-8/19	430	0.40	28.3	0.51	32	9.5	28	21.5	13.5	10.5	34.6	34.6	37.3	7820
8/7-8/20	400	0.42	30	0.56	33.5	10.8	30	23	14.5	11.5	38.8	38.8	41.9	7800
8/8-8/24	370	0.45	32.4	0.625	35.5	12.7	32.2	25.5	17	13.5	44.2	44.2	47.5	7760
8/9-8/29	340	0.49	35.4	0.70	38	15	35	28	19	16.0	51.1	51.1	54.1	7730

Δv_A (10^3 ft/sec)

Elliptic Capt. Orb. No Δv_A	Elliptic Capt. Orb. No Δv_A	16.8	18.5	22.4	18.8	Elliptic Capt. Orb. No Δv_A	2	

Total Impulse Velocity (Outbound)[1)] $= \Delta v_1 + \Delta v_{p,2} + \Delta v_A$

8/2-8/17	55	33	68.5	63.2	59.6	52.9	54.8	56.8	57.8	7840
8/3-8/19	60.3	37.8	73.1	68.3	64.2	57.6	62.9	64.9	65.6	7820
8/7-8/20	63.5	40.8	76.8	71.5	66.9	60.3	68.8	70.8	71.9	7800
8/8-8/24	67.9	45.1	81.4	76.4	71.8	64.7	76.6	78.6	79.9	7760
8/9-8/29	73.4	50.4	87.2	81.9	76.8	70.2	86.5	88.5	89.5	7730

1) The g - potential of the Jupiter Moons is neglected in these figures.

Tab. 2-17 JUPITER MISSIONS: DEPARTURE FROM JUPITER UNDER VARIOUS DEPARTURE CONDITIONS

JuDD (JD) 1989/90	T_2 (D)	$v^*_{\infty 3}$ (EMOS)	n = 3, r^*_P = 1.1		n = 30, r^*_P = 1.1		J I 1)	J II 1)	J III 2), r^*_P = 1.1		J IV 1), r^*_P = 1.1		n = 2, r^*_P = 50		n = 1, r* = 100	n = 1, r* = 50
			$2\Delta v_A$ (10^3 ft/sec) →	$\Delta v_{P,3}$ →	$2\Delta v_A$ →	$\Delta v_{P,3}$ →	Δv_3 →	Δv_3 →	Δv_A →	Δv_3 or $\Delta v_{P,3}$ →	Δv_A →	Δv_3 or $\Delta v_{P,3}$ →	$2\Delta v_A$ →	$\Delta v_{P,3}$ →	Δv_3 →	Δv_3 →
7790/810	580	0.341	45	28.6	18 2)	23.6 2)	30.2	27	-	25	-	24	5400	20.9	25	24
7820/840	550	0.372	45	29.1	18 2)	25.7 2)	31.3	29	-	26.5	-	25.8	5400	23.1	27.4	26.3
7855/875	520	0.412	45	30	36	7.3	33.2	31	-	29	-	28.5	5400	26.3	31	29.5
7885/905	490	0.452	45	30.9	36	8.2	35.2	32	-	31.5	18.8	9.3	5400	29.6	34.4	32.5
7920/940	460	0.503	45	31.9	36	9.2	37.5	36	-	35	18.8	10.5	5400	34	39	37
7950/470	430	0.557	45	33.3	36	10.8	41	40	22.4	13.5	18.8	11.8	5400	38.2	43.9	41.5
7980/800	400	0.619	45	35.1	36	12.6	44	44	22.4	15.2	18.8	13.5	5400	42.8	49.6	47
8000/020	370	0.675	45	37	36	14.2	48	48.5	22.4	17.1	18.8	15.4	5400	49	55	52
8030/050	340	0.759	45	39.9	36	17.1	53	54	22.4	20	18.8	18.5	5400	56.5	63	59.9

1) The g - potential of the Jupiter Moons is neglected; for J I and J II, departure from Moon orbits is most favorable. For J III and J IV, direct departure from the Moon is more favorable at low values of $v^*_{\infty 3}$, while at higher values of $v^*_{\infty 3}$, less velocity is required if departure occurs from periapsis of intermediate elliptic orbit.

2) At low values of $v^*_{\infty 3}$ it requires less velocity to enter the circular orbit at r* = 30 and depart from there.

Tab. 2-18 JUPITER MISSIONS: EARTH ARRIVAL CONDITIONS FOR ENTRY AT 50,000 ft/sec, FOR CAPTURE IN CIRCULAR ORBIT AT LUNAR DISTANCE AND AT NEAR-EARTH DISTANCE.

JuDD (JD) 1989/90	$v^*_{\infty 4}$ (EMOS)	v_E (10^3 ft/sec)	Δv_4 (v_E = 50k) (10^3 ft/sec)	Δv_4 (Enter Circ. Orbit at Moon Dist.)[1] (10^3 ft/sec)	Δv_A	Δv_4 EaCC[2] at n=1, r^*=1.1 (10^3 ft/sec)
7790/810	0.416	54.3	4.3	18.5	4.1	28.6
7820/840	0.420	55.1	5.1	19.3	4.1	29.4
7855/875	0.40	52.6	2.6	16.8	4.1	26.9
7885/905	0.406	54	4	18.2	4.1	28.3
7920/940	0.397	53.5	3.5	17.7	4.1	27.8
7950/970	0.409	54.2	4.2	18.4	4.1	28.5
7980/800	0.436	54.5	4.5	18.7	4.1	28.8
8000/020	0.482	59.9	9.9	24.1	4.1	34.2
803/050	0.509	61.9	11.9	26.1	4.1	36.2

1) Reducing to a perigee velocity of 35,800 ft/sec.

2) Reducing to a circular velocity of 25,700 ft/sec.

Tab. 2-19 SUMMARY JUPITER MISSIONS 1988

A. Effect of Ratio of Outbound to Return Transfer Time

T_1	460	430	400	370	340
$\Delta v_{outbound}$ (n = 3)	55	60.3	63.5	67.9	73.4
JuAD	7840	7820	7800	7760	7730
JuDD	7920	7900	7875	7840	7810
T_2	460	490	520	550	580
T_{cpt}	80	80	75	80	80
$\therefore T$	1000	1000	995	1000	1000
$2\Delta v_A$	45	45	45	45	45
$\Delta v_{P,3}$	31.9	30.9	30	29.1	28.6
$2\Delta v_A + \Delta v_{P,3}$	76.9	75.9	75	74.1	73.6
$\therefore \Delta v_4$ (EaCC)	27.8	28.3	26.9	29.4	28.6
$\Sigma\Delta v$	159.7	164.5	165.4	171.4	175.6
$\Delta v_{outbound}$ (n = 30)	33	37.8	40.8	45.1	50.4
$2\Delta v_A$ or Δv_A	36	36	36	18	18
$\Delta v_{P,3}$ or Δv_3	9.2	8.2	7.3	25.7	23.6
$\therefore \Delta v_4$	27.8	28.3	26.9	29.4	28.6
	106.0	110.3	111.0	118.2	120.6
$\Delta v_{outbound}$ (Callisto)	52.9	57.6	60.3	64.7	70.2
$\Delta v_{P,3}$ or Δv_3	10.5	9.3	28.5	25.8	24
Δv_A	18.8	18.8	--	--	--
$\therefore \Delta v_4$ (EaCC)	27.8	28.3	26.9	29.4	28.6
	110.0	114.0	115.7	119.9	122.8

B. Effect of Capture Period

T_1	460	430	400	370	340
$\Delta v_{outbound}$ (n = 3)	55	60.3	63.5	67.9	73.4
JuAD	7840	7820	7800	7760	7730
JuDD	8030	8030	8030	8030	8030
T_{cpt}	190	210	230	270	300
T_2	340	340	340	340	340
$\therefore T$	990	980	970	980	980
$2\Delta v_A$	45	45	45	45	45
$\Delta v_{P,3}$	39.9	39.9	39.9	39.9	39.9
$2\Delta v_A + \Delta v_{P,3}$	84.9	84.9	→	→	→
Δv_4 (EaCC)	36.2	36.2	→	→	→
$\therefore \Sigma\Delta v$	176.1	181.4	184.6	189	194.5
$\Delta v_{outbound}$ (n = 30)	33	37.8	40.8	45.1	50.4
$2\Delta v_A$	36	→	→	→	→
$\Delta v_{P,3}$	17.1	89.3 →	→	→	→
Δv_4 (EaCC)	36.2	→	→	→	→
$\therefore \Sigma\Delta v$	122.3	127.1	130.1	134.4	139.7
$\Delta v_{outbound}$ (Callisto)	52.9	57.6	60.3	64.7	70.2
Δv_A	18.8				
$\Delta v_{P,3}$	18.5	73.5			
Δv_4 (EaCC)	36.2				
$\therefore \Sigma\Delta v$	126.4	131.1	133.8	138.2	143.7

2.2.6 Summary of Impulsive Velocities for Mono-Elliptic One-Planet Missions

Tab. 2-20 summarizes the results of the mission discussions in the preceding paragraphs. Velocity bands are shown for missions to the four planets and for the various conditions indicated. For Mars and Venus, medium-fast missions are considered.

2.3 MISSIONS INVOLVING BI-ELLIPTIC TRANSFER PROFILES WITH PERIHELION BRAKE

The concept of the perihelion brake (PB) maneuver was developed for Mars-Earth return flights as part of earlier planetary mission studies undertaken for NASA/MSFC/FPO (ref. 3). It is applicable to all missions which involve close perihelion passage (0.6 to 0.4 A.U.) and relatively steep intersection with the Earth orbit at the point of Earth return, resulting in very hyperbolic excess velocities.

This type of transfer profile is found for Mars-Earth transfers, especially during the unfavorable mission years (Fig. 2-36). However, similar profiles can be found for the return flight from any of the outer planets, for instance from Jupiter. Par. 2.2.5 discusses the constraints imposed on mono-elliptic return flights from Jupiter, primarily in order to avoid excessive Earth approach velocities. Fig. 2-37 shows an example of a round-trip mission profile to Jupiter. The return flight, as specified in Fig. 2-37, involves perihelion passage at 0.378 A.U. and a hyperbolic excess velocity at Earth approach of 1.0298 EMOS, corresponding to a geocentric Earth approach velocity of 105,000 ft/sec (32 km/sec). A geocentric retro-maneuver to return into a near-Earth satellite orbit would involve an impulsive maneuver of 79,000 ft/sec (24.1 km/sec); a stiff requirement even for vehicles with very high specific impulse.

In evaluating the effectiveness of PB maneuvers, their potential accomplishments must be kept in mind. Their usefulness obviously depends on the usefulness of what they can accomplish, which is the following:

(1) Reduction of unretarded Earth approach velocity by a maneuver which is smaller than a GEAR maneuver.

(2) Opening up of return departure windows from an outer planet when returning to Earth. By means of the PB maneuver a relatively invariant Earth return condition can be maintained over time periods during which a GEAR maneuver would vary by a larger amount than the PB maneuver needed to keep the Earth return conditions invariant. (The extent to which this fact can be utilized depends, of

Fig. 2-36. MARS-EARTH TRANSFER PROFILE WITH PERIHELION BRAKE

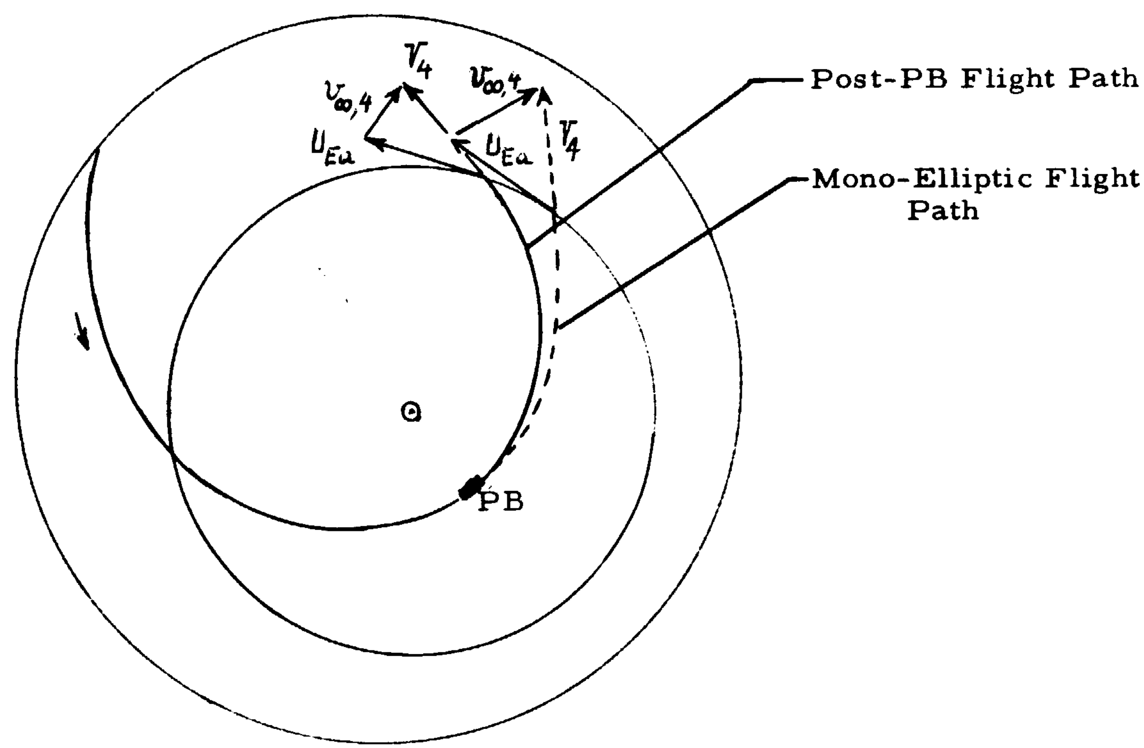

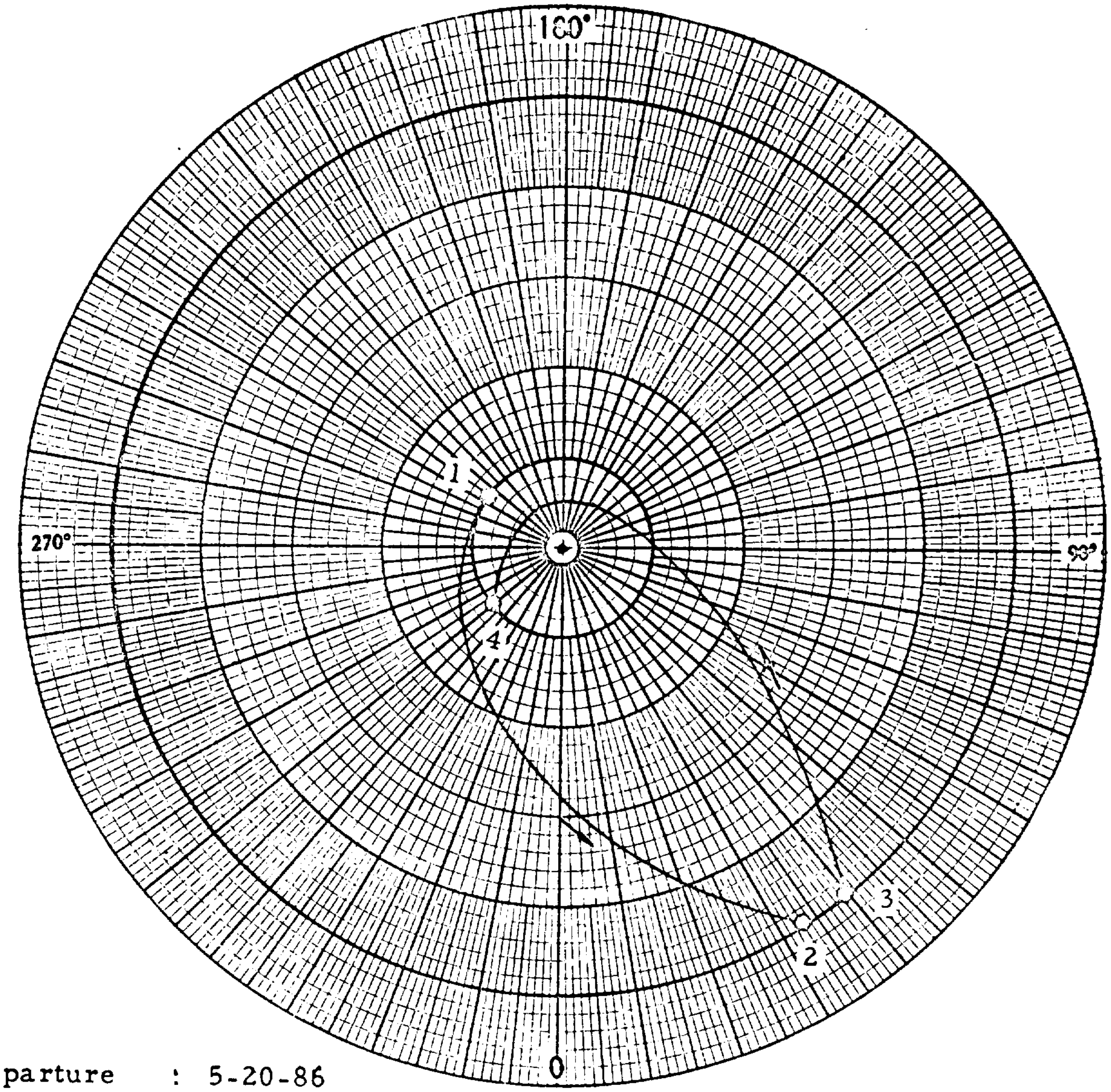

1 Departure : 5-20-86
T_1 = 610 days

T_{cpt} = 70 days

3 Departure ♃ : 3 -30-88
T_2 = 490 days

Fig. 2-37 EARTH - JUPITER ROUND-TRIP

Tab. 2-20 REPRESENTATIVE VELOCITY RANGES FOR PLANETARY MISSIONS (10^3 ft/sec)

Planet	Mode	One-Way		Round-Trip
		Fly-By	Capture	Capture
Me	$n = 1$; $r_P^* = 1.1$ $T_1 = 80\text{-}110$; $T = 330\text{-}330$	24-27	55-60	90-105 (UHE) 100-110 (50k)
Ve	$n = 8$; $r_P^* = 1.1$ $T_1 = 120\text{-}140$; $T = 400\text{-}420$	12-14	17-19	33-36 (UHE) 25-28 (UHE; no ΔV_A) 39-41 (40k) 31-32 (40k; no ΔV_A) 52-54 (EaCC) 44-45 (EaCC; no ΔV_A)
	$n = 1$; $r_P^* = 1.1$ $T_1 = 120\text{-}140$; $T = 400\text{-}420$	12-14	25-27	40-42 (UHE) 44-45 (40k) 59-60 (EaCC)
Ma	$n = 1$; $r_P^* = 1.3$ $T_1 = 160\text{-}200$; $T = 420\text{-}450$	12-17	30-33	43-53 (UHE) 44-71 (50k) 53-81 (40k) 67-95 (EaCC)
Ju	$n = 3$; $r_P^* = 1.1$ $T_1 = 460$; $T = 1000\text{-}1050$	24-28	55-60	130-135 (UHE) 135-140 (50k)
	$n = 30$; $r_P^* = 1.1$	24-28	30-35	75-80 (UHE) 80-85 (50k) 105-110 (EaCC)

course on the variation of the planet departure maneuver as the capture period is extended).

(3) Use of propulsion systems at the perihelion which are more advantageous than those available for the GEAR maneuver.

The figure of merit for the first accomplishment is the exchange ratio $\Delta v_E/\Delta V_{PB}$, where Δv_E represents the GEAR maneuver, the other the PB maneuver for equal geocentric velocity at mission termination. This exchange ratio obviously is poor (less than unity) if a very large plane change is involved in the PB maneuver. Investigation of many Mars-Earth return flights with PB maneuver, however, have shown that this condition can always be avoided. For near-planar PB maneuvers, the exchange ratio tends to increase with decreasing perihelion distance and with increasing aphelion distance of the mono-elliptic transfer orbit.

During the unfavorable Mars mission years, the perihelion distance for mono-elliptic return transfers is smaller than in favorable mission years during which similarly small perihelion distances can be attained only under conditions which increase the Mars departure maneuver. The exchange ratio therefore tends to be smaller in the favorable mission years where a PB maneuver is less urgently needed in the first place because the Earth approach velocities are lower. Relatively poor exchange ratios (1.3 - 1.5) are limited to the relatively most favorable mission years (1986 and 1988). Good exchange ratios are not so limited. Values of 1.7 to 1.8 were found for the 1975 mission year (ref. 3) as well as for 1982 (ref. 4). In 1984 values around 1.6 were found (ref. 4). Fig. 2-38 shows a typical example for return from Mars in 1982.

No similarly systematic investigation was carried out for return flights from Jupiter and Saturn. However, taking the example shown in Fig. 2-37 above, Tab. 2-21[1]) shows the background data for the case of a PB maneuver which changes the semi-major axis of the heliocentric transfer orbit from 4.0 to 2.0 AU. It is seen that this requires a reduction in perihelion velocity ((9) & (10)) by $\Delta V_{PB} \sim 17{,}000$ ft/sec, resulting in a reduction in Earth entry velocity, i.e. velocity very near Earth, of ((17) & (18)) $\Delta v_E \sim 42{,}100$ ft/sec. The exchange ratio for reducing the geocentric arrival velocity from 104,900 to 62,800 ft/sec is

$$\Delta v_E / \Delta V_{PB} \sim 42{,}100/17{,}000 = 2.48$$

There is no reason why the PB maneuver could not have been stronger,

1) Data are approximate, since read from charts.

Fig. 2-38 PERIHELION MANEUVER AND REDUCTION IN EARTH ENTRY VELOCITY VS PERIHELION-EARTH FLIGHT TIME

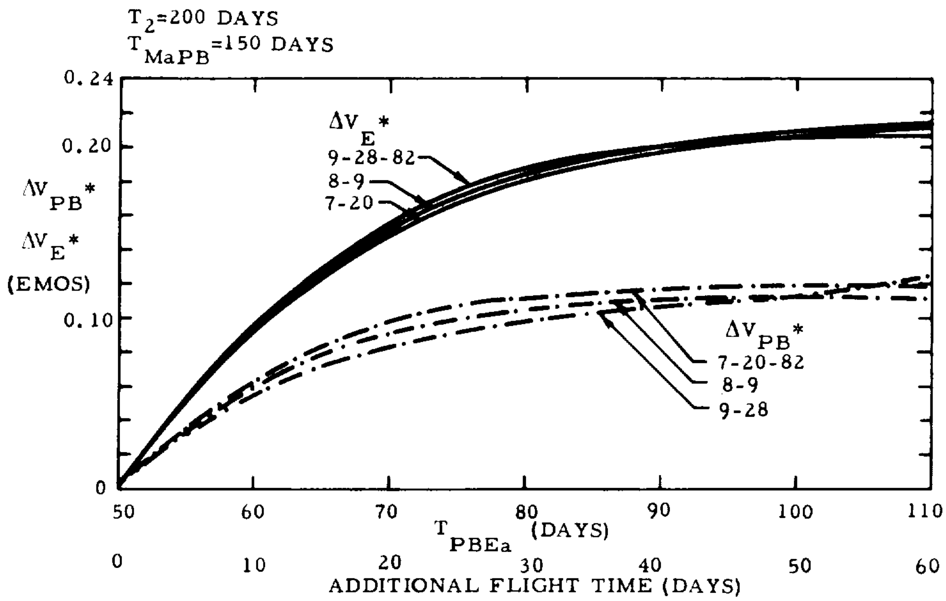

Tab. 2-21. DETERMINATION OF EXCHANGE RATIO OF PERIHELION BRAKE MANEUVER DURING JUPITER RETURN FLIGHT ALONG MISSION PROFILE SHOWN IN FIGURE 2-37

MONO-ELLIPTIC DATA	BI-ELLIPTIC (PB) DATA
1. $R_P = 0.378$ AU	2. $R_P = 0.378$ AU
3. $R_A = 0.764$ AU	4. Reduced to $R_A = 1.622$ AU
5. $a \sim 4.0$ AU	6. Reduced to $a = 2.0$ AU
7. $V_{c,P} \sim 160,000$ ft/sec	8. $V_{c,P} \sim 160,000$ ft/sec
9. $V_P \sim 221,000$ ft/sec	10. Reduced to $V_P \sim 204,000$ ft/sec
11. $\theta_{arr} \sim 50^o$	12. Reduced to $\theta_{arr} \sim 38^o$
13. $V_{arr} \sim 130,000$ ft/sec	14. Reduced to $V_{arr} \sim 96,000$ ft/sec
15. $\overrightarrow{\Delta V} = v_\infty \sim 101,000$ ft/sec $v_\infty^* \sim 1.034$ EMOS	16. Reduced to $v_\infty \sim 51,000$ ft/sec $v_\infty^* \sim 0.521$ EMOS
17. UHE Velocity $v_E \sim 104,900$ ft/sec	18. Reduced to $v_E \sim 62,800$ ft/sec
19. GEAR Maneuver to Circular Velocity near Earth $\Delta v_{GEAR} \sim 104,900 - 25,900$ $\sim 79,000$ ft/sec (impulsive)	20. Reduced to $\Delta v_{GEAR} \sim 37,000$ ft/sec (impulsive)

R_P = perihelion distance; R_A = aphelion distance; a = semi-major axis; $V_{c,P}$ = circular velocity at perihelion; V_P = perihelion velocity; θ_{arr} = path intersection angle at Earth arrival; V_{arr} = heliocentric velocity at arrival reducing the geocentric arrival velocity to between 50,000 to 40,000 ft/sec, probably with a still slightly better exchange ratio. On the other hand, the PB maneuver described in Tab. 2-21 is planar. In reality some plane change is almost invariably involved, degrading the exchange ratio somewhat[2]. Therefore, it appears fair to expect that accurately computed (non-planar) PB maneuvers during Jupiter-Earth return flights with close perihelion passages will yield an exchange ratio of the order of 1.9 to 2.1.

For return flights from Saturn, the exchange ratio should be still somewhat higher because of larger aphelion distances of the mono-elliptic return path.

The attractiveness of the second accomplishment depends on the desirability of an extended capture period. The desirability could be based on scientific reasons or on safety reasons, if it must be feared that failures or operational complexities at the target (such as due to secondary missions, e.g. surface excursion or excursions to a planet moon) render the probability of a fixed departure date after a minimum capture period to be low.

The effectiveness of the third accomplishment, in terms of reducing the ODW (increasing the payload fraction), depends on the propulsion system which would be used for the PB and on the propulsion systems available to the HISV for the other principal maneuvers of the mission. For instance, use of a solar heat exchanger (SHE) drive which is characterized by low mass and relatively elevated specific impulse (700 sec or more) represents an improvement over the use of chemical propulsion for HISV's equipped with chemical or nuclear (SCR/G) drives. It would offer no improvement for HISV's using nuclear pulse or nuclear-electric drives.

The importance of the velocity exchange ratio as a figure of merit lies, of course, in the strong reduction in ODW suggested by it. Since the flight time from perihelion to Earth is of the order of 60 to 90 days for return from Mars and of the order of 50 to 70 days for return from Jupiter, the crew must retain a larger payload weight at the perihelion than for the GEAR maneuver with subsequent Earth entry, in which case the payload for the GEAR maneuver is reduded to the Earth entry module (EEM). In such cases, for the PB maneuver to be competitive with the GEAR maneuver, the operational payload must be designed in such a manner that it is possible for the crew to eliminate all items no longer needed during the remaining portion of the mission. This has been discussed in greater detail in ref. 3. For exchange ratios of about 1.8, the perihelion payload can be about twice

2) For instance, some Mars return flights should yield an exchange ratio close to 2. Due to some plane change involved, such high values have not been found so far.

the mass of the GEAR payload, if a SHE drive is used compared to a chemical drive for the GEAR maneuver, and still a reduction in ODW of about 500,000 lb (20 - 25%) in HISV's using SCR/G propulsion for the other main maneuver. ODW reductions of over 40% are achieved for chemical HISV's. For an NP HISV, the same propulsion system would, of course, be used for the PB as for all other principal maneuvers. If the vehicle is to be abandoned at mission termination and the crew returns to Earth via high-speed entry, a PB maneuver would, therefore not offer any advantages. It probably would cause in increase in ODW.

The situation is radically different, however, if the NP vehicle is not to be abandoned but to be returned into an Earth capture orbit (low altitude or distant orbit; circular or elliptic). In that case, the mass to be slowed down during the GEAR maneuver is significantly larger. The ratio of masses to be decelerated at the PB and the GEAR maneuver no longer is 1.5:1 to 2:1, but more like 1.2:1 to 1.1:1. In such a case a PB maneuver is extremely effective in terms of reducing ODW (increasing the payload fraction) for any HISV, be it NP or SCR or chemical.

The exchange ratio is even more effective in improving the payload fraction if a shuttle operation to another planet in which passengers and other return destination payload to Earth is involved.

2.4 MISSIONS INVOLVING BI-ELLIPTIC TRANSFER WITH A PLANET FLY-BY

Such mission profiles were investigated earlier for Mars-Earth return using the gravitational field of Venus in conjunction with a moderate powered maneuver to reduce the Earth approach velocity (ref. 5). The same technique was applied earlier to the use of Jupiter for shortening the transfer time to Saturn and post-Saturn planets and to enter strongly inclined extra-ecliptic orbits (ref. 6). The method has been extended to use Venus in flights to and from Mercury.

While the reduction in mission velocity, and consequently the gain in payload fraction can be considerable, bi-elliptic transfer orbits with a planet fly-by necessarily demand more precise timing, they are not available as frequently and, in the inner solar system they practically always increase the transfer time.

2.4.1 Mars-Earth Transfer with Venus Powered Fly-By

Mission velocity charts for the 1979 and the 1982 Mars mission windows are presented in ref. 4.

Under favorable transfer conditions a Mars round-trip mission with VePFB on return requires a mission velocity of 42, 000 to 47, 000 ft/sec (12.8 to 14.3 km/sec) for geocentric approach velocities of 39, 000 to 42, 000 ft/sec; compared to at least 53, 000 ft/sec mission velocity for mono-elliptic round-trip missions (cf. Tab. 2-20).

2.4.2 Earth-Mercury Missions With Venus Powered Fly-By

No systematic search for suitable mission windows could be carried out within the frame of this study. A typical comparison of the velocity reduction attainable by using Venus during the outbound flight is presented subsequently.

Dep Ea: 4-6670.5; 8-28-1986
Dep. velocity: $v_{\infty 1}^{*}$ = 0.115 EMOS; Δv_1 = 12,000 ft/sec = 3.66 km/sec
Transfer time T_{EaVe} = 174d
Ar Ve: 4-6844.5; 2-18-87
Dep Ve: 4-6844.5; 2-18-87
Δv_{VePFB} ~ 2000 ft/sec = 0.61 km/sec
Transfer time T_{VeMe} = 70 d
Ar Me: 4-6914.5; 4-29-87
Arrival maneuver (capture, n = 1, r* = 1.1)
v_{∞}^{*} = 0.1905 EMOS; Δv_2 = 13,500 ft/sec = 4.12 km/sec

Transfer velocity:
12000 + 2000 + 13,500 = 27,500 ft/sec = 8.39 km/sec
Transfer time: 174 + 70 = 244 d.

Comparison with Tab 2-3 shows that the mono-elliptic transfer velocity is at least twice as large, but the transfer time is 80 - 110 days.

It must be emphasized again that without systematic search through a large number of mission windows it is not possible to judge whether this example represents a particularly favorable case. Celestial latitude of Venus at VeDD is 2.65 deg., that of Mercury at MeAD is -2.88 deg at a heliocentric distance of 0.348 AU. This means that Mercury is not at extreme elevation (about 7^{o}) and close to mean distance (0.387 AU) at the time of arrival. Thus, there should occasionally be even more favorable Ea-VePFB-Me transfer conditions, while there should be others which are less favorable. Fig. 2-39 shows several opportunities between 1978 and 1987.

If the departure from Mercury is timed so that Venus is used during the return transfer also, the overall mission velocity to Mercury should be reduced to 55,000 to 60,000 ft/sec with terminal Earth orbital capture, or 40,000 to 45,000 ft/sec with mission termination by Earth

Fig. 2-39. MISSION WINDOWS FOR EARTH-MERCURY TRANSFER VIA VePFB

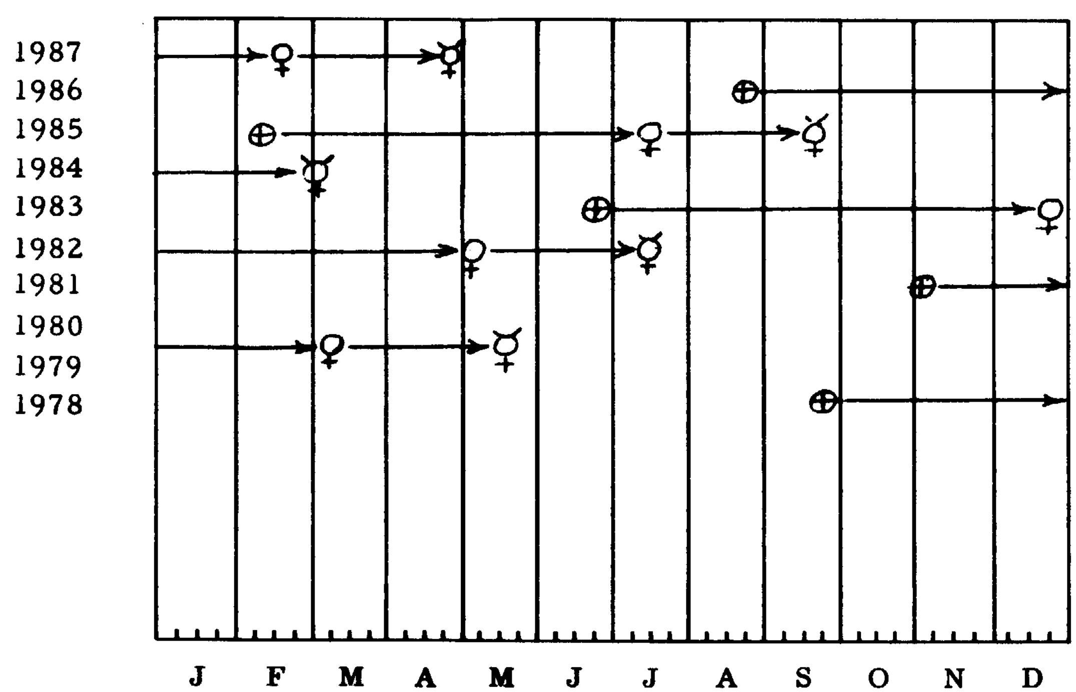

atmospheric entry at 40,000 to 45,000 ft/sec. This enormous saving, compared to a mono-elliptic round-trip mission profile (cf. Tab. 2-20) is bought at the expense of very long Mercury capture periods, because of the long synodic period between Venus and Earth and long transfer periods both ways.

It is, therefore, most likely more practical to combine a favorable mono-elliptic transfer condition one way with a favorable VePFB transfer window the other way. In this case the overall round-trip mission velocity should lie between 60,000 and 80,000 ft/sec for hyperbolic Earth entry velocity of 50,000 ft/sec, instead of 100,000 to 110,000 ft/sec, and correspondingly for terminal Earth orbital capture.

2.4.3 Interaction with the Gravitational Fields of Jupiter and Saturn

Fig. 2-40 shows the positions of Jupiter and Saturn in the 1970-2000 period. Both planets have orbits of low inclination and low eccentricity. Transfer orbit computations show that the effect of eccentricity supersedes that of inclination for both planets. Arrival near the respective perihelion produces favorable transfer conditions, whereas comparatively unfavorable conditions exist upon arrival near the aphelion. A "boomerang" mission is shown with the orbit involving a retrograde circum-navigation of Jupiter at a closest distance of about 11.7 Jupiter radii (i.e. between the Moons J II and J III). The transfer period Earth-Jupiter and back is approximately 1.9 years each, Shorter mission periods are obtained by circum-navigating Jupiter more closely. A "slingshot" mission to Saturn is shown, involving use of the Jovian gravitational field for the purpose of reducing the transfer time to Saturn at no or little additional propellant cost. For heliocentric parabolic transfer from Earth to Jupiter (1.1 year transfer time) a gain of 40,000 ft/sec (from 60,600 ft/sec heliocentric approach velocity to 100,200 ft/sec after the hyperbolic encounter) is obtained. The vehicle is now hyperbolic with respect to Sun with a heliocentric hyperbolic excess of 80,000 ft/sec.

Fig. 2-41 shows the positions of Uranus and Neptune which during the 1970 to 2000 period cover only a relatively small portion of their respective orbits. As time progresses during this period, Uranus moves away from its perihelion, Neptune moves away from its aphelion. Jupiter or Saturn can be used to reduce the flight time to Uranus or Neptune. The use of Jupiter's gravitational field for reducing the mission energy to Saturn is possible in the years 1976-1979 and perhaps 1980 and then again in 1995-1999. For reaching Uranus, Jupiter's field can be used in 1978-1980 and 1991-1993, Saturn's field in 1978-1982 and then again after 2000. For reaching Neptune, Jupiter's field can be used in 1978-1980 and 1002-1994, Saturn's field in 1975-1978 and thereafter beyond 2000. Thus Jupiter, besides being more

POSITIONS OF JUPITER & SATURN 1970-2000
POSITIONS REFER TO BEGINNING YEAR INDICATED

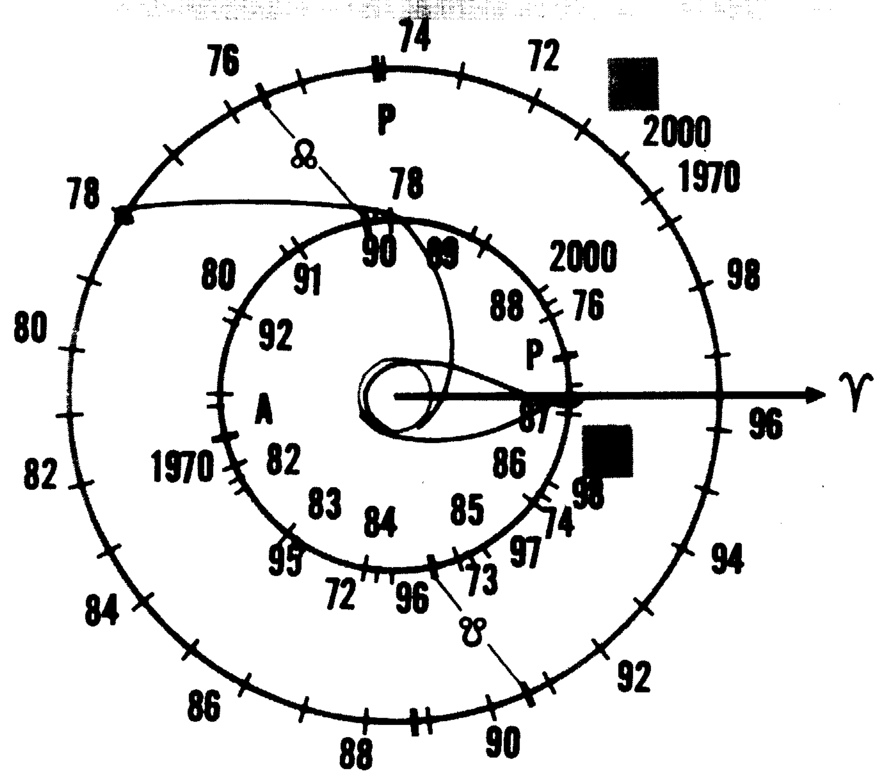

Fig. 2-40

POSITIONS OF JOVIAN PLANETS 1970 2000 — POSITIONS REFER TO THE BEGINNING OF THE YEAR INDICATED

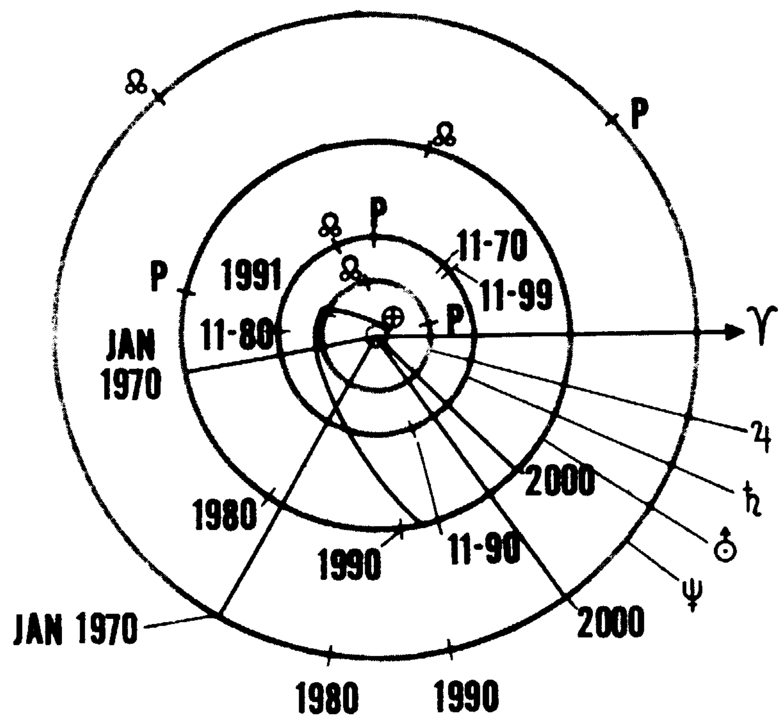

Fig. 2-41

effective, is also comparatively more frequently available. In fact, for all practical purposes Saturn is not at all available in this century when space technology has reached a level at which such missions can be considered. If a powered maneuver is carried out during Jupiter fly-by, the available time period can be extended in both directions.

2.5 BI-PLANET CAPTURE MISSIONS

Bi-planet capture missions require less stringent timing than capture/ fly-by missions, since capture periods are inserted between transfers which permit adaptation of the overall mission profile to favorable transfer windows between any two planets and Earth. The philosophy underlying the bi-planet capture missions is simply that, if a favorable transfer window does not exist between planets A and B, it may exist between A and C, and subsequently between C and B.

Tab. 2-22 shows three characteristic bi-elliptic capture mission profiles in the inner solar system. A favorable mission window for an Ea-Ma-Ve-Ea round-trip mission exists in 1975. In 1978 it is more advantageous to reverse the sequence. It is seen that the mission periods are longer (600 to 740 d) than for mono-elliptic Mars or Venus round-trip missions (400 to 450 d), but the mission velocities are not larger than those found for mono-elliptic Mars missions with 40,000 to 50,000 ft/sec Earth entry velocity (cf. Fig. 2-27).

The Ea-Ve-Me-Ea mission actually results in a shorter mission period and a lower mission velocity than mono-elliptic round-trip missions to Mercury. This is a particularly favorable case. While the mission velocity, as a rule can be held to 90,000-95,000 ft/sec, compared to 100,000-110,000 ft/sec for mono-elliptic missions (for both modes the hyperbolic entry velocity was limited to 50,000 ft/sec), the mission period is longer or shorter, depending on the specific Mercury departure conditions.

These examples, which are representative as far as mission velocities are concerned, show that for bi-planet capture missions involving Venus and Mars, mission velocities are of the order of 60,000 to 70,000 ft/sec. Shorter transfer orbits tend to increase the mission velocity without significantly (if at all) reducing the mission period, so long as favorable transfer corridors are to be used at all, because the increased capture period resulting from waiting for the favorable transfer corridor to the next planet about eliminates any time gain. The possibilities for reducing the mission period of bi-planet capture missions are in general far more limited than those available to one-planet round-trip missions.

Bi-planet capture missions involving Venus and Mercury require mission velocities of 90,000 to 95,000 ft/sec and, therewith indicate a velocity saving compared to mono-elliptic Mercury mission profiles.

Tab. 2-22. **THREE BI-PLANET CAPTURE MISSION PROFILES**

Earth-Mars-Venus-Earth, 1975-1977

EaDD	10-5-75	**MaAD**	3-13-76	**MaDD**	4-20-76	**VeAD**	10-27-76	**VeDD**	12-30-76	**EaAD**	6-8-77	**Total:**
	4-2690.5		4-2850.5		4-2888.5		4-3078.5		4-3142.5		4-3302.5	**Mission Period T = 612 d**
T_t (d)	160	$v^*_{\infty 2}$	0.1754	T_t	190	$v^*_{\infty,4}$	0.2340	T_t	160	$v^*_{\infty 6}$	0.1096	**Mission Vel. (impulsive)**
$v^*_{\infty,1}$	0.1760	Δv_2	12,191 (3.717)	$v^*_{\infty,3}$	0.1797	Δv_4	16,600 (5.060)	$v^*_{\infty,5}$	0.1639	v^*_E	0.389	**69,928 ft/sec**
Δv_1 (ft/sec)(km/sec)	14,237 (4.34)	($n = 1$; $r^* = 1.3$)		Δv_3	(13,900)(4.238)	($n = 1$, $r^* = 1.1$)		Δv_5	13,000 (3.97)	v_E	39,000 (11.9)	**21.33 km/sec**
($r^* = 1.1$)		T_{cpt} (d)	38	($n = 1$; $r^* = 1.3$)		T_{cpt}	64	($n - 1$, $r^* = 1.1$)				

Earth-Venus-Mars-Earth, 1978-1980

EaDD	8-29-78	**VeAD**	12-27-78	**VeDD**	4-10-79	**MaAD**	10-27-79	**MaDD**	1-11-80	**EaAD**	9-7-80	**Total:**
	4-3759.5		4-3869.5		4-3973.5		4-4173.5		4-4249.5		4-4489.5	**Mission Period T = 740 d**
T_t (d)	110	$v^*_{\infty 2}$	0.1639	T_t	200	$v^*_{\infty,4}$	0.1454	T_t	250	$v^*_{\infty,6}$	0.3116	**Mission Vel. (impulsive)**
$v^*_{\infty,1}$ (EMOS)	0.1043	Δv_2	13,400 (4.1)	$v^*_{\infty,3}$	0.2098	Δv_4	10,300 (3.15)	$v^*_{\infty,5}$	0.1893	v^*_E	0.49	**64,900 ft/sec**
Δv_1 (ft/sec)(km/sec)	12,000 (3.66)	($n = 1$; $r^* = 1.1$)		Δv_3	15,700 (4.8)	($n = 1$; $r^* = 1.3$)		Δv_5	13,500 (4.12)	v_E	47,900 (14.6)	**19.83 km/sec**
($r^* = 1.1$)		T_{cpt} (d)	104	($n = 1$; $r^* = 1.1$)		T_{cpt}	76	($n = 1$; $r^* = 1.3$)				

Earth-Venus-Mercury-Earth, 1986-1987

EaDD	8-20-86	**VeAD**	12-8-86	**VeDD**	2-18-87	**MeAD**	4-29-87	**MeDD**	4-29-87	**EaAD**	9-12-87	Total:
	4-6662.5		4-6772.5		4-6844.5	4-691	4-6914.5		4-6960.5		4-7050.5	Mission Period T = 396 d
T_t (d)	110	$v^*_{\infty 2}$	0.1808	T_t	70	$v^*_{\infty,4}$	0.1905	T_t	90	$v^*_{\infty,6}$	0.47	Mission Vel. (impulsive)
$v^*_{\infty,1}$ (EMOS)	0.0979	Δv_2	13,900 (4.25)	$v^*_{\infty,3}$	0.2609	Δv_4	13,500 (4.12)	$v^*_{\infty,5}$	0.25	v^*_E	0.63	88,800 ft/sec
Δv_1 (ft/sec)(km/sec)	11,500 (3.5)	($n = 1$; $r^* = 1.1$)		Δv_3	18,350 (5.6)	($n = 1$, $r^* = 1.1$)		Δv_5	18,600 (5.67)	Δv_6	13,000 (3.96)	27.10 km/sec
($r^* = 1.1$)		T_{cpt} (d)	82	($n = 1$; $r^* = 1.1$)		T_{cpt}	44	($n = 1$; $r^* = 1.1$)		(for $v^*_E = 0.50$	15 km/s)	

3. TRANSPORTATION METHODOLOGY

Transportation of a payload from Earth surface to the destination is divided into three principal transportation phases, as shown in Tab. 3-1.

The Earth-to-orbit logistic phase is necessary to render the interorbital space vehicle (ISV) space-borne and, if necessary, to carry out orbital assembly and fueling. No comparison of Earth launch vehicles (ELV's) is carried out in this report. Three ELV's are defined in Tab. 1-1. They are regarded as representative of the Earth-to-orbit transportation capability from the early seventies to the late eighties.

Transportation from Earth satellite orbit into an orbit about the target represents the primary mission in terms of duration and frequently also in terms of velocity requirement. In fact, the terms mission period and mission velocity refer to this interorbital portion of the mission in cislunar or heliocentric space. The transportation vehicles for this phase are referred to as ISV, cislunar ISV's (CISV) for lunar missions and heliocentric ISV's (HISV) for interplanetary missions.

The vicinity of the target body represents the general destination of the ISV. Depending on the overall mission objective, secondary missions (sub-missions) may have to be undertaken. The three possible types of secondary missions are listed in Tab. 3-1. A separate DSV is considered for these secondary missions. At least some of these missions could be carried out by the ISV proper, especially excursions from the capture orbit into one or several different orbits, and excursions to a planetary moon. However, unless the specific impulse of the ISV is very high, it does not pay (i.e. causes an unnecessary degradation of the ISV's payload fraction) to maneuver the large vehicle and its heavy operational payload any more than necessary.

In a mission leading directly to a moon of the target planet, the definition of the planetary moon excursion as a secondary mission does not apply. In such case it is presumed that the moon, rather than a capture orbit, represents the target of the ISV.

On the basis of various planetary mission studies it does not appear that DSV's represent a particular bottleneck or pace setter for the feasibility of manned planetary missions, so far as propulsion system selection is concerned. The pace setting characteristics refer primarily to surface excursion vehicles and are rather due to the implications of a so far largely unknown environment on the design criteria of the DSV.

Therewith, the scope of systems comparison in this report is based primarily on the ISV.

Tab. 3-1. TRANSPORTATION METHODOLOGY

Transportation Phase	Transportation Vehicle (TV)	Location	Mission	Payload
Destination	Destination Space Vehicle (DSV)	Target Body	Surface Excursion Orbital Excursion Planet Moon Excursion	Destination Payload
Interorbital	Interorbital Space Vehicle (ISV)	Cisluner or Heliocentric Space	Interorbital Transfer	Transport Payload Intransit Payload Operational Payload
Earth-to-Orbit	Earth Launch Vehicle (ELV)	Earth	Orbit Delivery	ISV

4. VEHICLE PROPULSION MODULE ANALYSIS

4.1 DEFINITION OF PROPULSION MODULES

Every transportation vehicle (TV) is broken down into propulsion modules (PM) and payload. In ELV's, a PM usually is identical with a stage. In ISV's the number of PM's is at least as large as the number of principal maneuvers of the mission; if the same engines are used for several maneuvers, the PM for all but the last of these maneuvers consists of jettisonable propellant containers. In other words, the engines, in this case, are counted in with the last of the series of maneuvers for which they are used. For the preceding maneuvers the wet inert weight reduction following each maneuver is restricted to the elimination of propellant containers and residuals.

If the velocity change for a maneuver is significantly larger than the exhaust velocity attainable by the PM involved (roughly, for factors in excess of 1.4 to 1.5) it pays to stage. This staging process may involve the jettisoning of a complete set of engine(s) and tankage; in which case the PM actually consists of more than one stage[1]; or it may involve the jettisoning of tankage only, or the jettisoning of engines only, during the maneuver.

Because of these variations it was found useful, conceptually speaking, to differentiate between a stage and a PM. In the subsequent discussion the "reference" PM will be regarded as consisting of propellant, propellant continers and thurst systems.

For analytical purposes, a PM, whether it is part of an Earth launch vehicle or an interorbital space vehicle, is divided into 3 portions:

useful propellant, W_p

wet inert weight, W_b

payload, W_λ

---

1) In this type of analysis it does not matter whether the stages are arranged in tandem or in parallel. If differences in structural weight per unit of propellant weight result between these two arrangements, they show up in the mass fraction x (cf. below)

where the useful propellant weight is defined as the propellant expended to execute a maneuver of ideal velocity change Δv_{id}, designating the sum total of actual velocity change plus the velocity equivalent of gravitational and drag losses, if any. If these losses are zero, the ideal velocity change becomes equal to the impulsive velocity change. Hence,

$$\Delta v_{id} = \Delta v_{imp} + \Delta v_g + \Delta v_d \tag{4-1}$$

the latter two terms on the right hand side representing the gravitational and drag loss components, respectively. Dividing Δv_{id} or Δv_{imp} by the weight/mass conversion factor g* yields

$$\tau = \Delta v_{id}/g^* \quad \text{or} \quad \Delta v_{imp}/g^* \tag{4-2}$$

which has the same dimension as the specific impulse I_{sp} (sec). The vehicle weight at the beginning of the maneuver may be W_A, at termination of the maneuver, W_B. Then the definition for W_p is

$$W_p = W_A - W_B = W_B\,(\mu - 1) = W_B\,(e^{\tau/I_{sp}} - 1) \tag{4-3}$$

where μ is the mass ratio

$$\mu = \frac{W_A}{W_B} = e^{\tau/I_{sp}} \tag{4-4}$$

4.2 SCALING COEFFICIENTS AND MASS FRACTION

The wet inert weight is the weight of the entire propulsion module plus residuals, i.e. the weight of the thrust system, tankage, plumbing and all other items which can be regarded as part of the propulsion system.

The (gross) payload is everything else. A definition of payloads is presented at the beginning of Par. 2-1.

The propulsion module consists of the wet inert weight and the useful propellant weight.

The following discussion refers to all vehicles except the nuclear (or solar) electric (NE) propulsion systems.

The wet inert weight consists of the thrust (F) dependent and the propellant dependent weight portions,

$$W_b = K_f F + K_p W_p \tag{4-5}$$

The propellant weight is a function of mass ratio, payload weight, thrust and the thrust and propellant dependent scaling coefficient,

$$W_p = \frac{(\mu-1)(W_\lambda + K_f F)}{1 - K_p(\mu-1)} \tag{4-6}$$

or, in terms of initial weight, where $W_\lambda / W_A = \lambda$, $F/W_A = n_o$ and $W_p/W_A = \Lambda$,

$$\Lambda = \frac{(\mu-1)(\lambda + K_f n_o)}{1 - K_p(\mu-1)} \tag{4-7}$$

This is a fundamental relation of the general analysis when based on scaling coefficients as an expression of the design characteristics of the propulsion module. Specifically, the thrust dependent scaling coefficient is defined by the relation

$$K_f = k_e + k_{ts} + k_{tsi} + k_{phi} + k_{c,f} \tag{4-8}$$

k_e = engine scaling coefficient

k_{ts} = thrust structure scaling coefficient

k_{tsi} = thrust structure insulation scaling coefficient

k_{phi} = propellant heating insulation coefficient

$k_{c,f}$ = contingency scaling coefficient ("future growth")

Propellant dependent scaling coefficient is

$$K_p = k_s + k_{tms} + k_{res} + k_{refrig} + k_{ss} + k_{c,p} \tag{4-9}$$

k_s = structures (tanks and adapters) scaling coefficients

k_{tms} = thermo-meteoroid shield scaling coefficient

k_{res} = residuals scaling coefficient

k_{refrig} = refrigeration (active propellant cooling) scaling coefficient

k_{ss} = subsystems (pressurization, propellant utilization etc.) scaling coefficient

$k_{c,p}$ = contingencies scaling coefficient

Both, K_f and K_p are not necessarily always expressed exactly in the form of the coefficients given in Eqs. (4-8) and (4-9); but, in one form or another, K_f and K_p contain all detail coefficients which ar e relevant for the particular propulsion module.

The mass fraction x of a PM is defined as ratio of wet inert weight to the sum of wet inert and useful propellant weight. While the mass fraction can be computed more accurately from the propellant and the thrust dependent scaling coefficients, it also offers a convenient way of estimating the weight of a propulsion module as function of the propellant weight only, if K_p and K_f are not known in detail from preceding design studies. The reason for this lies in the fact that x usually is less sensitive to variations in design than the scaling coefficients. The mass fraction for a "reference" PM is defined by the relations

$$x = \frac{W_p}{W_b + W_p} = \frac{1}{1 + W_b/W_p} = \frac{1}{1 + K_f \frac{F}{W_p} + K_p} \qquad (4\text{-}10a)$$

$$x = \frac{1}{1 + K_f n_o \frac{1}{\Lambda} + K_p} = \frac{1}{1 + K_p + K_f n_o \frac{\mu}{\mu - 1}} \qquad (4\text{-}10b)$$

$$x = \frac{1}{1 + K_p + K_f n_o \left(1 - e^{-\tau/I_{sp}}\right)^{-1}} \qquad (4\text{-}10c)$$

The term 1/x is used frequently in the subsequent relations.

If the PM for the particular maneuver consists of propellant containers only, it follows

$$x = \frac{1}{1 + K_p} \tag{4-10d}$$

If the PM for the particular maneuver consists of two or more stages, the maneuver must be subdivided into a number of sub-maneuvers ($\tau = \tau' + \tau'' + \ldots\ldots$), equal to the number of stages. For each of these stages, x is computed according to one of Eqs. (4-10a) through (4-10c) if the stages consist of engines and tankage; or according to Eq. (4-10d) if the staging process consists of jettisoning tankage during the maneuver; or according to

$$x = \frac{1}{1 + K_f \dfrac{F'}{W_p}} \tag{4-10e}$$

if the staging process consists of jettisoning thrust units F' units of thrust.

4.3 DEFINITION OF VEHICLE CONFIGURATIONS BY PROPULSION MODULE DESIGN

For the purpose of assuring conceptual precision, the following definitions are set forth in this paragraph, preceding the analysis of the payload fractions of these vehicles.

One-Stage vehicle: A vehicle possessing one complete propulsion module (for one or several maneuvers). No tankage or engines are jettisoned during a given maneuver or between any two maneuvers.

Multi-Stage vehicle: A vehicle possessing several complete propulsion modules, jettisoning a depleted module after each principal maneuver. Any one of these propulsion modules consists of one or more complete stages, arranged in tandem or in parallel. If the stages of a PM are arranged in parallel, it is assumed that the engines of all stages are burning at the beginning of the maneuver. In tandem arrangement, this assumption can, of course, not be made. This distinction has a bearing on the use of the graphs for mass fractions and payload fractions presented below in this report.

One-Stage, propellant tankage modularized vehicle: A vehicle possessing one thrust system which is used for the one or the number of maneuvers involved in the mission; but which jettisons depleted propellant containers between maneuvers, or even during a maneuver, in extreme cases.

Two-Stage, propellant tankage modularized vehicle: A vehicle consisting of two complete propulsion modules. The thrust system of one or of both PM's is used for a series of maneuvers; say, series A for PM-1 and series B for PM-2. PM-2 is part of the overall payload of PM-1 during maneuver series A which may consist of two principal maneuvers. Then, thrustors and tankage required to hold the useful propellant for the second maneuver are counted into the second maneuver which is followed by a staging of this portion of PM-1. Tankage is required to hold the useful propellant for the first maneuver, since this tankage is assumed to be jettisoned between the first and second maneuver. The procedure is analogous for the series B maneuvers.

Multi-Stage, propellant tankage modularized vehicle: A vehicle consisting of more than two complete propulsion modules. The thrust system of one or several of these modules is used for a series of maneuvers between which only tankage weight is eliminated[2].

One-Stage, engine modularized vehicle: A vehicle possessing one propellant container system which is used for one or the number of maneuvers involved in the mission; but which jettisons thrust units during or between maneuvers.

Two-Stage, or multi-stage, engine modularized vehicle: A vehicle consisting of two or more complete propulsion modules. One or several of these PM's are characterized by eliminating thrust units during or between principal maneuvers, whereas the propellant container system remains unchanged during the period of employment of the given PM.

Examples:

One-stage vehicles: Very advanced ELV's; ISV's of the nuclear pulse (NP), nuclear electric (NE) or gaseous core reactor (GCR) variety on missions whose total velocity is small enough so that τ / I_{sp} is well below one.

Multi-stage vehicles: Less advanced ELV's; ISV's with chemical drives or powered by solid core reactor, graphite based (SCR/G) engines on missions whose principal maneuvers are of such magnitude that engine operating life and post-cut-off cooling considerations suggest a complete propulsion module staging following each principal maneuver.

One-stage, propellant tankage modularized vehicle: Advanced ELV's; ISV's with NP, NE, GCR, long-duration SCR (e.g. SCR/W or SCR/N) and chemical (C) drives.

---

2) Payload weight may be eliminated also, but this is not relevant here.

Two-stage, or multi-stage, propellant tankage modularized vehicle: ISV's consisting of such combinations as C-NE, SCR/G-NE, SCR drives for all but one principal maneuver for which a chemical or solar heat exchanger (SHE) drive is employed, or a GCR/SCR combination for missions where high Earth departure weight makes the use of a high thrust GCR engine worthwhile for the first one or two maneuvers; but where the remaining mission maneuvers are handled more efficiently with smaller and lighter SCR engines[3)]

One-stage engine modularized vehicle: The Atlas ELV; chemical ISV's jettisoning engines during an extended maneuver, but retaining tankage for reasons of avoiding excessive complexity. Engine modularized vehicles are inherently a rarer species than tankage modularized vehicles.

The equations in the subsequent analysis reflect the distinctions defined in this paragraph.

4.4 One Stage Vehicle

The principal weights are the ignition weight, the cut-off weight (at the end of one of several maneuvers; or burn-out weight at propellant depletion and the net weight for a given maneuver:

ignition weight: $$W_A = W_b + W_p + W_\lambda \tag{4-11}$$

cut-off weight: $$W_B = W_A - W_p = W_b + W_R \tag{4-12}$$

net weight: $$W_N = W_b + W_p \tag{4-13}$$

where W_R designates the "remaining" weight of the vehicle at termination of the maneuver. In a one-maneuver vehicle, $W_R = W_\lambda$; in a multi-maneuver one-stage vehicle W_R contains the gross payload plus remaining propellant for the subsequent maneuvers (the associated hardware weight is part of W_b).

The gross payload fraction (GPF) is given by

$$\lambda = W\ /W_A = 1 - \frac{1 - 1/\mu}{x} = 1 - \frac{\Lambda}{x} \tag{4-14a}$$

---

3) Retaining very heavy thrust units too long involving excessive overall velocities can seriously degrade the payload fraction in spite of high specific impulse. This is particularly true in cases where a heavy thrust unit is retained until its weight becomes a significant fraction of the remaining propellant load.

$$\lambda = 1 - \frac{1}{x} \left(1 - e^{-\tau/I_{sp}} \right) \tag{4-14b}$$

$$\lambda = 1 - n_o K_f - \Lambda \left(1 + K_p\right) \tag{4-14c}$$

The mass fraction, in terms of payload fraction, is therefore given by

$$x = \frac{\Lambda}{1 - \lambda} \tag{4-15}$$

From the definition of the GPF (first of Eq. (4-19a)) it follows that W_A can be computed once the GPF and the weight W_λ are known. This, of course, yields the correct ignition weight only, if the GPF does not vary during the mission.

Suppose, the mission consists of 4 maneuvers, M-1 through M-4; for instance, a cislunar round-trip mission with payload delivery into a circumlunar capture orbit. Then, this being a single-stage vehicle, the Earth orbit departure and lunar capture maneuver velocities can be added up and treated, in effect, as one maneuver. The same can be done with the lunar departure and Earth arrival maneuver. This results in two combination maneuvers, Δv_{12} and Δv_{34} with the ignition weights W_{A1} at Earth orbit departure and W_{A4} at M-4 ignition. Let the gross payload (GP) at the latter point be $W_{\lambda 4}$. Then the associated GPF is

$$\lambda_4 = W_{\lambda 4}/W_{A4} \tag{4-16a}$$

Neglecting any small payload changes during the cislunar return flight, it is then

$$\lambda_3 = \frac{W_{A4}}{W_{A3}} = \frac{W_{\lambda 4} + W_{p4}}{W_{A3}} \tag{4-16b}$$

and

$$W_{A3} = \frac{W_{\lambda 4}}{\dfrac{W_{\lambda 4}}{W_{A4}} \quad \dfrac{W_{A4}}{W_{A3}}} = \frac{W_{\lambda 4}}{\lambda_4 \ \lambda_3} \tag{4-16c}$$

Let the payload eliminated between maneuvers 3 and 2 be $D_{\lambda 2}$. Now

$$\lambda_2 = \frac{W_{A4} + W_{p3} + D_{\lambda 2}}{W_{A2}} = \frac{W_{A3}}{W_{A2}} \left(1 + \frac{D_{\ 2}}{W_{A3}} \right) \tag{4-16d}$$

$$W_{A2} = \frac{W_{\lambda 4}}{\lambda_4 \lambda_3 \lambda_2} \left(1 + \lambda_4 \lambda_3 \frac{D_{\lambda 2}}{W_{\lambda 4}}\right) \quad (4\text{-}16e)$$

and, neglecting again small changes in payload during outbound cislunar transfer

$$\lambda_1 = \frac{W_{A2}}{W_{A1}} \quad (4\text{-}16f)$$

$$W_{A1} = \frac{W_{A2}}{\lambda_1} = \frac{W_{\lambda 4}}{\lambda_4 \lambda_3 \lambda_2 \lambda_1} \left(1 + \lambda_4 \lambda_3 \frac{D_{\lambda 2}}{W_{\lambda 4}}\right) \quad (4\text{-}16g)$$

The Earth orbital departure weight (ODW) is, in this case found from the product of the gross payload fractions for the individual maneuvers, the GP for the terminal maneuver and the ratio of delivered payload to GP for the terminal maneuver. If the latter is zero, Eq. (4-19b) is simplified to the case of a multi-stage vehicle with constant payload.

4.5 MULTI-STAGE VEHICLE

Overall propellant weight of vehicle,

$$W_p = W_{p1} + W_{p2} + W_{p3} + \ldots\ldots\ldots = \Sigma W_p \quad (4\text{-}17a)$$

Overall wet inert (primarily, hardware) weight of vehicle

$$W_b = W_{b1} + W_{b2} + W_{b3} + \ldots\ldots$$

$$= W_{p1} \left(\frac{1}{x_1}\right) - 1 \quad + W_{p2} \left(\frac{1}{x_2} - 1\right) + W_{p3} \left(\frac{1}{x_3} - 1\right) + \ldots \text{(etc.)} \quad (4\text{-}17b)$$

Overall vehicle propellant fraction

$$\Lambda = \Sigma W_p / W_{A1} \quad (4\text{-}17c)$$

Overall mass ratio

$$\mu = \mu_1 \ \mu_2 \ \mu_3 \ \ldots\ldots = \Pi \mu \quad (4\text{-}17d)$$

Overall payload fraction

$$\lambda = \lambda_1 \; \lambda_2 \; \lambda_3 \; \ldots\ldots = \Pi\,\lambda = \Pi\left[1 - 1/x\left(1 - e^{-\tau/I_{sp}}\right)\right] \tag{4-17e}$$

provided that the last maneuver GP, $W_{\lambda n}$, is unchanged throughout the mission, so that the ODW can be found from $W_{A1} = W_{\lambda n}/\Pi\,\lambda$.

Assuming a mission consisting of 4 principal maneuvers, and a payload change D_λ after the first, second and third maneuver, the value of W_{A1} is found with the following relations

$$W_{A4} = \frac{W_{\lambda 4}}{\lambda_4} \tag{4-18a}$$

$$W_{A3} = \frac{W_{\lambda 4}}{\lambda_4 \; \lambda_3}\left(1 + \lambda_4 \; \frac{D_{\lambda 3}}{W_{\lambda 4}}\right) \tag{4-18b}$$

$$\frac{W_{\lambda 4}}{W_{A3}} = \frac{\lambda_4 \; \lambda_3}{1 + \lambda_4 \; \dfrac{D_{\lambda 3}}{W_{\lambda 4}}} \tag{4-18c}$$

$$W_{A2} = \frac{W_{\lambda 4}}{\lambda_4 \; \lambda_3 \; \lambda_2}\left(1 + \lambda_4 \; \frac{D_{\lambda 3}}{W_{4}}\right)\left(1 + \frac{D_{\lambda 2}}{W_{\lambda 4}} \; \frac{W_{\lambda 4}}{W_{A3}}\right) \tag{4-18d}$$

$$\frac{W_{\lambda 4}}{W_{A2}} = \frac{\lambda_4 \; \lambda_3 \; \lambda_2}{\left(1 + \lambda_4 \; \dfrac{D_{\lambda 3}}{W_{\lambda 4}}\right)\left(1 + \dfrac{D_{\lambda 2}}{W_{\lambda 4}} \; \dfrac{W_{\lambda 4}}{W_{A3}}\right)} \tag{4-18f}$$

$$W_{A1} = \frac{W_{\lambda 4}}{\lambda_4 \; \lambda_3 \; \lambda_2 \; \lambda_1}\left(1 + \lambda_4 \; \frac{D_{\lambda 3}}{W_{\lambda 4}}\right)\left(1 + \frac{D_{\lambda 2}}{W_{\lambda 4}} \; \frac{W_{\lambda 4}}{W_{A3}}\right)\left(1 + \frac{D_{\lambda 1}}{W_{\lambda 4}} \; \frac{W_{\lambda 4}}{W_{A2}}\right) \tag{4-18g}$$

The inputs required are seen to be the terminal GP, $W_{\lambda 4}$, the product of the GPF's and the ratio of GP eliminated to terminal GP for each principal maneuver.

If any of the propulsion modules (PM) consists of two stages, say, PM-3, then, making the likely assumption that the payload remains constant, maneuver M-3 is divided into two consecutive sub-maneuvers for which the GPF's are

$$\lambda_3' = 1 - \frac{\Lambda_3'}{x_3'} \tag{4-19a}$$

$$\lambda_3'' = 1 - \frac{\Lambda_3''}{x_3''} \tag{4-19b}$$

and the GPF for M-3,

$$\lambda_3 = \lambda_3' \quad \lambda_3'' \tag{4-19c}$$

and analogously for more than two stages.

4.6 PROPELLANT TANKAGE MODULARIZED VEHICLES

If only propellant tankage is jettisoned between maneuvers, then the vehicle can be regarded as single-stage as far as the engines are concerned. The (propulsive) weight difference from one maneuver to the next is $W_p + K_p W_p$, whence, in this case the mass fraction becomes as defined in Eq. (4-10d) and the GPF for the maneuver preceding the jettisoning is

$$\lambda = 1 - \Lambda \ (1 + K_p) \tag{4-20a}$$

except for the last maneuver for which Eq. (4-14c) applies.

If the (non-propulsive) payload varies, the ODW of the vehicle is computed according to Eqs. (4-18).

If tankage is jettisoned during a given maneuver, then, assuming constant payload, the maneuver is divided into the respective sub-maneuvers for which the GPF's are

$$\lambda' = 1 - \Lambda' \ (1 + K_p') \tag{4-20b}$$

$$\lambda'' = 1 - \Lambda''(1 + K_p'') \tag{4-20c}$$

etc., resulting in a GPF for the individual maneuver of

$$\lambda = \lambda' \ \lambda'' \ \ldots\ldots. \tag{4-20d}$$

4.7 ENGINE MODULARIZED VEHICLES

If engines only are jettisoned between maneuvers, the (propulsive) weight difference from one maneuver to the next is $W_p + K_f F'$ where F' is the thrust of jettisoned engines. The mass fraction is, in this case, defined by Eq. (4-10e). The GPF for the maneuver preceding the jettisoning of the thrust system generating thrust F' is

$$\lambda = 1 - \Lambda \ (1 + K_f F) = 1 - \Lambda \left(1 + \frac{K_f \ n_o}{\Lambda}\right) \tag{4-21}$$

For the last maneuver Eq. (4-14c) applies. If engines are jettisoned during a given maneuver, the analysis is analogous to that of Eqs. (4-21).

4.8 EQUIVALENT MASS FRACTION

For a given type of PM, an average value of mass fraction can be determined for a specified size range, within which this mass fraction yields representative values of GPF or W_b.

Similarly, for a given vehicle type an average value of equivalent mass fraction, x_{eq}, can be determined for a specified size range and mission range, within which this equivalent mass fraction yields representative values of overall vehicle GPF. This equivalent mass fraction is given by the equation

$$x_{eq} = \frac{\Sigma W_p / W_{A1}}{1 - W_\lambda / W_{A1}} \tag{4-22a}$$

By evaluating this equation for a sufficient number of ISV's of given type for a given mission type, a characteristic value of x_{eq} can be determined. Using this value, the representative GPF of an ISV of given type is found from

$$\lambda = 1 - \frac{\Lambda}{x_{eq}} \tag{4-22b}$$

where Λ is defined by Eq. (4-17c).

The ISV propulsion systems to be compared in this report are listed in Par. 1.4. They are discussed individually in the subsequent paragraphs. The chemical drive is restricted to O_2/H_2.

4.9 CHEMICAL PROPULSION MODULES

Chemical propulsion (C) is represented by a system of the following specifications:

- Propellant: O_2/H_2
- Mixture ratio: 5:1
- LH_2 tank: Titanium
- LO_2 tank: Steel
- Nominal LH_2 tank pressure: 26 psia
- Nominal LO_2 tank pressure: 32 psia

The ratio $W_b/W_p = K_f (F/W_p) + K_{p,1} + K_{p,2}$ (4-23)

$$K_{p,1} = k_{tms} + k_{refrig} \tag{4-24a}$$

$$K_{p,2} = k_s + k_s + k_{ss} + k_{c,p} \tag{4-24b}$$

The variation of $K_{p,1}$, $K_{p,2}$ and K_f with W_p is shown in Fig. 4-1 and can be represented by the equation

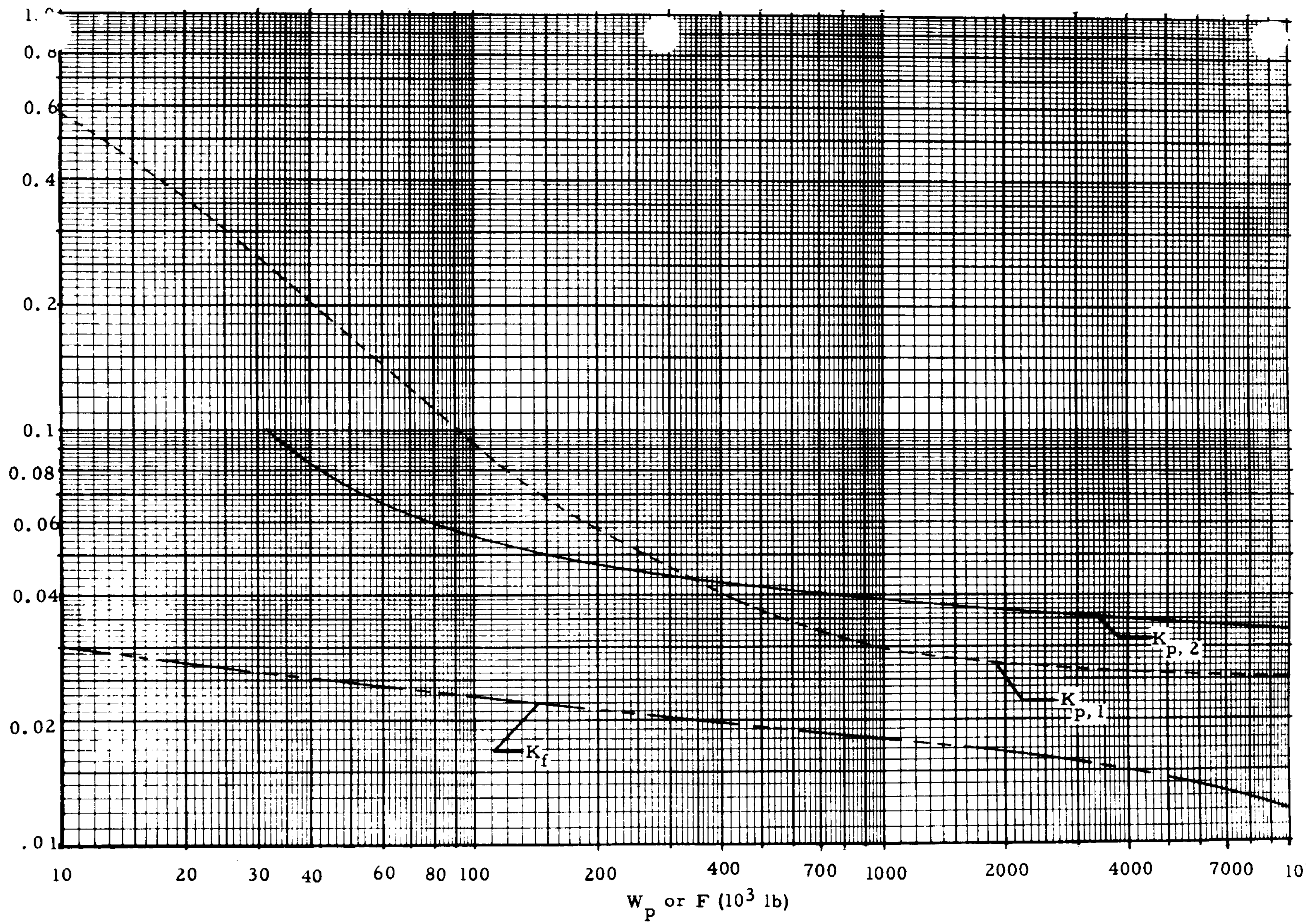

Fig. 4-1 VARIATION OF SCALING COEFFICIENTS FOR CHEMICAL HISV

$$K_{p,1} = 0.057 \left(\frac{200,000}{W_p}\right)^{0.79} \qquad (2 \cdot 10^4 \leq W_p \leq 2 \cdot 10^5 \text{ lb}) \tag{4-25}$$

$$K_{p,1} = 0.029 \left(\frac{10^6}{W_p}\right)^{0.42} \qquad (2 \cdot 10^5 \leq W_p \leq 10^6 \text{ lb}) \tag{4-26}$$

$$K_{p,1} = 0.025 \left(\frac{10^7}{W_p}\right)^{0.079} \qquad (10^6 \leq W_p \leq 10^7 \text{ lb}) \tag{4-27}$$

$$K_{p,2} = 0.049 \left(\frac{200,000}{W_p}\right)^{\frac{12,000}{W_p}} \qquad (2 \cdot 10^4 \leq W_p \leq 2 \cdot 10^5 \text{ lb}) \tag{4-28}$$

$$K_{p,2} = 0.033 \left(\frac{10^7}{W_p}\right)^{0.134} \qquad (2 \cdot 10^5 \leq W_p \leq 10^7 \text{ lb}) \tag{4-29}$$

$$K_f = 0.0145 \left(\frac{10^7}{F}\right)^{0.09} \qquad (10^4 \leq F \leq 10^7 \text{ lb}) \tag{4-30}$$

Therewith Eq. (4-23) assumes the form

$$W_b/W_p = 0.0145 \frac{F}{W_p} \left(\frac{10^7}{F}\right)^{0.09} + a \left(\frac{A}{W_p}\right)^y + d \left(\frac{D}{W_p}\right)^z \tag{4-31}$$

where the second and third term on the right hand side represent any one of the equations for $K_{p,1}$ and $K_{p,2}$, respectively. The mass fraction follows then from the second Eq. (4-10a). With the aid of Eq. (4-10c) an alternate relation can be defined for W_b/W_p,

$$W_b/W_p = a \left(\frac{A}{W_p}\right)^y + d \left(\frac{D}{W_p}\right)^z + 0.0145\, n_o \left(\frac{10^7}{F}\right)^{0.09} \left(1 - e^{-\tau/I_{sp}}\right) \tag{4-32}$$

A suitable value for n_o is readily selected. A value or a limited range of W_p values may be selected with respect to constraints imposed by a given ELV transport capability. For chemical vehicles the propellant weight is 70 to 80 percent of the weight of a stage. The thrust F should, therefore, be about 50 percent of the local weight of the stage. Therewith W_b/W_p and x become a function of the performance parameters τ and I_{sp} only.

Since the exponent of Eq. (4-30) is very small, the term in parenthesis is always close to one. This approximation is true with even more accuracy if the coefficient 0.0145 is replaced by 0.02. Therewith one can write

$$W_b/W_p \approx a\left(\frac{A}{W_p}\right)^y + d\left(\frac{D}{W_p}\right)^z + 0.02\, n_o \left(1 - e^{-\tau/I_{sp}}\right) \tag{4-33}$$

thus eliminating functional dependency upon F. By specifying n_o, it is now possible to correlate W_b/W_p or x with W_p and τ/I_{sp}; one being the independent, the other the parametric variable. Assuming that the thermal/meteoroid shield is jettisonable, the mass fraction should be determined under the condition of $a\,(A/W_p)^y = 0$. For this condition and for $n_o = 0.4$, the variation of x with W_p is shown in Fig. 4-2 for two values of τ/I_{sp}.

4.10 SOLAR HEAT EXCHANGER (SHE) PROPULSION MODULES

In this vehicle, the SHE drive is applied to the PB maneuver. Mass fractions (rather than scaling coefficients) were developed for the SHE drive under the following nominal specifications:

- Nominal operating distance: 0.6 AU
- Nominal thrust value: 10 lb
- Efficiency of converter-heater system: 0.6
- Structure: Titanium
- Tank pressure: 17 psia
- Helium purge on the ground (if LH_2 fueled)
- Propellant: LH_2
- Efficiency of thrust unit: 0.70

For further details on the SHE drive cf. ref. 7.

Two cases were considered: One conservative design involving a non-jettisonable thermal meteoroid shield, represented by the relation

$$x = 0.712\left(\frac{W_p}{10,000}\right)^{0.059} \qquad \left(10^4 \le W_p \le 8 \cdot 10^4 \text{ lb}\right) \tag{4-34}$$

and one more advanced design with a jettisonable thermal/meteoroid shield, defined by the relation

$$x = 0.794\left(\frac{W_p}{10,000}\right)^{0.063} \qquad \left(10^4 \le W_p \le 8 \cdot 10^4 \text{ lb}\right) \tag{4-35}$$

Within the range of specific impulse $600 \le I_{sp} \le 800$ sec, the mass fraction is affected only to a negligible degree. Within this range of specific impulses the mass fraction is therefore considered invariant. Fig. 4-3 shows the variation of x with the propellant weight.

In the above equations the exponents are so small that the term in parenthesis varies only between 1.0 and 1.13 or 1.14, respectively, the range of propellant weights. One can, therefore, with fair accuracy put these terms equal to one if the factors are changed to the following values

$$x \approx 0.791 \text{ (non-jettisonable T/M shield)} \tag{4-36}$$

$$x \approx 0.887 \text{ (jettisonable T/M shield)} \tag{4-37}$$

For the chemical propulsion modules the data of Par. 4.4 are valid.

4.11 SOLID CORE REACTOR (SCR) PROPULSION MODULES

The distinguishing characteristics of different SCR powered vehicles refer to structural configuration as well as to the type of SCR engine.

Because these ISV's use LH_2, their mean density is low and volume limitation of ELV payload sections sometimes impose constraints before the ELV payload weight limitation does. For this reason, the structural configuration of SCR-ISV's is strongly influenced by ELV compatibility considerations.

In previous manned planetary exploration studies, two standardized designs for nuclear-powered HISV's were developed (ref. 8): one to be Saturn V Mod. compatible (Fig. 4-4), the other post-Saturn compatible (Fig. 4-5). Both were carefully evolved for maximum mission flexibility, mission safety and minimum structural weight commensurate with crew safety and cost considerations, including ELV compatibility. They are characterized by the predominance of clustered tanks. They are based on use with SCR/G engines of limited operational life, requiring a complete new stage for every principal maneuver.

For a Saturn V compatible HISV a single tank version was selected, shown in Fig. 4-6. For use with SCR engines of longer expected operating life, such as for the SCR/N and the SCR/W (cf. Par. 1-4), which require only propellant tank jettisoning following each principal maneuver another design was developed, briefly referred to as -23 Configuration, also shown in Fig. 4-7.

The scaling coefficients for the Saturn V Mod compatible standardized configuration are shown in Fig. 4-7 and 4-8. The standardized configurations are designed for three principal maneuvers: Earth departure (PM-1), target planet arrival (handled by PM-2) and target planet departure (PM-3). Powered fly-by maneuvers en route, perihelion brake maneuvers or Earth retro-

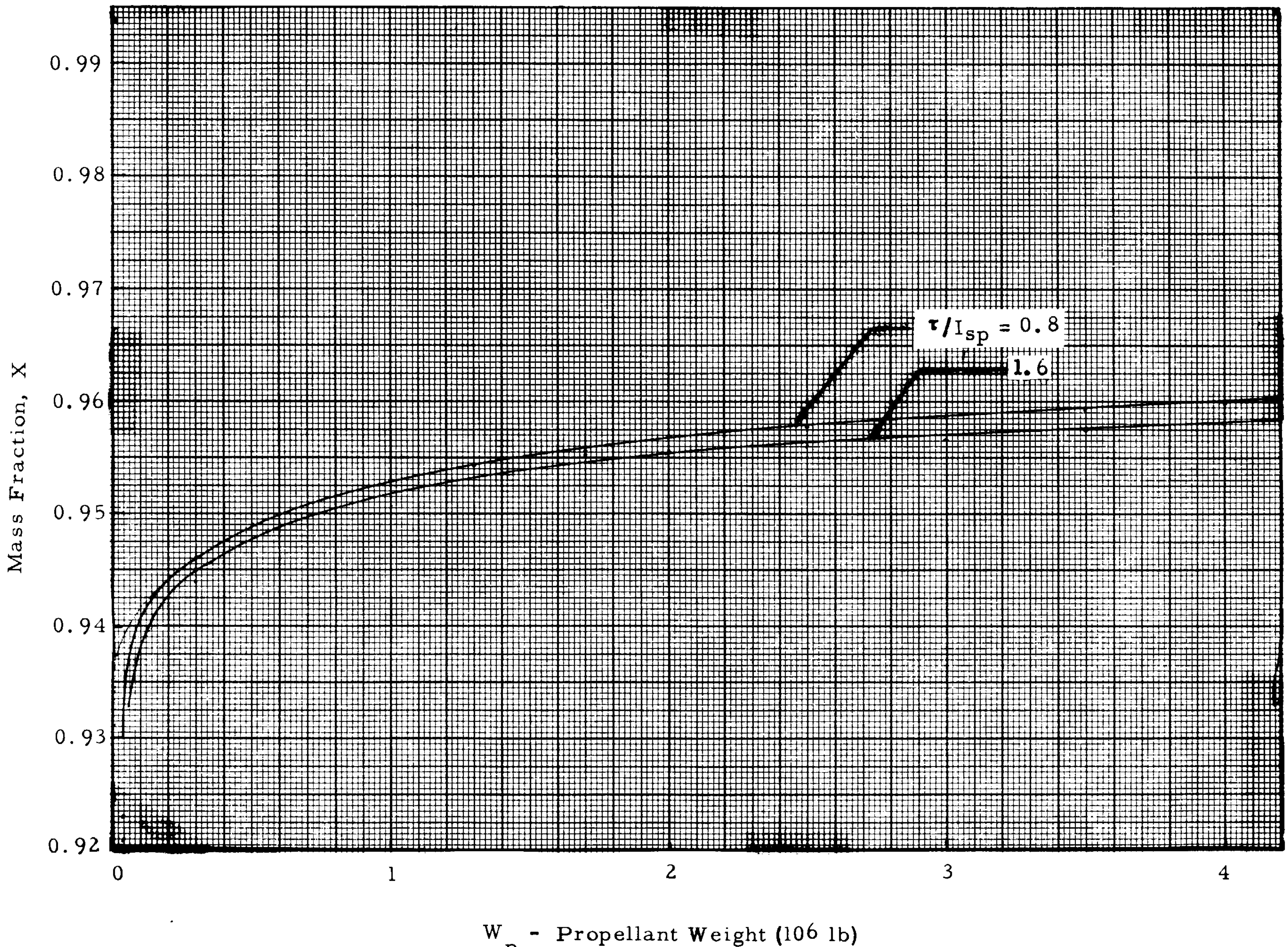

Fig. 4-2 CHEMICAL PROPULSION MODULE: VARIATION OF MASS FRACTION WITH PROPELLANT WEIGHT

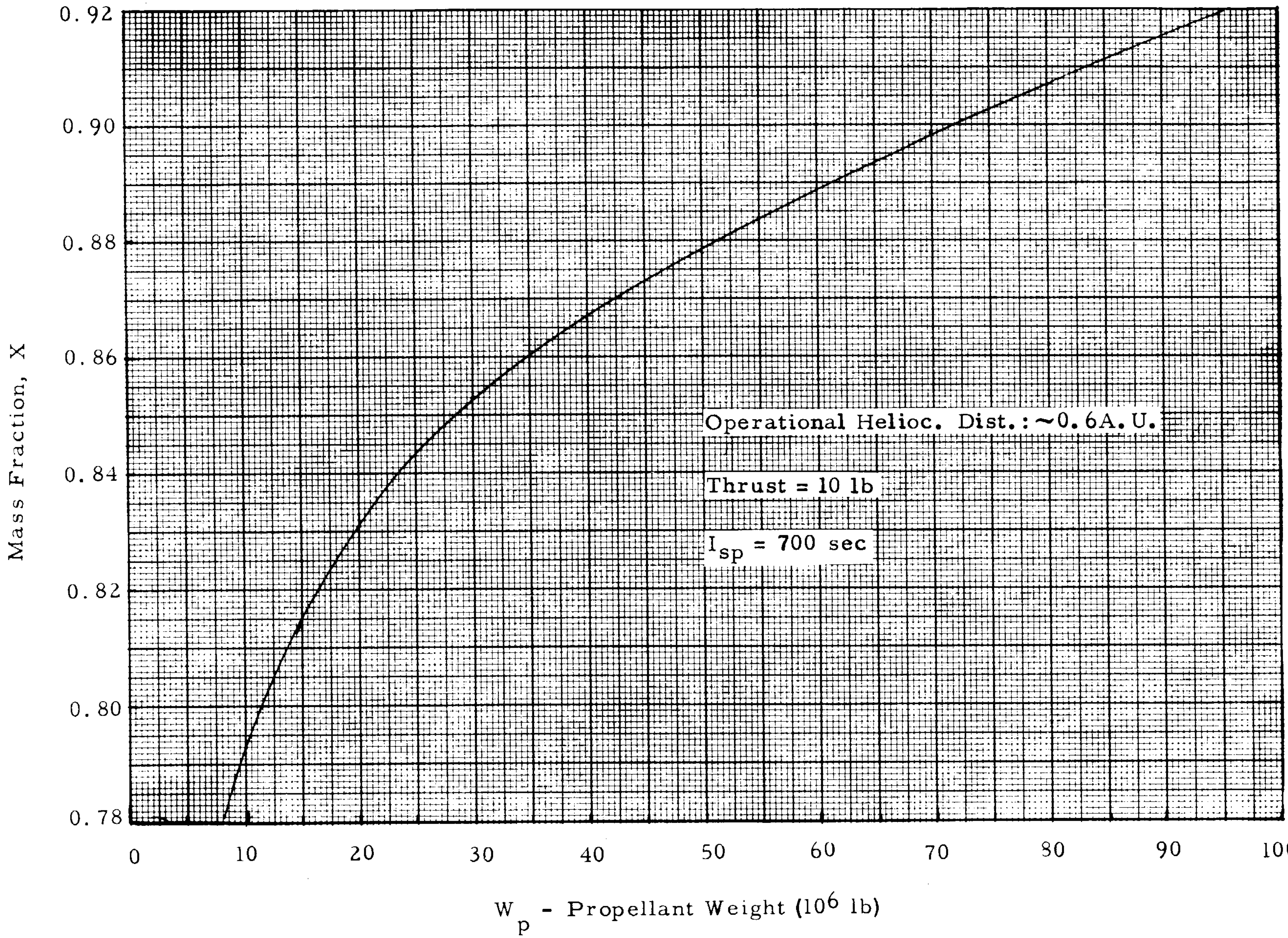

Fig. 4-3 SOLAR HEAT EXCHANGER PROPULSION MODULE: MASS FRACTION VS PROPELLANT WEIGHT

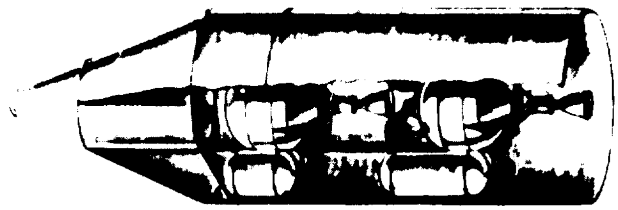

SERVICE

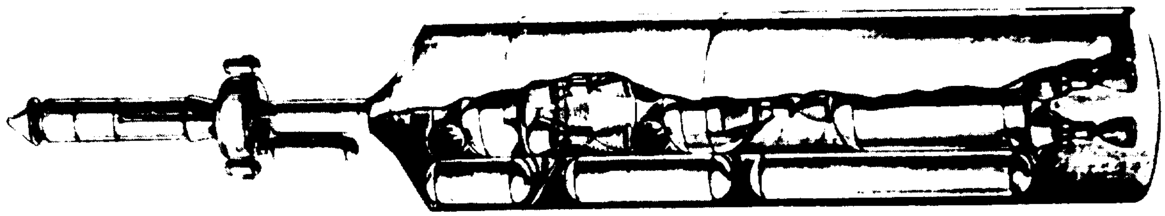

CREW

Nominal Mars Convoy Vehicle

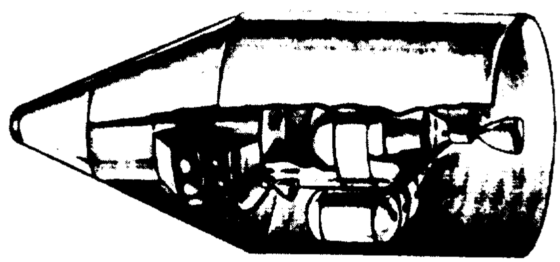

SERVICE

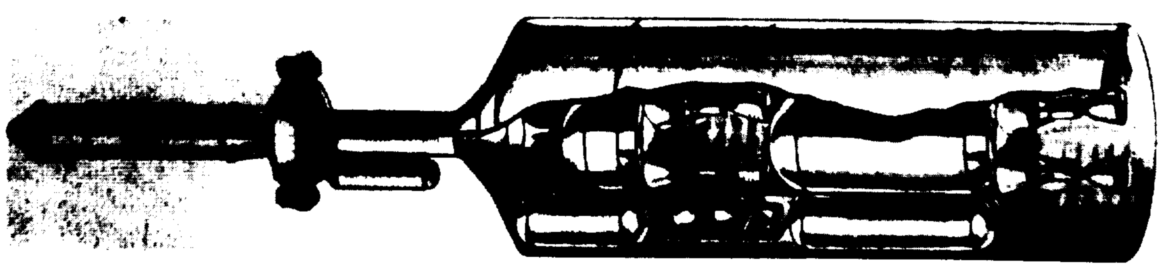

CREW

Nominal Venus Convoy Vehicle

Fig. 4-4 NOMINAL MARS AND VENUS CONVOY VEHICLES

SERVICE

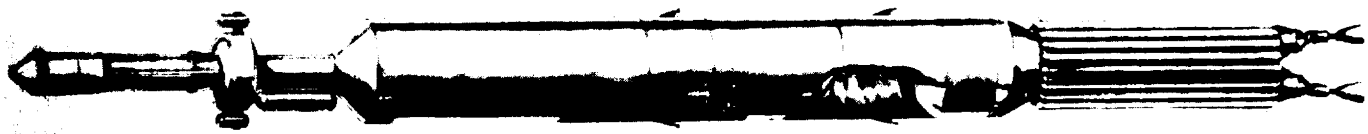

CREW

Fig. 4-5 NOMINAL VENUS CONVOY VEHICLE
(ELV: Adv. SATURN V)

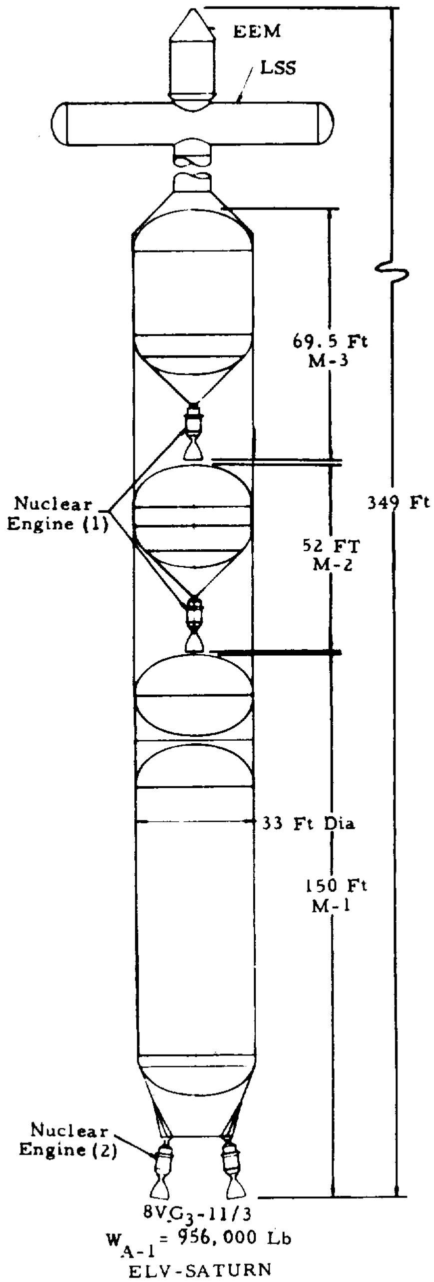

Saturn V Compatible HISV

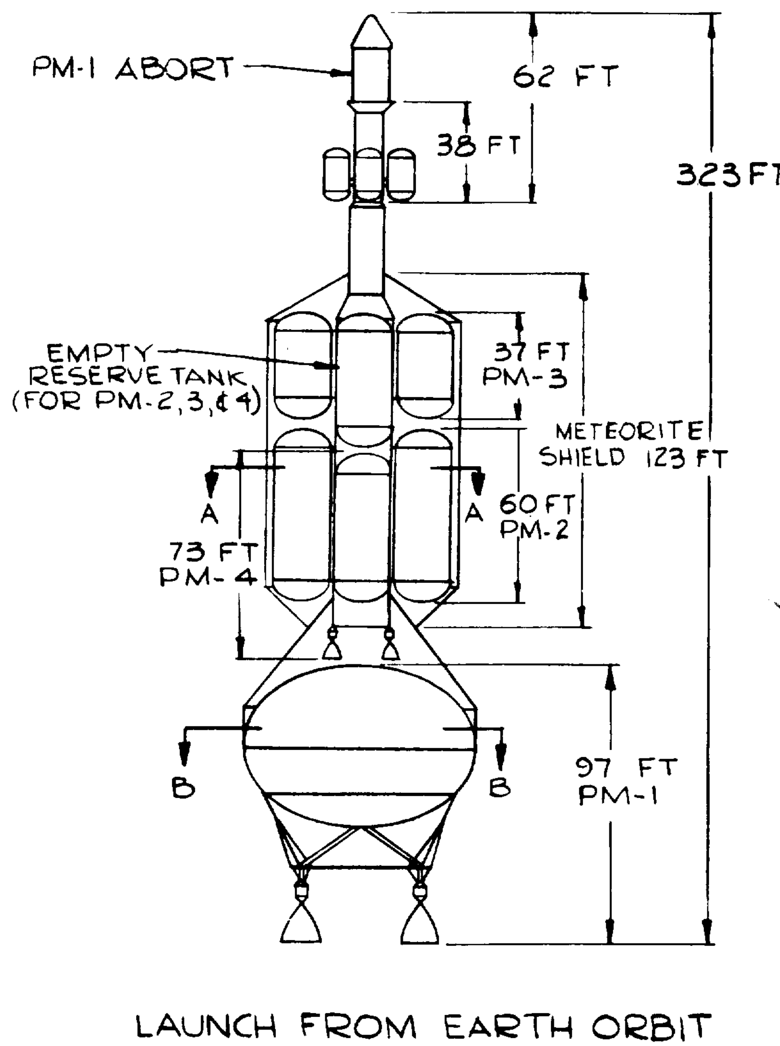

Configuration -23
(Post - Saturn Compatible)

Fig. 4-6 SATURN V COMPATIBLE HISV AND HISV-23 DESIGN BASED ON ONE SET OF NUCLEAR ENGINES FOR ALL MANEUVERS EXCEPT EARTH DEPARTURE

Fig. 4-7 SCR-ISV, SATURN V MOD. COMPATIBLE CONFIGURATION : K_p FOR W_{b2} & W_{b3}

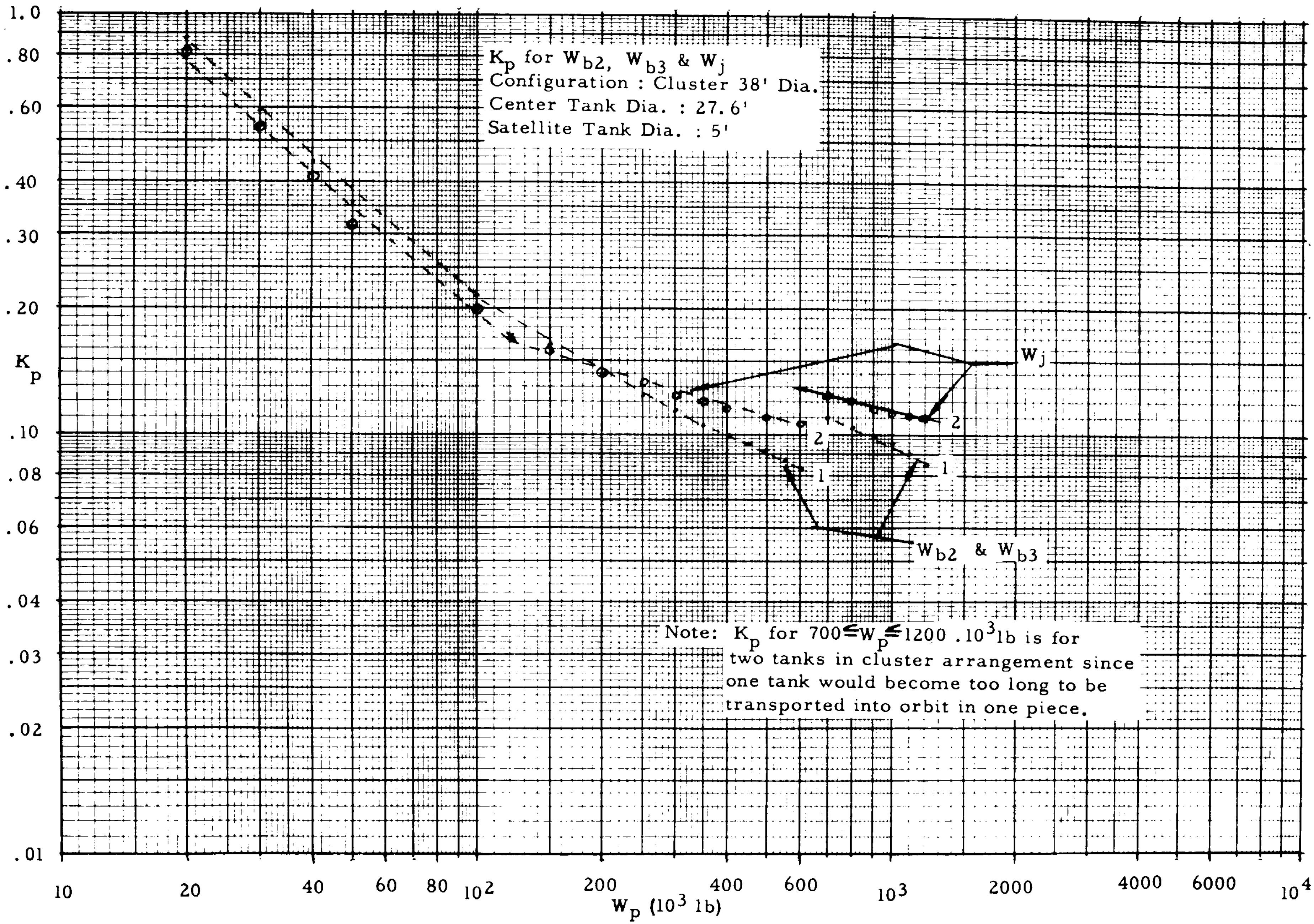

Fig. 4-8 SCR - ISV, SATURN V MOD. COMPATIBLE CONFIGURATION : K_p FOR W_{bl}

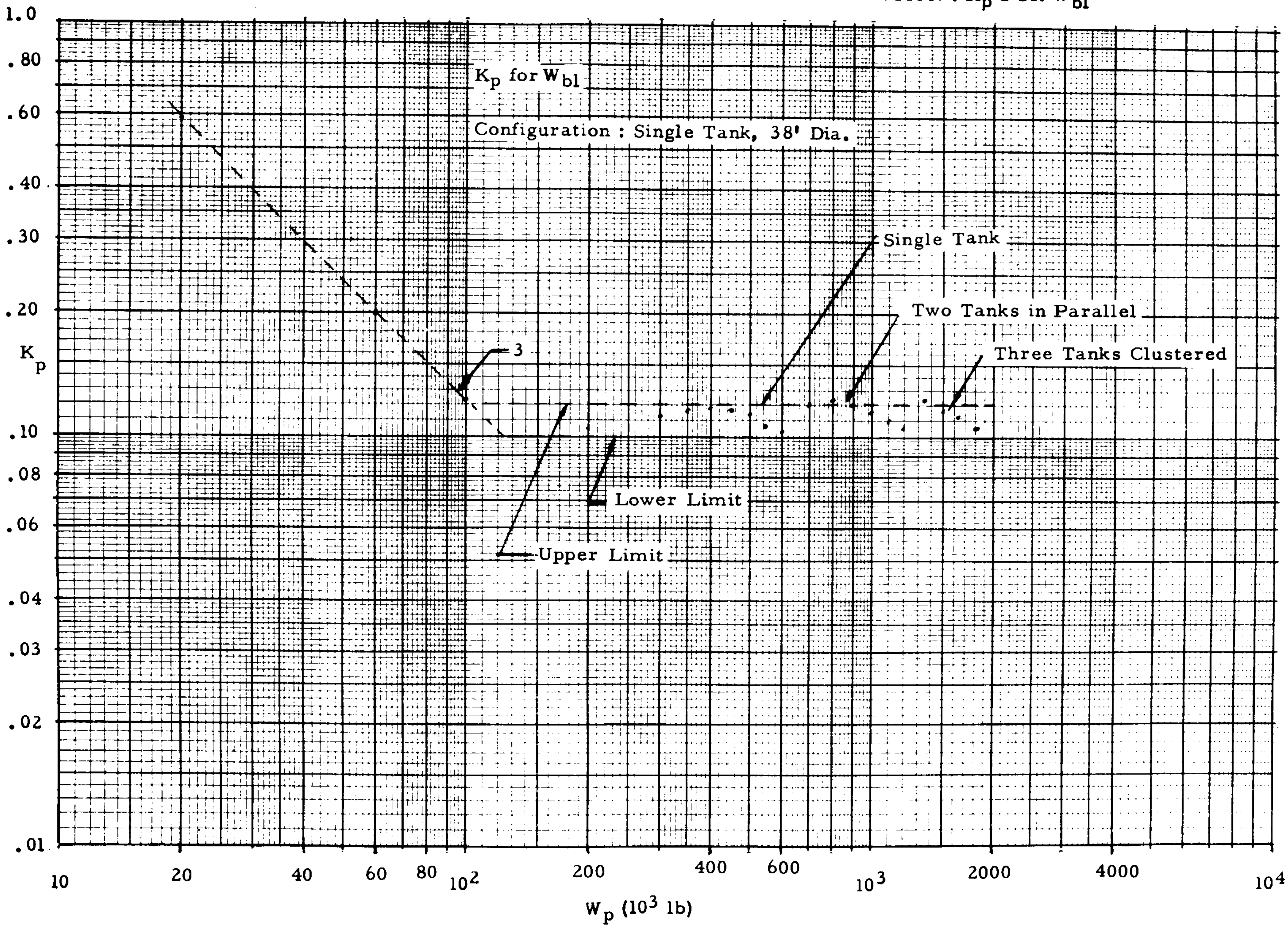

maneuvers may either be handled by a separate chemical or SHE or possibly by an additional nuclear stage, if the maneuver is large enough to render its addition worthwhile. In Fig. 4-6, curve 1 show the K_p of PM-2 and -3 without the (jettisonable) thermo/meteoroid (T/M) shield. Curve 2 marked W_j for jettisonable weight accounts for the T/M shield. The dots and circles represent specific values based on HISV sizing studies. The dashed line represents an approximate variation of K_p with W_p over certain W_p ranges, permitting a simpler analytic formulation. Using the numbers given at the curves as subscript, these equations are as follows:

$$K_{p,1} = 5,135\ W_p^{-0.8756} \qquad (20k \le W_p \le 100\ k) \tag{4-38}$$

$$K_{p,1} = 152\ W_p^{-0.569} \qquad (100\ k \le W_p \le 350\ k) \tag{4-39}$$

$$K_{p,1} = 27.47\ W_p^{-0.436} \qquad (350\ k \le W_p \le 599\ k) \tag{4-40}$$

$$K_{p,1} = 68.53\ W_p^{-0.4781} \qquad (600\ k \le W_p \le 1200\ k) \tag{4-41}$$

$$K_{p,2} = 5,166\ W_p^{-0.8846} \qquad (20\ k \le W_p \le 120\ k) \tag{4-42}$$

$$K_{p,2} = 4177.6\ W_p^{-0.8644} \qquad (120\ k \le W_p \le 599\ k) \tag{4-43}$$

$$K_{p,2} = 3.21\ W_p^{-0.241} \qquad (600\ k \le W_p \le 1200\ k) \tag{4-44}$$

For PM-1 in Fig. 4-8 one obtains

$$K_{p,3} = 9139\ W_p^{-0.9742} \qquad (20\ k \le W_p \le 119\ k) \tag{4-45}$$

Beyond 119,000 lb, the variations indicated by the detail analyses are bracketed by an upper and a lower limit,

$$K_p = 0.12 \text{ (upper limit) } (100\ k \le W_p \le 2000\ k) \tag{4-46}$$

$$K_p = 0.10 \text{ (lower limit) } (100\ k \le W_p \le 200\ k) \tag{4-47}$$

Similarly Figs. 4-9 and 4-10 show the mean variation of the K_p values for the Saturn V and the post-Saturn compatible ISV's. The analytical relations

Fig. 4-9 SCR-ISV, SATURN V COMPATIBLE CONFIGURATION : K_p

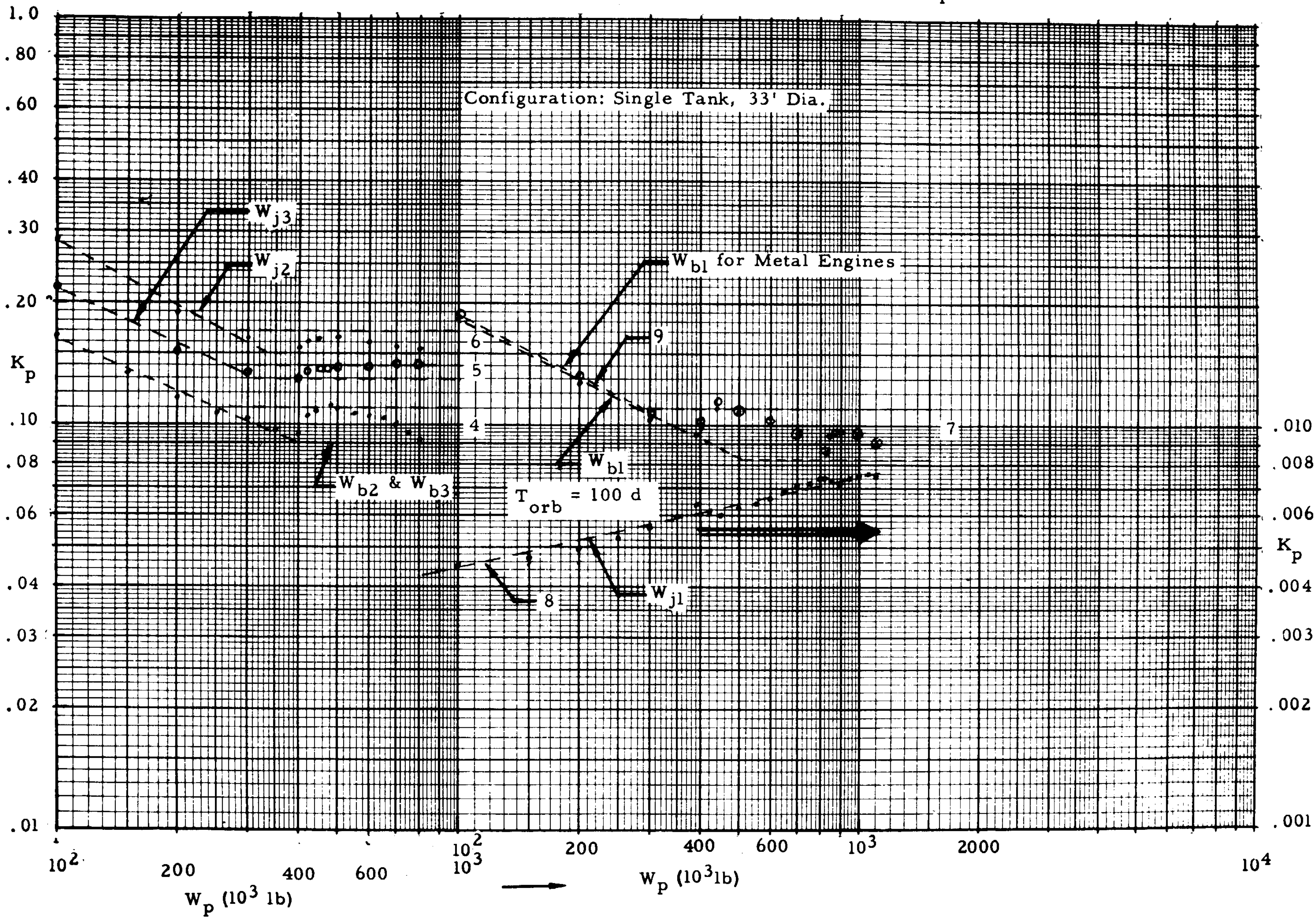

Fig. 4-10 SCR-ISV, POST-SATURN COMPATIBLE CONFIGURATION: K_p

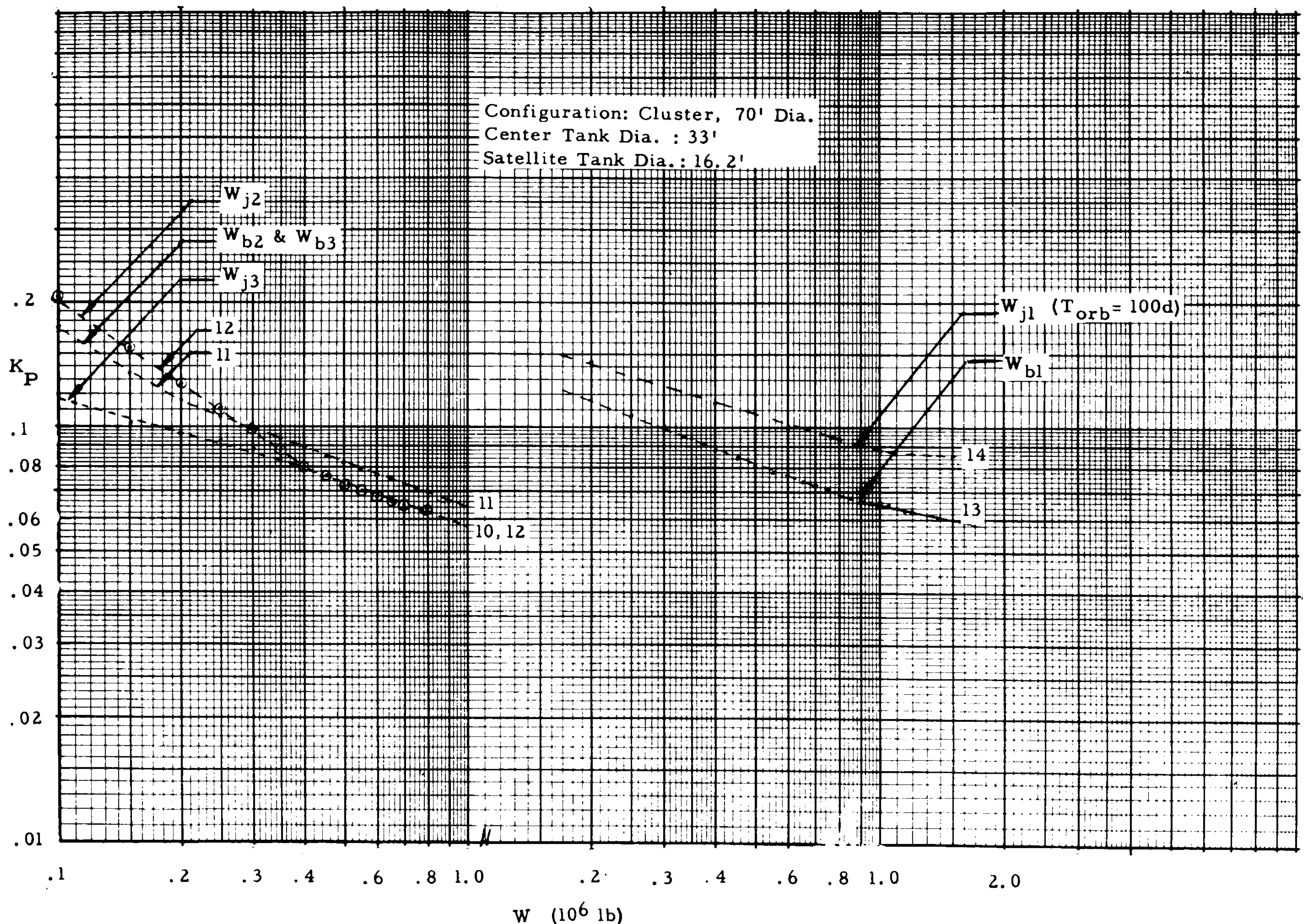

are

$$K_{p,4} = 26.74\, W_p^{-0.4414} \qquad (100\text{ k} \leq W_p \leq 400\text{ k}) \tag{4-47}$$

$$K_{p,4} = 0.11 \text{ (upper limit)} \qquad (2.5\text{ k} \leq W_p \leq 10^3\text{ k}) \tag{4-48}$$

$$K_{p,4} = 0.09 \text{ (lower limit)} \qquad (400\text{ k} \leq W_p \leq 10^3\text{ k}) \tag{4-49}$$

$$K_{p,5} = 32.96\, W_p^{-0.4359} \qquad (100\text{ k} \leq W_p \leq 300\text{ k}) \tag{4-50}$$

$$K_{p,5} = 0.14 \text{ (upper limit)} \qquad (270\text{ k} \leq W_p \leq 10^3\text{ k}) \tag{4-51}$$

$$K_{p,5} = 0.13 \text{ (lower limit)} \qquad (300\text{ k} \leq W_p \leq 10^3\text{ k}) \tag{4-52}$$

$$K_{p,6} = 139\, W_p^{-0.5375} \qquad (100\text{ k} \leq W_p \leq 330\text{ k}) \tag{4-53}$$

$$K_{p,6} = 0.17 \text{ (upper limit)} \qquad (270\text{ k} \leq W_p \leq 10^3\text{ k}) \tag{4-54}$$

$$K_{p,6} = 0.15 \text{ (lower limit)} \qquad (350\text{ k} \leq W_p \leq 10^3\text{ k}) \tag{4-55}$$

$$K_{p,7} = 52.35\, W_p^{-0.4913} \qquad (100\text{ k} \leq W_p \leq 500\text{ k}) \tag{4-56}$$

$$K_{p,7} = 0.11 \text{ (upper limit)} \qquad (300\text{ k} \leq W_p \leq 1500\text{ k}) \tag{4-57}$$

$$K_{p,7} = 0.082 \text{ (lower lower limit)} \qquad (500\text{ k} \leq W_p \leq 1500\text{ k}) \tag{4-58}$$

$$K_{p,8} = 8.96 \times 10^{-35} W_p^{+5.617} \qquad (800\text{ k} \leq W_p \leq 1100\text{ k}) \tag{4-59}$$

$$K_{p,9} = K_{p,7}$$

and, correspondingly for the post-Saturn compatible configuration,

$$K_{p,10} = 4.285\ W_p^{-0.31218} \qquad (100\ k \leq W_p \leq 1000\ k) \qquad (4\text{-}60)$$

$$K_{p,11} = 162.5\ W_p^{-0.59356} \qquad (100\ k \leq W_p \leq 200\ k) \qquad (4\text{-}61)$$

$$K_{p,11} = 10.55\ W_p^{-0.3695} \qquad (200\ k \leq W_p \leq 1000\ k) \qquad (4\text{-}62)$$

$$K_{p,12} = 507.8\ W_p^{-0.6788} \qquad (100\ k \leq W_p \leq 400\ k) \qquad (4\text{-}63)$$

$$K_{p,12} = K_{p,10} \qquad (400\ k \leq W_p \leq 1000\ k) \qquad (4\text{-}64)$$

$$K_{p,13} = 10.3\ W_p^{-0.36757} \qquad (200\ k \leq W_p \leq 900\ k) \qquad (4\text{-}65)$$

$$K_{p,13} = 1.05\ W_p^{-0.2013} \qquad (900\ k \leq W_p \leq 1500\ k) \qquad (4\text{-}66)$$

$$K_{p,14} = 51.76\ W_p^{-0.4616} \qquad (200\ k \leq W_p \leq 100\ k) \qquad (4\text{-}67)$$

$$K_{p,14} = 0.1068\ W_p^{-0.01402} \qquad (1000\ k \leq W_p \leq 1500\ k) \qquad (4\text{-}68)$$

Finally, for the -23 configuration, the following K_p relations apply:

For PM-1 the relations for $K_{p,13}$ and $K_{p,14}$ apply, if PM-1 is to be powered by an SCR/G propulsion system. For W_{b2} and W_{b3},

$$K_{p,15} = 0.06 \left(\frac{330,000}{W_p}\right)^{0.44} \qquad (10\ k \leq W_p \leq 330\ k) \qquad (4\text{-}69)$$

$$K_{p,15} \approx 0.06 \qquad (330\ k \leq W_p \leq 500\ k) \qquad (4\text{-}70)$$

For W_{j2} and W_{j3},

$$K_{p,16} = 0.086 \left(\frac{330,000}{W_p}\right)^{0.428} \qquad (30\ k \leq W_p \leq 330\ k) \qquad (4\text{-}71)$$

$$K_{p,16} = 0.07 \left(\frac{500,000}{W_p} \right)^{0.09} \qquad (330 \text{ k} \leq W_p \leq 500 \text{ k}) \qquad (4\text{-}72)$$

and, for a fourth, smaller stage, $K_{p,17}$ for W_{b4}

$$K_{p,17} = 0.11 \left(\frac{60,000}{W_p} \right)^{1.65} \qquad (30 \text{ k} \leq W_p \leq 60 \text{ k}) \qquad (4\text{-}73)$$

For W_{j4},

$$K_{p,18} = 0.094 \left(\frac{60,000}{W_p} \right)^{0.68} \qquad (30 \text{ k} \leq W_p \leq 60 \text{ k}) \qquad (4\text{-}74)$$

The second characteristic of the SCR propulsion modules is their engine. The following K_f values were established in previous studies (ref. 9)

- Metal-based, non-moderated engine (SCR/N) of F = 50 k and no specific limit on its operating life:

1 engine: $K_f = 0.10$ (F = 50 k)

2 engines: $K_f = 0.11$ (F = 100 k)

3 engines: $K_f = 0.107$ (F = 150 k)

4 engines: $K_f = 0.103$ (F = 200 k)

- Graphite-based, NERVA-type engine of about 45 minutes operating life (used in the analysis model as an assumption; the actual operating life of the engine has not yet been established). Thrust structure for this engine or engine cluster is based on a single tank of 33' diameter.

1 engine: $K_f = 0.31$ (F = 63 k) (4-75)

2 engines: $K_f = 0.325$ (F = 126 k) (4-76)

3 engines: $K_f = 0.32$ (F = 189 k) (4-77)

4 engines: $K_f = 0.32$ (F = 252 k) (4-78)

- Graphite-based "second generation" engine of 250 k thrust and 45 minutes (by NASA Study direction) operating life:

1 engine: $K_f = 0.105$ (F = 250 k) (4-79)

2 engines: $K_f = 0.105$ (F = 500 k) (4-80)

For thrust values from 75K to 250k, the non-moderated metal reactor (SCR/N) and the water moderated metal reactor engine (SCR/W) are expected to be comparable in weight and lighter than the SCR/G engine.

Therefore, the following relation was used for both, SCR/N and SCR/W engines in the $75k \leq F \leq 250k$ thrust range

$$K_f = 0.09 \left(\frac{100,000}{F}\right)^{1/8} \qquad (75\ k \leq F \leq 250\ k) \qquad (4\text{-}81)$$

In the SCR/N-HISV the same engines can be used for several or all maneuvers. Using the last of Eqs. (4-10a), x for a given set of engines can be determined for a range of W_p to obtain a curve for which x-values associated with the approximate HISV ignition weight for each maneuver can be estimated. An alternate approach, analogous to the $W_{p,ST}/W_{p,CT}$ method used in Par. 4.12, is discussed in Example No. 2 of Sect. 5.

The SCR/N engines may be usable for more than one maneuver, depending upon their operating life. Fig. 4-11 compares the mass fractions as function of propellant weight for tankage without engines and for tankage with two and four SCR/N engines, respectively. The higher mass fraction indicated for the tankage without engines demonstrates the advantage associated with reusable nuclear engines. Example No. 2 in Sect. 5 compares the SCR/N powered HISV without and with reusable engines and also discusses an alternate approach to the determination of gross payload fractions for this vehicle type. This approach is analogous to the $W_{p,ST}/W_{p,CT}$ method presented in Par. 4-12.

4.12 GASEOUS CORE REACTOR (GCR) PROPULSION MODULES

The propellant dependent scaling coefficient is determined on the basis of a structural configuration which consists of a center tank which is permanently attached to the spine and life support section. This center tank serves as propellant container for the last and, possibly next to the last principal maneuver. In the latter case it is subdivided. The GCR engine is attached to its aft end. The center tank is surrounded by a cluster of satellite tanks which contain propellant for the preceding principal mission maneuvers. The satellite tanks feed propellant into the center tank from where a main feeding system supplies LH_2 to the engine. It is assumed that the engine can be throttled to half its maximum thrust value.

Propellant for the Earth departure maneuver (M-1) is contained in the PM-1 tanks. These satellite tanks are located between the LSS and the central tank, parallel to the spine. Depleting these forward tanks during M-1 shifts the vehicle CG aft, thus providing a more favorable dynamic

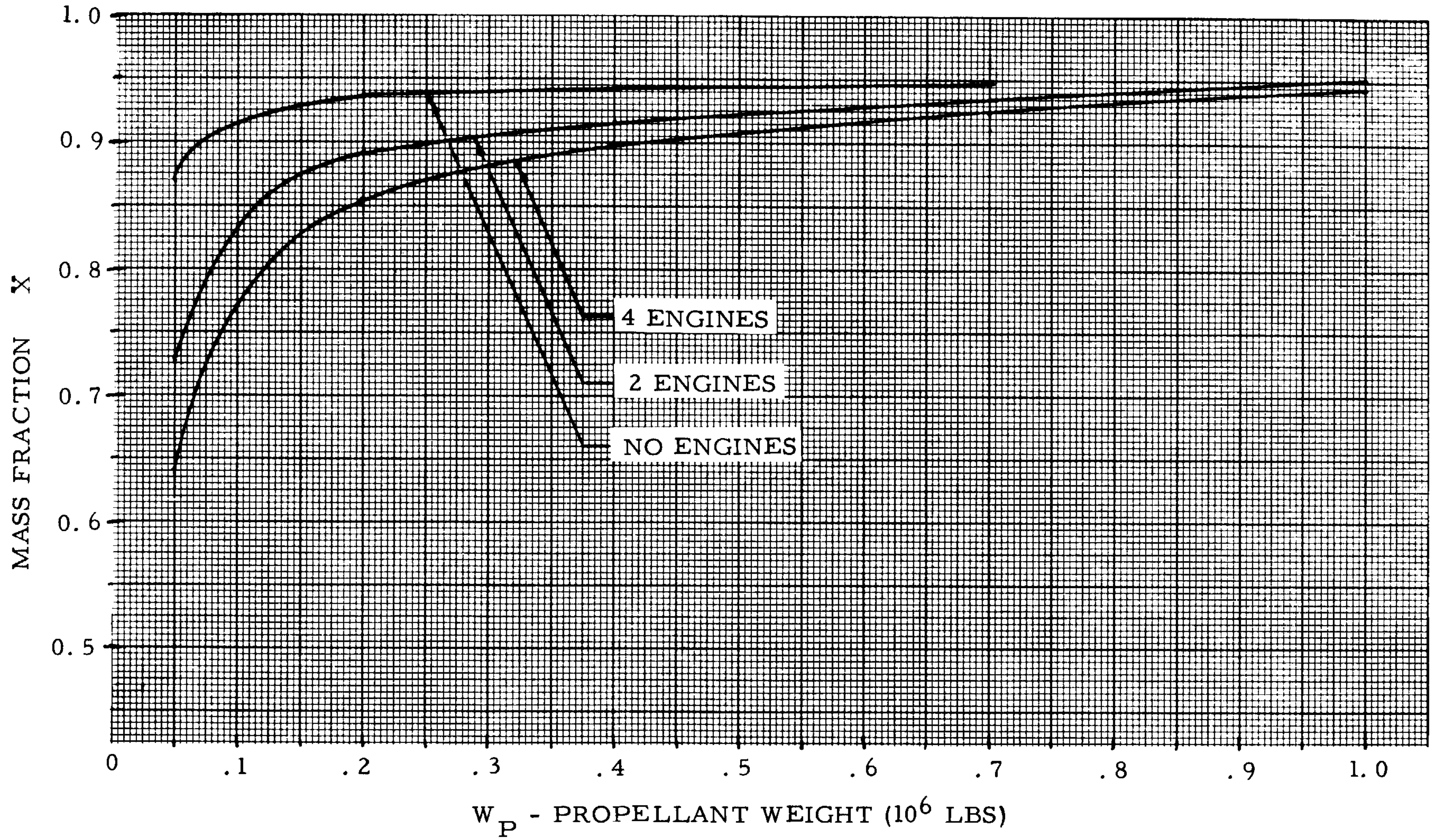

Fig. 4-11a SCR/N - HISV: VARIATION OF MASS FRACTION WITH PROPELLANT LOAD OF THE -23 CONFIGURATION

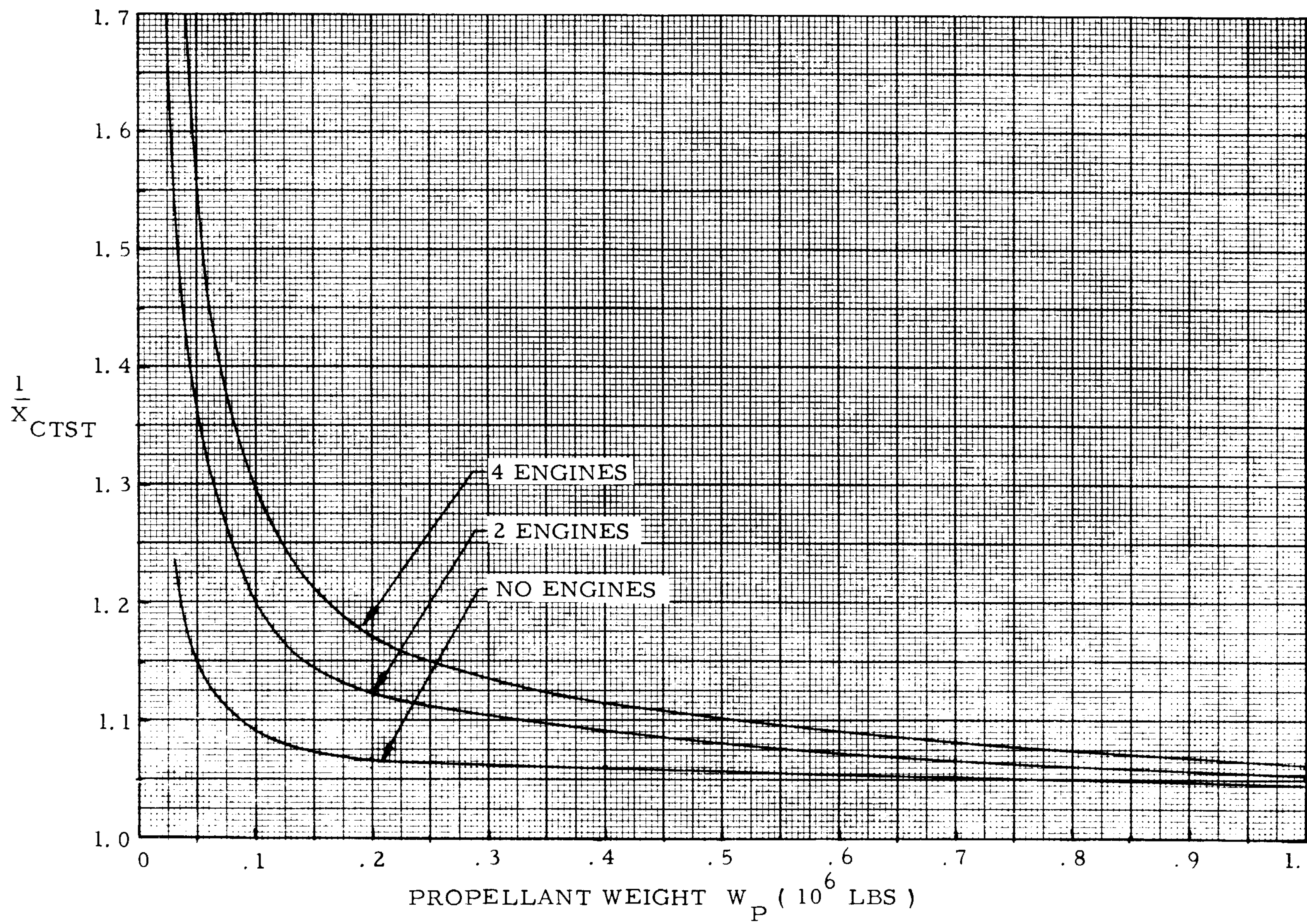

Fig. 4-11b SCR/N - HISV: VARIATION OF 1/X WITH PROPELLANT LOAD OF THE -23 CONFIGURATION

condition for gravity provisions in the LSS through ISV tumbling. The PM-2, PM-3 etc. satellite tanks are attached to the center tank into which they feed.

The K_p data are based on a tank pressure of 16 psi. A 10% contingency is provided. The thermo/meteoroid shield is jettisoned from the tanks about to be depleted just prior to the respective maneuver.

Engine thrust levels ranging from 1000 k to 4000 k for the individual thrust chamber were considered. The probability that GCR engine thrust levels will be high provides a constraint which prevents using the high specific impulse to reduce the ODW. Its superior performance is reflected rather in a larger payload capability.

For this reason a center tank of 38' diameter was chosen for the reference configuration, making it transportable by the Saturn V Mod. Satellite tanks of 17' diameter each surround the center tank. They consist of three or more sets in tandem arrangement. The most forward set represents the PM-1 tanks, the set behind it the PM-2 tanks and so forth. The length of these tanks can be varied, thereby providing the versatility required of the standardized vehicle to adapt itself to characteristic variations in planetary mission velocity from one mission window to the next. The propellant capacity of the center tank varies between 200 and 700 $\cdot 10^3$ lb; that of the individual satellite tanks ranges from 20,000 to 100,000 lb.

The overall propellant dependent scaling coefficient is the sum of the scaling coefficients for the center tank and for the satellite tanks,

$$K_p = K_{p,CT} + K_{p,ST} \tag{4-82}$$

$$K_{p,CT} \approx 0.1 \qquad (200\text{ k} \leq W_p \leq 560\text{ k}) \tag{4-83}$$

$$K_{p,CT} \approx 0.1 \left(\frac{560,000}{W_p}\right)^{0.304} \qquad (560\text{ k} \leq W_p \leq 675\text{ k}) \tag{4-84}$$

$$K_{p,CT} \approx 0.0945 \left(\frac{675,000}{W_p}\right)^{2.34} \qquad (675\text{ k} \leq W_p \leq 725\text{ k}) \tag{4-85}$$

$$K_{p,ST} \approx 0.0725 \left(\frac{20,000}{W_p}\right)^{\frac{6000}{W_p}} \qquad (20\text{ k} \leq W_p \leq 100\text{ k}) \tag{4-86}$$

The thrust dependent scaling coefficient is given by

$$K_f \approx 0.01 + 0.0091 \frac{40 \cdot 10^6}{1.2 \cdot F(\mathrm{lb})} \qquad (10^6 \leq F \leq 4 \cdot 10^6) \tag{4-87}$$

Therewith a relation for x can be established. Eq. (4-10c) is not used, because $n_o = F/W_A$ may vary greatly. Using the third of Eq. (4-10a),

$$x = \frac{1}{1 + K_{p,CT} \frac{W_{p,CT}}{W_p} + K_{p,ST} \left(1 - \frac{W_{p,CT}}{W_p}\right) + \left(0.01 + 0.0091 \frac{40 \cdot 10^6}{1.2F(\mathrm{lb})}\right) \frac{F}{W_p}} \tag{4-88a}$$

This equation applies to those cases where the GCR-HISV is treated as a 1-stage vehicle, with the same configuration returning into a near-Earth orbit as departed from a near-Earth orbit. In view of the high specific impulse attainable with the GCR, this assumption is plausible, at least for some missions, such as lunar supply and not too high planetary supply missions. The variation of $K_{p,CT}$, $K_{p,ST}$ and K_f is shown in Fig. 4-12 and 4-13. The variation of x with W_p is shown in Figs. 4-14 through 4-17. The thrust is produced by one engine, at the base of the center tank. The same engine is used for all maneuvers.

For missions whose economic execution depends upon jettisoning empty propellant tanks and which, therefore, must be evaluated in a maneuver-for-maneuver manner, the methodology for computing the mass fraction is similar as in the case of the -23 configuration. For the last one or two maneuvers, depending on the magnitude of the velocity changes involved, a center tank plus GCR engine combination is assumed. For all other maneuvers, satellite tanks without engine are assumed, in addition to the center tank plus engine configuration. Therewith two equations for x are involved in this case. For the center tank plus engine configuration

$$x_{CT} = \frac{1}{1 + K_{p,CT} + K_f \frac{F}{W_p}} \tag{4-88b}$$

where K_f is given by Eq. (4-87). For the satellite additions,

$$x_{ST} = \frac{1}{1 + K_{p, ST}} \qquad (4\text{-}88c)$$

For the last one or two maneuvers, Eq. (4-88b) applies. For the preceding maneuvers, if they involve satellite tanks, the combined mass fraction is defined by the equation,

$$x_{CTST} = \frac{W_{p, CT} + W_{p, ST}}{W_{c, CT} + W_{b, ST} + W_{p, CT} + W_{p, ST}} \qquad (4\text{-}88d)$$

or, after some adjustments,

$$x_{CTST} = \frac{1}{1 + \frac{1}{x_{CT}} - 1 \quad 1 + W_{p, ST}/W_{p, CT} \quad + \frac{1}{x_{ST}} - 1 \quad 1 + \frac{1}{W_{P,ST}/W_{p,CT}}}$$

The variation of x_{CT}, $1/x_{CT}$ and x_{ST}, $1/x_{ST}$ is presented in Figs. 4-18 through 4-20.

The variation of x_{CT} with $W_{p, CT}$ is considerably larger than that of x_{ST}. It is, therefore, possible without undue loss of accuracy, to fix x_{ST} by selecting a mean value for it. It should be recognized, in this connection, that the values of x_{ST}, shown in Fig. 4-20, are based on the W_p value of the individual satellite tank. Suppose, for example, $W_{p, ST}$ = 800, 000 lb. Then, if it is assumed that this propellant is housed in 10 satellite tanks @ 80, 000 lb, the mass fraction for the full 800, 000 lb is 0.9432. If, on the other hand, $W_{p, ST}$ is assumed to be housed in 5 satellite tanks @ 160, 000 lb, x_{ST} is 0.9448. There is a simplification involved here, inasmuch as the mass fraction of a number of satellite tanks is taken to be the same as that of a single tank shown in Fig. 4-20. Because of the small variation of x_{ST} with $W_{p, ST}$, this simplification appears permissible without undue loss of accuracy. By specifying a mean value of x_{ST}, Eq. (4-88d) remains a function only of x_{CT} and $W_{p, ST}/W_{p, CT}$. Fig. 4-21 shows the variation of x_{CTST} with $W_{p, ST}/W_{p, CT}$ and with X_{CT}.

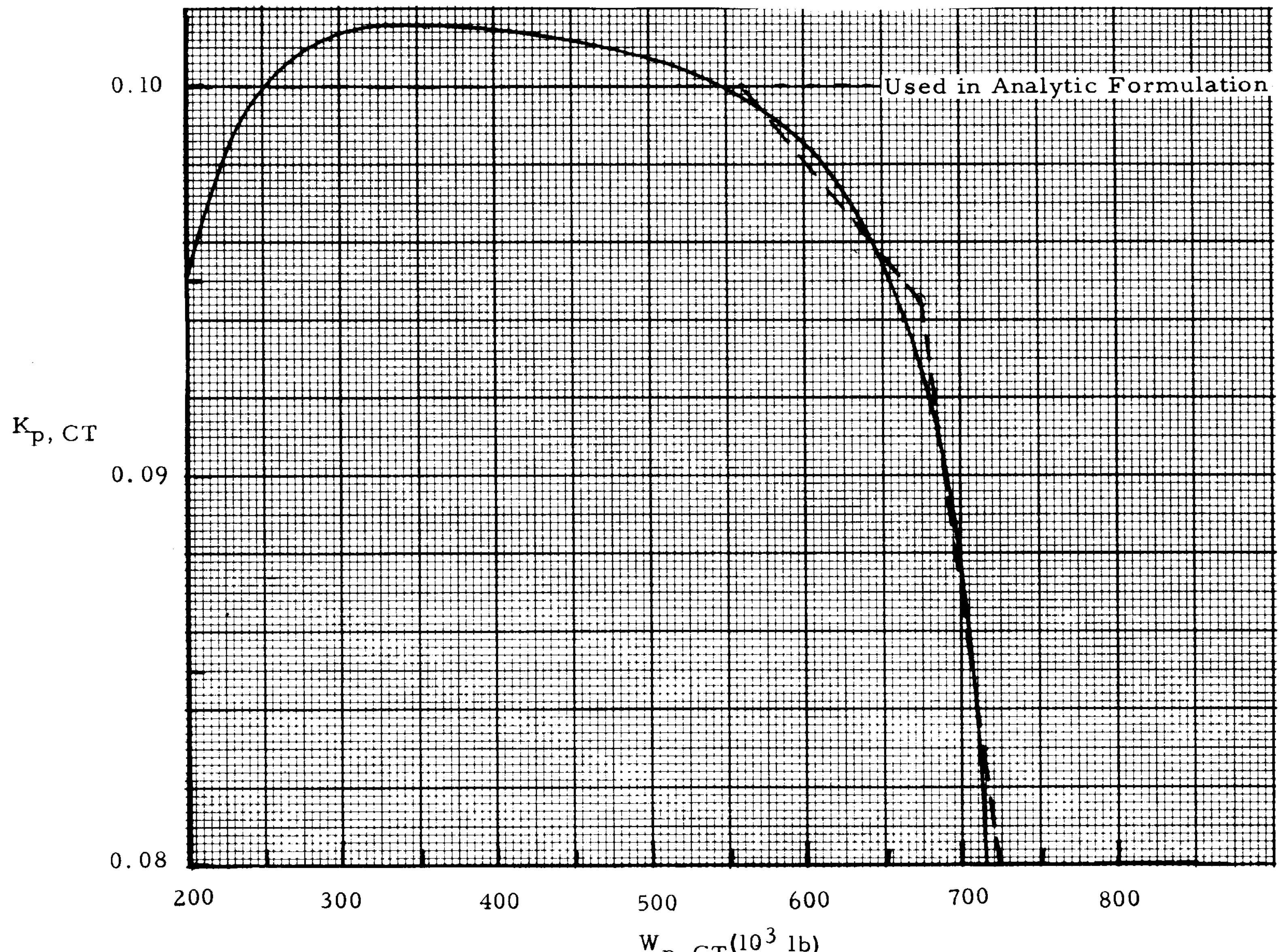

Fig. 4-12a $K_{p,CT}$ vs. $W_{p,CT}$ FOR 38' DIAMETER CENTRAL TANK

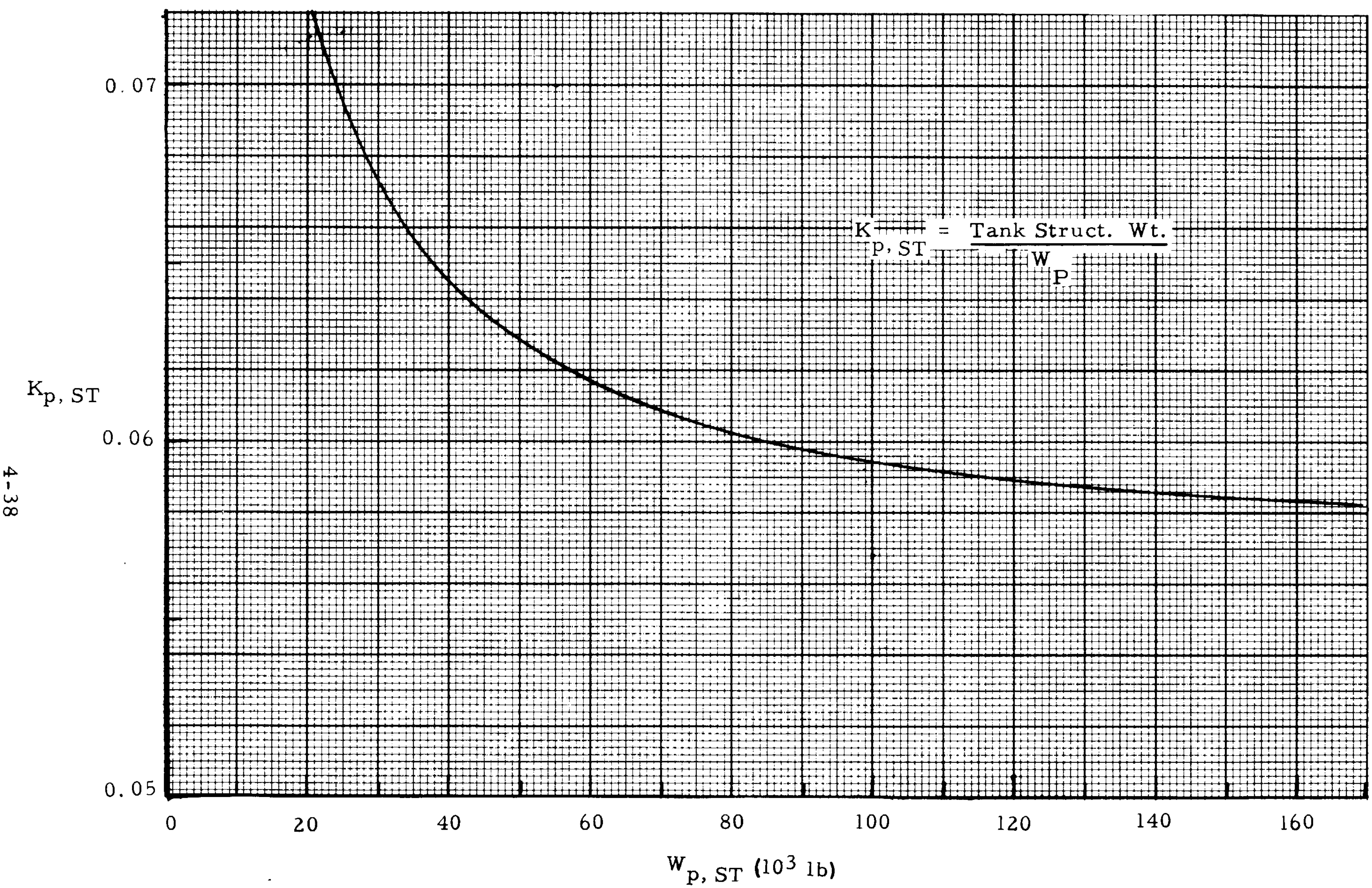

Fig. 4-12b $K_{p,ST}$ FOR SATELLITE TANKS OF THE GCR-HISV

Fig. 4-13 K_f FOR GASEOUS CORE REACTOR ENGINES

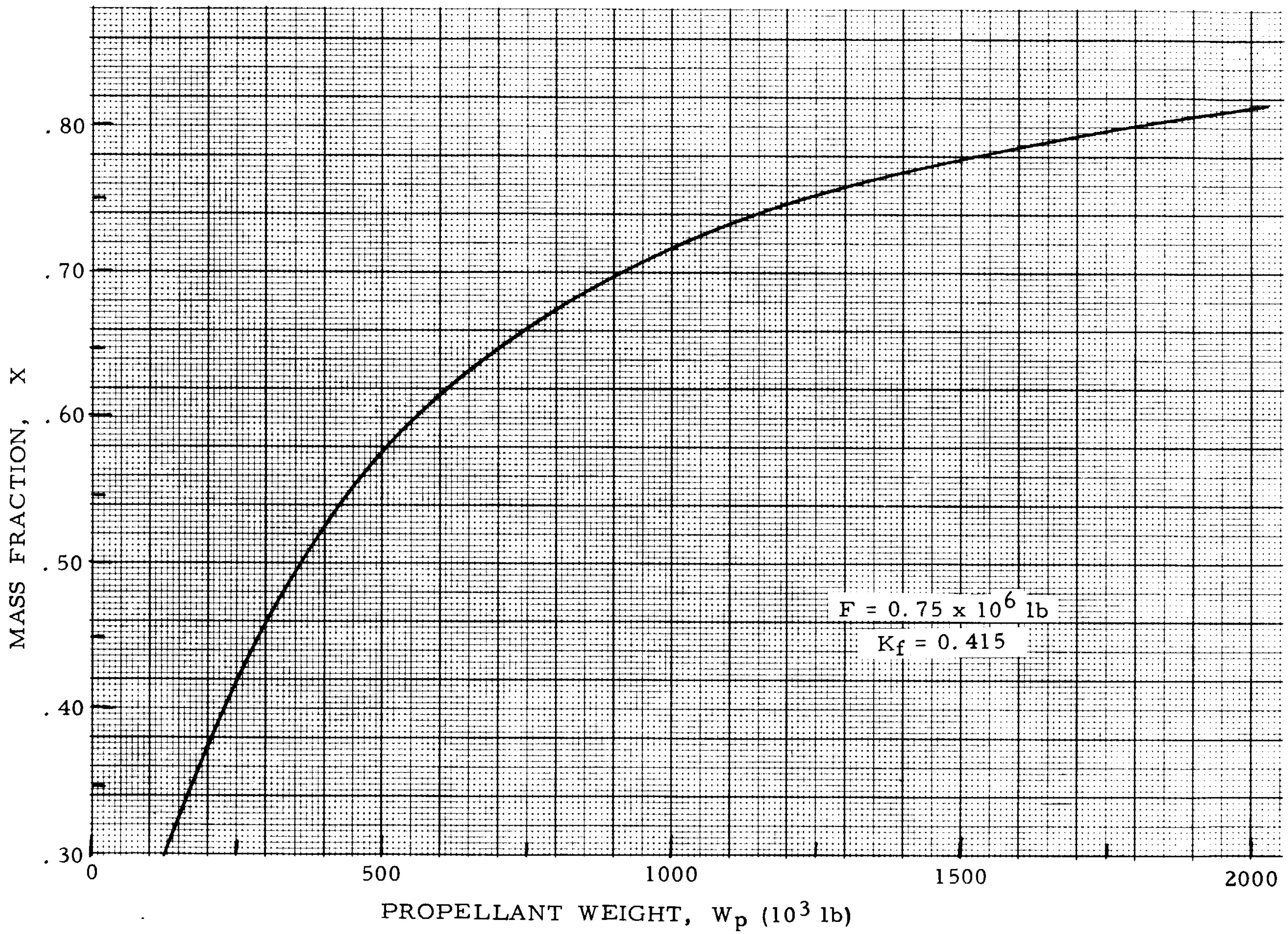

Fig. 4-14 GAS CORE REACTOR -- HISV -- MASS FRACTION vs. PROPELLANT WEIGHT

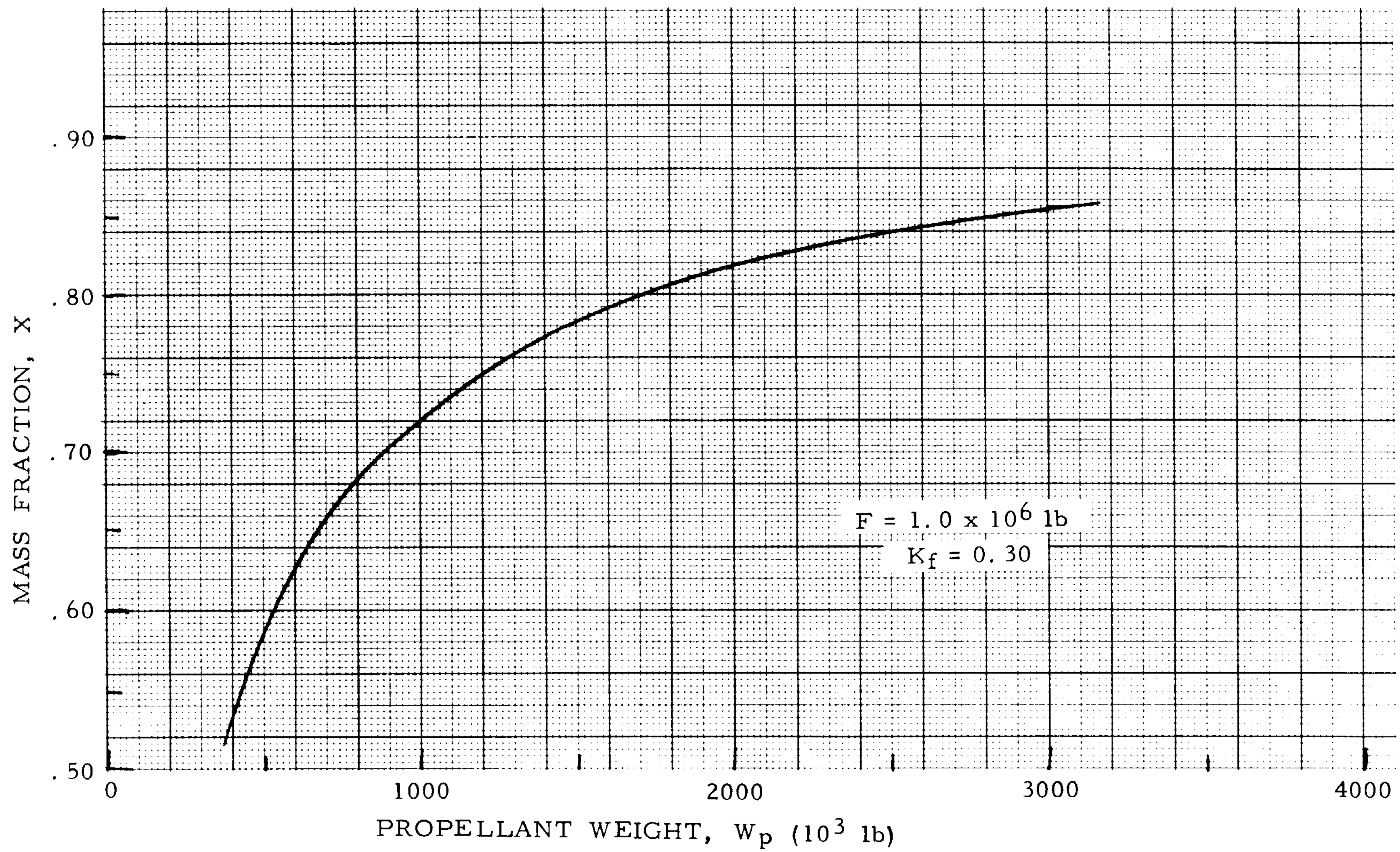

Fig. 4-15 GAS CORE REACTOR -- HISV--- MASS FRACTION vs. PROPELLANT WEIGHT

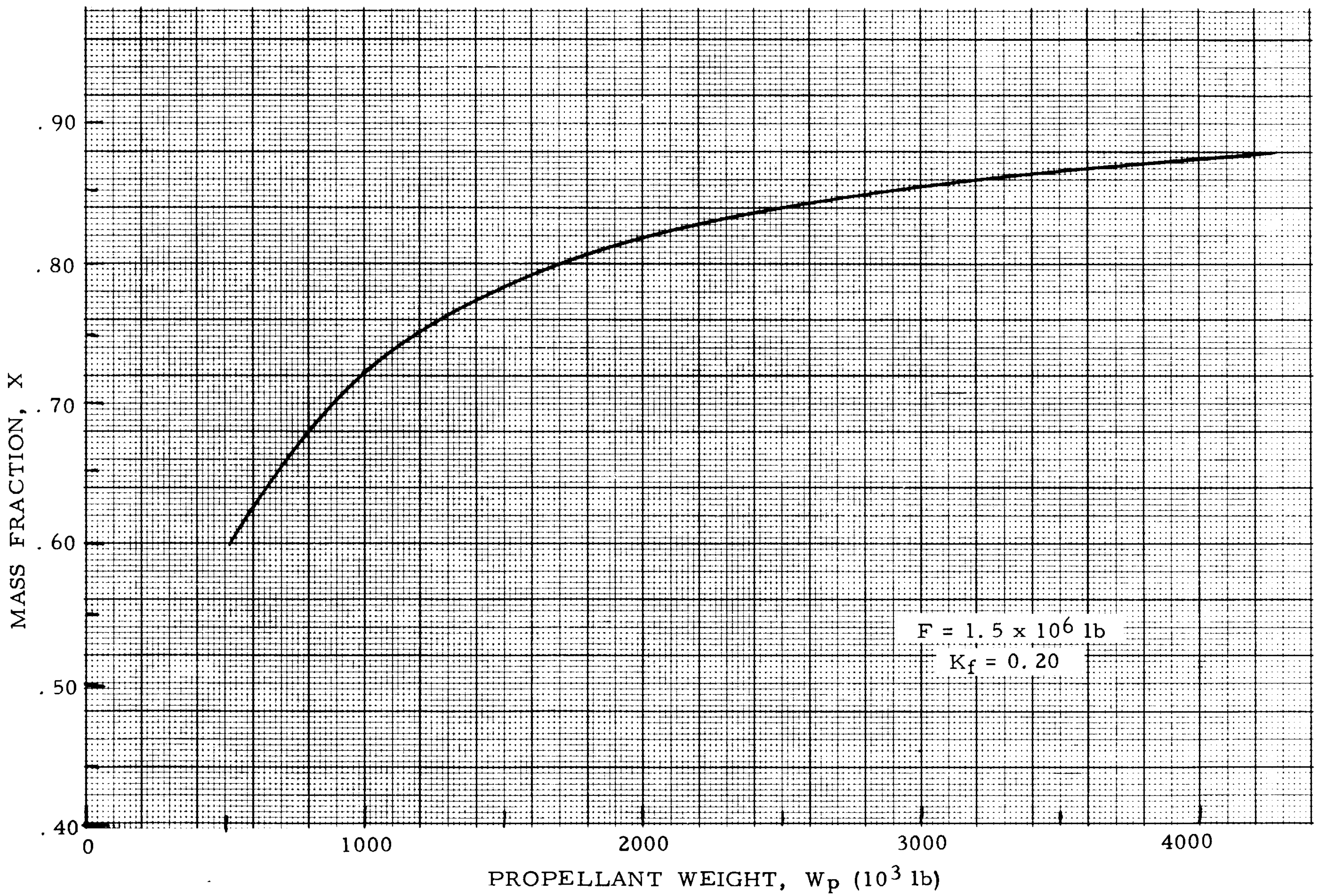

Fig. 4-16 GAS CORE REACTOR -- HISV -- MASS FRACTION vs. PROPELLANT WEIGHT

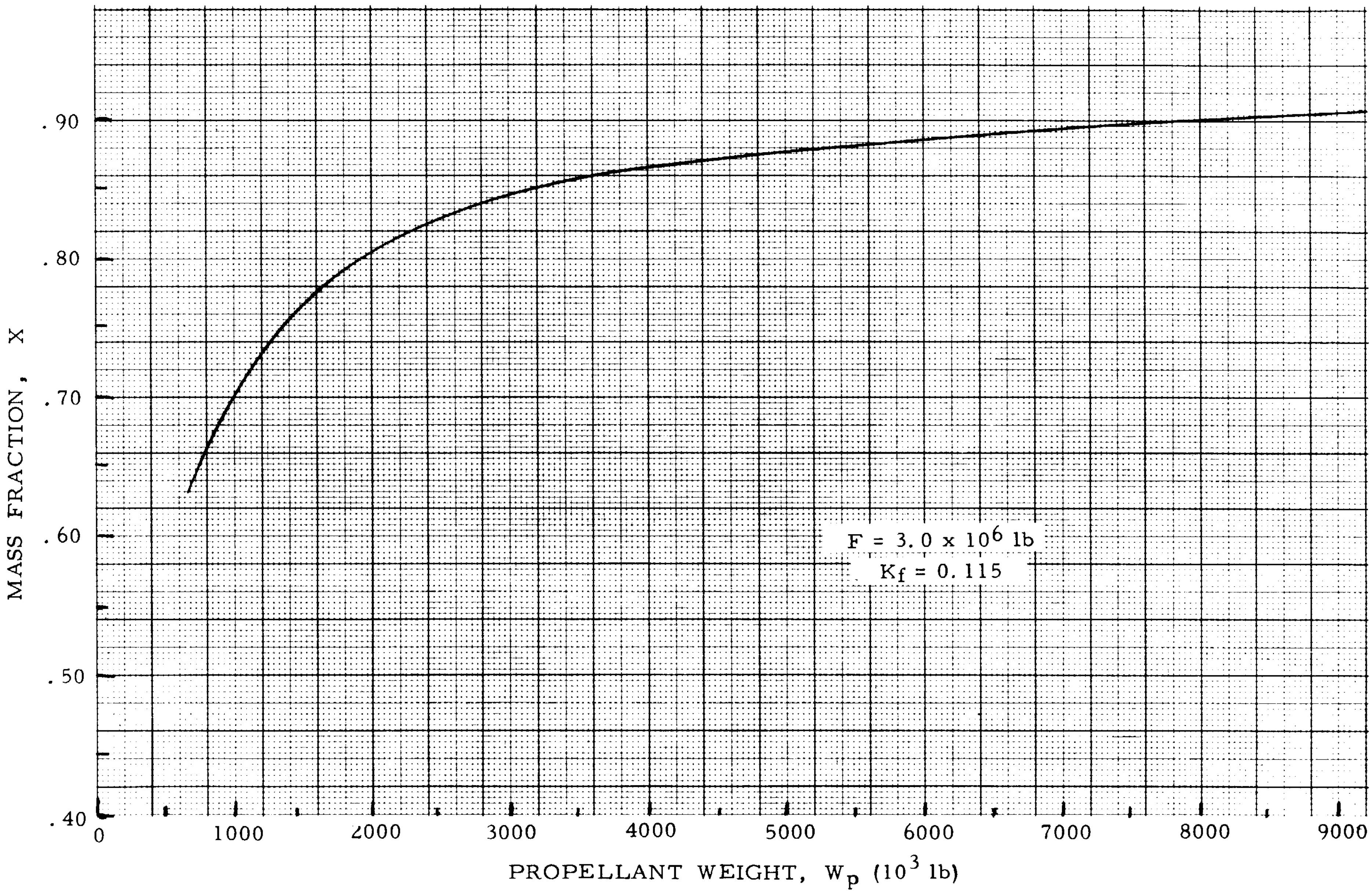

Fig. 4-17 GAS CORE REACTOR --- HISV -- MASS FRACTION vs. PROPELLANT WEIGHT

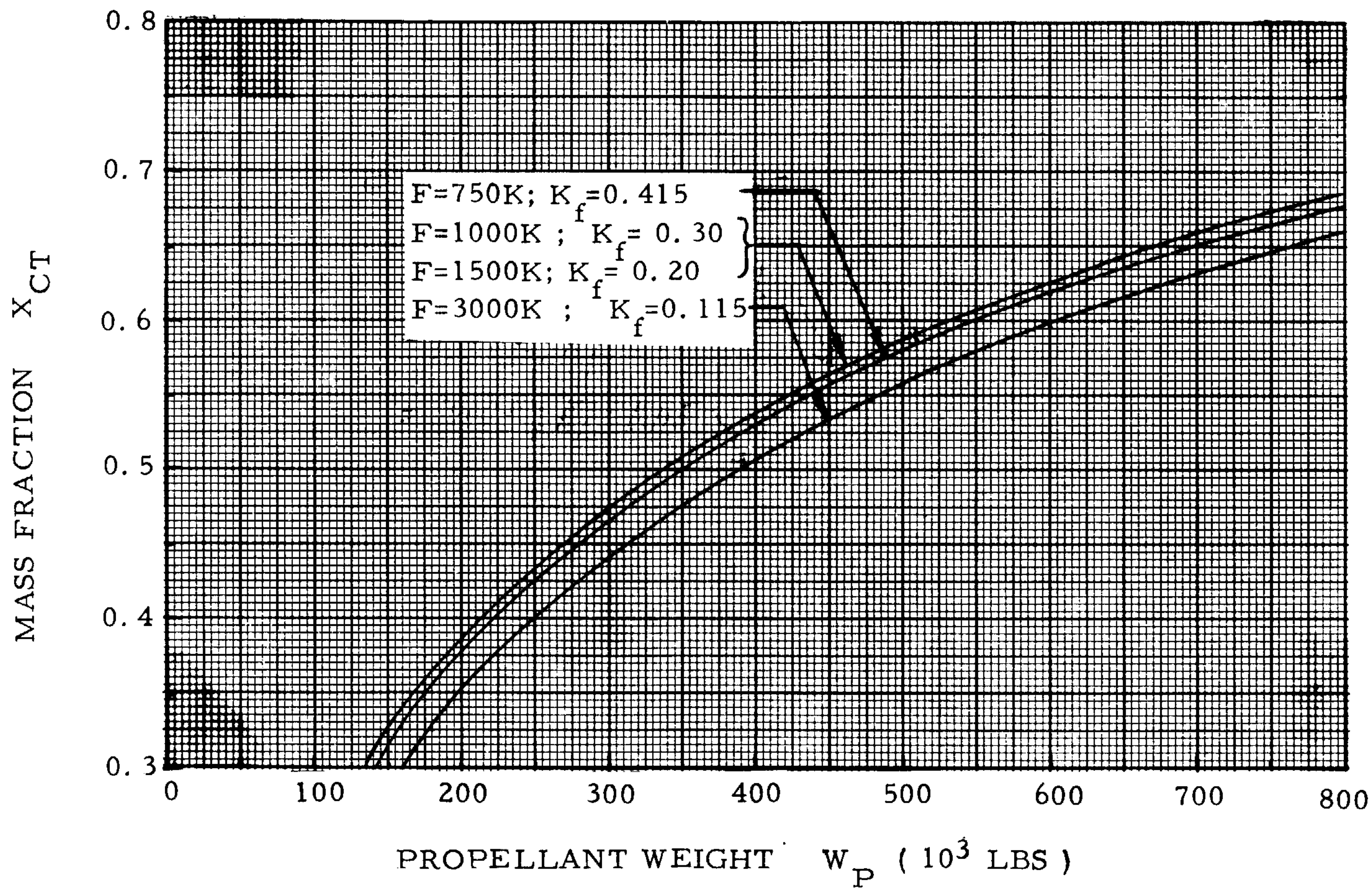

Fig. 4-18 GCR-HISV : VARIATION OF MASS FRACTION FOR CENTER TANK PLUS ENGINE CONFIGURATION

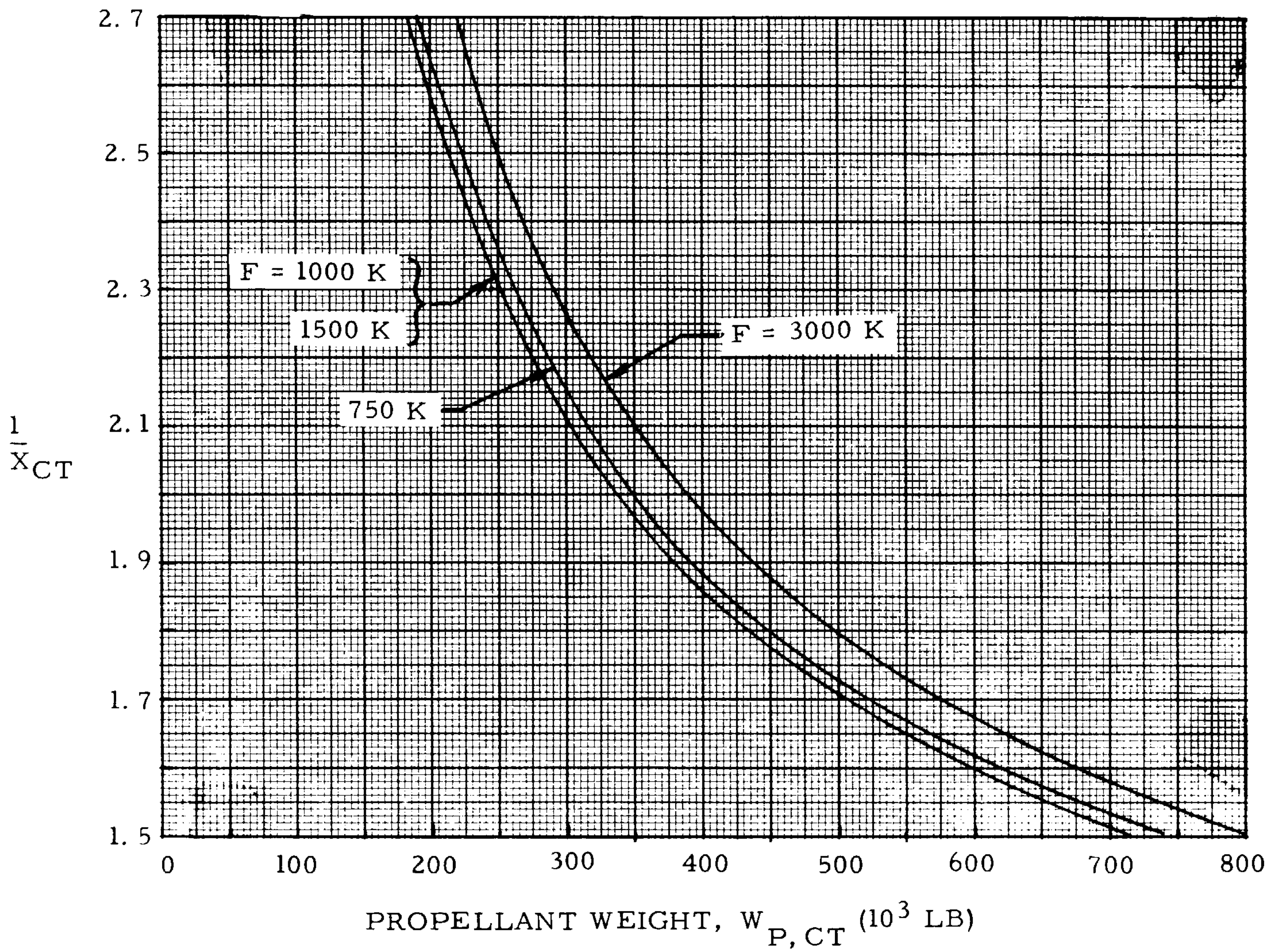

Fig. 4 - 19 GCR - HISV: RECIPROCAL OF MASS FRACTION FOR CENTER TANK PLUS ENGINE CONFIG.

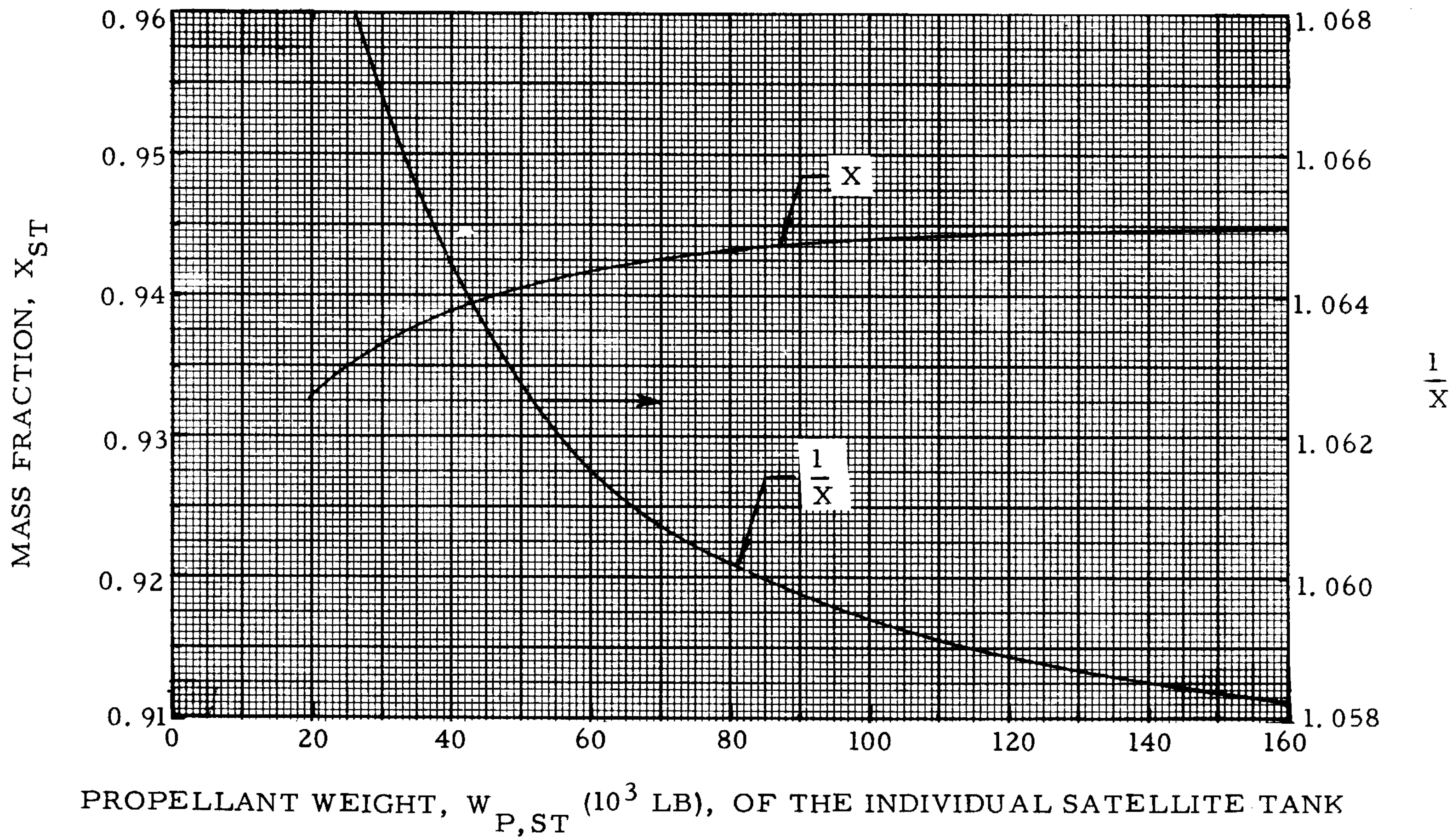

Fig. 4 - 20 GCR - HISV: VARIATION OF MASS FRACTION AND 1/X FOR SATELLITE TANKS

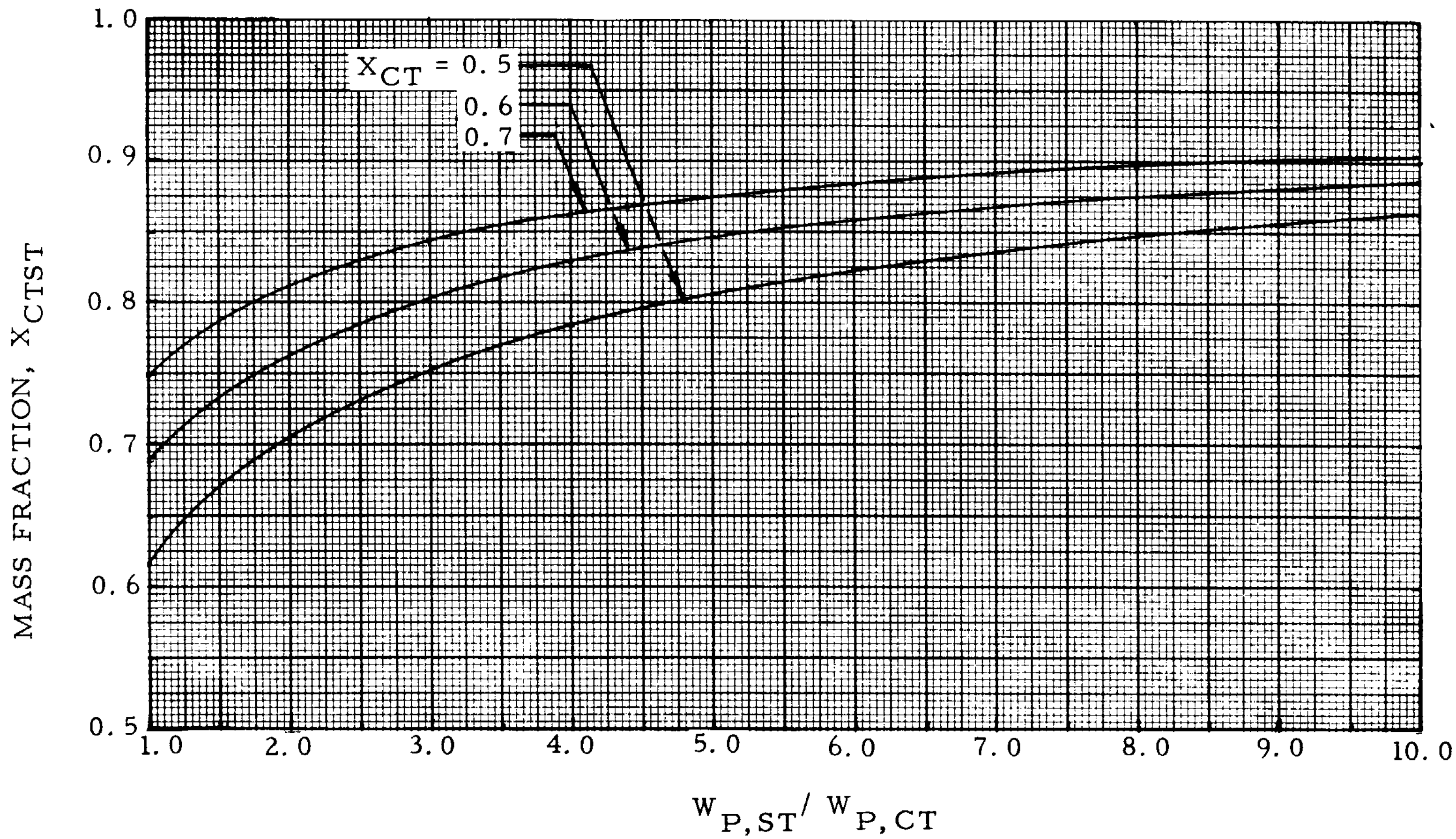

Fig. 4 - 21 GCR - HISV: OVERALL MASS FRACTION X_{CTST} AS FUNCTION OF $W_{P,ST}/W_{P,CT}$ FOR SEVERAL VALUES OF X_{CT}

5. GENERAL VEHICLE/MISSION INTEGRATION

The general vehicle/mission integration synthesizes the results of mission analysis and propulsion module analysis to obtain the gross payload fraction which represents the principal non-dimensional figure of merit.

Before the mission gross payload fraction (MGPF) can be determined, it is necessary to determine the gross payload fraction GPF on the basis of individual maneuvers. This can be done on the basis of scaling coefficients or of mass fractions. The GPF for a given maneuver is determined by the relation

$$\lambda = 1 - \frac{1}{x}\,\frac{\mu - 1}{\mu} = 1 - \frac{\Lambda}{x} = 1 - \frac{1}{x}\left(1 - e^{-\tau/I_{sp}}\right)$$

whichever is more convenient, and in lieu of x a suitable relation, containing the scaling coefficients, can be used.

The correlation between GPF, mass fraction, mass ratio and τ/I_{sp} can be presented in a completely universal, non-dimensional vehicle/mission integration chart (Fig. 5-1). This chart is based on the fact that the GPF for a given mass fraction is a function of mass ratio, and τ/I_{sp} can be used directly to determine the GPF, if the mass fraction is known. The chart can be used in several ways, depending upon the choice of the independent variable. If τ/I_{sp} is the independdnt variable, one moves from the upper abscissa vertically down to the point of intersection with the τ/I_{sp} curve. From there one moves horizontally to the left or the right until the x-curve which applies to the particular propulsion module is intersected. From that point one moves vertically downward to read the corresponding GPF value. The process is reversed if one wants to determine the attainable τ/I_{sp} for a given set of GPF and x-values. The chart permits rapid determination of the effect of a change (or uncertainty) in mass fraction, ideal velocity requirement or specific impulse. For the latter two, the value if τ/I_{sp} varies accordingly. One moves along the τ/I_{sp} curve from one to the other limiting τ/I_{sp} value and from either point curves horizontally to intersect the given x-curve (or point of interpolation between two curves). From the resulting two points of intersection one can determine the associated variation of the GPF. The correlation between Λ and τ/I_{sp} is shown in Fig. 5-1a.

In order to be able to use this chart properly, the mass fractions of the propulsion modules used for the maneuver must be known. These mass fractions are, basically a function of the propellant content. If,

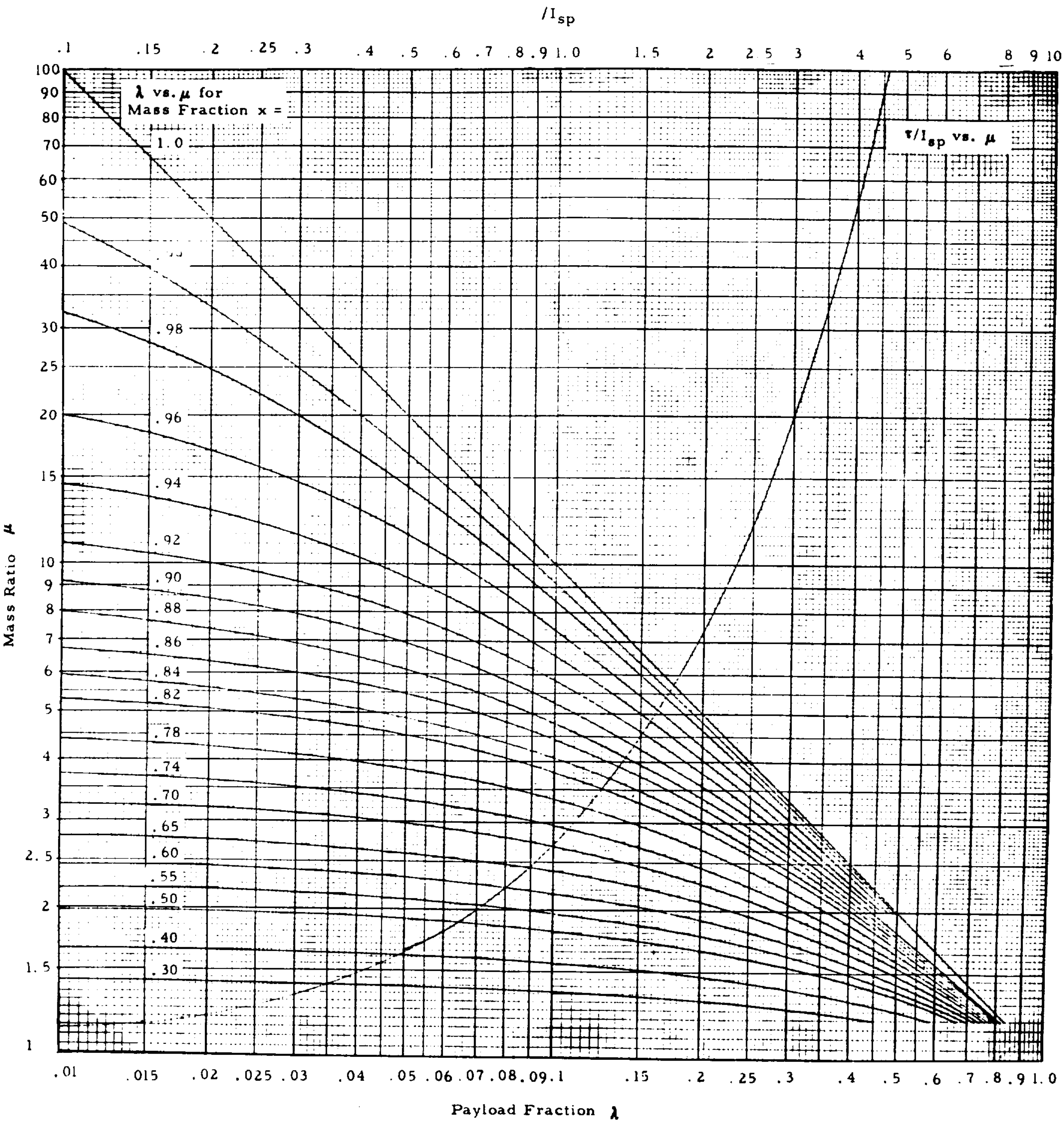

Fig. 5-1 UNIVERSAL VEHICLE/MISSION INTEGRATION CHART

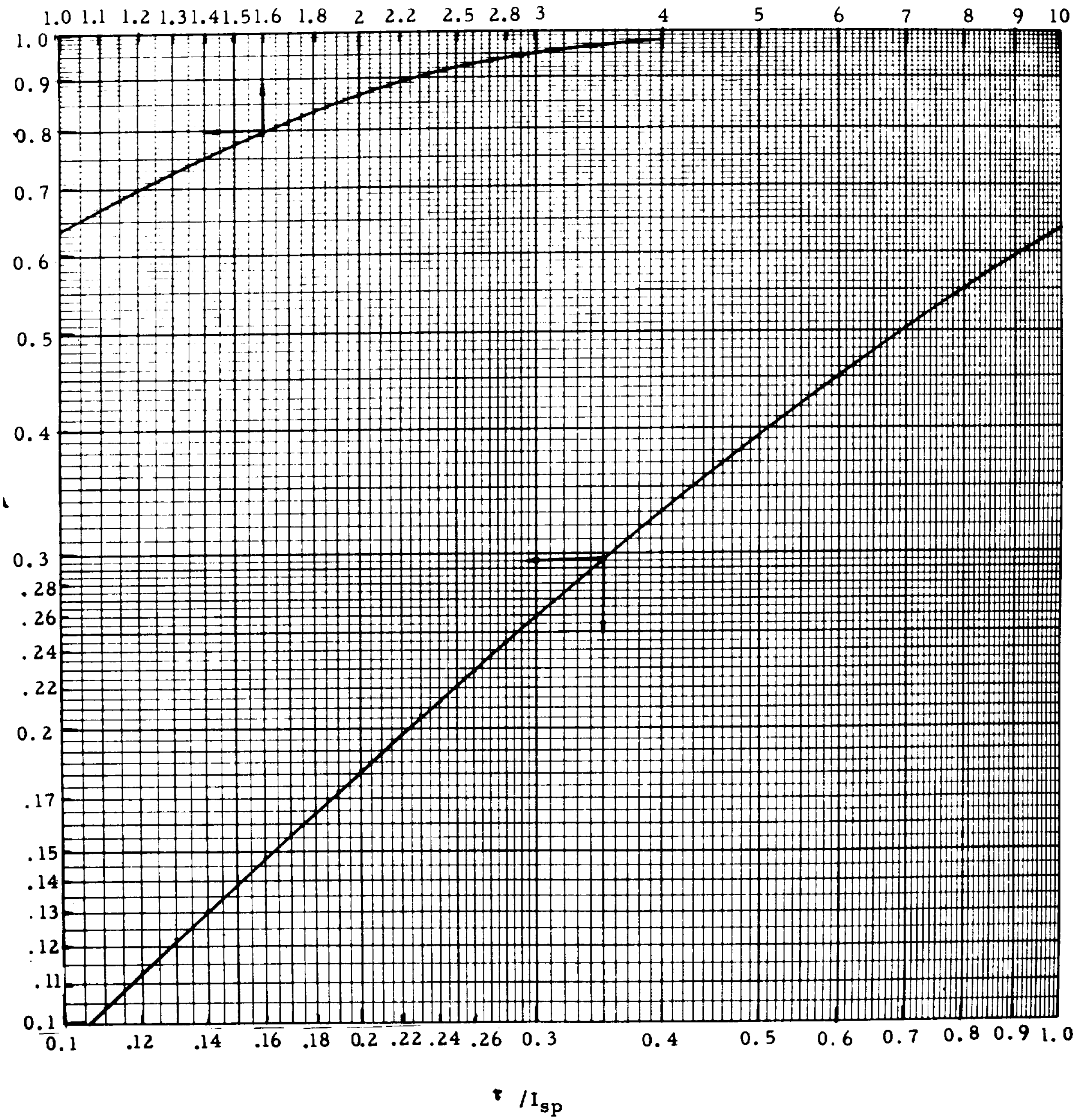

Fig. 5-1a PROPELLANT FRACTION Λ Vs. τ / I_{sp}

for a given design point, x is known, as well as τ/I_{sp}, then the GPF can be determined as described. Now, if τ/I_{sp} is varied because of a variation in I_{sp}, the x-value does not change. If τ/I_{sp} is increased, because Δv_{id} is increased, for the purpose of determining the reduction in GPF with increasing maneuver velocity, without changing the propellant load of the fully fueled module, then the x-value also does not change. If, however, τ/I_{sp} is reduced, because Δv_{id} is reduced, and if a corresponding reduction in propellant loading is assumed, then the x-value changes. Maintaining an invariant x-value when the propellant weight is changed from the design point for which x was determined, means that one must assume an average mass fraction which, in the range in question, is not a function of the propellant load W_p.

Mass fractions can be selected for a given propulsion module from the graphs presented in the preceding Section; or they can be determined from the equations given.

For the convenience of the reader, a number of graphs are presented in this section, showing λ directly for each of the propulsion modules covered in the preceding section. These graphs show λ vs. W_p for discrete values of τ/I_{sp}; and λ vs. τ/I_{sp} for discrete values of W_p. They were computed from the equations for x or the associated scaling coefficients presented in the preceding section. With their use, the need for determining x first, is eliminated.

Figs. 5-2 through 5-4 represent chemical stages.

Figs. 5-5 and 5-6 apply to the SHE driven stage or vehicle.

Figs. 5-7 and 5-8 show the Saturn V Mod. compatible, standardized SCR/G-powered PM-1 (Earth orbit launch stage) with one SCR/G engine @ 250 k thrust. Figs. 5-9 and 5-10 show the same with two SCR/G engines @ 250 k. Figs. 5-11 and 5-12 refer to the other propulsion modules (PM-2, PM-3 etc.) of this interplanetary vehicle configuration, using one SCR/G engine; Figs. 5-13 and 5-14 apply to the same propulsion modules but with two SCR/G engines.

The post-Saturn compatible, standardized SCR/G-powered HISV is presented in Figs. 5-15 and 5-16. Up to 500,000 lb propellant the vehicle is powered by one SCR/G engine @ 250 k thrust; beyond 500,000 lb propellant, two engines are employed. Due to the large masses involved, the addition of a second engine is hardly noticeable.

Figs. 5-17 and 5-18 apply to the Saturn V compatible HISV.

Fig. 5-2 CHEMICAL VEHICLE PAYLOAD FRACTION AS FUNCTION OF PROPELLANT WEIGHT AND τ/I_{sp}

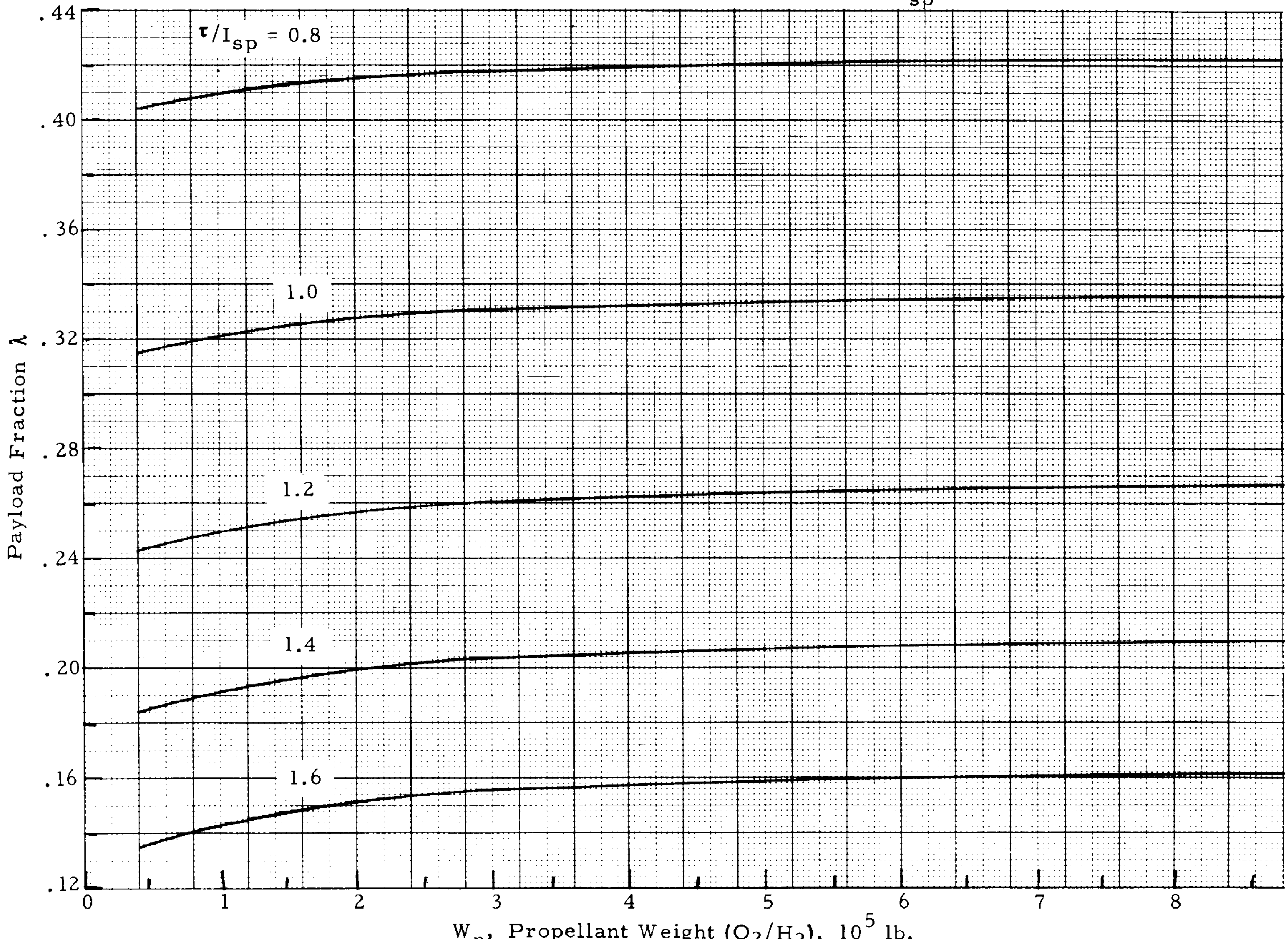

Fig. 5-3 CHEMICAL VEHICLE PAYLOAD FRACTION AS FUNCTION OF PROPELLANT WEIGHT AND τ/I_{sp}.

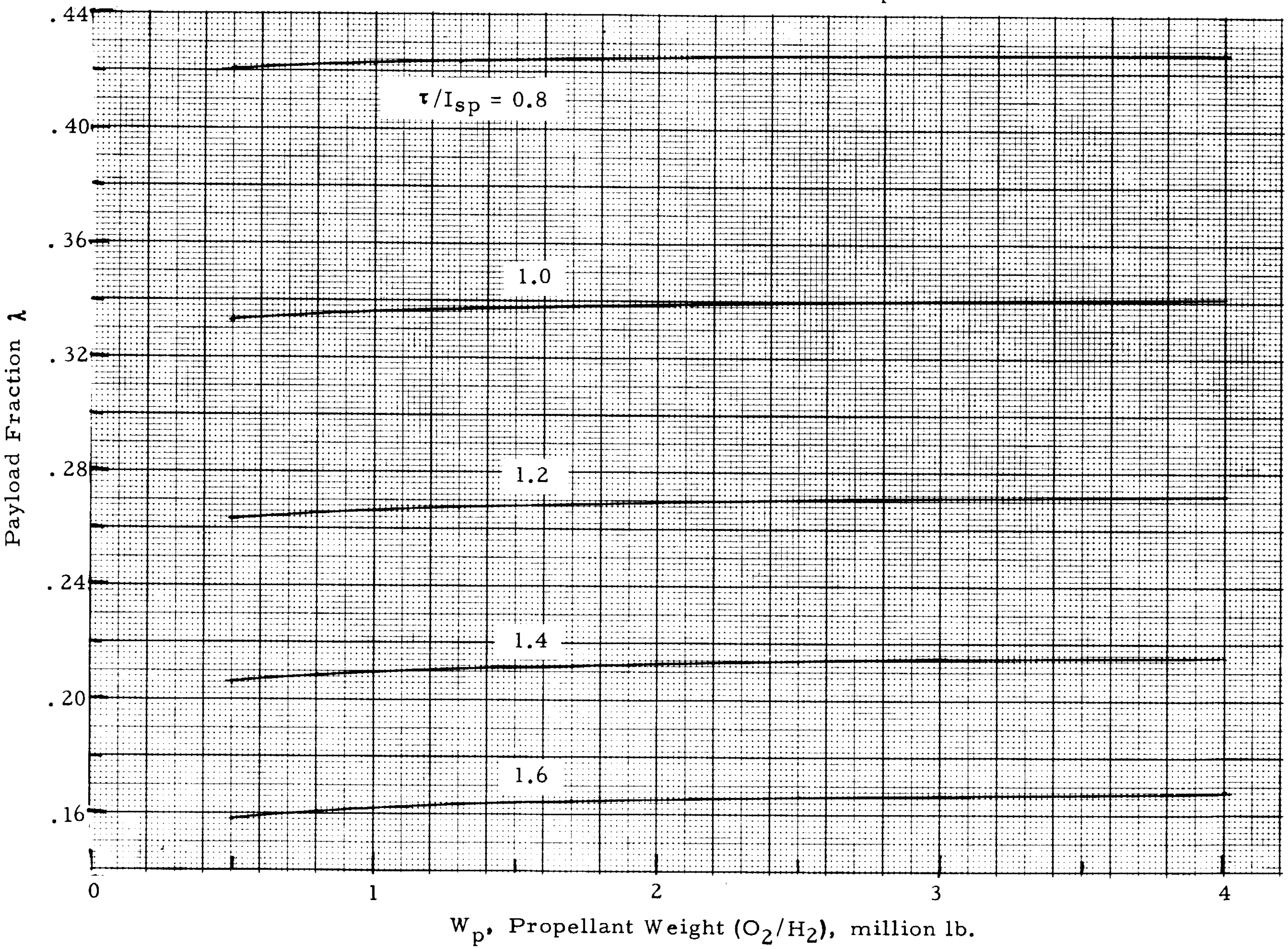

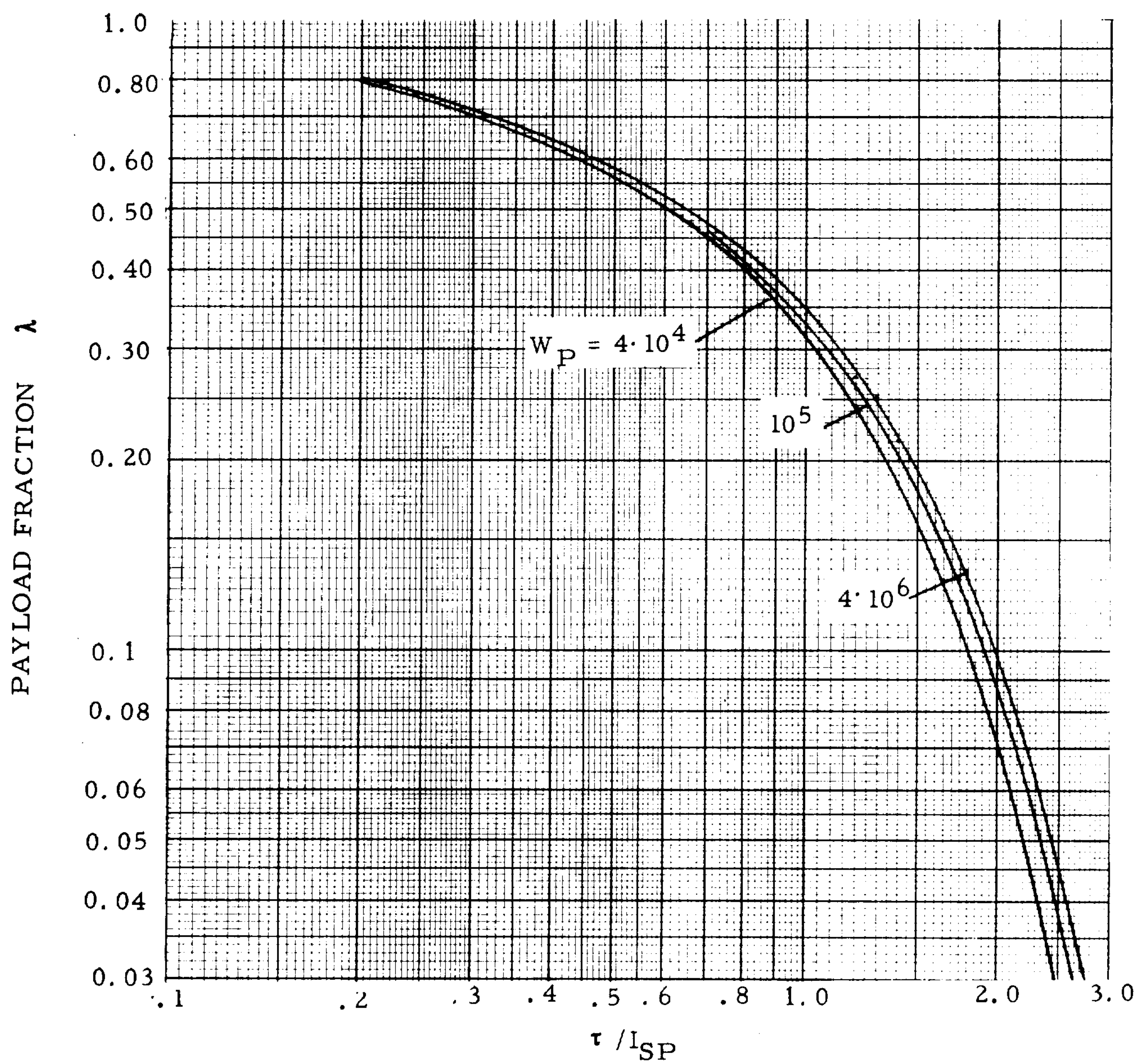

Fig. 5-4 CHEMICAL STAGES: λ VS τ/I_{SP}

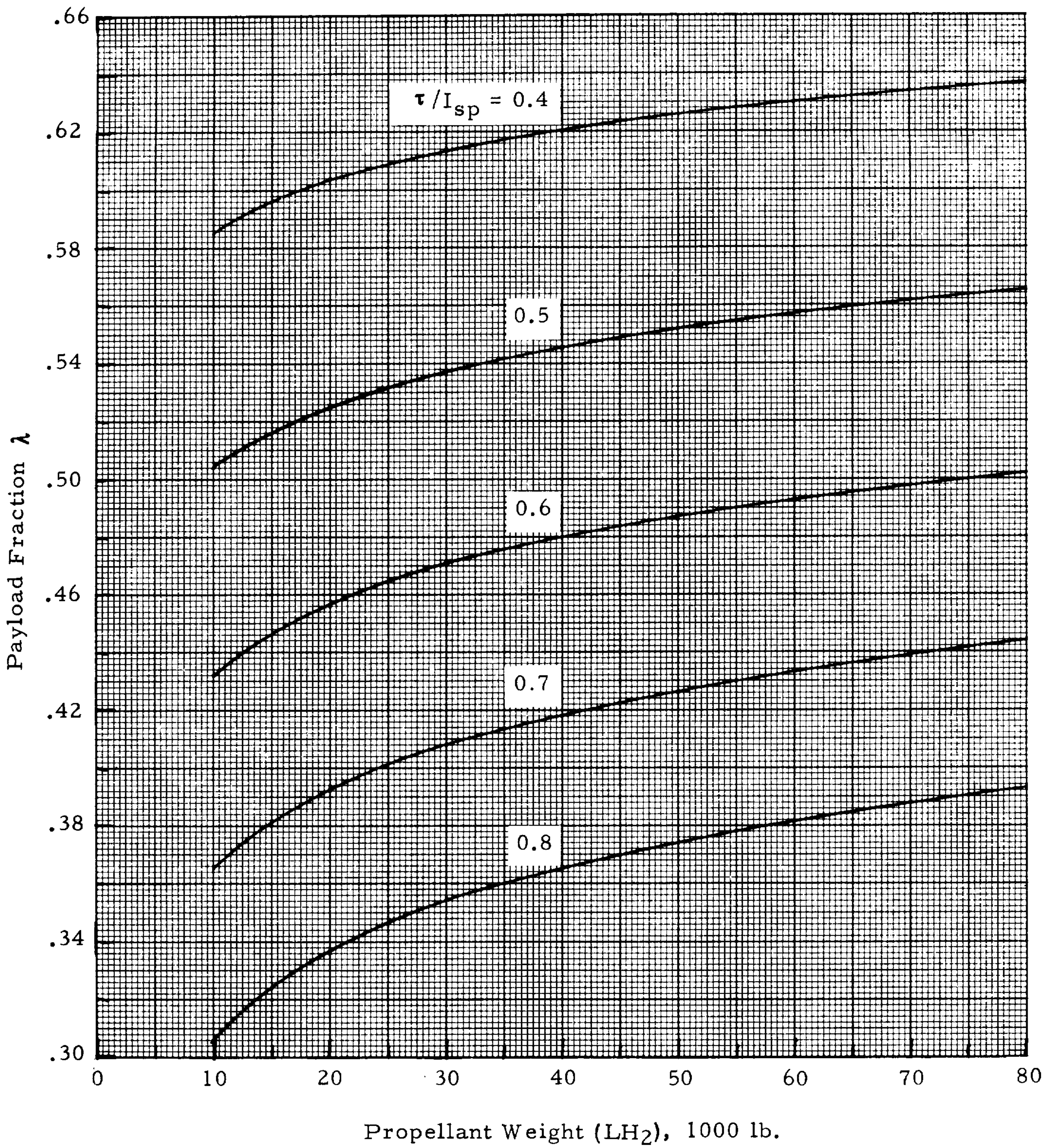

Fig. 5-5 SHE VEHICLE PAYLOAD FRACTION AS FUNCTION OF PROPELLANT WEIGHT AND τ/I_{sp}

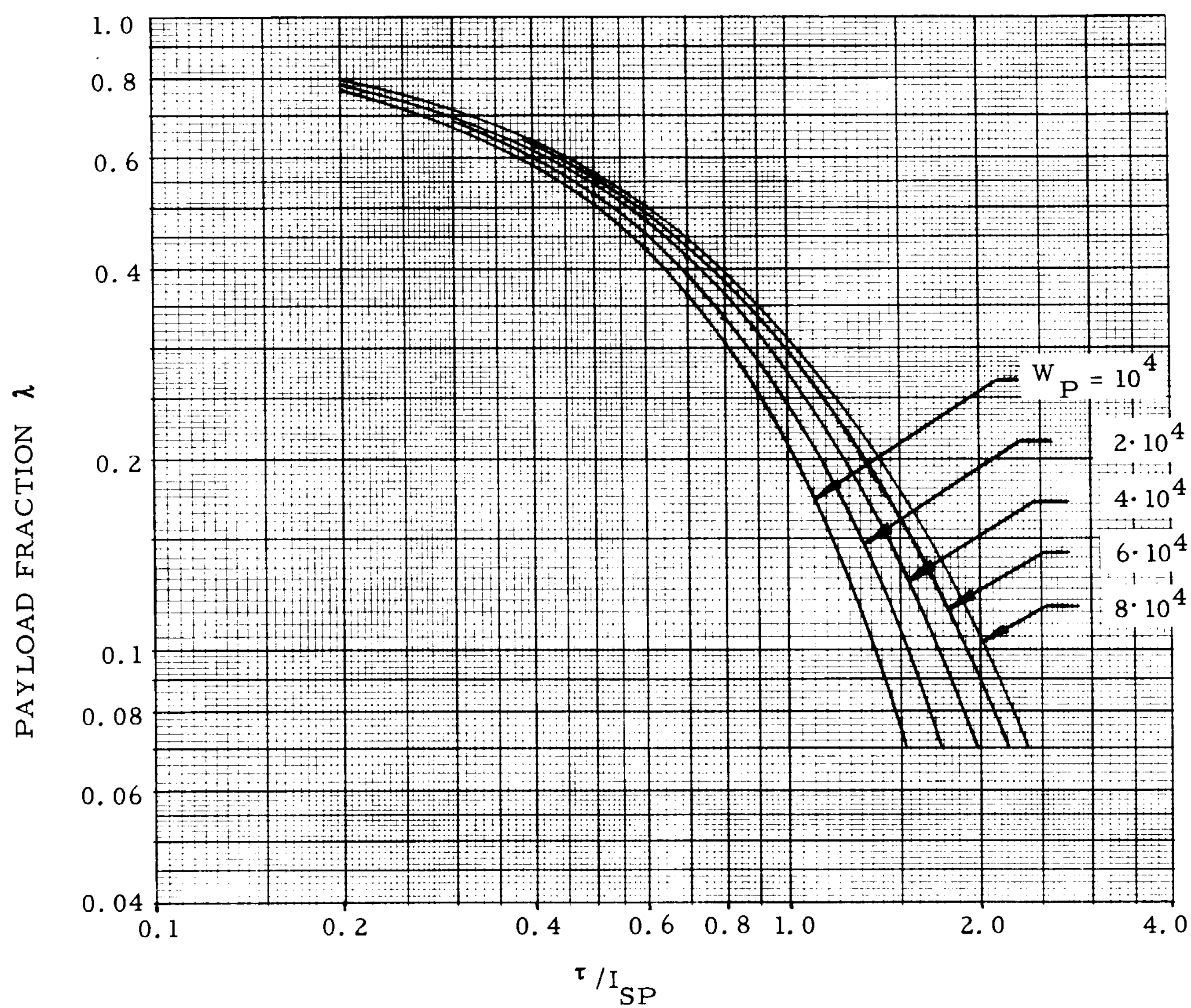

Fig. 5-6 HISV STAGE WITH SHE DRIVE: λ VS τ/I_{SP}

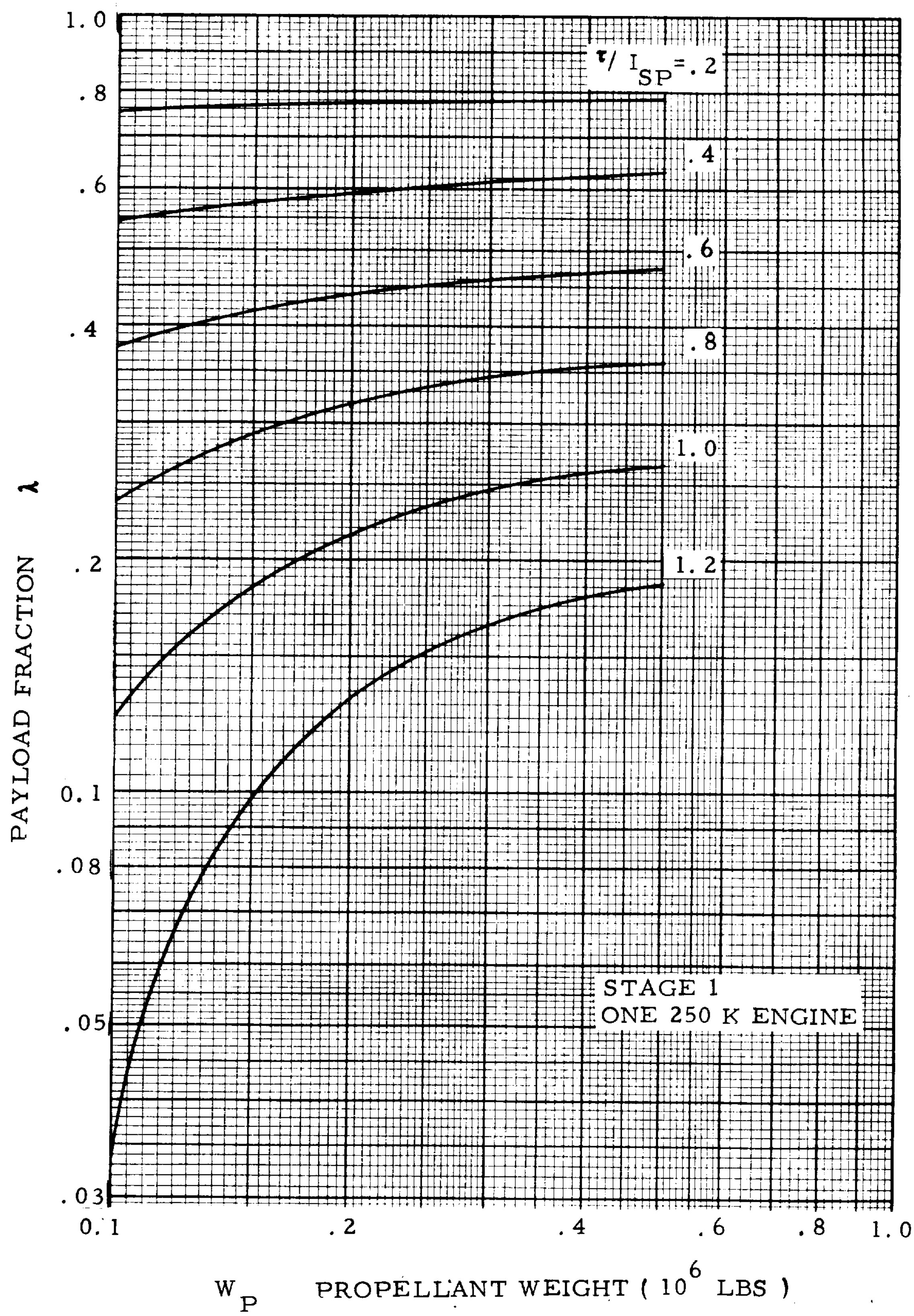

FIG. 5-7 SCR PROPULSION MODULE - PAYLOAD FRACTION VS PROPELLANT WEIGHT FOR VARIOUS τ/I_{SP} RATIOS

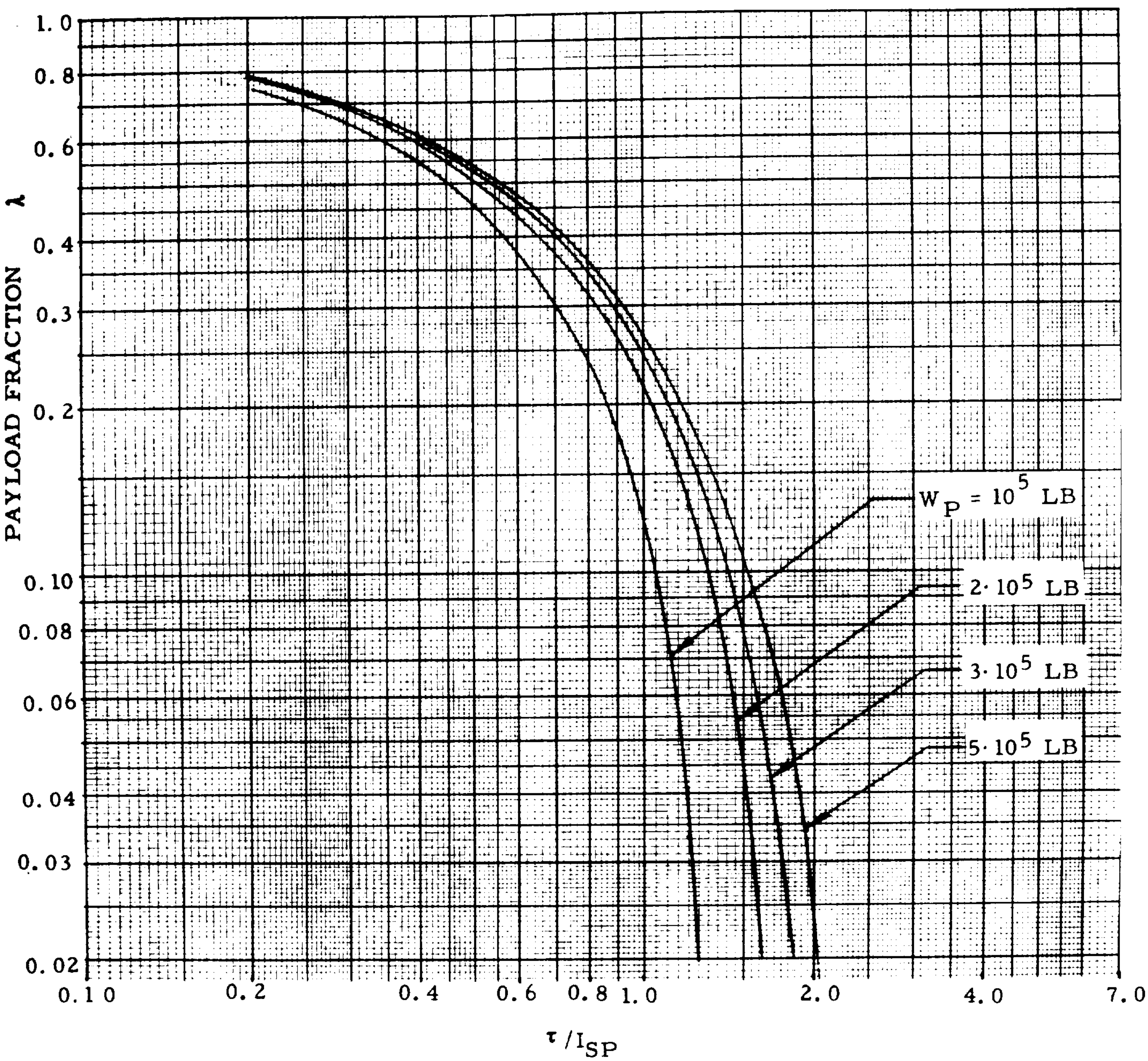

Fig. 5-8 PM-1 CLUSTER (38'DIA.; 1 SCR/G ENGINE @ 250 k): VARIATION OF λ WITH τ/I_{SP}

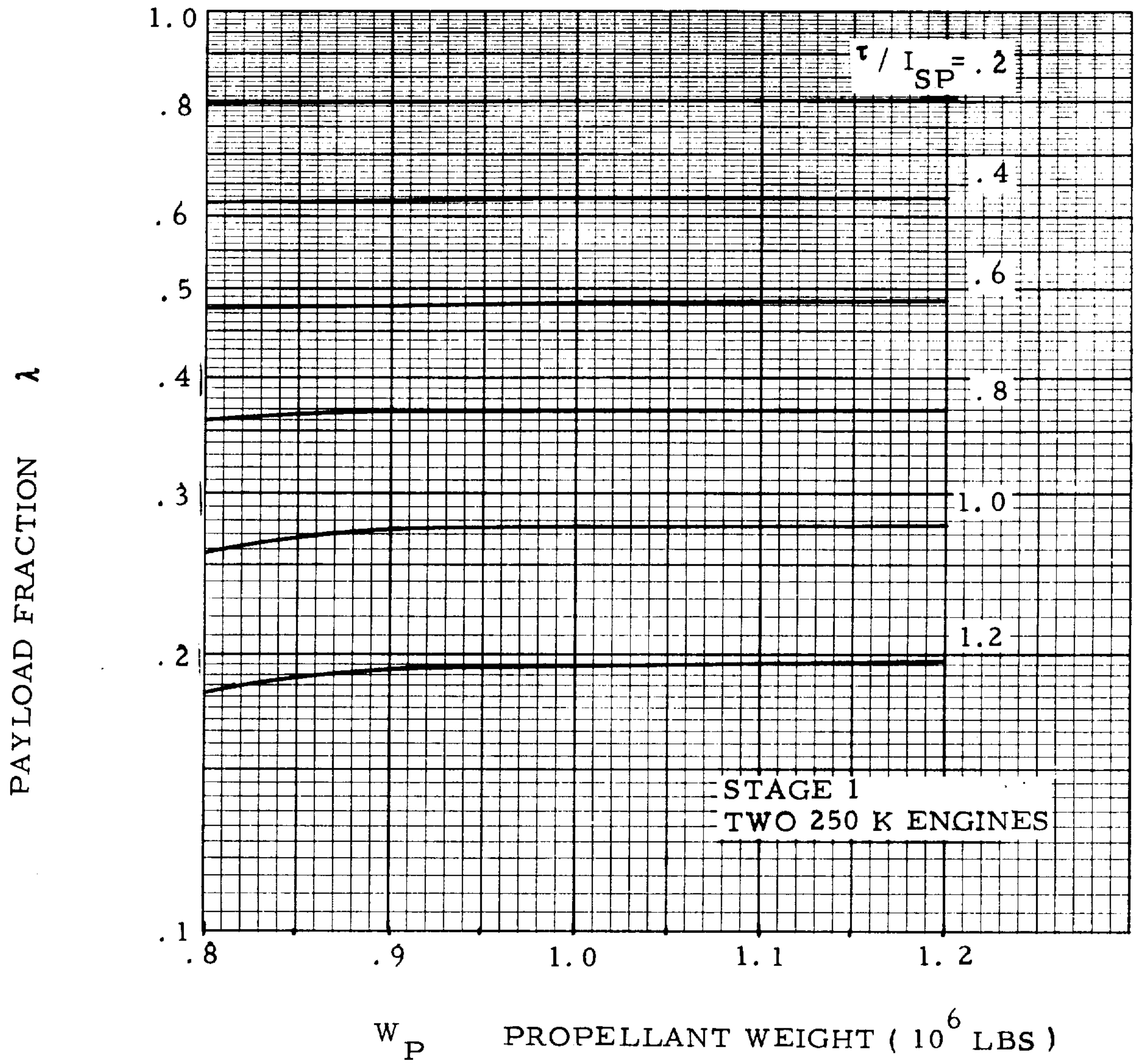

FIG. 5-9 SCR PROPULSION MODULE - PAYLOAD FRACTION VS PROPELLANT WEIGHT FOR VARIOUS τ/I_{SP} RATIOS

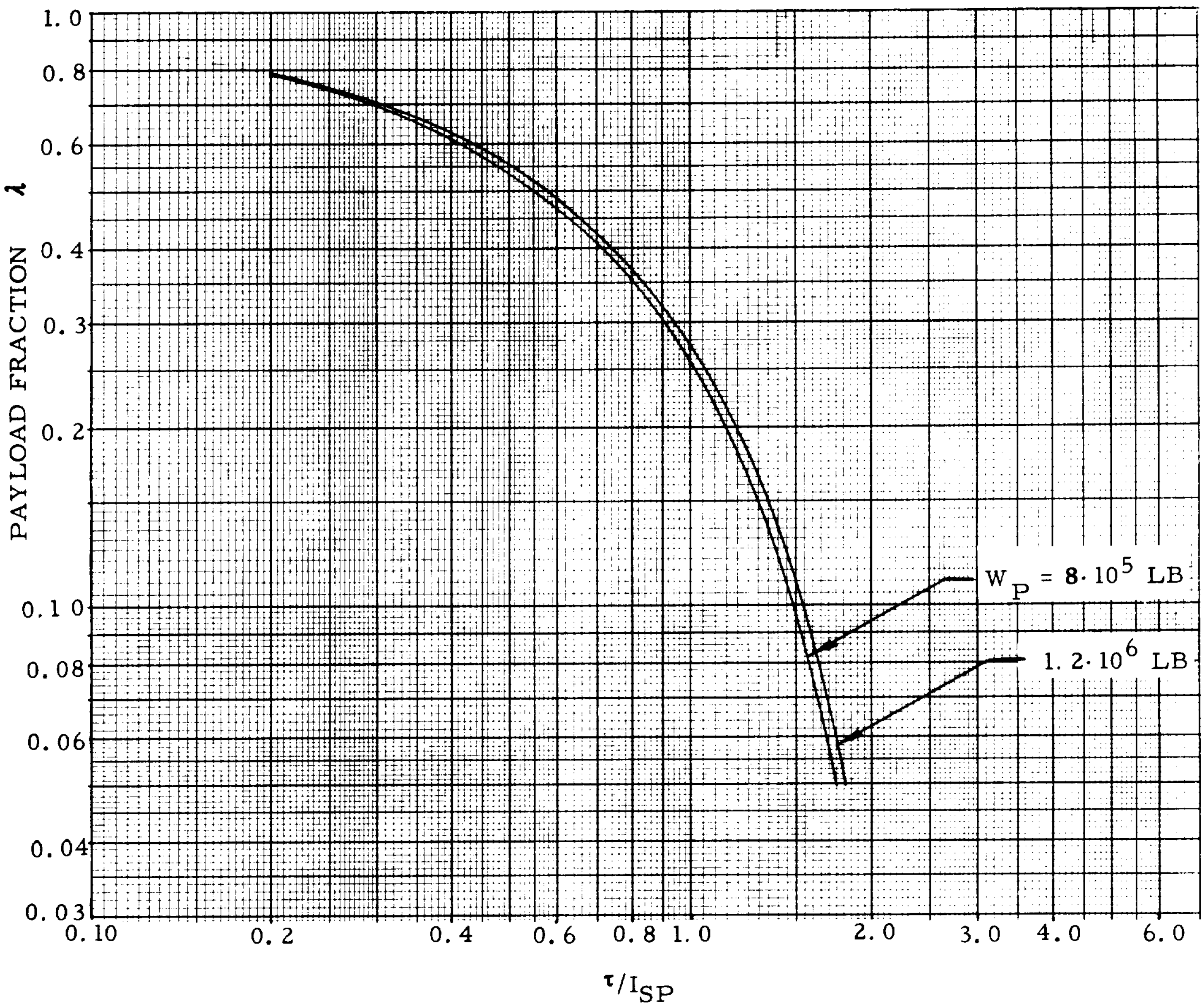

Fig. 5-10 PM-1 CLUSTER (38' DIA.; 2 SCR/G ENGINES @ 250 K)

VARIATION OF λ WITH τ/I_{SP}

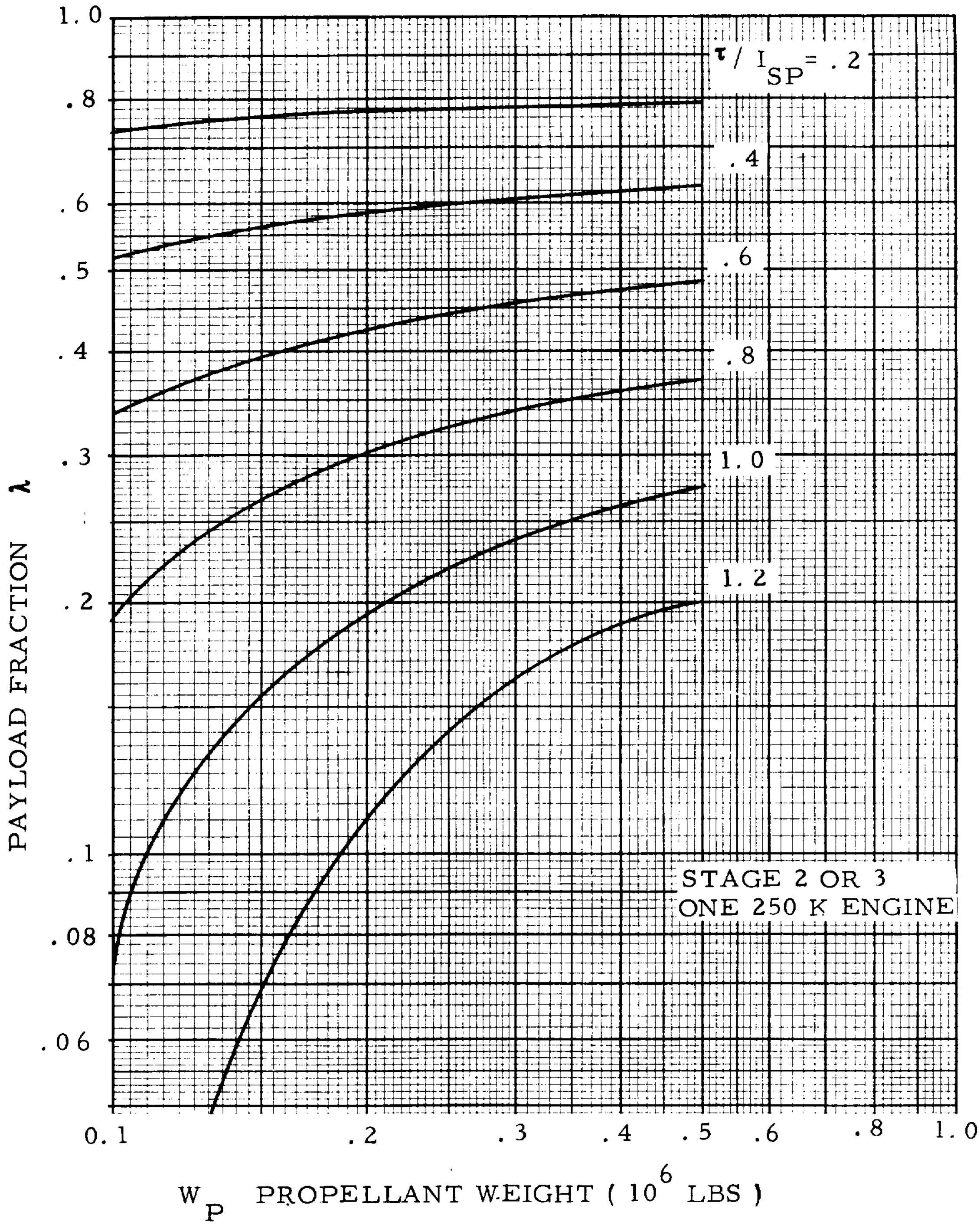

FIG. 5-11 SCR PROPULSION MODULE - PAYLOAD FRACTION VS PROPELLANT WEIGHT FOR VARIOUS τ/I_{SP} RATIOS

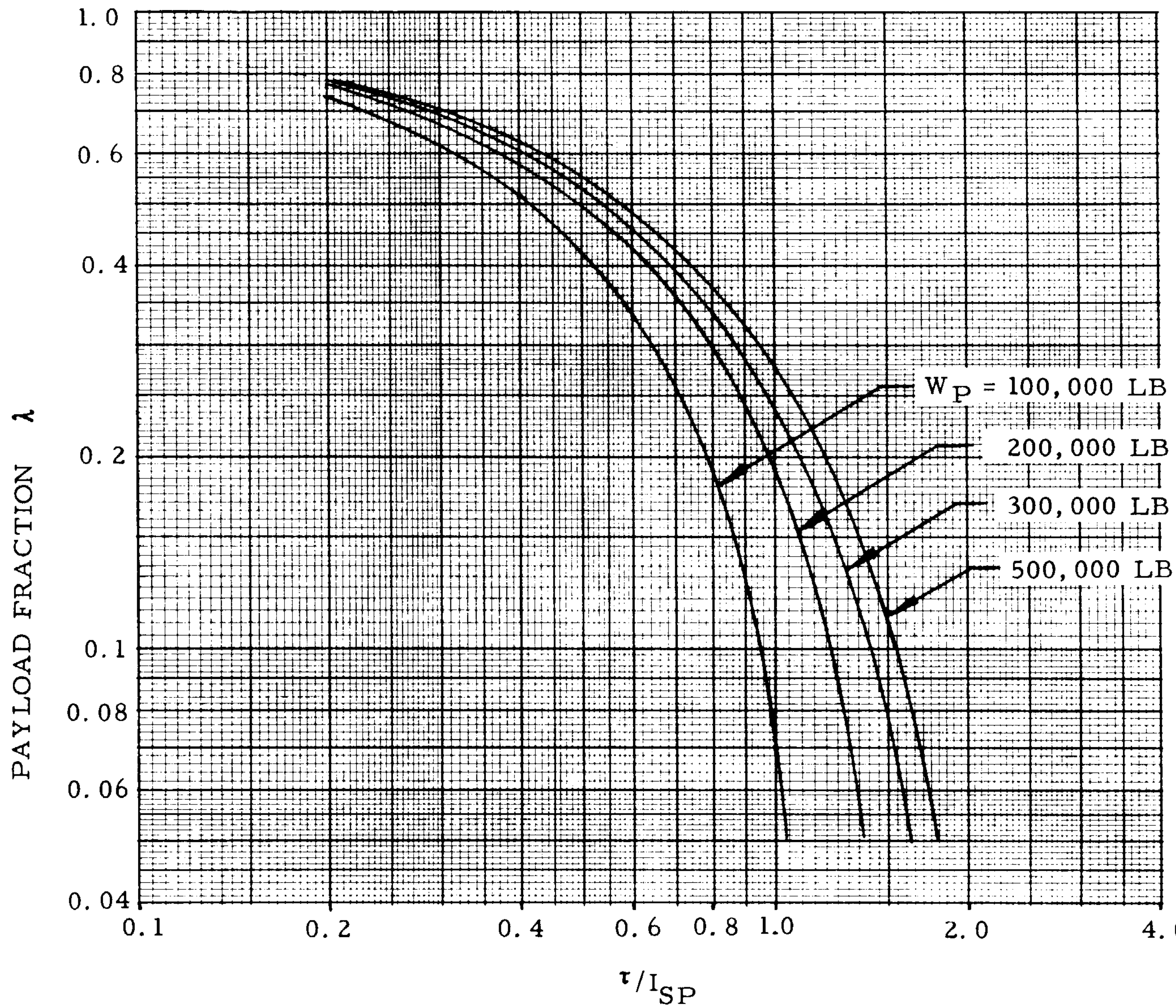

Fig. 5-12 HISV CLUSTER (38' DIA.; 1 SCR /G ENGINE @ 250 K): VARIATION OF λ WITH τ/I_{SP}

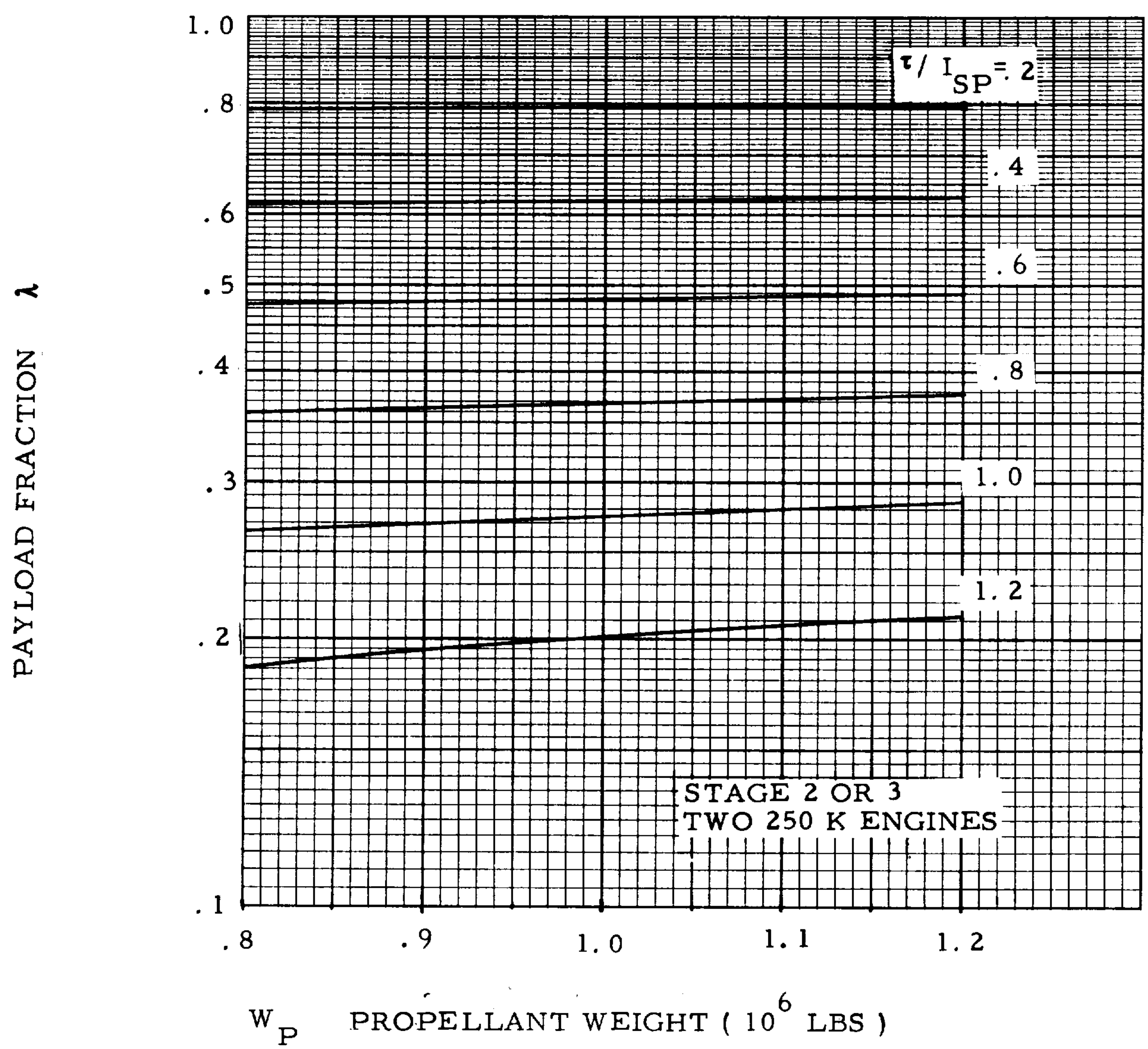

FIG. 5-13 SCR PROPULSION MODULE - PAYLOAD FRACTION VS PROPELLANT WEIGHT FOR VARIOUS τ/I_{SP} RATIOS

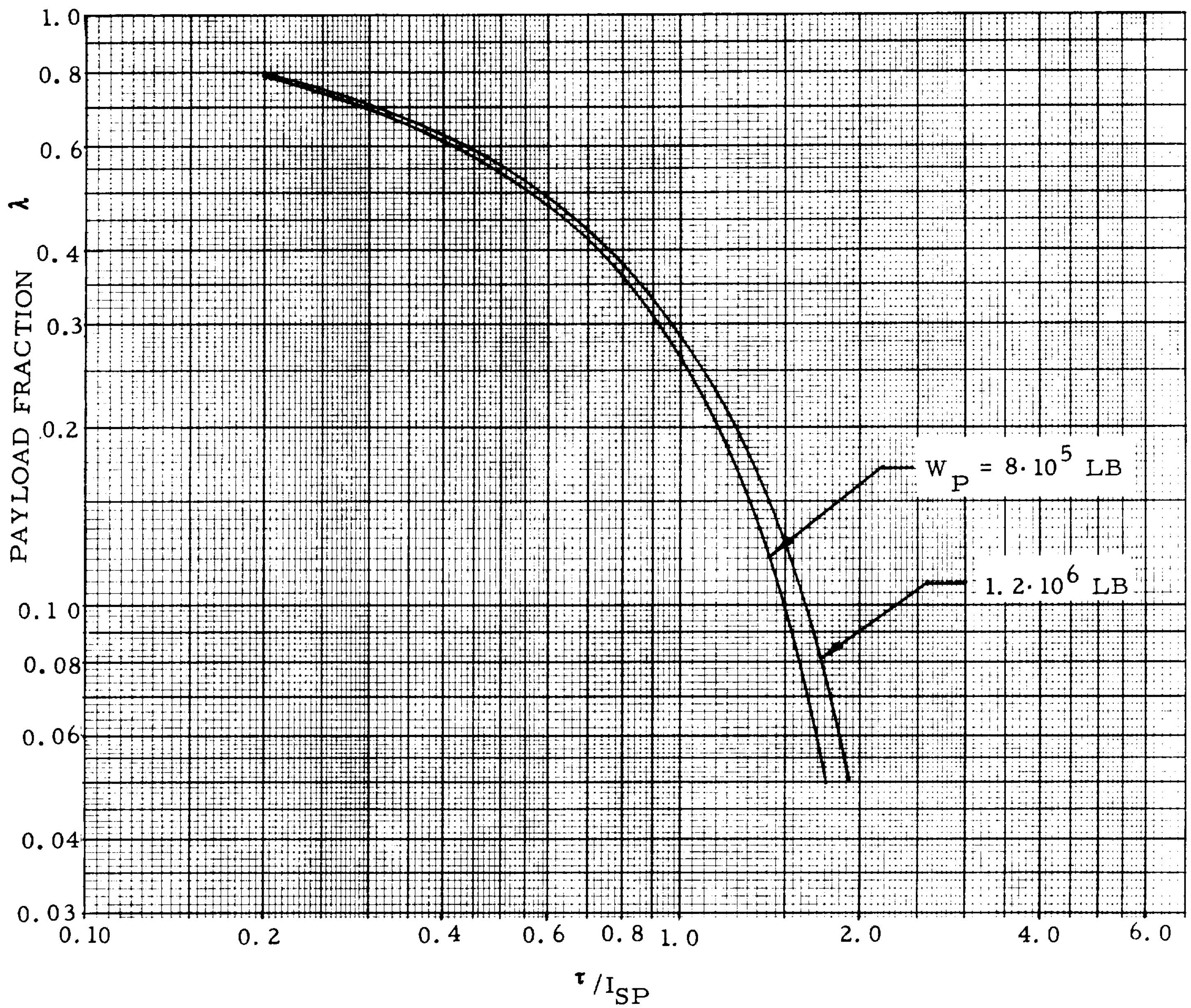

Fig. 5-14 HISV CLUSTER (38' DIA.; 2 SCR/G ENGINES @ 250 K)

VARIATION OF λ WITH τ / I_{sp}

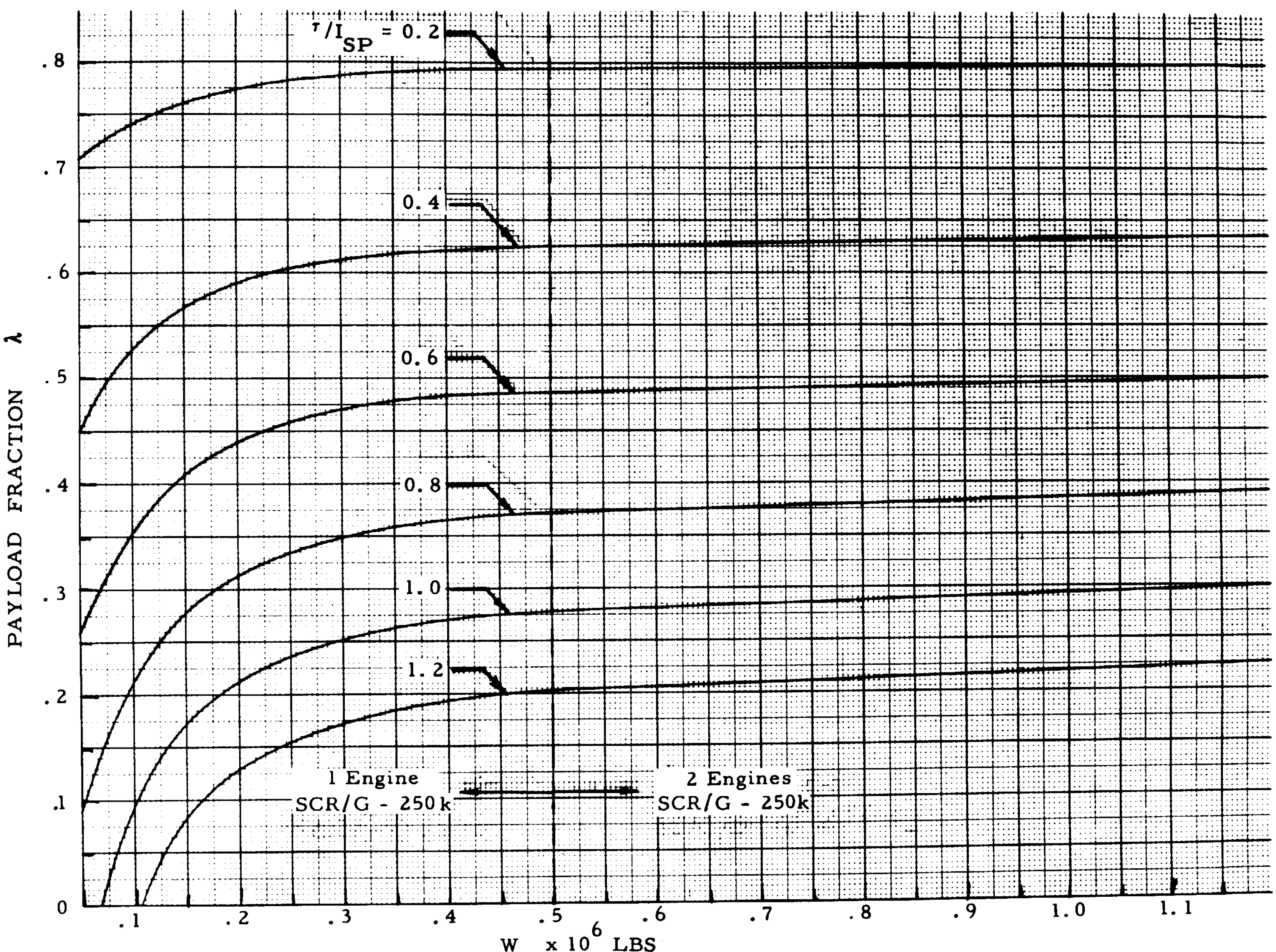

FIG. 5-15 PAYLOAD FRACTION VS τ/I_{SP} AND PROPELLANT WEIGHT FOR 70 FT. DIAMETER POST SATURN COMPATIBLE VEHICLE . Propulsion: SCR/G Engines - 250k

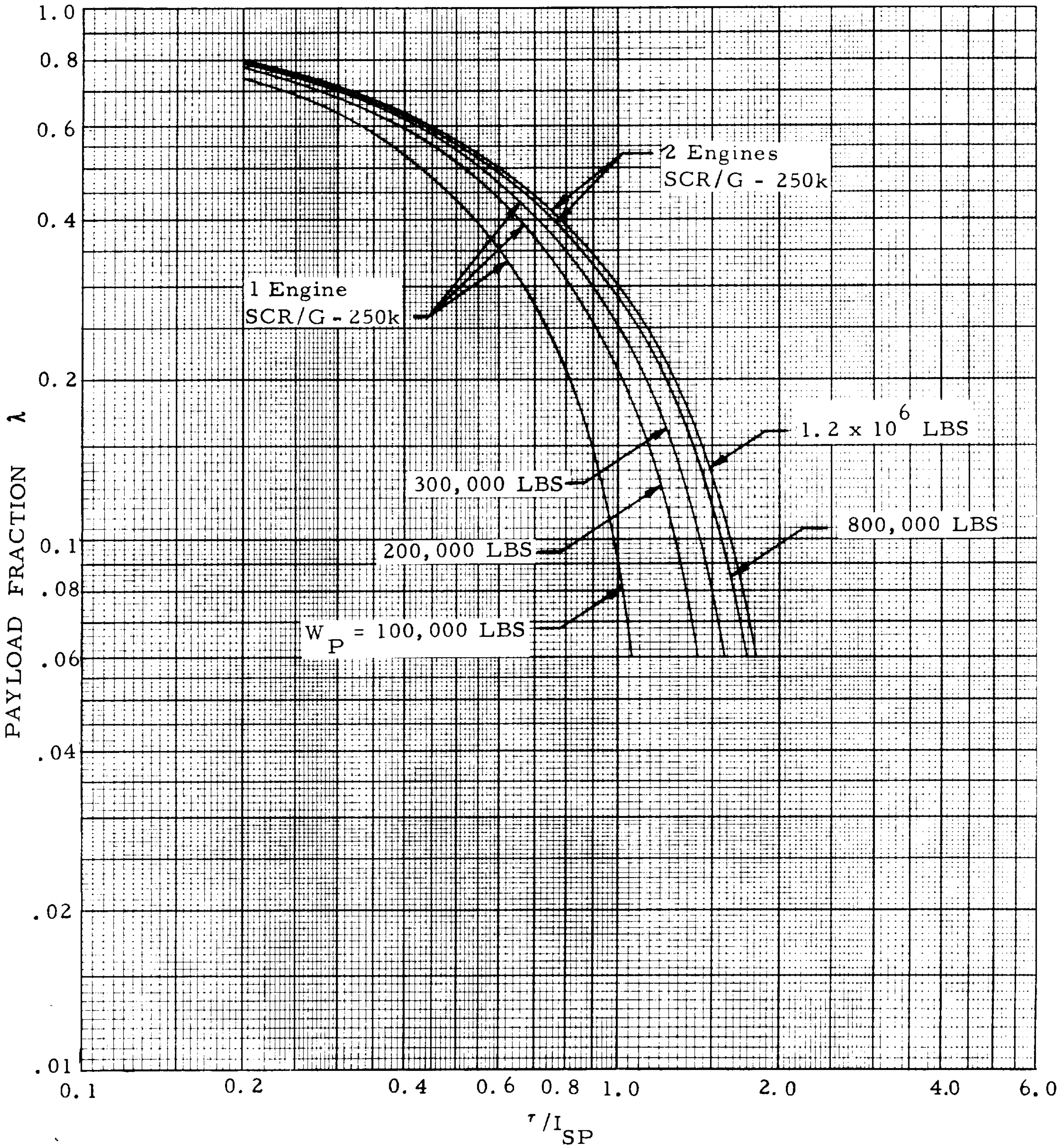

FIG. 5-16 HISV PAYLOAD FRACTION VS τ/I_{SP} AND PROPELLANT WEIGHT FOR CLUSTERED 70 FT. DIAMETER POST SATURN COMPATIBLE VEHICLE

PROPULSION : SCR/G Engine - 250k

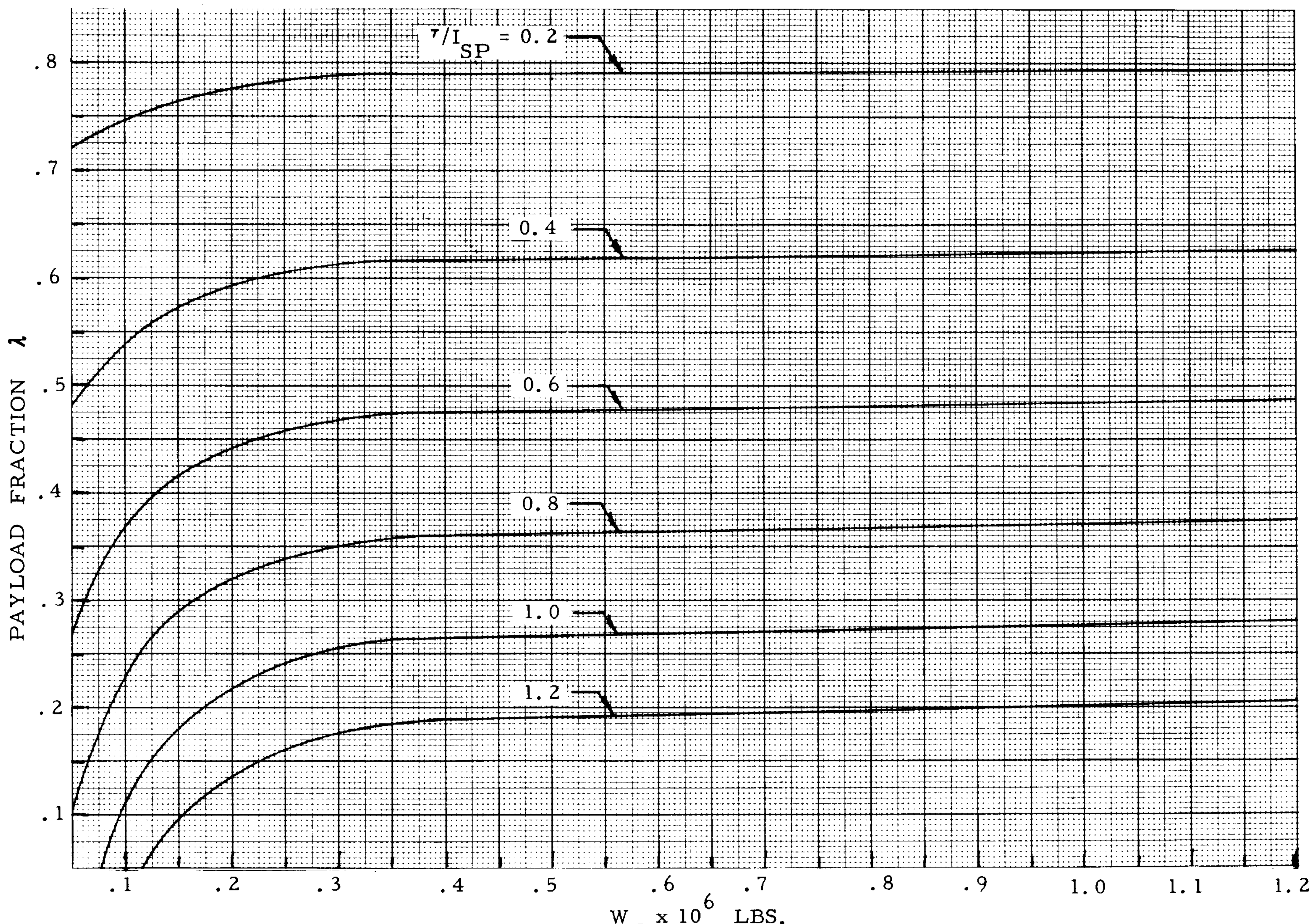

FIG. 5-17 PAYLOAD FRACTION VS τ/I_{SP} AND PROPELLANT WEIGHT FOR 33 FT. DIAMETER SATURN V COMPATIBLE STAGES

Propuls(: 1 SCR/G Engine - 250k

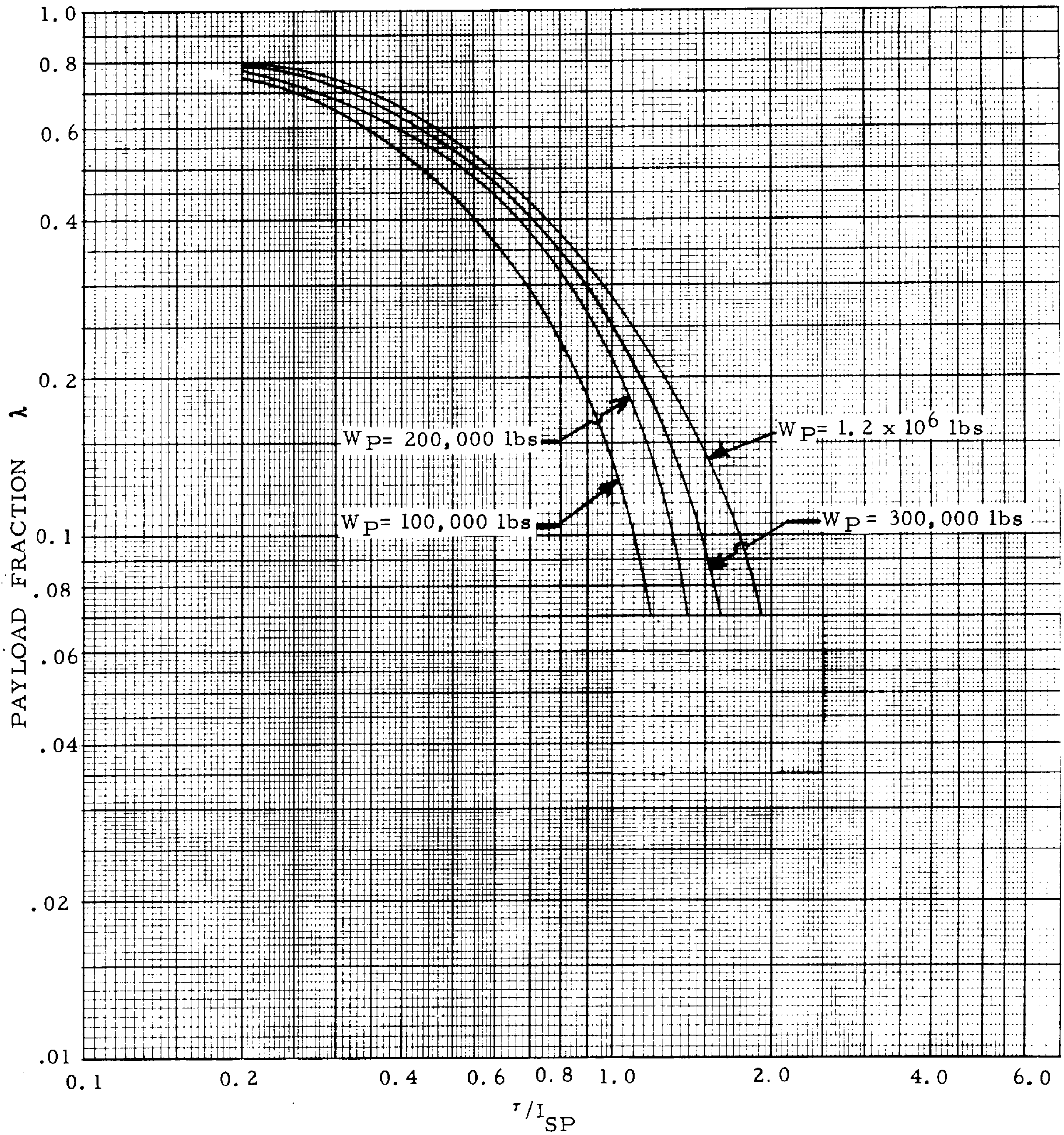

FIG. 5-18 HISV PAYLOAD FRACTION VS τ/I_{SP} AND PROPELLANT WEIGHT FOR 33 FT. DIAMETER SATURN V COMPATIBLE STAGES

PROPULSION: 1 SCR/G Engine - 250k

Conditions for the -23 Class vehicle are shown in Figs. 5-19, 5-20, for the tankage without engines (since in this configuration the same engines are used throughout the mission and only tankage is jettisoned between the individual maneuvers); Figs. 5-21, 5-22 for tankage with 2 SCR/N engines; and Figs. 5-23, 5-24 for tankage with 4 SCR/N engines. The engines have 50 k thrust each and are of the non-moderated metal-base type.

Figs. 5-25 through 5-32 apply to the GCR HISV of the configuration described in the preceding section. Only single-engine versions were considered. The same engine is used for all maneuvers. It is assumed that its thrust can be throttled to 25% of its full-thrust value. Four thrust levels were considered, namely, 0.75, 1.0, 1.5 and $3 \cdot 10^6$ lb. Since a distribution is made in this configuration, between the scaling coefficient for the center tank, $K_{p,\,CT}$ and that for the satellite tanks, $K_{p,\,ST}$, Eq. (4-88a) was used for the computation of x, where the total quantity of propellant, W_p, was divided into center tank propellant and satellite tank propellant. These conditions are the basis for the payload fraction charts of the GCR-HISV's.

Finally, Figs. 5-33 and 5-34 show plots of GPF versus τ/I_{sp} or Λ for the Saturn V compatible nuclear pulse vehicle NP-1.

With the use of these graphs, mission payload fractions can be determined. The following information must be given:

- Number of maneuvers constituting the mission
- Ideal velocity change Δv_{id} for each maneuver. The ideal velocity is defined as the sum of actual velocity change plus the velocity equivalent of gravitational losses, drag losses where relevant and of propellant losses due to thrust vector misalignment or aftercooling (the latter only insofar as it has not already been taken into account by lowering the specific impulse). From the known ideal velocity, the value of τ is obtained for each maneuver.
- Type of propulsion module for each maneuver.
- Specific impulse I_{sp} of each propulsion module.

The method of evaluation is demonstrated in the subsequent examples:

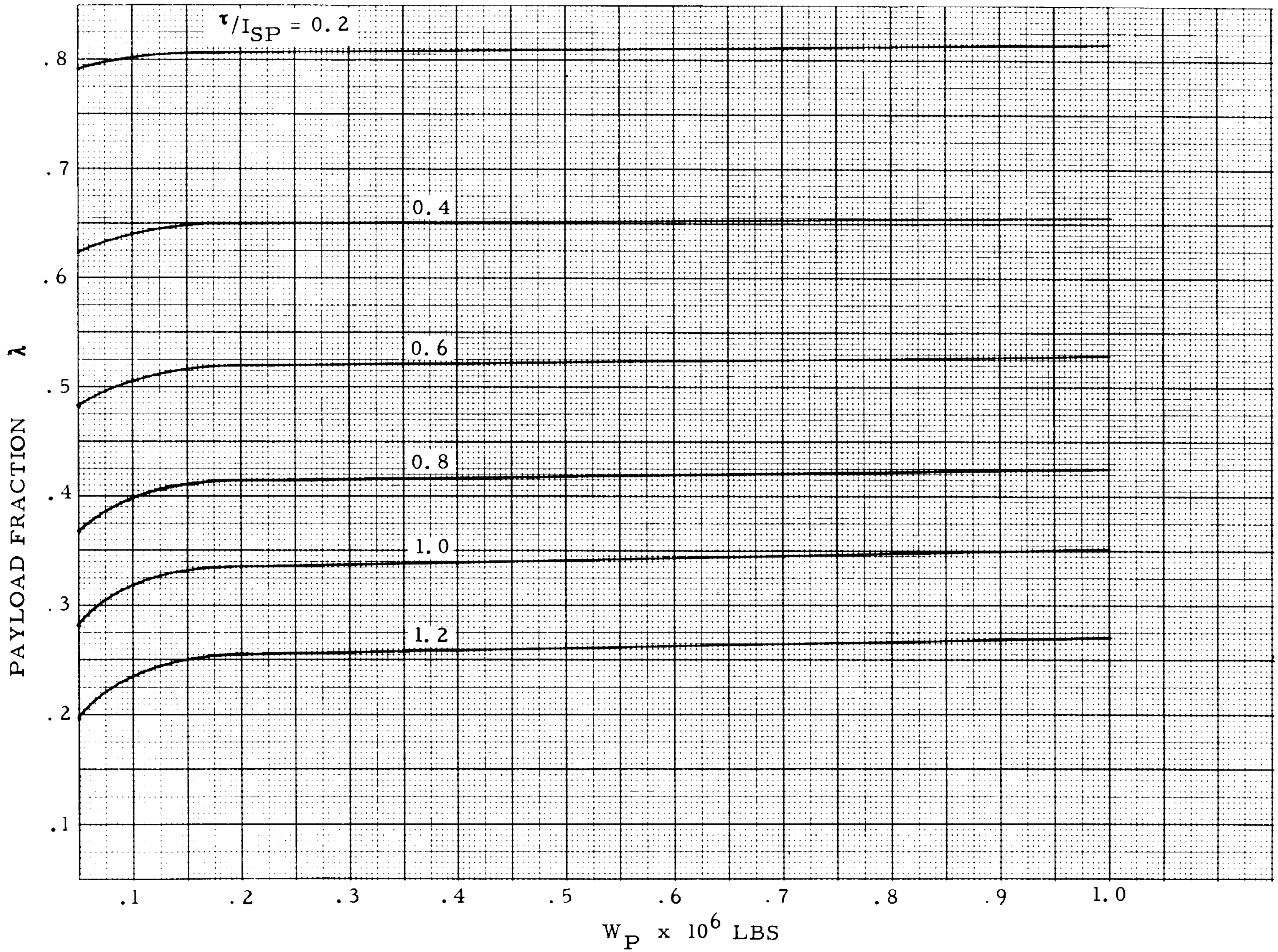

Fig. 5-19 PAYLOAD FRACTION VS τ/I_{SP} AND PROPELLANT WEIGHT FOR -23 CONFIGURATION WITHOUT ENGINES

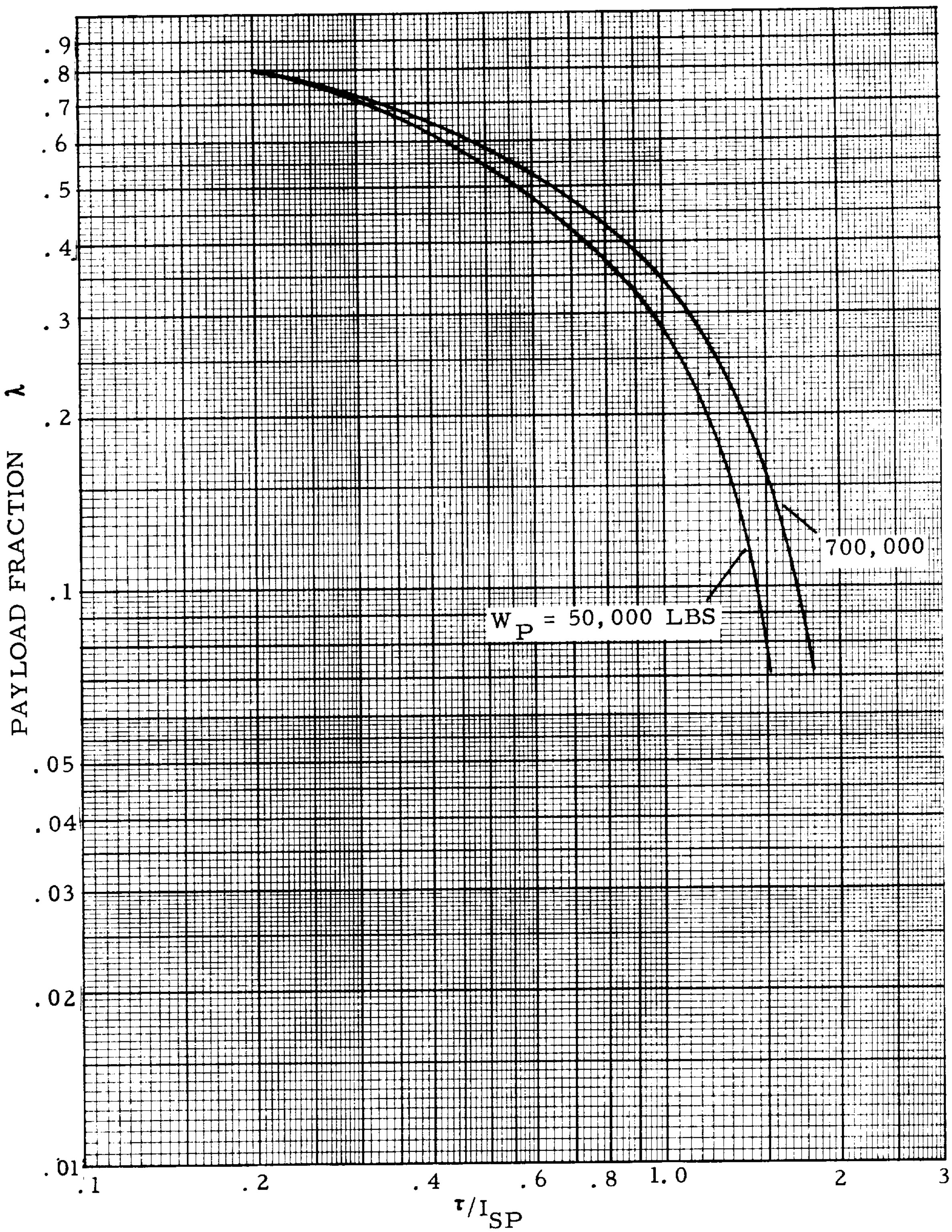

Fig. 5-20 PAYLOAD FRACTION VS τ/I_{SP} AND PROPELLANT WEIGHT FOR -23 CONFIGURATION WITHOUT ENGINES

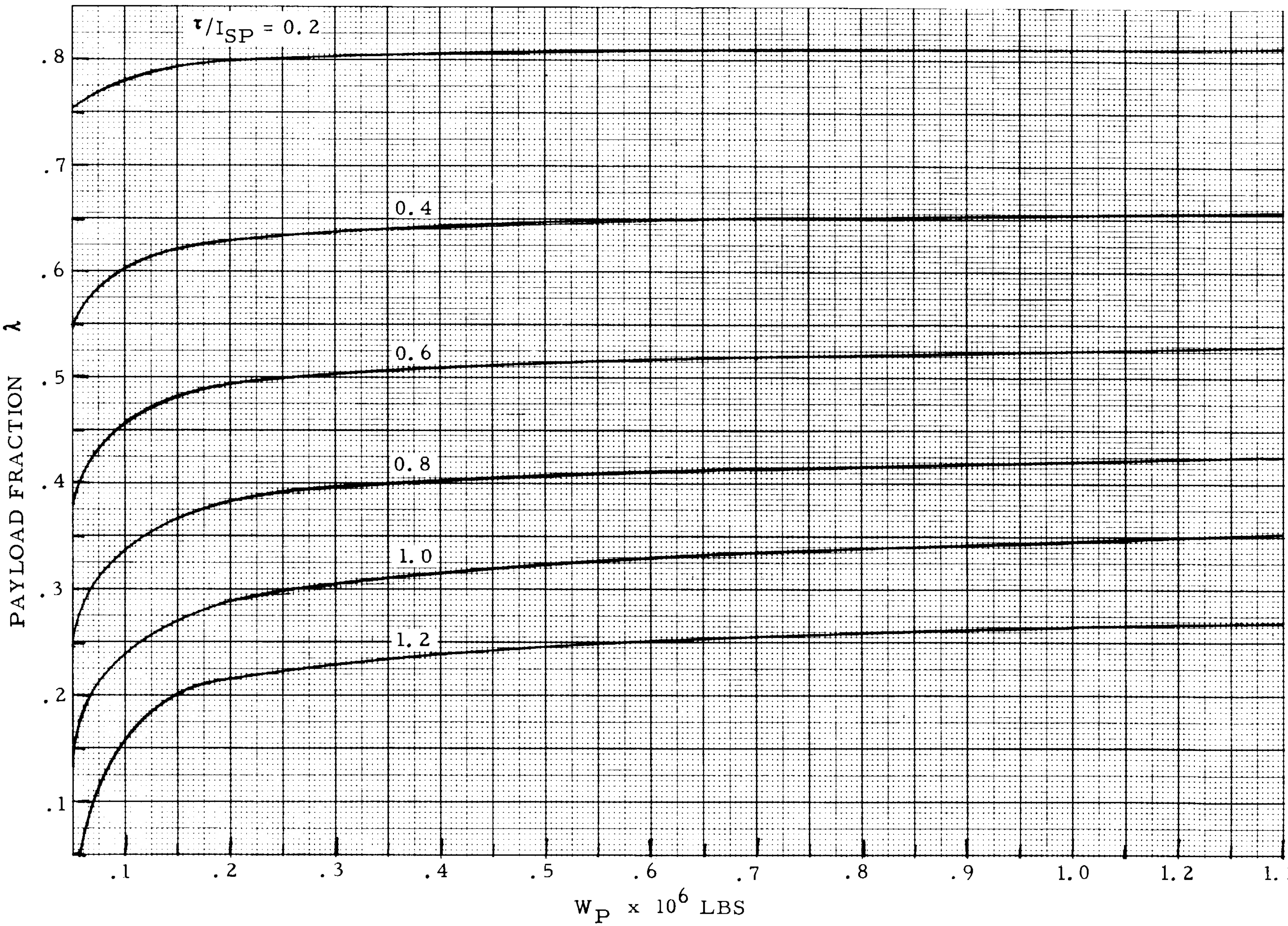

Fig. 5-21 PAYLOAD FRACTION VS τ/I_{SP} AND PROPELLANT WEIGHT FOR -23 CONFIGURATION WITH 2 METAL CORE ENGINES

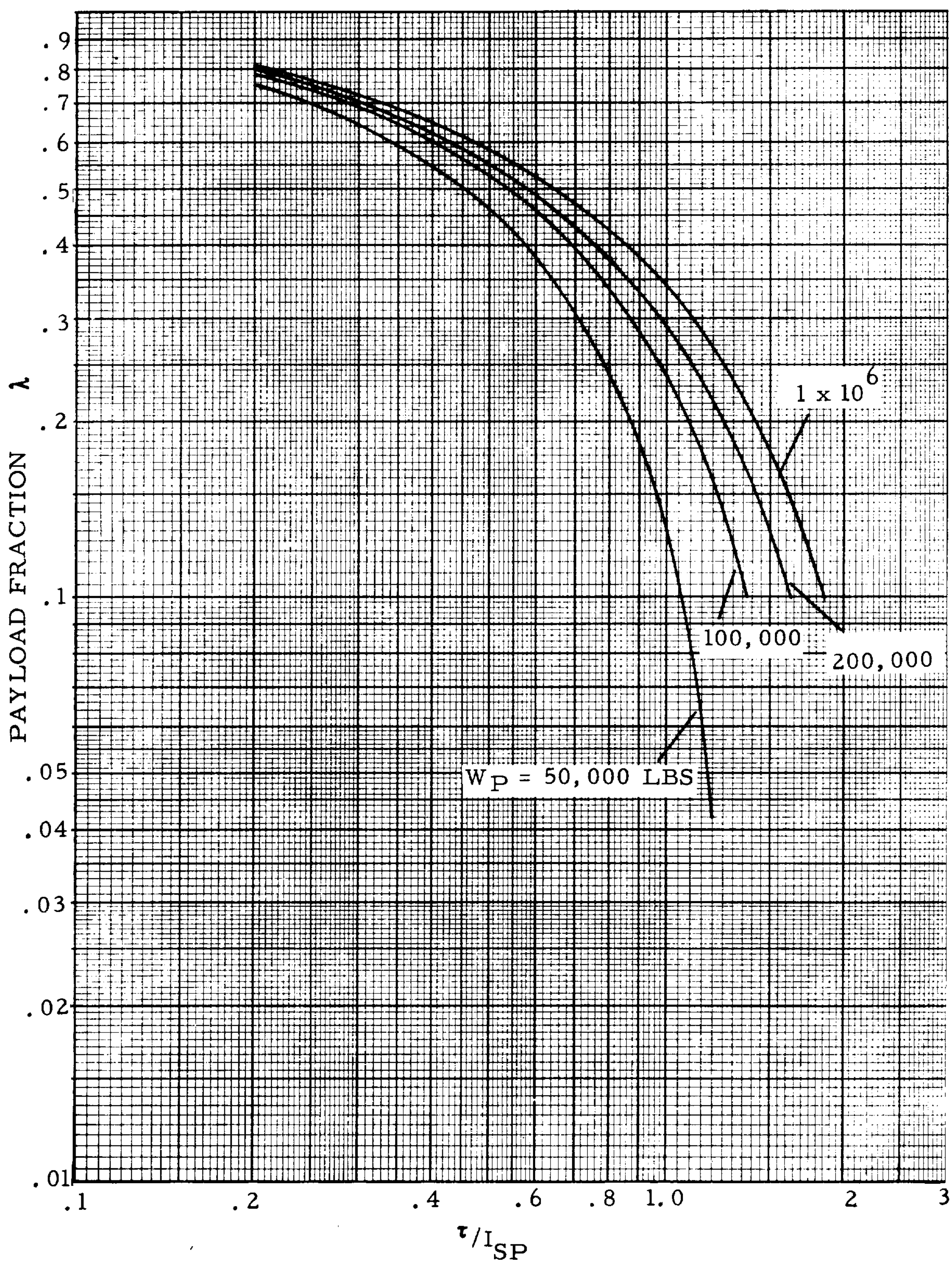

Fig. 5-22 PAYLOAD FRACTION VS τ/I_{SP} AND PROPELLANT WEIGHT FOR -23 CONFIGURATION WITH 2 METAL CORE ENGINES

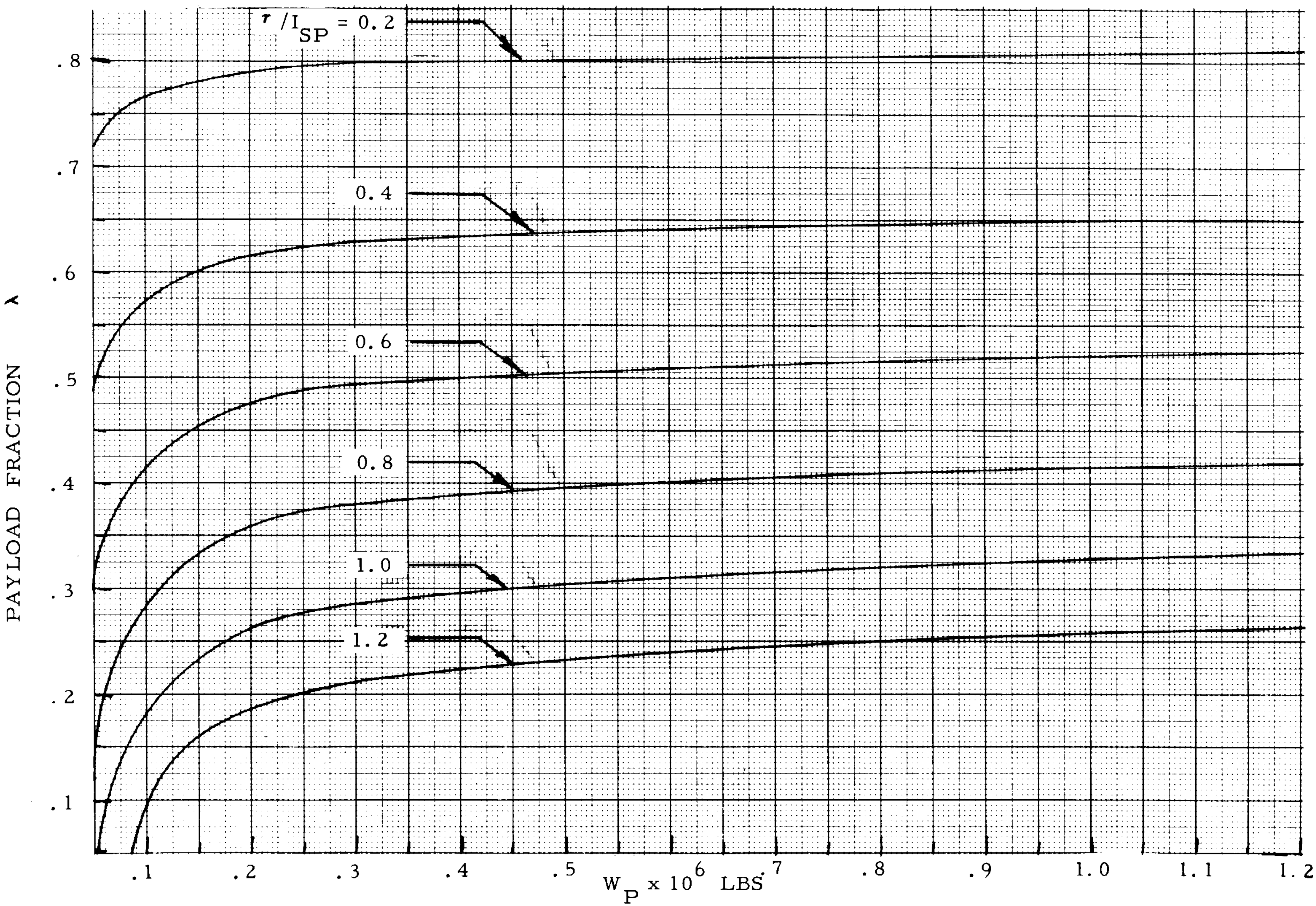

FIG. 5-23 PAYLOAD FRACTION VS τ/I_{SP} AND PROPELLANT WEIGHT FOR -23 CONFIGURATION WITH 4 METAL CORE ENGINES

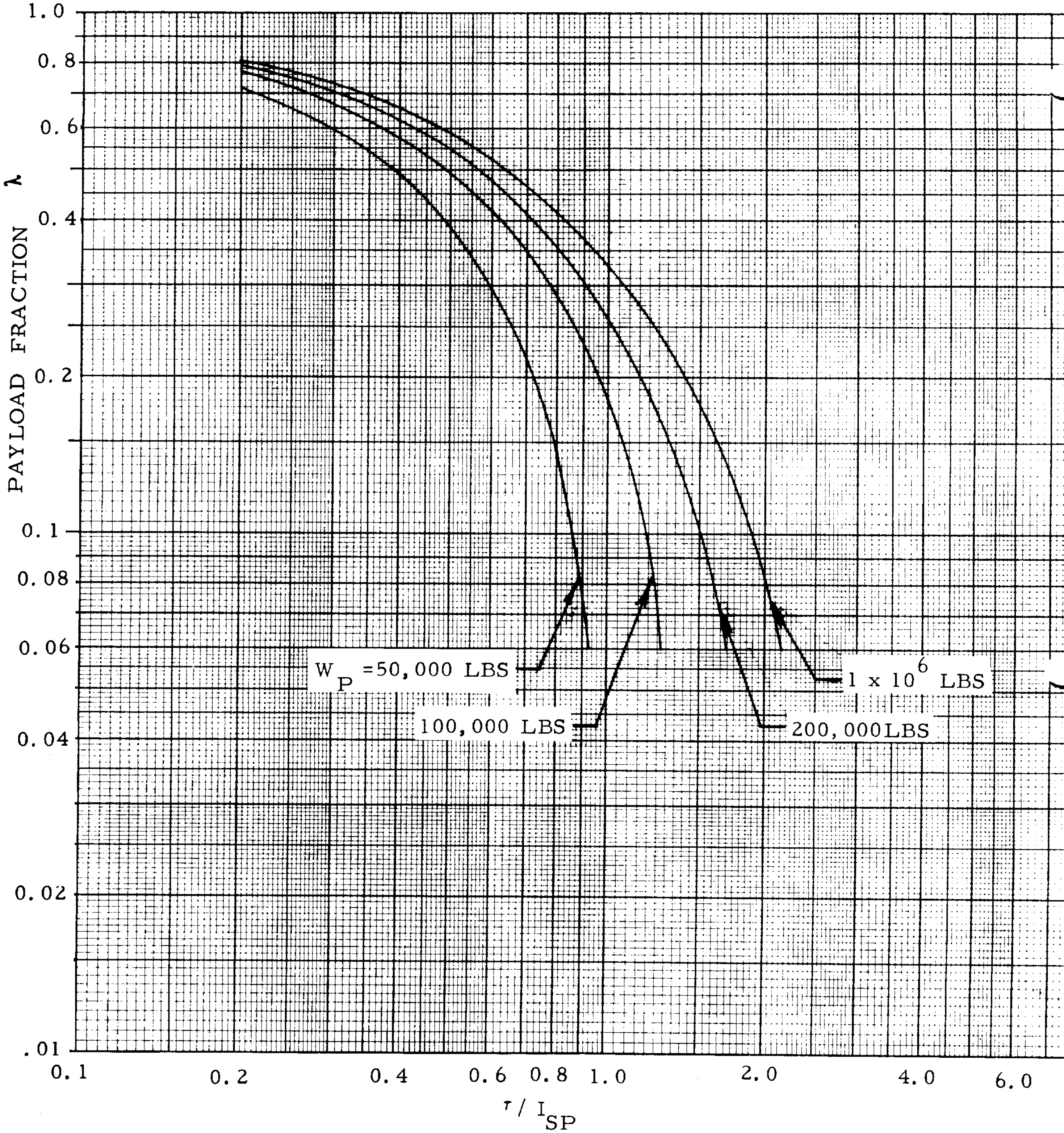

FIG. 5-24 HISV PAYLOAD FRACTION VS τ/I_{SP} AND PROPELLANT WEIGHT FOR -23 CONFIGURATION WITH 4 METAL CORE ENGINES

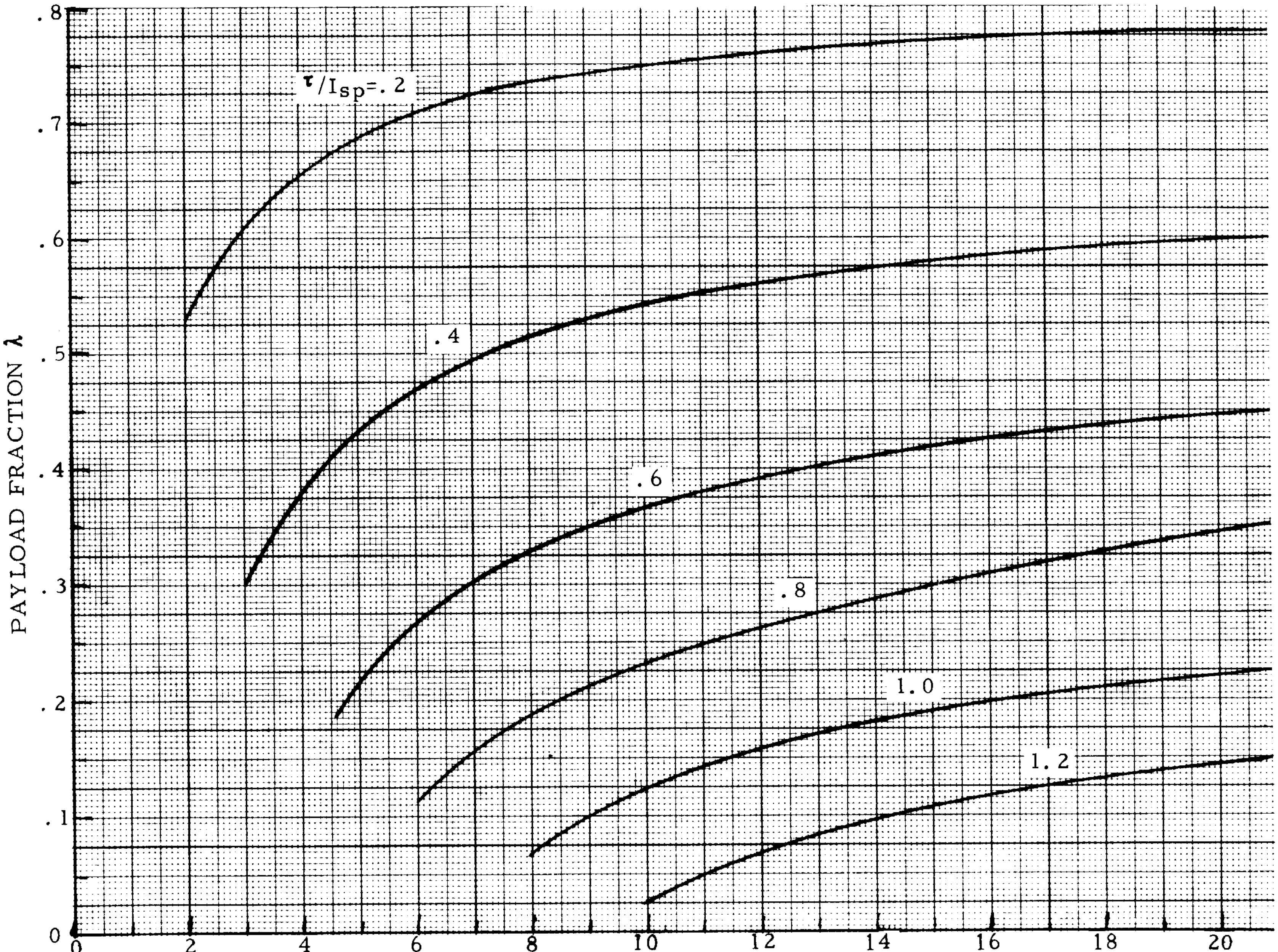

Fig. 5-25 GCR HISV: VARIATION OF PAYLOAD FRACTION WITH PROPELLANT WEIGHT FOR VARIOUS VALUES OF τ/I_{sp} ($F = .75 \times 10^6$ LB)

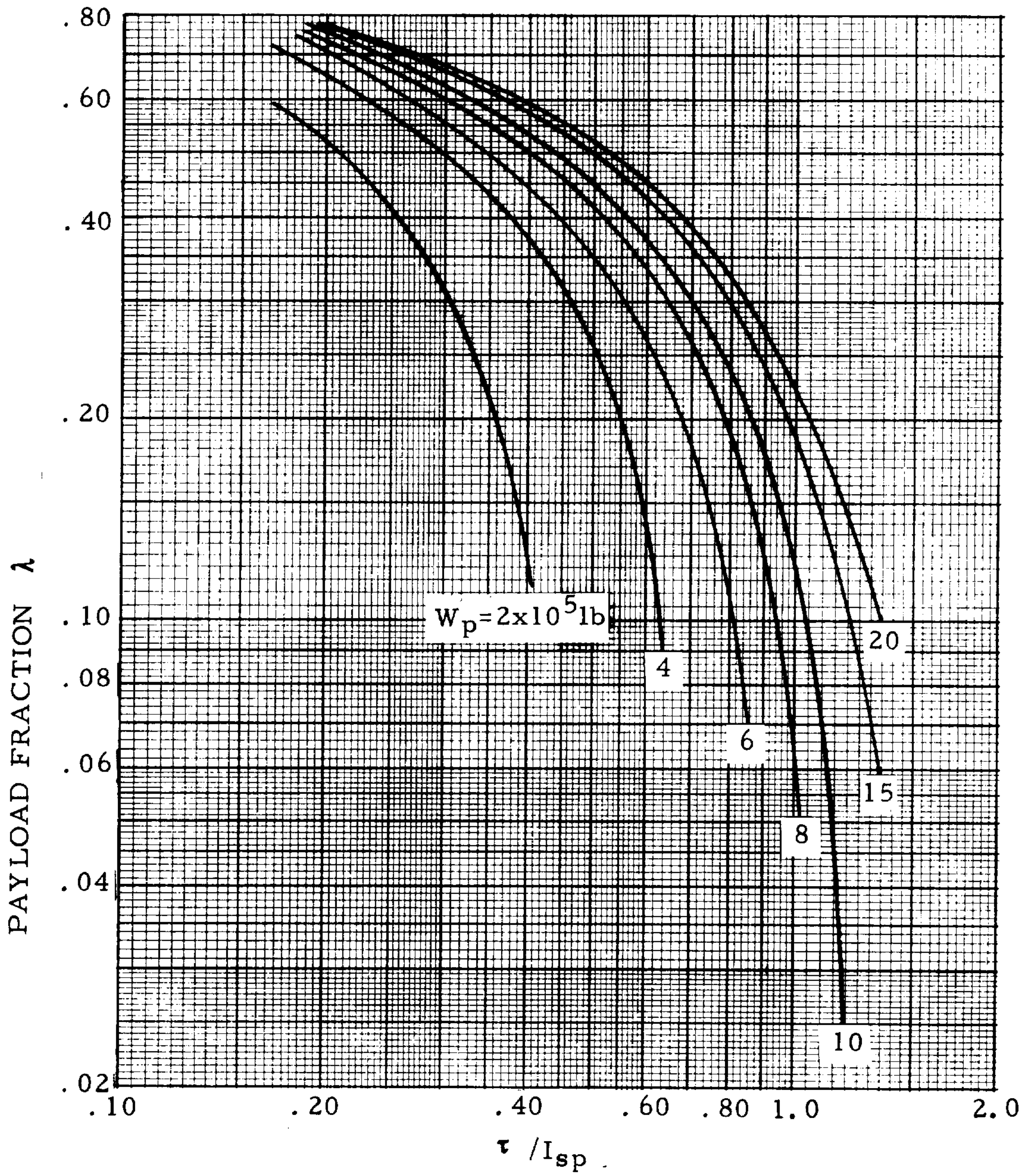

Fig. 5-26 GCR HISV λ vs. τ /I_{sp}

(F= .75x10^{6}LB)

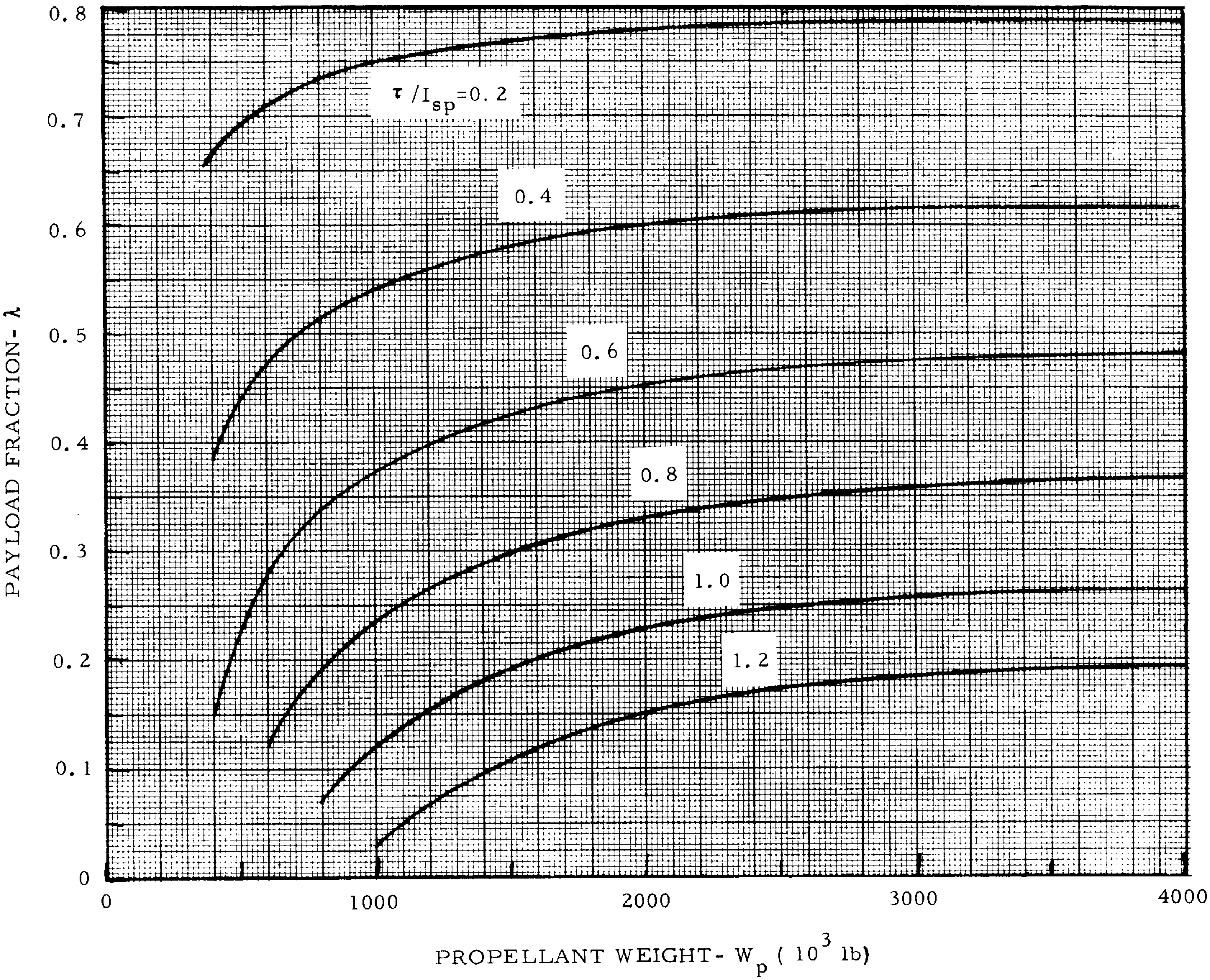

Fig. 5-27. GCR HISV – VARIATION OF PAYLOAD FRACTION WITH PROPELLANT WEIGHT FOR VARIOUS VALUES OF τ/I_{sp}. $F=10^6$ lb.

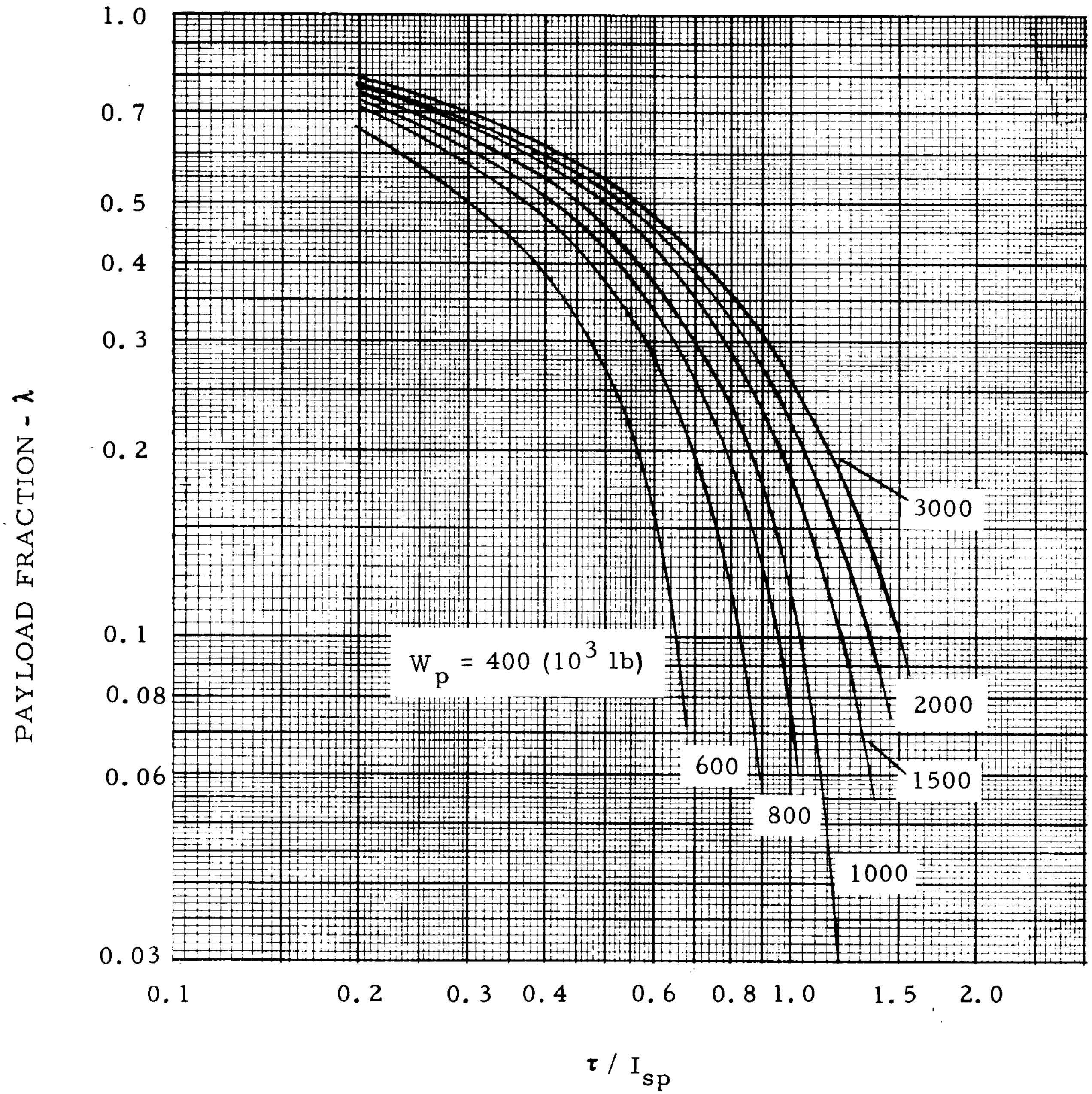

Fig.5-28 GCR HISV (F= 10^6 lb)

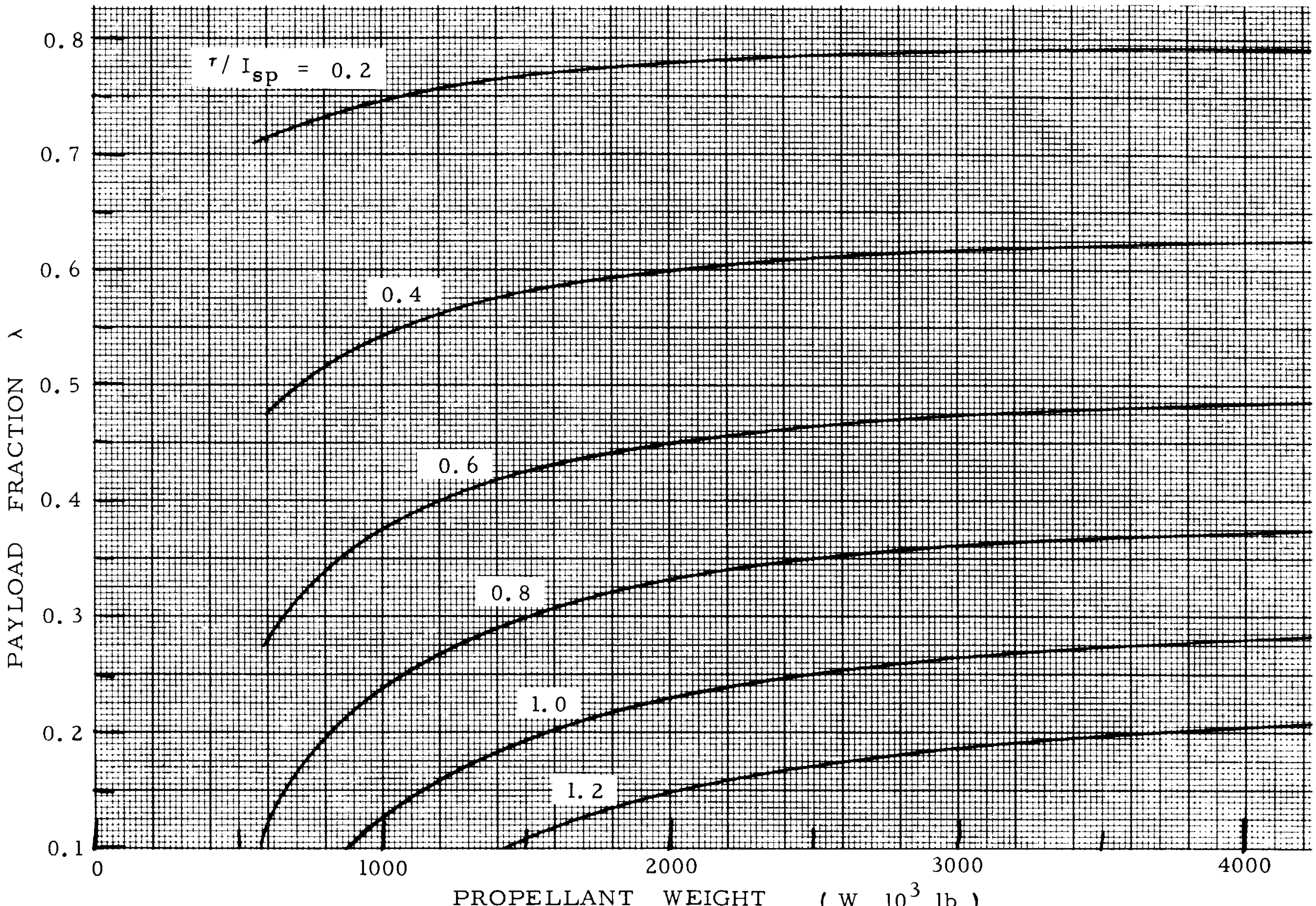

Fig.5-29 GCR HISV VARIATION OF PAYLOAD FRACTION WITH PROPELLANT WEIGHT FOR VARIOUS VALUES OF τ/I_{sp}

($F = 1.5 \times 10^6$ lb)

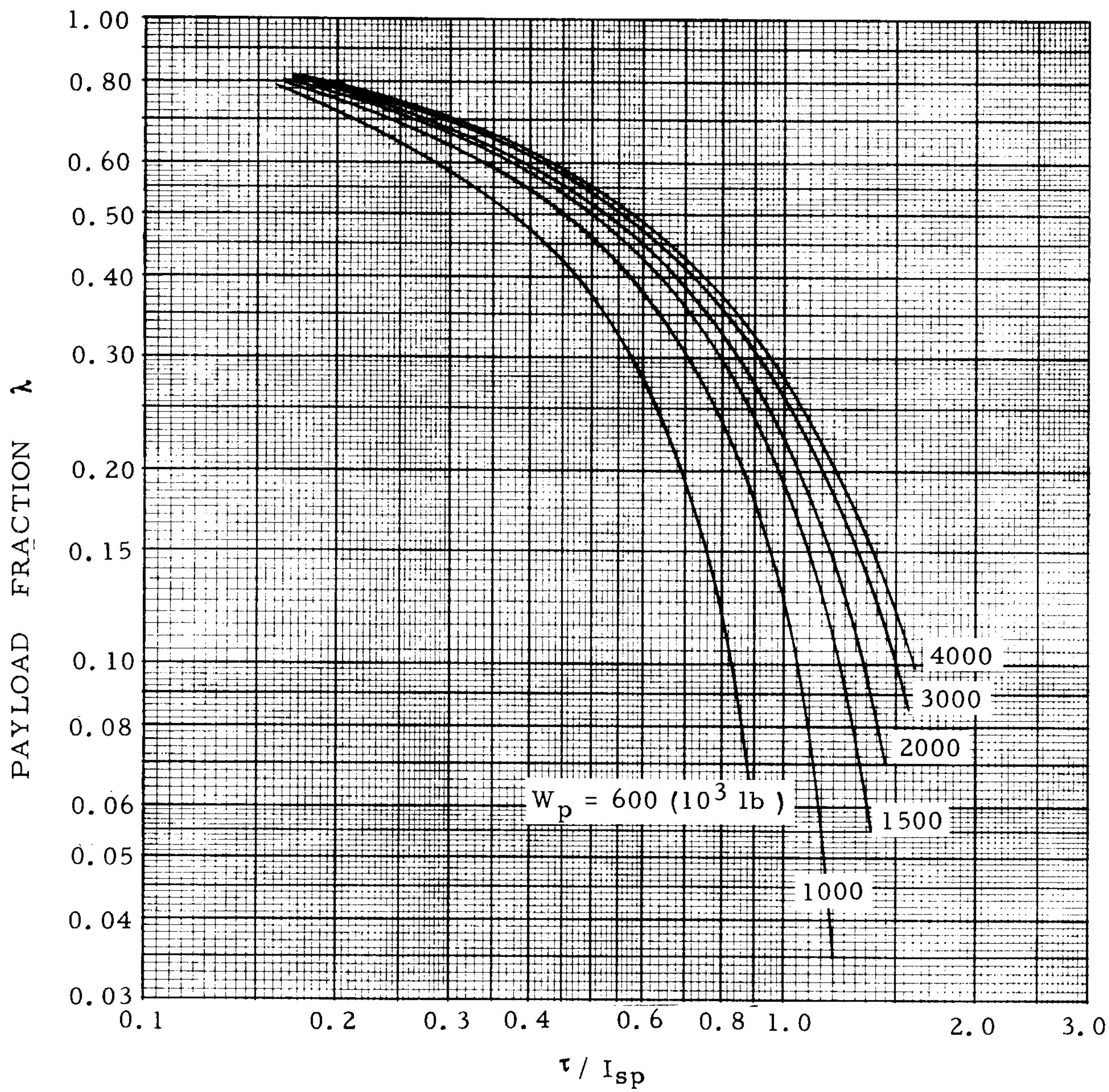

Fig. 5-30 GCR HISV ($F = 1.5 \times 10^6$) λ vs. τ / I_{sp}

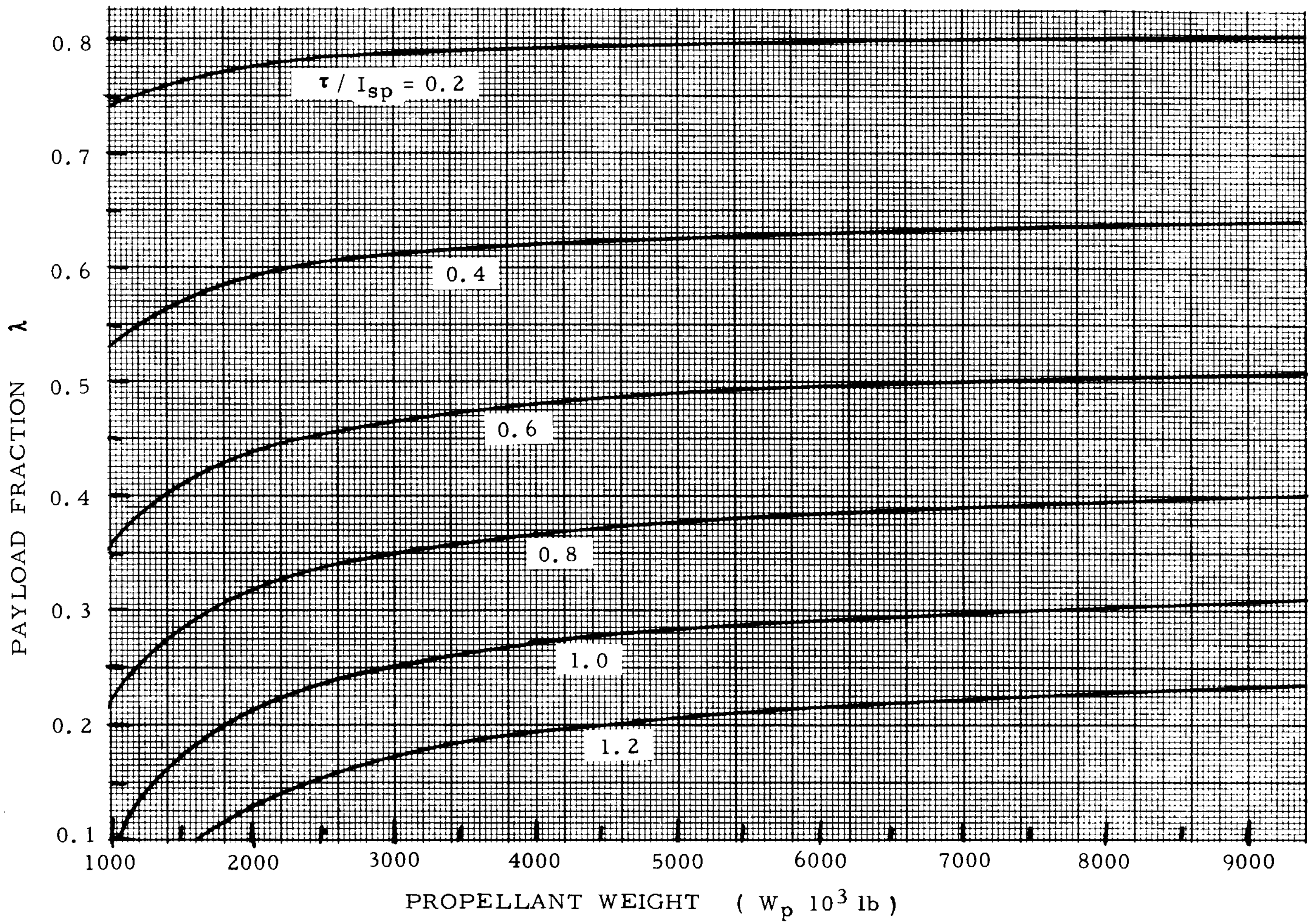

Fig.5-31 GCR HISV VARIATION OF PAYLOAD FRACTION WITH PROPELLANT WEIGHT FOR VARIOUS VALUES OF τ / I_{sp}
($F = 3 \times 10^6$ lb)

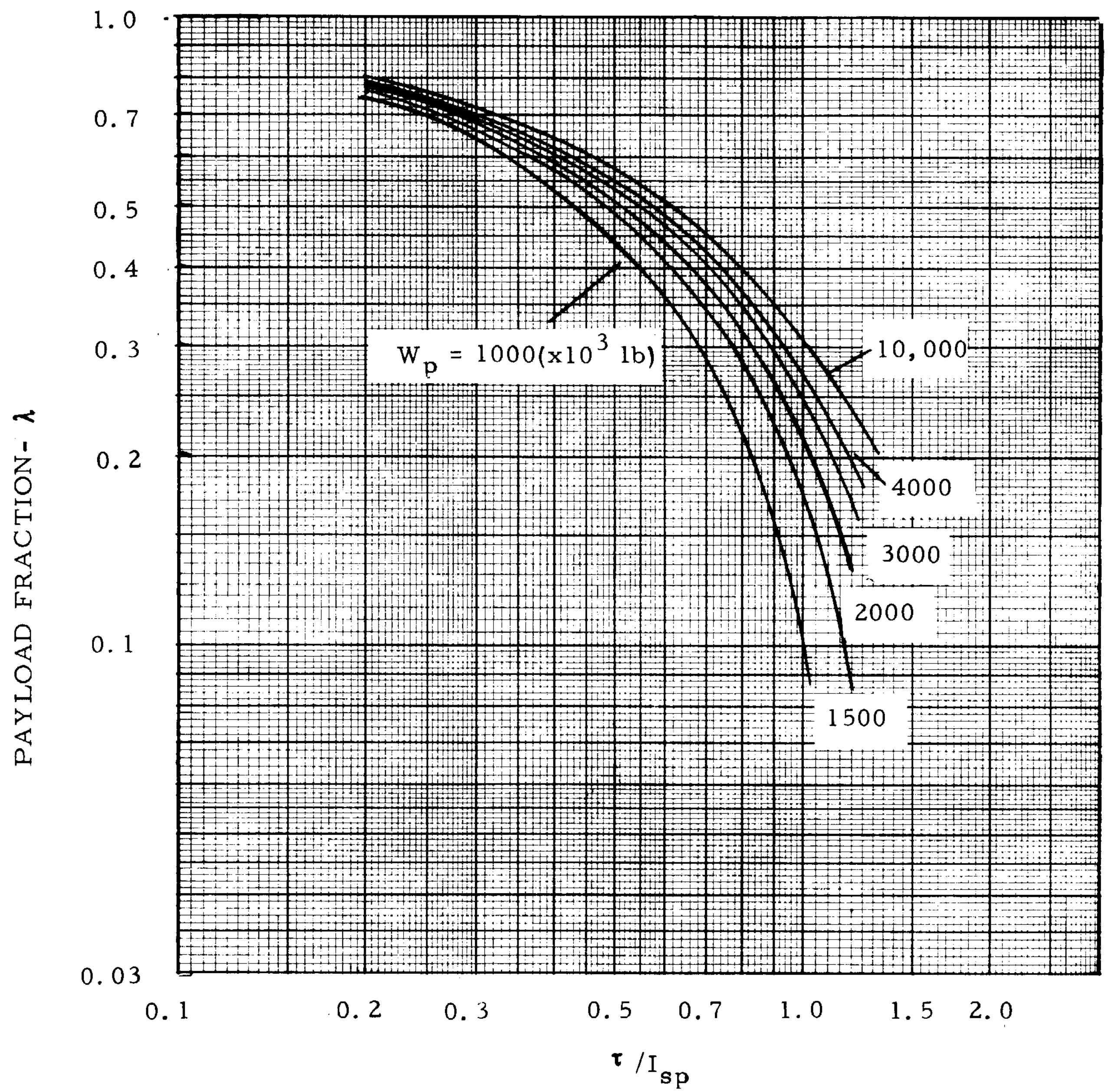

Fig. 5-32. GCR HISV ($F = 3x10^6 lb$).

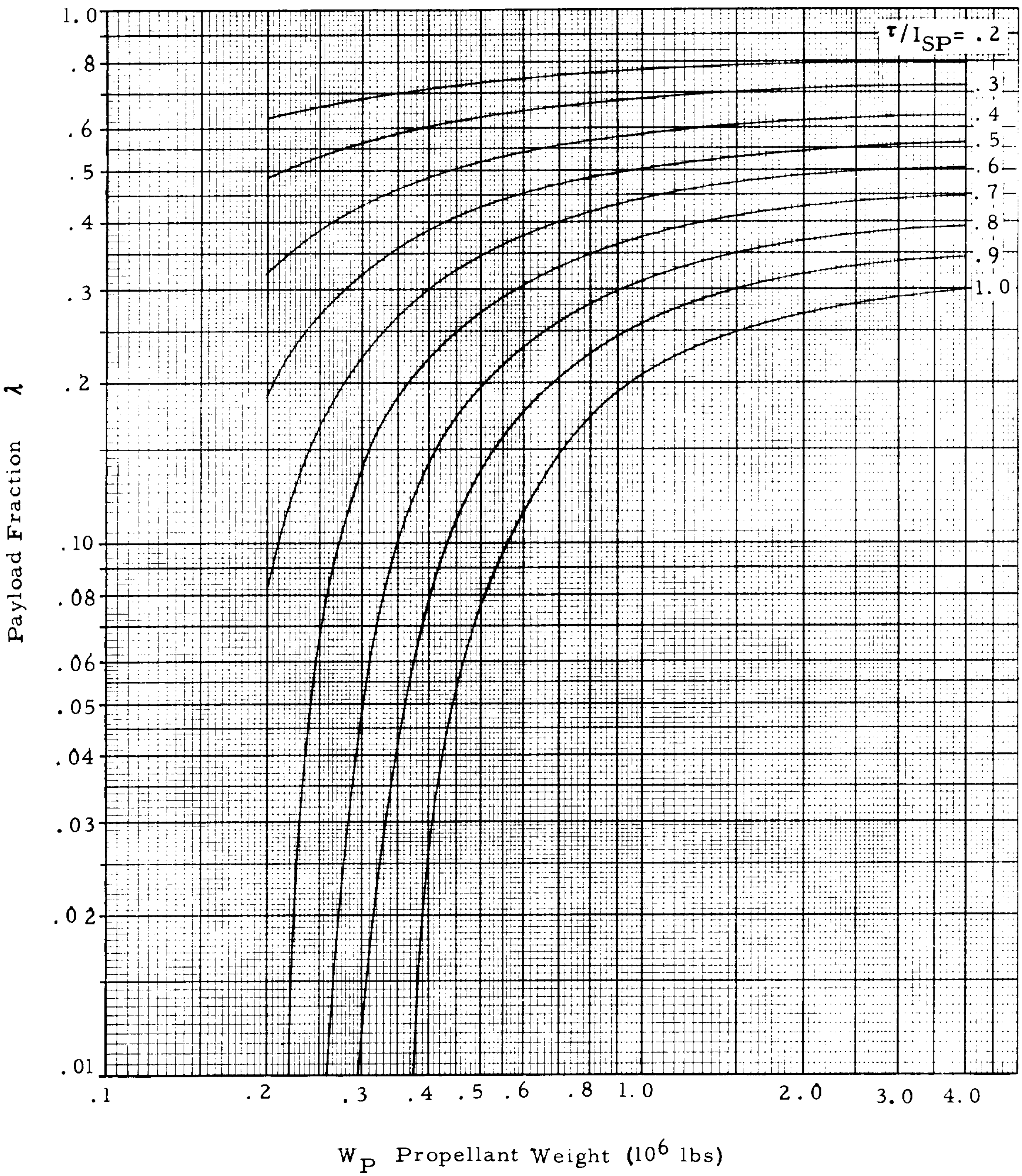

Fig. 5-33 NP-1, NUCLEAR PULSE HISV - PAYLOAD FRACTION VS PROPELLANT WEIGHT FOR VARIOUS τ/I_{sp} VALUES

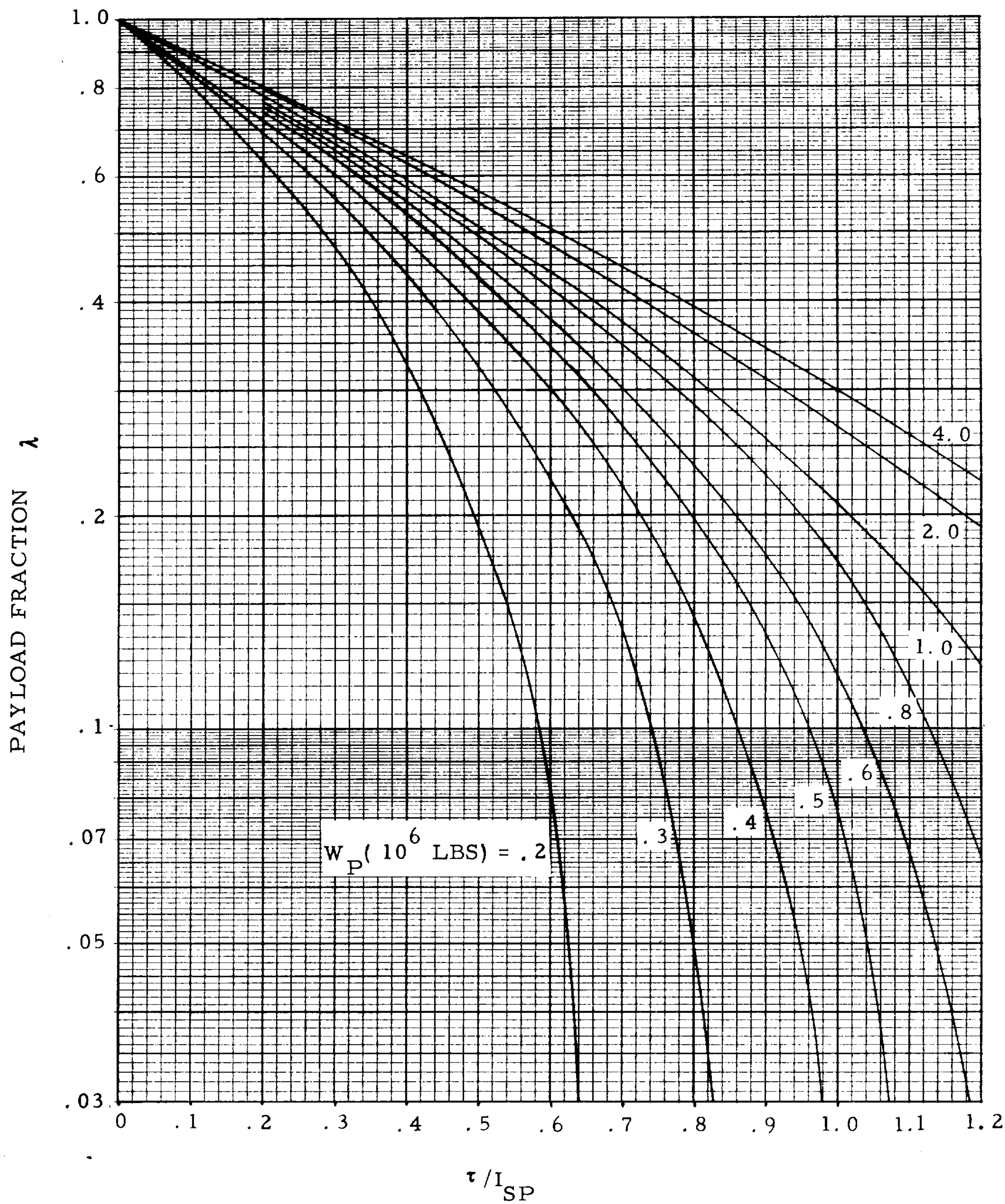

FIG. 5-34 NP-1, NUCLEAR PULSE HISV PAYLOAD FRACTION VS τ/I_{SP}

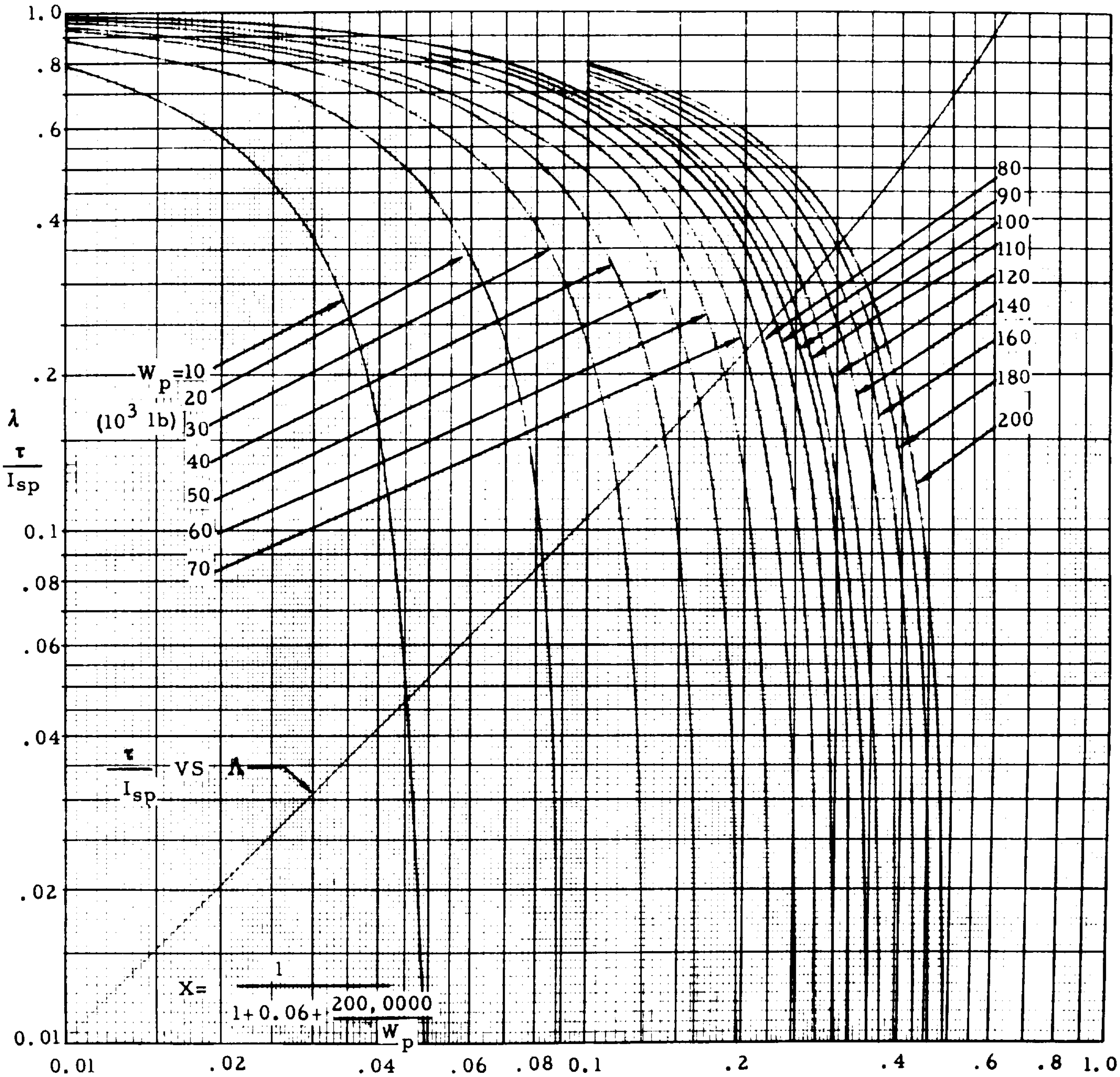

Fig. 5-35 VARIATION OF λ AND τ/I_{sp} WITH Λ FOR SATURN V COMPATIBLE NUCLEAR PULSE VEHICLE NP-1 BASED ON MASS FRACTION RELATION GIVEN ON CHART

Example No. 1: Compare the MGPF of a chemical HISV with that of a chemical HISV using SHE propulsion for a perihelion brake maneuver at return transfer to Earth.

1.1 Specifications and Solution

Mission: Mars round-trip mission, 1982.
Number of maneuvers: 4

Maneuver	M-4	M-3	M-2	M-1
Δv_{imp} (ft/sec)	9300 (C) 5900 (C/SHE)	20,750	12,400	12,000
Δv_{id} (ft/sec)	9600 6100	24,600	12,800	12,400
Propulsion Modules	C SHE	C	C	C
Specific Impulse (sec)	450 700	450	450	450
τ / I_{sp}	0.663 0.27	1.70	0.885	0.855
λ	0.475 0.72	0.13	0.385	0.40
DGPF	0.154 for both types			
MGPF	0.0095 (C) 0.0144 (C/SHE)			

1.2 Discussion: Fig. 5-4 shows that the gross payload fraction (GPF) varies little with the size of the propulsion module. Therefore, average values can be selected with good accuracy. Fig. 5-6 shows that for the SHE drive, the GPF is relatively more dependent on the absolute size of the propulsion system. A propellant weight of $W_p = 4 \cdot 10^4$ lb was selected as a mean value for the fourth maneuver.

The impulsive velocity changes are designated Δv_{imp}. The ideal velocities include losses and, in the case of Mars departure, a 3000 ft/sec velocity allowance for orbit plane change.

The use of SHE drive and perihelion brake maneuver results in considerable improvement of the mission gross payload fraction (MGPF). The MGPF of the C-HISV is 0.66 of that of the C/SHE-HISV. Based on this result, the orbital departure weight (ODW) of the latter is 66 percent of that of the C-HISV. This is true of course, only if the gross payloads at each maneuver are the same for both vehicles. In the present case, this is not so in the 4th maneuver. The C-HISV executes M-4 at geocentric Earth approach with a gross payload which represents the Earth entry module (EEM). The C/SHE-HISV carries out the perihelion maneuver some 70 to 90 days prior to mission termination with a gross payload which consists of the EEM and additional operational payload needed for the final part of the mission. From the fact that the gross payload is the same for all maneuvers, except M-4, one could be led to the conclusion that the ODW simply depends on the ratio of gross payloads carried by the respective HISV's during M-4. While this provides a more realistic approach to estimating the effect of the MGPF on the ODW, it too can be unduly misleading. Comparing, for example, the M-4 gross payload fraction (GPF) of the two HISV's, their ratio is found to be 0.72/0.475 = 1.515, implying that a gross payload ratio of 1.515 for the two vehicles would result in equal ODW. This would be correct only if the difference in GPF were due only to a difference in v_4; or due only to a difference in $I_{sp,4}$. In the present example, however, the GPF difference is due to a difference in maneuver velocity as well as in specific impulse at M-4. Since for the C/SHE-HISV the M-4 involves smaller velocity change as well as larger specific impulse, one is correct in concluding that the GPF ratio for which equal ODW is attained is larger than 1.515. In fact, as will be shown subsequently, the ratio is larger than 2. The reason why a ratio larger than 1.515 can be expected is that the M-4 net weight W_{N4} for the C/SHE-HISV must be considerably smaller than that of the C-HISV. For equal ODW, however, the sum of gross payload and M-4 net weight must be the same at M-3, because that represents the total load to be accelerated during M-4,

$$W_{\lambda 4} + \Delta W_{\lambda} = W_{N4} = W_{\lambda 3} + W_{N3} = W_{L3}$$

The elimination of weights during manned lunar or planetary missions is another factor which must be kept in mind when estimating the ODW from the MGPF. Using the M-4 gross payload would lead to an erroneous ODW, usually underestimating it. In order to estimate the ODW, the payload weight additions between maneuvers, starting with the last one and working backwards, must be known. For example:

Interval	M-4	I_{34}	M-3	I_{23}	M-2	I_{12}	M-1
Gross payload							
Growth: C-HISV		63,500		20,000		5,000	
C/SHE-HISV		44,500		20,000		5,000	
Gross pld.: C-HISV	16,500		80,000		100,000		105,000
C/SHE-HISV	35,500		80,000		100,000		105,000
Ignition Weight,							
W_A, C-HISV	35,000		758,000		2,020,000		5,070,000
C/SHE-HISV	49,300		721,000		1,928,000		4,840,000

The M-4 gross payload of the C/SHE-HISV is more than twice as large as that of the C-HISV, resulting in a higher M-4 ignition weight. The net weight W_{N4} is smaller, however; namely, 49, 300 - 35, 500 = 13, 800 lb for the C/SHE-HISV, compared to 35, 000 - 16, 500 = 18, 500 lb. The total load for M-3 is 16, 500 + 63, 500 + 18, 500 = 98, 500 lb for the C-HISV 35, 500 + 44, 500 + 13, 800 = 93, 800 lb for the C/SHE-HISV. The lower load for the C/SHE-HISV results in the slightly lower ODW, in spite of the fact that the M-4 gross payload is more than twice as large. The ODW of either HISV is considerably larger than the values obtained by 16, 500/0. 0095 = 1, 7350, 000 lb and 35, 500/0. 0144 = 2, 470, 000 lb. In addition the trend is reversed, a larger ODW for the HISV whose ODW actually is smaller. It is of interest to note the mean equivalent payload which is 0. 0095 · 5, 070, 000 = 48, 200 lb and 0. 0144 · 4, 840, 000 = 69, 600 lb, respectively, for the C-HISV and the C/SHE-HISV. The larger mean equivalent payload of the C/SHE-HISV indicates its higher quality as a transportation vehicle. The ratio of the two mean equivalent payloads is approximately the same as the ratio of the MGPF of the two vehicles.

Example No. 2: Compare the SCR/G driven HISV with the -23 configuration, a GCR version and a Saturn V compatible NP-HISV.

2.1 Specifications and Solution

Mission is terminated by capture in a highly eccentric Earth capture orbit at a perigee velocity of 35, 000 ft/sec. For the SCR/G - HISV the Saturn V Mod compatible 38 ft diameter cluster tank configuration is assumed. The -23 configuration is based on a 70 ft diameter tank cluster configuration which is post-Saturn compatible. PM-1 of this vehicle is powered by four SCR/N engines @ 50 k thrust each. Two of these engines are jettisoned following Earth departure. The other two are used for all subsequent maneuvers. The GCR-HISV configuration is as described in Sect. 4. The engine thrust selected is 750 k. One engine is used for all maneuvers. For the NP-HISV, the selected configuration is Saturn V compatible. The thrust is 750 k.

Mission: 440-day Mars round-trip mission, 1984.
Number of maneuvers: 4

Maneuver	M-4	M-3	M-2	M-1
Δv_{imp} (ft/sec)	18, 350	19, 200	13, 820	11, 620
Δv_{id} (ft/sec)	19, 000	22, 800	14, 300	12, 000
Propulsion Modules				
Vehicle A	SCR/G	SCR/G	SCR/G	SCR/G
B	SCR/N	SCR/N	SCR/N	SCR/N
C (F = 750 k)	GCR	GCR	GCR	GCR
D (F = 750k)	NP	NP	NP	NP

Specific impulse (sec)					
	A	800	800	800	800
	B	1000	1000	1000	1000
	C	1800	1800	1800	1800
	D	2500	2500	2500	2500
τ / I_{sp}					
	A	0.737	0.885	0.555	0.466
	B	0.59	0.709	0.445	0.373
	C	0.328	0.394	0.247	0.207
	D	0.236	0.238	0.178	0.149

Vehicle A is treated as a multi-stage vehicle with a 1-stage propulsion module (PM) for each principal maneuver.

For reasons of comparison, vehicle B is treated as a multi-stage vehicle with a 1-stage PM for each maneuver (version B'); and as a two-stage, tankage modularized vehicle (version B''). In version B'' four SCR/N engines are assumed for PM-1. Two of these engines are jettisoned, together with tankage, at termination of M-1. The other two are used for remaining three maneuvers. Therefore, for version B'', the last maneuver (M-4) must be based on two engines (Fig. 5-22), M-3 and M-2 on zero engines (Fig. 5-20) and M-1 again on two engines (Fig. 5-22). If 6 engines were assumed for M-1 with four jettisoned following M-1, then M-1 would have to be based on four engines (Fig. 5-24). For version B', 4 engines are assumed for M-1, 2 engines each for the remaining maneuvers. The PM's are arranged in tandem so that only one PM can operate at a time. Thus M-1 must be based on 4 engines (Fig. 5-24), all other maneuvers on two engines (Fig. 5-22).

Vehicle C is based on Fig. 5-26 for M-4. For M-3 through M-1, satellite tanks with $K_p = 0.06$ (Fig. 4-12) are assumed, yielding $x = 0.944$.

For vehicle D, Fig. 5-34 is used for M-4. For M-3 through M-1, propellant magazines are jettisoned, assuming $K_p + K_{p,c} = 0.06$, or $x \approx 0.944$.

Subsequently, the GPF values for each maneuver (from left to right: M-4 to M-1) are given, together with the figure numbers from which the value was obtained.

Vehicle A	0.24 (5-12)	0.315 (5-14)	0.515 (5-12)	0.58 (5-10)
B'	0.39 (5-22)	0.40 (5-22)	0.59 (5-22)	0.68 (5-24)
B''	0.39 (5-22)	0.45 (5-20)	0.61 (5-20)	0.69 (5-22)

Vehicle C	0.24 (5-26)	$0.658^{1)}$	$0.714^{1)}$	$0.737^{1)}$
D	0.65 (5-34)	$0.72^{1)}$	$0.749^{1)}$	$0.761^{1)}$

1) Computed from $\lambda = 1 - \Lambda/x$; $\Lambda = (\mu - 1)/\mu$; and μ from Fig. 5-1 for λ/I_{sp} values listed above.

Therewith the following DGPF and MFPF values are obtained

HISV	A	B'	B''	C	D
	0.299	0.40	-	-	-
MGPF	0.0226	0.063	0.0735	0.135	0.265

2.2 Discussion:

The tankage modularized version B'' of vehicle B achieves an increase in MGPF by 16 percent. However, comparison with vehicles C and D clearly shows that improvements in specific impulse have a far more powerful effect on the MGPF than structural and design improvements, even though the inert weight of both vehicles C and D is far higher than that of vehicle B.

The destination gross payload fraction (DGPF) of vehicles B'', C and D cannot be computed from the GPF values given for the individual maneuvers. With tankage modularized or engine modularized vehicles the maneuver for which an overall GPF is to be determined must be treated like a "terminal" maneuver by including the propulsion system (or tankage, respectively, In the case of vehicle C, for example, the M-2 GPF of 0.714 must be replaced by 0.67 (Fig. 5-26). The DGPF is then $0.737 \cdot 0.67 = 0.49$.

An alternate method of estimating the GPF of the GCR-HISV (vehicle C) is by using Figs. 4-18 and 4-21. Assume $x_{CT} = 0.57$. Then, for M-4

$$\lambda_4 = 1 - \left(\frac{1}{0.57}\right)\left(1 - e^{-0.328}\right) = 1 - 1.75\,(1 - 0.715) = 0.519$$

For M-3 a ratio of $W_{p,ST}/W_{p,CT} = 2$ is selected as a plausible ratio, whence, from Fig. 4-21, $x_{CTST} = 0.74$ and

$$\lambda_3 = 1 - \frac{1}{0.74}\left(1 - e^{-0.394}\right) = 1 - 3.5\,(1 - 0.62) = 0.487$$

For M-2 a propellant ratio of 3.5 is selected, whence $x_{CTST} = 0.81$ and

$$\lambda_2 = 1 - \frac{1}{0.795}\left(1 - e^{-0.247}\right) = 1 - 1.26\,(1 - 0.78) = 0.723$$

For M-1 a propellant ratio of 4.5 is selected, yielding $x_{CTST} = 0.82$ and

$$\lambda_1 = 1 - \frac{1}{0.82}\left(1 - e^{-0.207}\right) = 1 - 1.22\,(1 - 0.812) = 0.771$$

These individual gross payload fractions result in a DGPF of 0.560 and a MGPF of 0.141. These values are slightly higher, but not very different, from those found by the other method before. The latter method, however, permits a somewhat better estimate as to whether or not the results are optimistic. The ratio of propellants has been selected conservatively and probably is higher. In the latter case, the individual mass fractions would be higher and so would be the gross payload fractions.

The payload fractions of the SCR/N-HISV (vehicle B') can also be computed according to an alternate method. For M-4 the GPF is the same as before. Fig. 5-22 shows that the GPF for M-4 corresponds to $W_p \sim 60,000$ lb. With 2 engines, Fig. 4-11b[1] indicates a corresponding value of $1/x$ of 1.3 or $x = 0.77$. For M-3 and M-2, propellant tanks are added successively, computing the mission backwards. The propellant load of these satellite tanks is 100,000 lb and above. Since $1/x$ for the satellite tanks varies little with W_p, an average value of $1/x = 1.07$ ($x = 0.935$) is assumed. Therewith, using Eq. (4-88d)

$$x_{CTST} = \frac{1}{1 + (1.3 - 1)\left[\dfrac{1}{1 + W_{p,ST}/60k}\right] + (1.07 - 1)\left[\dfrac{1}{1 + \dfrac{1}{W_{p,ST}/60k}}\right]}$$

$$= \frac{1}{1 + 0.3\left[\dfrac{1}{1 + W_{p,ST}/60k}\right] + 0.07\left[\dfrac{1}{1 + \dfrac{1}{W_{p,ST}/60k}}\right]}$$

Selecting $W_{p,ST} = 150,000$ lb for M-3 yields

$x_{CTST} = 0.88$ and

$$\lambda_3 = 1 - \frac{1}{0.88}\left(1 - e^{-0.709}\right) = 1 - 1.137\,(1 - 0.493) = 0.425$$

1) Fig. 4-11a shows the corresponding x-value

For M-2 a value of $W_{p, ST}$ = 360, 000 lb is selected as plausible value, yielding

x_{CTST} = 0.905 and

$$\lambda_2 = 1 - \frac{1}{0.905} \left(1 - e^{-0.445}\right) = 1 - 1.105 \, (1 - 0.64) = 0.602$$

For M-1 the value (4 engines) is the same as in the preceding method. Therewith DGPF = 0.68 · 0.602 = 0.410 and MGPF = 0.39 · 0.425 · 0.410 = 0.068. Again, the agreement between the two methods is satisfactory.

6. GENERAL TRANSPORTATION COST ANALYSIS

Based on the general MGPF analysis, a non-dimensional transportation cost analysis can be developed.

The operating cost of the transportation vehicle is

$$K^*_{TV} (\$) = K^*_i + K^*_d \tag{6-1}$$

where K^*_i and K^*_d are the indirect and direct operating cost. The <u>gross payload transportation cost effectiveness</u> (GPTCE) is, therefore,

$$T^{**}_{\lambda} (\$/lb) = \frac{K^*_{TV}}{W_\lambda} = \frac{K^*_{TV}}{W_A} \frac{1}{\lambda} \tag{6-2}$$

This leads to the definition of the <u>gross payload transportation cost effectiveness index</u> (GPTCEI)

$$I^*_\lambda = \frac{T^*_{GP}}{K^*_{TV}/W_A} = \frac{1}{\lambda} \tag{6-3}$$

Since, according to the payload break-down presented in Par. 2.1 it is

$$\lambda = \lambda_D + \lambda_I + \lambda_T + \lambda_O \tag{6-4}$$

the payload transportation cost effectiveness (PTCE) and the associated index (PTCEI) can be formulated readily with respect to any particular payload group; e.g. for the destination payload

$$T^*_D (\$/lb) = (K^*_{TV}/W_A)\ (1/\lambda)\ (\lambda/\lambda_D) = (K^*_{TV}/W_A)\ (1/\lambda_D) \tag{6-5}$$

$$I^*_D = (1/\lambda)\ (\lambda/\lambda_D) = (1/\lambda_D) \tag{6-6}$$

If the individual payload groups are formulated in terms of gross payload fractions (e.g. λ_D/λ, λ_O/λ, etc.) then the general relations using the gross payload fractions, i.e. the first eqs. (6-5) and (6-6), are adequate.

For a 1-stage vehicle

$$T_\lambda^{**}(\$/\text{lb}) = \frac{K_{TV}^*}{W_A} \frac{1}{1-\frac{\Lambda}{x}} = \frac{K_{TV}^*}{W_A} \frac{1}{1-n_o K_f - \Lambda(1+K_p)} \tag{6-7}$$

$$I_\lambda^* = \frac{1}{1-n_o K_f - \Lambda(1+K_p)} \tag{6-8}$$

For a 2-stage vehicle, for constant GP,

$$T_\lambda^{**}(\$/\text{lb}) = \frac{K_{TV}^*}{W_{A1}} \frac{1}{\lambda_2 \lambda_1} = \frac{K_{TV}^*}{W_{A1}} I_{\lambda 12}^* \tag{6-9}$$

For a 2-stage vehicle, the transportation cost with respect to the terminal GP, $W_{\lambda 2}$, is, for the case of variable payload,

$$T_\lambda^{**}(\$/\text{lb}) = \frac{K_{TV}^*}{W_{\lambda 2}} = \frac{K_{TV}^*}{W_{\lambda 2}} \frac{W_{A1}}{W_{\lambda 2}}$$

$$= \frac{K_{TV}^*}{W_{A1}} \frac{1+\lambda_2 \frac{D_{\lambda 1}}{W_{\lambda 2}}}{\lambda_2 \lambda_1} \tag{6-10}$$

For a 4-stage vehicle, the transportation cost with respect to the terminal payload, $W_{\lambda 4}$, is, for the case of variable payload,

$$T_\lambda^{**}(\$/\text{lb}) = \frac{K_{TV}^*}{W_{\lambda 4}} = \frac{K_{TV}^*}{W_{A1}} \frac{W_{A1}}{W_{\lambda 4}} \tag{6-11}$$

where $W_{A1}/W_{\lambda 4}$ follows from Eq. (4-18g).

For a 4-stage vehicle, the transportation cost with respect to the destination payload, $W_{\lambda, D}$, is, for the case of variable payload, derived from the following relations

$$W_{\lambda D} = D_{\lambda 2} \left(1 - D'_{\lambda 2}/D_{\lambda 2}\right) \tag{6-12}$$

where $D'_{\lambda 2}$ represents that portion of the payload eliminated between maneuvers 2 and 3, which is not destination payload,

$$T^{**}_{\lambda} (\$/\mathrm{lb}) = \frac{K^{*}_{TV}}{W_{\lambda, D}} = \frac{K^{*}_{TV}}{W_{A1}} \; \frac{1}{\dfrac{D_{\lambda 2}}{W_{A1}} \left(1 - D'_{\lambda 2}/D_{\lambda 2}\right)} \tag{6-13}$$

where

$$\frac{D_{\lambda 2}}{W_{A1}} = \frac{D_{\lambda 2}}{W_{\lambda 4}} \; \frac{W_{\lambda 4}}{W_{A1}} \tag{6-14}$$

with $D_{\lambda 2}/W_{\lambda 4}$ being an independent variable in the Eqs. (4-18) and $W_{\lambda 4}/W_{A1}$ following from Eq. (4-18g). Eq. (6-14) is general and applies particularly to missions in which the mass of D_{λ} eliminated after M-1, M-2 and M-3, respectively, is a substantial fraction, or larger, than $W_{\lambda 4}$. In that case Eqs. (4-18) apply which require knowledge of $W_{\lambda 4}$, and of the $D_{\lambda}/W_{\lambda 4}$ ratios, to compute W_{A1} and $D_{\lambda 2}$.

There are cases, however, which lend themselves to a simplified analysis. Three cases are treated subsequently.

Case 1: <u>Reconnaissance Missions</u>

Planetary reconnaissance missions are frequently envisioned of terminating in hyperbolic entry into the Earth atmosphere, preceded by a retro-maneuver (let it be called M-4) to reduce the entry velocity to an acceptable value. The gross payload (GP) for M-4 is the weight of the Earth entry module (EEM), including crew. The EEM is a small part of the operational payload (life support section (LSS), consisting of various mission modules) which is carried through M-3 (target planet departure) and the heliocentric return/ coast phase, to be jettisoned just prior to M-4. In other words, $D_{\lambda 3}$ (LSS) is much larger than $W_{\lambda 4}$ (EEM). $W_{\lambda 4}$ is comparatively so small that even

$D_{\lambda 1}$ (the payload weight eliminated on the outbound coast phase Earth to target planet) is a significant fraction of, or larger than, $W_{\lambda 4}$, so that $D_{\lambda 1}/W_{\lambda 4}$ cannot very well be neglected.

A considerable simplification can be achieved, at relatively small loss in accuracy, by eliminating M-4 and beginning the computation of $W_{\lambda 1}$ (Eq. 4-18)) with $W_{\lambda 3}$. The GP of W_{A3} consists of $W_{\lambda 4}$, W_{N4} and $D_{\lambda 3}$. The GP for M-4, namely the EEM, can be defined comparatively readily. For a given mission or group of missions, a representative value of W_{N4} can be determined readily once the propulsion system is selected. For a given crew size and mission class, the LSS, i.e. $D_{\lambda 3}$, carried through M-3 can also be determined with relatively fair accuracy. Compared to

$$W_{\lambda 3} = W_{\lambda 4} + W_{N4} + D_{\lambda 3} \tag{6-15}$$

the value of $D_{\lambda 1}$ is, in most cases, small and, in first approximation, can be neglected. With this simplification, and bearing in mind that the above consideration reduce this mission from a 4-maneuver to a 3-maneuver event, follows, remembering Eqs. (4-18),

$$W_{A2} = \frac{W_{\lambda 3}}{\lambda_{32}} \left(1 + \lambda_3 \frac{D_{\lambda 2}}{W_{\lambda 3}}\right) \tag{6-16}$$

$$W_{A1} = \frac{W_{\lambda 3}}{\lambda_{321}} \left(1 + \lambda_3 \frac{D_{\lambda 2}}{W_{\lambda 3}}\right) \tag{6-17}$$

leaving $D_{\lambda 2}$ (essentially destination payload) as the principal payload change during the mission. In that case, Eq. (6-14) becomes

$$\frac{D_{\lambda 2}}{W_{A1}} = \frac{D_{\lambda 2}}{W_{\lambda 3}} \frac{W_{\lambda 3}}{W_{A1}} \tag{6-18a}$$

$$= \frac{D_{\lambda 2}}{W_{\lambda 3}} \frac{\lambda_{321}}{1 + \lambda_3 \dfrac{D_{\lambda 2}}{W_{\lambda 3}}} \tag{5-18b}$$

$$= \lambda_2 \left(1 - \frac{\lambda_1}{1 + \lambda_3 \dfrac{D_{\lambda 2}}{W_{\lambda 3}}} \right) \qquad (6\text{-}18c)$$

Case 2: <u>Shuttle Missions with One-Way Destination Payload</u>

In some cislunar and interplanetary shuttle missions which, by definition involve reusable ISV's, $D_{\lambda 1}$ and $D_{\lambda 3}$ are small compared to $D_{\lambda 2}$ which consists almost entirely of destination payload (i.e. $D'_{\lambda 2}/W_{\lambda, D} \approx O$) and to $W_{\lambda 4}$ which comprises essentially the operation payload. Thus, setting, in first approximation, $D_{\lambda 1} = D_{\lambda 3} = O$, it follows from Eqs. (4-18g) after some manipulations

$$\frac{D_{\lambda 2}}{W_{A1}} = \frac{1 - \lambda_{21}}{1 + \dfrac{D_{\lambda 2}}{W_{\lambda 4}} \lambda_{43}} \qquad (6\text{-}19)$$

where $\lambda_{43} = \lambda_4 \lambda_3$ and analogously for λ_{4321}; and

$$T_{\lambda}^{**} = \frac{K_{TV}^{*}}{W_{A1}} \frac{1 + \dfrac{D_{\lambda 2}}{W_{\lambda 4}} \lambda_{43}}{\left(1 - \lambda_{21}\right)\left(1 - \dfrac{D'_{\lambda 2}}{D_{\lambda 2}}\right)} \qquad (6\text{-}20)$$

where $D'_{\lambda 2}$ can be put equal to zero if only destination payload is eliminated following the second maneuver.

Case 3: <u>Shuttle Missions with Two-Way Destination Payloads</u>

In other shuttle missions, not only is outbound destination payload delivered to the target body, but return destination payload is carried back to Earth. In that case, $D_{\lambda 2}$ would be unloaded and return destination payload loaded. Nominally, this amounts to an increase in $W_{\lambda 4}$ so far as the transportation system is concerned. For example, if a fraction of f_D of $D_{\lambda 2}$ is loaded back as Earth return destination payload $W_{\lambda 4}$ in the denominator of Eq. (6-15) changes from $W_{\lambda 4} = W_{\lambda, O}$ (operational payload only) to

$W_{\lambda 4} \equiv f_D D_{\lambda 2} + W_{\lambda, O}$. Eq. (6-15) becomes

$$\frac{D_{\lambda 2}}{W_{A1}} = \frac{1 - \lambda_{21}}{1 + \cfrac{\lambda_{43}}{1 + \cfrac{W_{\lambda, O}}{f_D D_{\lambda 2}}}} \tag{6-21}$$

with $f_D = 1$, if as much destination payload is unloaded at the target body as is returned from the target body to Earth.

7. PAYLOAD ANALYSIS

Payload analysis is the "other half" of the space vehicle analysis, the "first half" being, of course, the propulsion module analysis. Moreover, payload analysis bridges general and special mission engineering analysis, because the special analysis is based on weights and volumes, while the former operates with non-dimensional figures of merit.

Payload analysis is a large subject area in its own right and as such outside the scope of this report. Moreover, payload analysis is not only a function of mission characteristics but also of mission objectives and therefore of the activity of the destination which may range from a relatively modest fly-by project to the supply of a large and active base. Beyond everything else, however, payload weights must maintain a measure of compatibility with the payload capability of ELV's, as do ISV's in general. This limits payloads for heliocentric missions to the range of 60, 000 to 150, 000 lb; and to about 220, 000 lb for lunar and orbit launch missions, in cases where Saturn V is involved; and from 250, 000 - 600, 000 lb to about 880, 000 lb where a post-Saturn ELV with 10^6 lb maximum payload capacity is involved.

Because of the parametric nature of the payload data involved in this report, no consequent differentiation between destination, intransit, transportation and operational payload groups is maintained. Rather the following payload "packages" are identified, in accordance with the analysis in Sections 5 and 6:

$D_{\lambda 1}$ = payload differential eliminated between maneuvers M-1 and M-2

$D_{\lambda 2}$ = payload differential eliminated between maneuvers M-2 and M-3

and so forth for all periods between principal maneuvers,

$W_{\lambda 3}$ = in a 4-maneuver round-trip mission, the gross payload of the ISV at departure from the target body and injection into a return orbit to Earth. For a mission with more or fewer principal missions, the numerical subscript is changed correspondingly,

$W_{\lambda 4}$ = in a 4-maneuver round-trip mission, the gross payload at the last principal maneuver prior to Earth arrival either for atmospheric entry or for capture in an Earth satellite period.

Thus, in a 4-maneuver round-trip mission, the payload build-up from terminal to initial mission conditions proceeds as follows:

$$W_{\lambda 4} \text{----} W_{\lambda 4} + W_{N4} + D_{\lambda 3} = W_{\lambda 3} \text{----} W_{\lambda 3} + W_{N3} + D_{\lambda 2} = W_{\lambda 2}$$

$$\text{----} W_{\lambda 2} + W_{N2} + D_{\lambda 1} = W_{\lambda 1} \qquad (7\text{-}1)$$

where W_N is the net weight of each stage, i. e. the sum of propellant weight and wet inert weight required for each principal maneuver. Although no distinction is made between the functional payload groups mentioned above, it is apparent that, in the example of a 4-maneuver mission, $D_{\lambda 2}$ represents predominantly destination payload, $W_{\lambda 3}$ and $W_{\lambda 4}$ predominantly operational payload; and $D_{\lambda 1}$ and $D_{\lambda 3}$ consist primarily of propellant expenditures for attitude control, correction maneuvers as well as possibly for spin-up and spin-down operations, of thermo-meteoroid shielding jettisoned just prior to the next principal maneuver from the tanks about to be emptied during that maneuver, and of damaged parts and refuse. In some instances the values of $D_{\lambda 1}$ and $D_{\lambda 3}$ are small enough, compared to $D_{\lambda 2}$, $W_{\lambda 3}$ and W_{A1}, to be neglected in a comparative analysis such as the one carried out in this report.

Tab. 7-1 lists the values used in the subsequent special analysis.

Tab. 7-1 PAYLOAD WEIGHTS USED IN SPECIAL ANALYSIS

(Unit: 10^3 lb)

Mission	Computation	$D_{\lambda 1}$	$D_{\lambda 2}$	$D_{\lambda 3}$	$D_{\lambda 4}$	$W_{\lambda 3}$	$W_{\lambda 4}$
Mercury Capture	3 Maneuvers	0	100	-	-	120	-
	4 Maneuvers (Nucl. Vehicles)	0	100	0	-	-	90
	4 Maneuvers (Chem. Vehicles)	Method No. 4 applied (cf. Sect. 9)					
Venus Capture	3 Maneuvers	0	100	-	-	130	-
	4 Maneuvers	0	100	40	-	-	90
	4 Maneuvers (Very Fast)	0	100	0	-	-	90
Earth Orbit Launch (Reusable OLV) (3 Maneuvers)	Chemical	220	0	-	-	6	-
	SCR/G; SCR/N	220	0	-	-	6	-
	GCR	880	0	-	-	6	-
	NP	880	0	-	-	12	-
Lunar Missions	MoCC; C or SCR (48+48 hr Transf.)	0	220	0	-	-	22
	MoCC; GCR or NP (12+12 hr Transf.)	0	220	0	-	-	22
	MoSE; C or SCR	0	0	0	110	-	$W_{\lambda 6} = 11$
	MoFFD; NP	0	0	220	0	-	$W_{\lambda 6} = 22$
Mars Capture	3 Maneuvers	0	50	-	-	160	
	4 Maneuvers	0	50	0	-	-	90
	Very Fast; GCR, NP	0	100	-	-	160	
	" " " "	0	100	0	-	-	90
	Slo-Slo and	0	50	0	-	-	90
	Fast-Slo	17	220	11	-	-	90
	Synodic Missions	22	80	18	-	-	120
	Missions Comparing the Effect of PB:						
	Without PB	0	50	75.5	-	-	16.5
	With PB	0	50	70	-	-	22
Jupiter Capture Jupiter Callisto	4 Maneuvers	20	100	170	-	-	50

8. GENERALIZED GROSS PAYLOAD FRACTION (GPF) ANALYSIS

The general vehicle/mission integration is based on the selection of average x-values over a more or less wide range of propellant weight. With x no longer a function of W_p (within the specified range), the GPF is a function of Λ, hence of τ/I_{sp}, only and can readily be computed from $\lambda = 1 - \Lambda/x$. Unless the generalization of x is handled judiciously, the results can be seriously misleading, especially where heavy thrust units (such as GCR and NP engines) are applied to comparatively small maneuvers (τ/I_{sp} well under 1.0). Chemical systems are relatively most insensitive, hence for them x is most readily and accurately generalized, because of the small ratio of engine weight to thrust. SCR engine systems play an intermediate role. The regime in which the sensitivity to wide x-value generalization increases rapidly can readily be discerned by inspecting the λ vs. τ/I_{sp} graphs in Sect. 5. Thus, even in the general method, at least certain broad estimates of the payload weights involved must be made. The sensitivity of the general method to the x-value generalization can be minimized by avoiding small terminal maneuvers where W_p is small and compare different propulsion systems by computing the GPF for those mission maneuvers for which the propellant weight for either system is in the range where x is no longer very sensitive to variations in W_p. This case is outlined in "case 1" of Section 6.

9. SPECIAL GROSS PAYLOAD FRACTION AND COST ANALYSIS

In the special GPF analysis x is used as function of W_p. Numerical values are, therefore, involved as a means of obtaining greater accuracy in determining the mission gross payload fraction (MGPF) over wide ranges of propellant weights; and as a means of obtaining propellant weights and the overall ODW, in order to be able to determine the logistic demands on a given ELV supply system, as part of the special cost analysis.

Five methods are available in the special GPF analysis:

1. Given Λ, W_λ : Iterate W_p and λ to match.

   Procedure:

   $$\lambda W_p = \Lambda W_\lambda \quad ; \quad \Lambda = f(\tau / I_{sp})$$

   $$W_p = \frac{\Lambda W_\lambda}{\lambda}$$

   Assume λ to obtain W_p. Check with appropriate λ vs. τ / I_{sp} chart whether, for W_p and τ / I_{sp}, the assumed value for λ is obtained. If agreement is unsatisfactory, assume new λ value.

2. Given Λ, W_p : Read λ from chart.

   Procedure:

   Since $\Lambda = f(\tau / I_{sp})$, the value of λ can be read directly from appropriate λ vs. τ / I_{sp} chart.

   In a multi-maneuver mission with variable payload, this method is fast as well as accurate only for the last maneuver (which is computed first). For each of the subsequent maneuvers W_p must be estimated without knowing whether or not it yields the appropriate W_λ. Thus an iteration process to match W_p and W_λ is required for all subsequent maneuvers.

3. Given $\tau_n / I_{sp,n}$, $W_{\lambda,n}$, $W_{\lambda,n-1}$: Stepwise computation of ISV ignition weights by maneuvers.

   Procedure for a 4-maneuver mission for example:

Given: τ_4 / I_{sp4} , $W_{\lambda 4}$, $D_{\lambda 3}$

Estimate W_{p4}

Read λ_4

Compute $W_{A4} = W_{\lambda 4} / \lambda_4$

Read (or compute) $\Lambda_4 = \dfrac{\mu_{4-1}}{\mu_4}$

Compare

(mass ratio) $\mu_4 = \exp(\tau_4 / I_{sp4})$

Compute $W_{p4} = \Lambda_4 \; W_{A4}$

Repeat if agreement is unsatisfactory

Add $D_{\lambda 3}$ to obtain $W_{\lambda 3} = W_{A4} + D_{\lambda 3}$

Estimate W_{p3}

⋮

Compare

Compute $W_{p3} = \Lambda_3 \; W_{A3}$

Repeat if agreement is unsatisfactory

Add $D_{\lambda 2}$ to obtain $W_{\lambda 2} = W_{A3} + D_{\lambda 2}$

Estimate W_{p2} and read λ_2 to obtain W_{A2}

Add $D_{\lambda 1}$ to obtain $W_{\lambda 1} = W_{A2} + D_{\lambda 1}$

Estimate W_{p1} and read λ_1 to obtain W_{A1}

The determination of W_{A2} and W_{A1} as described is based on the premise that W_{p2} and W_{p1} are in a range in which x_1, hence λ, is adequately insensitive to errors in W_p estimate. If this is not the case, the iterative process used for the two preceding maneuvers must be repeated also for W_{A2} and W_{A1}.

4. Estimate W_p throughout all maneuvers and use the GFP's so obtained to find the ignition weights, in conjunction with the given terminal gross payload and D_λ-values for the periods between the other maneuvers.

5. For a given maneuver (τ/I_{sp}, Λ) and W_λ estimate the GPF λ to obtain W_A. The product ΛW_A yields W_p. Then using the mass fraction equation for the propulsion module in question in the form

$$\frac{1}{x} = 1 + K_p + K_f F/W_p$$

compute λ from

$$\lambda = 1 - \Lambda (1/x)$$

Compare the GPF so obtained with the original estimate and repeat, if necessary, until the difference between the two becomes acceptably small.

Of these five methods:

No. 1 offers the best compromise of speediness and accuracy,

No. 2 is most laborious and most accurate

No. 3 is comparable to No. 2,

No. 4 is the fastest and, except for chemical ISV's, the least accurate,

No. 5 is fast and accurate, if an x vs. W_p curve is available. Even if the equation for $1/x$ must be used, the method can be fast, if K_fF is a constant (which usually is the case for a given maneuver) and if K_p is not a function of W_p. The latter condition applies in the case of the NP, where the mass ratio of propellant magazines to propellant is constant, regardless of the quantity loaded, since the propellant can be stored in a number of packages of identical weight. In Par. 4.13 a K_p-value of 0.06 was selected for the NP vehicles. Taking, for example, the Saturn V compatible NP vehicle, K_fF is 200, 000 lb. Thus, the relation for $1/x$ assumes, in this case, the simple form

$$\frac{1}{x} = 1.06 + \frac{200,000}{W_p(\text{lb})}$$

Conditions are alleviated even further for the maneuvers preceding the terminal maneuver of the mission. For the terminal maneuver itself the above equation applies. For the preceding maneuvers, however, the same thrust system is used and, therefore, $1/x$ becomes now simply $1/x = 1.06$, and the GPF follows directly from the second of the above equations, without iteration.

The propellant magazines of the NP vehicle can be compared to clustered tanks in liquid propellant vehicles. Therefore, in cases where it can be assumed that the propellant is varied in quantities involving tank sizes within the range of which a constant average K_p-value can be used, an equation similar to the one given above for the NP vehicle can be developed. For example, for the GCR configuration described in Par. 4-12, an average K_p-value for the satellite tanks of $K_{p,ST} = 0.059$ is assumed in the numerical applications in the next Section. Fig. 4-12 shows that this is a fairly accurate mean value for satellite tanks in the capacity range of 100, 000 to 140, 000 lb of liquid hydrogen. In the GCR vehicle the engine is re-used for all maneuvers during which the GCR system is to operate. It is assumed further that, in the last GCR maneuver (which is not necessarily the terminal maneuver of the missions), the engine consumes the hydrogen contained in its central tank. Therefore, for this last maneuver

$$\frac{1}{x_{CT}} = 1 + K_{p,CT} + K_f F/W_p$$

Figs. 4-18 and 4-19 show x_{CT} and $1/x_{CT}$, respectively, as function of propellant load. Therefore, in the iteration process of method No. 5, Fig. 4-19 can be used to determine the GPF against which the originally assumed GPF can be checked. Once the GPF for this maneuver is determined, however, $1/x$ for the preceding maneuvers becomes simply $1/x_{ST} = 1.059$ and now the GPF follows directly without iteration. If greater accuracy is desired, then, instead of making $1/x_{ST}$ invariant, one can use Fig. 4-20.

Finally, method No. 5 can be used conveniently in cases where the capability of a specific Earth launch vehicle (ELV) is taken into account. Every given ELV has two practical limitations which are expressed in its payload weight capability and its payload section volume capability. Large ELV's, such as Saturn V or post-Saturn, have a volume capacity which exceeds their weight capacity, even if LH_2 is transported. For example, Saturn V has a maximum payload section volume of 115,000 ft^3 (Tab. 1-1), corresponding to about twice the load of LH_2 which it is actually capable of transporting. Conditions are even more extreme in the case of post-Saturn (Tab. 1-1). Therefore, if a given ELV is considered and if build-up of the ISV in orbit is involved, one does not have a free choice of selecting the propellant tank size. Moving up, on the x vs. W_p and λ vs. τ/I_{sp} charts, to larger and larger W_p values implies, of course, larger and larger size of the particular tank configuration to which the particular mass fraction curve applies. In fact, however, only two tank sizes need to be considered in this case: the size of a fully fueled tank (or tank plus engines) corresponding to the maximum payload weight of the ELV; or the size of a tank (or tank cluster) which occupies as much of the ELV's payload section volume as possible. In the latter case it must be assumed, of course, that the excess propellant load is carried aloft in tankers and transferred into the tank in orbit. This, however, is irrelevant as far as the determination of the GPF of the ISV is concerned. What matters is that there exist two limiting tank sizes, hence, two fixed mass fractions. If the two corresponding propellant weights turn out to be too small for some vehicle/mission combinations, it is tacitly assumed that a cluster (or super-cluster) of identical tanks (or tank cluster) "elements" is formed (with or without engines). If this is assumed, the mass fraction becomes independent of the propellant quantity, with good approximation; and then the GPF can be determined from the above equation without further iteration, requiring only knowledge of Λ and x.

Based on the evaluation of these five methods, No. 1 is applied where nuclear propulsion systems are involved and new engine-tank systems are required for each maneuver (such as for the SCR/G engine in those cases where a limited operating life is assumed). For chemical systems, either No. 1 or No. 4 can be used. Method No. 5 is especially attractive where the same thrust system is reused for several maneuvers and where the propellant is added (calculating backwards) in clusters of tanks of sufficiently limited size range to permit a constant K_p-value, independent of the amount of propellant involved. In addition, this method is convenient to use in those cases where the limits of the λ vs. τ/I_{sp} charts in Sect. 5 are exceeded, which can occur especially in the direction of low W_p-values.

Knowledge of propellant quantity and ODW allows computation of the logistic requirements. These can be computed either by determining the volume of each propulsion module (PM) and fitting it into the available payload section of the ELV (subject to the payload weight limitations), either in one piece or in sections; or by determining, or estimating, the equivalent mass fraction x_{eq} of the vehicle and by computing the overall mass ratio of the vehicle for the particular mission,

$$\mu_{tot} = \exp \left[\frac{\Sigma \tau}{I_{sp}} \right] \tag{9-1}$$

This method is suitable where the same propulsion system (not necessarily the same engines) is used throughout the mission, because then I_{sp} is constant. From μ_{tot} the overall propellant fraction Λ_{tot} is obtained which, together with x_{eq}, yields the equivalent MGPF

$$\lambda_{eq} = 1 - \frac{\Lambda_{tot}}{x_{eq}} \tag{9-2}$$

the overall wet inert weight fraction

$$b_{tot} = \Lambda_{tot} \frac{1 - x_{eq}}{x_{eq}} \tag{9-3}$$

Assuming an "average" or equivalent payload, taken to be constant throughout the mission, $W_{\lambda, eq}$, yields the associated ODW

$$W_{A1} = \frac{W_{\lambda, eq}}{\lambda_{eq}} \tag{9-4}$$

and, therewith, the overall wet inert weight

$$W_{b,tot} = b_{tot} W_{Al} \tag{9-5}$$

and propellant weight

$$W_{p,tot} = \Lambda_{tot} W_{Al} \tag{9-6}$$

The propellant volume follows from the propellant weight, knowing its mean density. The length L_p of the propellant column is determined by dividing the volume by the cross sectional area of the ELV's payload section. Specifying, from design considerations, a characteristic ratio of propellant volume to overall ISV volume [1] (this ratio is always less than one and ranges from 0.8 for chemical vehicles to as low as 0.3 for nuclear vehicles), one can define a configuration factor

$$j = L_p / L_{ISV} \tag{9-7}$$

so that the total length of the ISV propulsion modules is

$$L_{ISV} = L_p / jk \tag{9-8}$$

where k is the ELV payload section length utilization factor.

The number of ELV's carrying ISV modules is then, based on one ISV,

$$N_M = L_{ISV}/L_L \quad (\text{if } W_{b,tot}/N_M < W_{L,M}) \tag{9-9}$$

---

1) Considering the sum of propulsion modules only; i.e. disregarding spine and life support section, assumed to be carried aloft separately.

where L_L is the length of the ELV payload section and $W_{L,M}$ is the ELV module carrying payload capacity. Obviously, if $W_{b,tot}/N_M > W_{L,M}$ the number N_M must be increased until the ratio is smaller than $W_{L,M}$. If that is the case, a certain amount of propellant may be carried in the modules,

$$W_{p,M} = 0.9\, N_M\, (W_{L,M} - W_b/N_M) \tag{9-10}$$

Instead of 0.9, any other suitable factor can be used. An additional propellant is carried up in tankers for transfer into the modules in orbit. The propellant weight which remains to be delivered by tankers is

$$W_{p,T} = q\, W_{p,tot} - W_{p,M} \tag{9-11}$$

where q is the make-up propellant weight factor ($q > 1$, e.g. 1.2). The number of ELV tanker carriers without redundancy is, per ISV,

$$N_T = W_{p,T}/W_{L,T} \tag{9-12}$$

where $W_{L,T}$ is the payload weight available for propellant delivery in the ELV/Tanker combination.

The payload is assumed to be carried aloft separately; but since its weight, for heliocentric missions, is practically never larger than the payload of the largest ELV involved in the ETO logistic operation, it is consistent with the overall accuracy of the method to add one ELV to the sum of N_M and N_T, whence the number of ELV's required to prepare one ISV in Earth orbit is, <u>without redundancy and disregarding the logistic requirements of orbital assembly and fueling operations.</u>

$$N_{ELV,ISV} = N_M + N_T + 1 \tag{9-13}$$

Redundancies depend on the assumptions regarding the probabilities of successful delivery (P_D), mating (P_M) and fueling (P_S) which result in an overall probability of successful mission readiness achieved by the operation without redundancy

$$P^*_{act} = P_D^n P_M^m P_S^s \tag{9-14}$$

if s fuelings, m matings and $n = N_{ELV, ISV}$ deliveries are involved. If the actual overall mission readiness success probability P^*_{act} is not adequate, a desired overall probability, P^*, must be defined which forms the basis for determining the redundancies. For a somewhat more accurate determination of the redundancies, those required for orbital fueling, mating and eventually delivery should be computed separately. However, for a simpler, though less accurate, appraisal the factor P^*/P^*_{act} can be used, so that the total number of ELV's to be procured, i.e. the sum of required and redundant ELV's is

$$N^+_{ELV, ISV} = N_{ELV, ISV} (P^*/P^*_{act}) \tag{9-15}$$

The sum of redundant ELV's to be ordered is then

$$N_{ELV, ISV, R} = (N^+ - N)_{ELV, ISV} \tag{9-16}$$

If, for example, 2 ISV's are to be assembled in orbit, N_{ELV} doubles, but the redundancy does not necessarily double. How much it is to be increased depends on the number of tankers (which are interchangeable payload), on the interchangeability of the individual modules of the ISV's, on the number of module deliveries required, on the individual delivery proability P_D and on the overall delivery probability P^*_D. Assume $P^* = 0.75$. Then, since

$$P^* = P^*_D P^*_M P^*_S \tag{9-17}$$

and assuming all three values on the right hand side to be equal, it follows that very closely $P^*_D = 0.91$. If a lower limit for the individual delivery probability is set as $P_D = 0.85$ and an upper limit $P_D = 0.95$, then the number of ELV's to be procured (i.e. N^+_{ELV}) varies with the number of deliveries (N_{ELV}) as shown in Fig. 9-1 for the cases that all deliveries involve interchangeable payloads or that all deliveries involve non-interchangeable payloads.

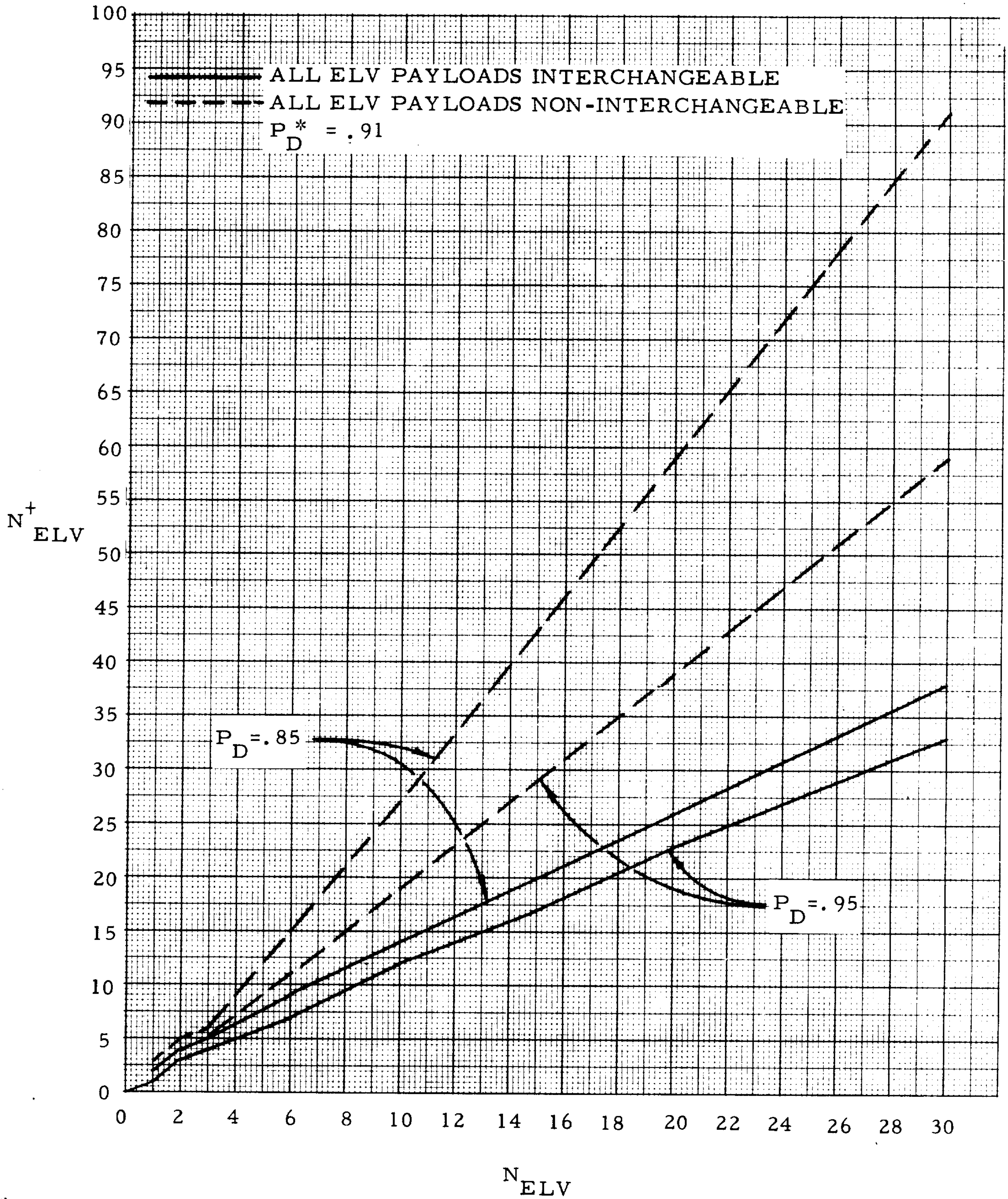

Fig. 9-1 EFFECT OF INTERCHANGEABILITY ON ELV PROCUREMENT REQUIREMENT N^+_{ELV} VS MINIMUM NUMBER OF DELIVERIES N_{ELV}

From the standpoint of this analysis, it makes no difference whether one or more ISV's are to be assembled. What counts is whether or not the modules are interchangeable. Examples below illustrate the method:

Example No. 1: One ISV is to be assembled. Required minimum number of module carriers is $N_M = 4$, number of tankers is $N_T = 10$. The same propellants are used in all modules. $P_D = 0.95$ for module carriers as well as tankers. $P_D^* = 0.91$. Then, from Fig. 9-1, $N_T^+ = 12$, because tankers are interchangeable, since propellants are the same; and $N_M^+ = 5$ if modules are all interchangeable; and $N_M^+ = 7$ if modules are non-interchangeable.

Example No. 2: As example No. 1, but the four modules consist of two pairs of modules, interchangeable within themselves but not between pairs. Theoretically, each pair should have a $P_{D,P}^*$ of $\sqrt{0.91} = 0.945$, if the same overall $P_D^* = 0.91$ is to be maintained. Neglecting this fact, the number is $N_{M,P}^+ = 3$ for each pair of modules, while N_T^+ remains the same as in the first example.

Example No. 3: Two ISV's, vehicle A and B, are to be assembled. Vehicle A requires $N_M = 5$, $N_T = 12$, vehicle B requires $N_M = 3$, $N_T = 8$. Within each vehicle the modules are interchangeable; between vehicles they are not interchangeable. Both vehicles use the same propellant. Therefore it can be set $N_T = 20$. Let $P_D = 0.85$. Then, from Fig. 9-1 for

Vehicle A: $N_M^+ = 8$

Vehicle B: $N_M^+ = 5$

Propellants for both: $N_P^+ = 26$

Example No. 4: As Example No. 3, but vehicles A and B use different propellants. Let P_D again be 0.85. In that case, from Fig. 9-1:

Vehicle A:	$N_M^+ = 8$	$N_T^+ = 17$
Vehicle B:	$N_M^+ = 5$	$N_T^+ = 12$

The logistic requirements, hence the direct operating cost of preparing the mission in orbit is higher than in Example No. 3. Corresponding effects are observed if different propellants are used in the various propulsion modules of one ISV.

The overall direct operating cost for a given mission can now be computed. The cost is defined as the sum of

- ETO transportation cost (cost of all ELV's and tankers procured and charged to this endeavor)
- Interorbital transportation cost (cost of all ISV's charged to this endeavor)
- Cost of destination, intransit, transportation and operational (DITO) payload of the ISV's
- Cost of orbital operation
- Miscellaneous costs, such as range cost, tracking and engineering support.

Thus, for direct operating cost (DOC) considerations only, Eq. (6-1) becomes

$$K_{TV}^{*} = K_{d}^{*} \qquad (\$/1b) \tag{9-18}$$

The ETO transportation cost is computed with the following relation

$$K_{ETO} = N_M^+ \, T_{GP} \, \frac{W_\lambda}{W_{L,M}} \, W_\lambda + N_T^+ \, T_{GP} \, \frac{W_\lambda}{W_{L,T}} \, W_\lambda \tag{9-19}$$

where T_{GP} is defined by Eq. (6-2) and W_λ is the gross payload of the ELV in question.

The interorbital transportation cost per ISV is

$$K_{ISV} = T_\lambda^{**} \, W_\lambda \tag{9-20}$$

where T_λ^{**} and W_λ depend on the choice of equations and conditions outlined in Section 6.

The cost of the DITO payload has not been investigated in detail in this report. Since it has little bearing on the systems comparison, it will be neglected. The same applies to miscellaneous costs and to the cost of the orbital operation, although it should be pointed out that the transfer of solid propellant magazines, as in the nuclear pulse vehicle, appears to be simpler, faster and therefore less expensive than the transfer of liquid propellants, especially of liquid hydrogen of which also larger quantities are needed than of nuclear pulse propellants.

For the comparative analysis, it appears therefore sufficient to compare the sum of those two DOC items which are most dependent upon transportation systems,

$$K^{*} = K_{ETO} + K_{ISV} \qquad (9\text{-}21)$$

The method of computing logistic requirements, outlined above in Equation (9-1) through (9-17) was applied parametrically, to determine the trend of ELV procurement requirements as a function of mission velocity, the three reference ELV's, and for chemical, SCR/G and NP systems of various specific impulses and mean equivalent payloads, i. e., constant payload masses throughout the mission. The results are presented in Fig. 9-2 through 9-5. It should be noted that the number of ELV's refers to the preparation of two identical vehicles in orbit.

Shown in Fig. 9-2 is the result of a parametric Earth-to-orbit logistics analysis for preparing manned planetary missions in Earth orbit as a function of mission velocity for different values of specific impulse of the interplanetary vehicle drives, for different initial payload weights, ranging from 100,000 lb for chemical vehicles to 500,000 lb for advanced vehicles with 5000 sec specific impulse. The ELV is Saturn V (Apollo). The redundancies are determined on the basis of the success probabilities listed. The abbreviations stand for: chemical (C), solid core reactor/graphite (SCR/G), and nuclear pulse (NP).

Because of the redundancy requirements involved, the number of ELV's shown represents primarily the procurement requirement and not necessarily the actual overall launch requirement, but rather the maximum launch requirement in order to assure 75% probability of success of assemblying and fueling two interplanetary vehicles of given initial payload, given overall mission velocity and given specific impulse (and associated propellant density) in orbit.

Fig. 9-3 shows the same parametric ELV procurement requirements as the previous chart, but with a modified Saturn V of improved payload capability and larger volume payload section.

Fig. 9-4 shows the same parametric ELV procurement requirements as the two previous charts, but for a Post Saturn launch vehicle.

Fig. 9-5 superimposes some of the results of the preceding three charts, namely, cases (1), (2), (3), and (6).

All of these charts make it apparent that Saturn V itself has a quite limited applicability as a logistics vehicle for manned planetary missions, unless the interplanetary vehicles have specific impulses of at least 1500 to 2200 sec. The applicability of lower specific impulses becomes increasingly practical and economic as the ELV capacity is enlarged. For very high mission velocities (above 70,000 ft/sec), both, a Post Saturn ELV and a nuclear pulse interplanetary vehicle, or a vehicle with a drive of similar specific impulse, are required. The trends indicated in these charts are in agreement with the results and evaluation of a more detailed special GPF and cost analysis presented in Sect. 11.

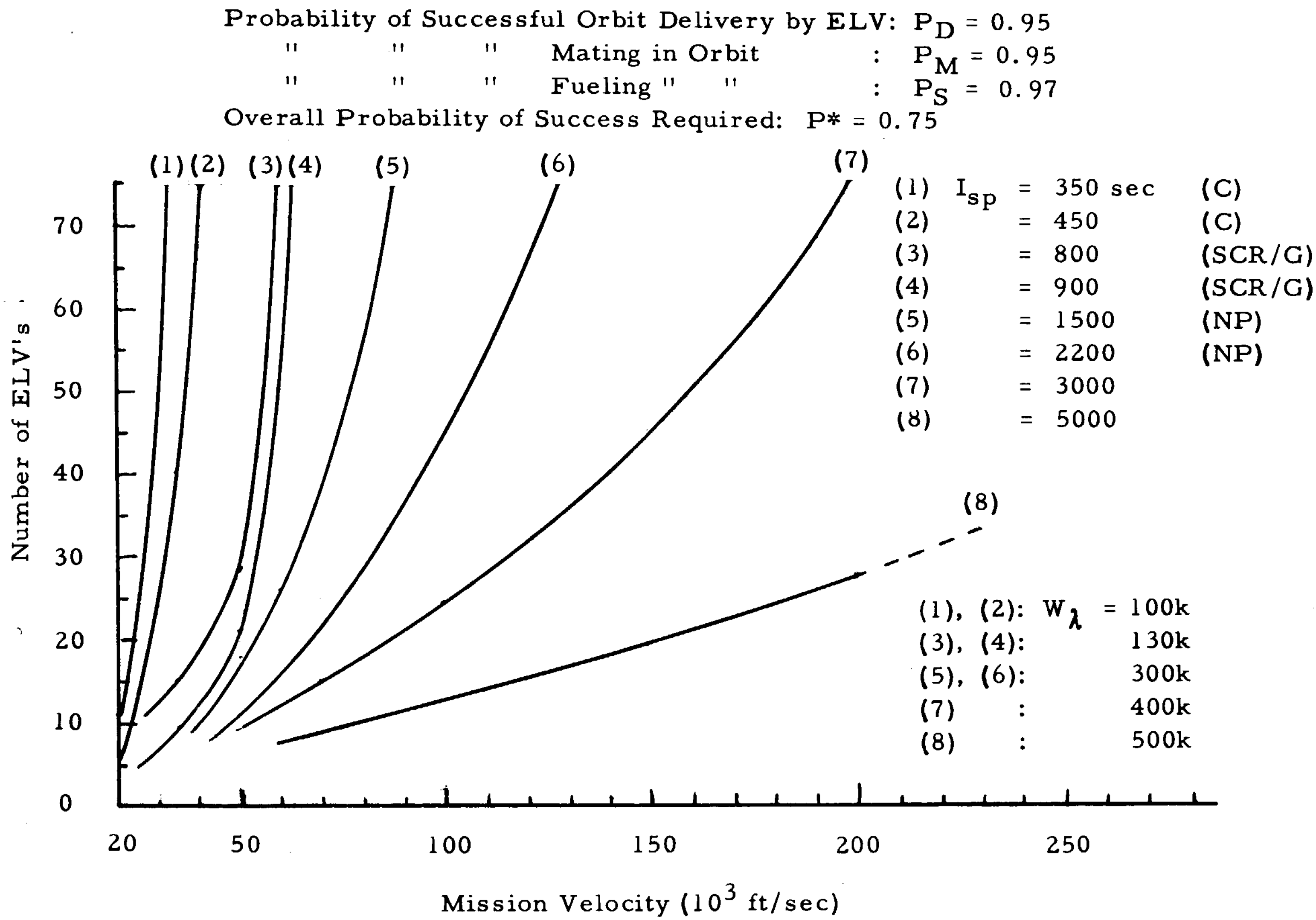

Fig. 9-2 Number of ELV's (incl. Redundancies) Required to Prepare Two Identical Interplanetary Vehicles of Initial Payload W_λ in Earth Orbit, ELV: Saturn V (Pld. 250k; 33' dia. Pld. Sect.)

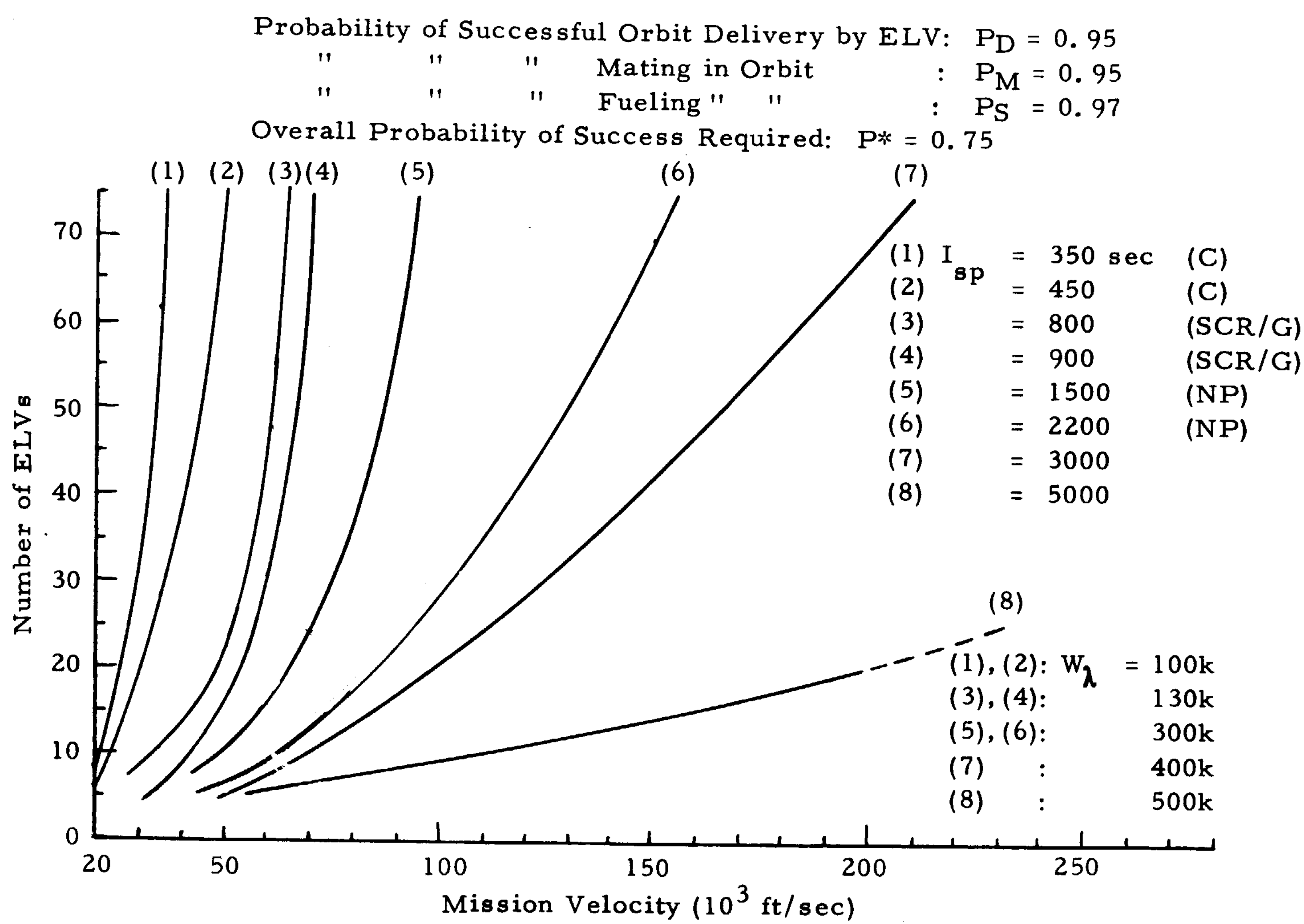

Fig. 9-3 Number of ELVs (incl. Redundancies) Required to Prepare Two Identical Interplanetary Vehicles of Initial Payload W_λ in Earth Orbit, ELV: Saturn V Mod. (Pld. 350k; 40' dia Pld. Sect.)

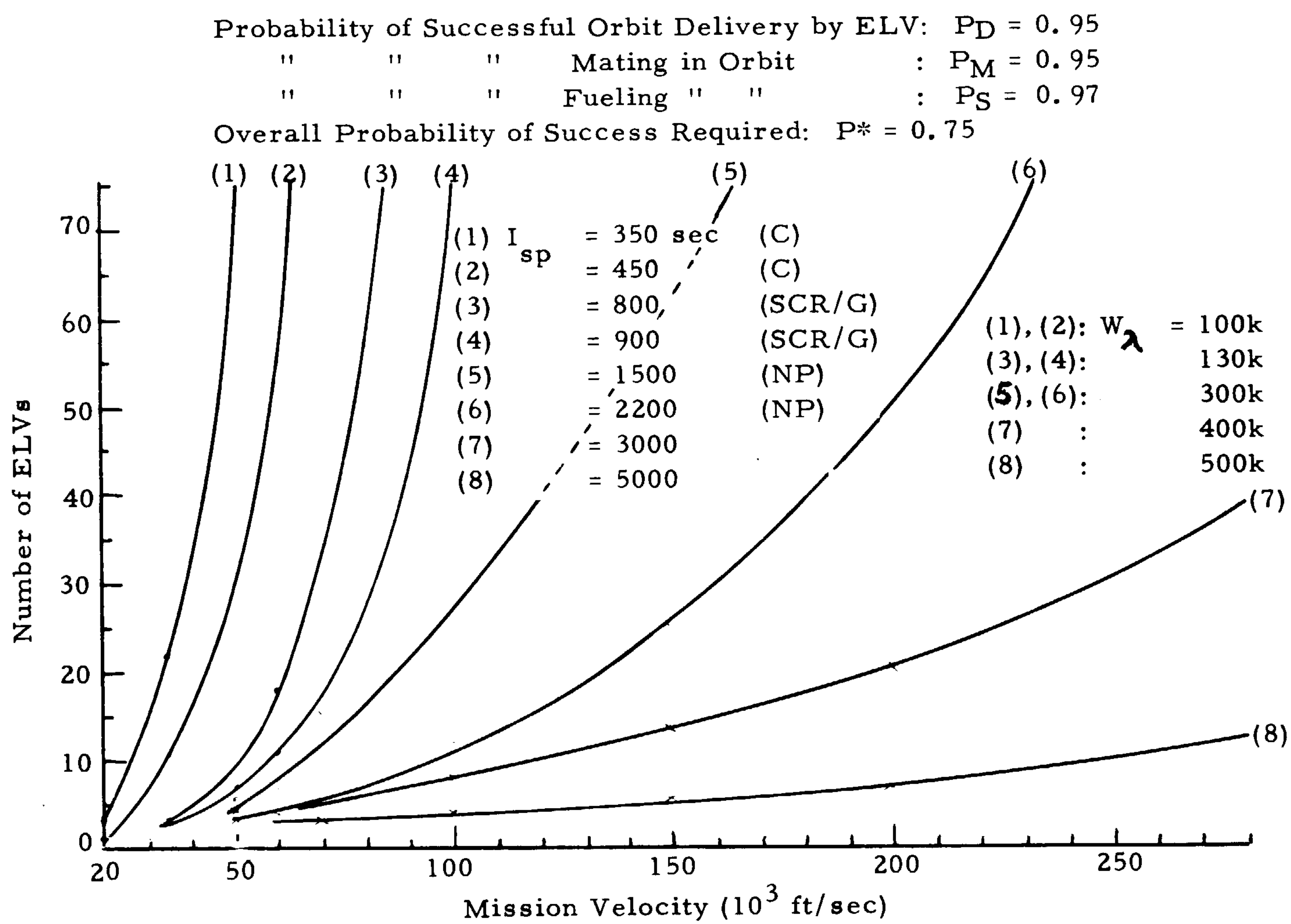

Fig. 9-4 Number of ELVs (incl. Redundancies) Required to Prepare Two Identical Interplanetary Vehicles of Initial Payload W_λ in Earth Orbit, ELV: Post Saturn (Pld. 1000k; 70' dia. Pld. Sec.)

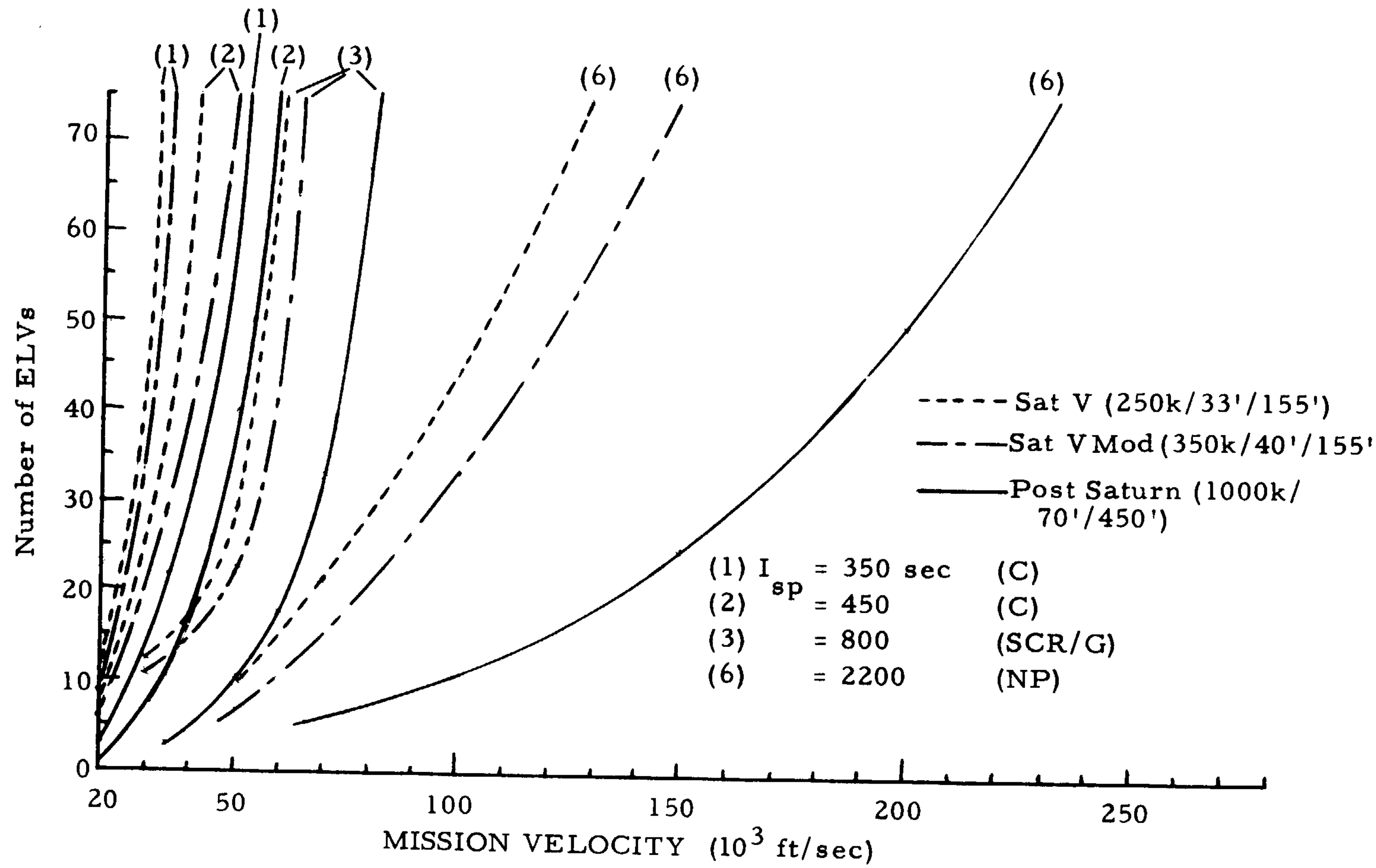

Fig. 9-5 Comparison of the Effect of I_{sp} and ELV Capability on Interplanetary Mission Capability

10 NUMERICAL APPLICATIONS

Special gross payload fractions (GPF) were computed for a large variety of missions, applying the methods No. 1, 4 and 5, explained in Sect. 9, the payload table given in Sect. 7, the charts for various vehicles and propulsion systems presented in Sections 5 and 4; and some of the mission data shown in Sect. 2. A typical computation form is shown in Fig. 10-1. The mission is briefly described in the upper right. The term "combination" refers to:

ELV Designation - ISV Designation - Terminal Mission Condition Designation

e.g. SaV - NP - 25k means the ELV is Saturn V, the ISV is a nuclear pulse vehicle and the terminal mission condition is a circular orbit at close Earth distance at 25,000 ft/sec velocity. Alternately, SaVM-G_3S-35k signifies the use of a modified Saturn V compatible ISV using SCR/G propulsion for three maneuvers and SHE propulsion for the fourth maneuver. Terminal mission condition is in an elliptic Earth capture orbit with a near-Earth perigee velocity of 35,000 ft/sec. Finally, PS-C_4-50k designates the use of a post-Saturn ELV, a chemical HISV for four maneuvers and return to Earth via hyperbolic atmospheric entry at 50,000 ft/sec. In a 3-maneuver mission for which the GPF is determined for 3 maneuvers; $W_\lambda = W_{\lambda 3}$, $D_{\lambda 2}$ and $D_{\lambda 1}$ must be specified (the fourth maneuver may either be nonexistent or its propulsion weight may be contained in the weight $W_{\lambda 3}$). If 4 maneuvers are computed, $W_{\lambda 4}$, $D_{\lambda 3}$, $D_{\lambda 2}$ and $D_{\lambda 1}$ must be specified. The velocity requirement (either impulsive or ideal, as can be noted under "Remarks",) for each maneuver is Δv. Next, $\tau/I_{sp} = \Delta v/g^*I_{sp}$ is determined. The specific impulse can be noted under "Remarks". The number of stages involved in each maneuver is specified next using the following symbols:

1 = a propulsion module consisting of one stage is employed for the maneuver

1P = The propulsion modules for each maneuver are mounted in parallel

2 = A propulsion module consisting of two stages in tandem, one of which is jettisoned during the maneuver. It is assumed that in that case, each stage brings up half of the maneuver velocity Δv, although this is not necessarily optimum.

2P = a propulsion module consisting of two stages in parallel. Conditions are the same as for "2", except that parallel stage arrangement permits the use of all engines at the beginning of the maneuver.

3 or 3P = a propulsion module consisting of three stages. In this case it is assumed that each stage brings up one third of the maneuver velocity.

CASE NO. ____________

MISSION ____________________

____

COMBINATION ____________________

____

W_λ = | $D_{\lambda 4}$ = | $D_{\lambda 3}$ = | $D_{\lambda 2}$ = | $D_{\lambda 1}$ =

Maneuver	1	2	3	4	5	Remarks
Δv (10^3 ft/sec)						
τ / I_{sp}						
# of Stages						
# or Thrust of Engine(s)						
Λ						
D_λ (10^3 lb)						
W_A (10^3 lb)						
W_λ (10^3 lb)						
ΛW_λ (10^3 lb)						
$W_p = \frac{\Lambda W_\lambda}{\lambda}$ (10^3 lb)						
λ (Stage)						
λ (Maneuver)						
λ (Mission)						
W_{A1} (10^3 lb)						

Fig. 10-1 COMPUTATION FORM

The number of stages is described by the requirement that for minimum W_b and W_p the ratio of τ / I_{sp} for a given stage should not exceed 1.4.

T = Only tanks or propellant magazines are jettisoned, rather than a full stage; indicating that the engine is reused for several maneuvers.

E = Engines are jettisoned, rather than a full stage; indicating that the propellant tankage is retained over several maneuvers.

The next line "Number or Thrust of Engine(s)" applies to GCR engines where the thrust should be specified and to the SCR/G or SCR/N engines where the selection of charts in Sections 5 and 4 depends on these specifications. The number of engines, together with No. of stages per maneuver 1, 2, or 1P, 2P indicates the amount of thrust initially available. Take, for instance SCR/N and a 4-maneuver mission. Then, the code

# of Stages	1P	2P	T	2P
# or Thrust of Engines	4	2	0	2

means that 8 engines burn at the first maneuver, 4 at the second, 2 on the third and fourth. Alternately,

# of Stages	1	1	1	1
# or Thrust of Engine(s)	2	1	2	1

means that propulsion modules are in tandem. M-1 operates with two engines, M-2 with one, M-3 with two and M-4 with one engine, respectively.

The next line "Λ" gives the useful propellant fraction and follows from τ / I_{sp} and Fig. 5-1b or from 5-1a by conversion from mass ratio μ. The value of $D_{\lambda 1}$ is listed under Maneuver 1, and so forth. W_A designates the ignition weight at the beginning of each maneuver. Each W_A is listed in such a manner that it can be most conveniently be added into the payload of the next lowe r stage. Thus W_{A4} is listed under Maneuver 3, W_{A3} is listed under maneuver 2, W_{A2} and Maneuver 1 and W_{A1} at the bottom of the table. The sum of D_λ and W_A under a given Maneuver column represent the gross payload W_λ for preceding propulsion module; i.e. the weight which must be divided by λ (stage) or λ (Maneuver) in the same colume to yield the next lower ignition we ight. The product ΛW_λ is required for iteration purposes in method No. 1 (cf. Sect. 9.). W_p follows from the iteration or the product ΛW_A. Finally, three lines for the GPF are provided: λ (Stage) is used only for those maneuvers for which "# of Stages" is larger than one. For these maneuver, λ (Maneuver) is equal to the square or the cube of λ (Stage), depending on the number of stages. λ (Mission) is the product of the λ (Maneuver) values for all maneuvers up to and including the maneuver in whose colume the λ (Mission) value is listed.

Several examples are presented in Tabs. 10-1 through 10-5 to illustrate the preceding description.

The results of a large number of computations are shown in Fig. 10-2 through 10-10.

Fig. 10-2 compares mission gross payload fractions (MGPF) versus mission period for a large number of Mars missions. The propulsion systems are indicated at the right. The subscripts designate the number of maneuvers for which they are used. The numbers designate the individual Mars missions, given by year and month of Earth departure. The graph is divided into three horizontal bands. The lower band shows the MGPF for three maneuvers (λ_{321}), namely, Mars departure for Earth, Mars arrival (circular orbit capture) and Earth departure. The missions are of the fast mission type (420-450 days). They are also typical for Mars missions with return via Venus fly-by with unretarded hyperbolic entry velocity up to about 45,000 ft/sec. In that case, however, the mission period is approximately 100 days longer. Gross payload at Mars departure is 160,000 lb, payload weight eliminated during Mars capture period is 50,000 lb. The Mars departure gross payload of 160,000 lb is kept constant throughout favorable and unfavorable mission years. Based on the variation of the Earth return conditions it would require more stringent mission termination conditions in 1977 than in 1986. On the basis of the first three maneuvers, the 1990 mission, rather than the 1977 mission, because the outbound maneuvers are particularly high. Fig. 10-3 shows the GPF and W_{A1} of the G_3 case (all three maneuvers using SCR/G engines). This is the case marked by little squares in Fig. 10-2. The lower band in Fig. 10-3 chemical, SCR/G and NP (Saturn V compatible) drives. In the central band are shown missions with 35,000 ft/sec Earth terminal capture velocity. The fast missions are represented by the SaV compatible NP drive. Comparing the MGPF's with these in the lower band shows a comparatively severe reduction. This is due to the relatively large weight of the propulsion system, especially the pusher plate. Even so, MGPF values of 10 to 15% are obtained. The comparatively larger scattering of the MGPF's than in the lower band, indicates the higher sensitivity to velocity conditions which characterizes every propulsion system as the ratio of τ/I_{sp} for the mission increases. It is seen that an NP vehicle returning into a highly elliptical Earth capture orbit (Mars departure gross payload 120k, Earth capture gross payload 90k) yields approximately the same MGPF as the SCR/G vehicle with a Mars departure gross payload of 160k, which is far less than required for Earth capture even with a much smaller payload. For very fast Mars round-trip missions of 190 to 250 days(with 10 days capture period) the MGPF values with the NP vehicle become comparble to those found for the chemical vehicle in the lower band. The central band also shows that for the synodic (conjunction)

Note: It lies in the nature of Method No. 4 that no distinction can be made between true payload and other weight elimination, such as jettisoning thermo-meteoroid shielding. Therefore the GPF of 0.0368 tends to be on the high side so far as true payload is concerned. The value should be multiplied by about 0.7. Then, if $W_{\lambda 3}$ is 125,000 lb, $W_{A1} = 4.85 \cdot 10^6$ lb.

CASE NO. Example

MISSION Mars; Circular Capture
T = 160/50/240d; EaDep
3-31-86

COMBINATION PS - C_3 - UHE (50.3k)

(UHE = Unretarded Hyperbolic Entry

W_λ = $D_{\lambda 4}$ = $D_{\lambda 3}$ = $D_{\lambda 2}$ = $D_{\lambda 1}$ =

Maneuver	1	2	3	4	5	Remarks
Δv (10^3 ft/sec)	11.98	13.92	16.82			Impulse Values
τ / I_{sp}	0.825	0.96	1.16			I_{sp} = 450 sec
# of Stages	1	1	1			
# or Thrust of Engine(s)	Not specified					
Λ	Not specified					Method No. 4 is used[1)]
D_λ (10^3 lb)	"	"				"
W_A (10^3 lb)	"	"				"
W_λ (10^3 lb)	"	"				"
ΛW_λ (10^3 lb)	"	"				"
$W_p = \frac{\Lambda W_\lambda}{\lambda}$ (10^3 lb)	2000	1000	40			W_p values assumed to be representative of tank modules
λ (Stage)	-	-	-			
λ (Maneuver)	0.42	0.35	0.25			
λ (Mission)		0.147	0.0368			0.147 = DGPF
W_{A1} (10^3 lb)						

1) cf. Sect. 9

DGPF = Delivery Gross Payload Fraction

Tab. 10-1 COMPUTATION FORM APPLYING METHOD NO. 4 TO CHEMICAL HISV ON MARS ROUND-TRIP MISSION 1986

Note: Because of comparative low sensitivity of mass fraction for chemical propulsion modules of this size, the number of chemical engines need not be specified.

CASE NO. Example

MISSION Mars; Circular Capture

T = 160/30/240; EaDep 10-5-75

COMBINATION PS - G_3C - 50k

$W_\lambda = 16.5 \cdot 10^3$ lb $D_{\lambda 4}$ = - $D_{\lambda 3} = 75.5$ $D_{\lambda 2} = 50$ $D_{\lambda 1} = 0$

Maneuver	1	2	3	4	5	Remarks
Δv (10^3 ft/sec)	14.3	12.8	19.9	20.3		Impulse Values
τ / I_{sp}	0.555	0.497	0.772	1.40		$G_3 = I_{sp} = 800$ sec C : $I_{sp} = 450$
# of Stages	1	1	1	1		PM-4 would better have been a 2-stager
# or Thrust of Engine(s)	2 250k	1 250k	1 250k	Not Specif.		See note on top of page
Λ	0.424	0.392	0.538	0.750		
D_λ (10^3 lb)	0	50	75.5			
W_A (10^3 lb)	931	457	84.6			
W_λ (10^3 lb)	931	507	160.1	16.5		
ΛW_λ (10^3 lb)	395	199	86	12.37		
$W_p = \frac{\Lambda W_\lambda}{\lambda}$ (10^3 lb)	760	365	245	68.6		
λ (Stage)	-	-	-	-		
λ (Maneuver)	0.52	0.545	0.35	0.195		
λ (Mission)		0.284	0.0992	0.0193		
W_{A1} (10^3 lb)	1790					

Tab. 10-2 COMPUTATION FORM APPLYING METHOD NO. 1 TO SCR/G_3-C HISV ON MARS ROUND-TRIP MISSION 1975

CASE NO. Example

MISSION Mercury Capture

T = ; EaDep 2-

COMBINATION PS - N_3 - W 3

Note: $W_{\lambda 3} = W_{\lambda}$ given below

$W_{\lambda} = 120 \cdot 10^3$ lb $D_{\lambda 4}$ = - $D_{\lambda 3}$ = - $D_{\lambda 2}$ = 100 $D_{\lambda 1}$ = 0

Maneuver	1	2 a/b	3 a/b	4	5	Remarks
Δv (10^3 ft/sec)	25.6	41.4	38.6			Impulse Values
τ / I_{sp}	0.935	1.512	1.41			I_{sp} = 850 sec
# of Stages	1P	2P	2P			2b = T 3a = T
# or Thrust of Engine(s)	10	6/2	2/2	a/b		F = 50k a/b = 1st St./2nd St.
Λ	0.608	0.53 0.53	0.505 0.505	a b		a = First stage b = Second stage
D_{λ} (10^3 lb)	0	100	0			Note:
W_A (10^3 lb)	3760	1655 635	293 -	a b		3760=W_{A2a}=St. 1 of PM-2 1655=W_{A2b}=St. 2 of PM-2
W_{λ} (10^3 lb)	3760	1655 732	120			632=W_{A3a}=St. 1 of PM-3 293=W_{A3b}=St. 2 of PM-3
ΛW_{λ} (10^3 lb)	2285	878 388	148 60.6	a b		PM = Propulsion Module
$W_p = \frac{\Lambda W_{\lambda}}{\lambda}$ (10^3 lb)	6450	2000 878	319 147.8	a b		PM-1 is composed of cluster of 10^6 lb propellant tanks, applying method No. 5. The rest is computed acc. to method No. 1
λ (Stage)	0.355	0.440 0.442	0.464 0.410	a b		
λ (Maneuver)	0.355	0.194	0.190			
λ (Mission)			0.0131			
W_{A1} (10^3 lb)	10,600					

Tab. 10-3 COMPUTATION FORM APPLYING METHODS NO. 1 AND 5 TO SCR/N HISV ON MERCURY ROUND-TRIP MISSION 1984

CASE NO. Example

MISSION Venus Ell. Capt. $(n=8; r_p^*=1.1)$

T =

COMBINATION SaVM - $(GCR)_3N$ - 25k

$W_\lambda = 90\cdot 10^3$ lb $\quad D_{\lambda 4}$ = - $\quad D_{\lambda 3} = 40 \quad D_{\lambda 2} = 100 \quad D_{\lambda 1} = 0$

Maneuver	1	2	3	4	5	Remarks
Δv (10^3 ft/sec)	12.53	5.23	15.03	22.31		
τ / I_{sp}	0.218	0.0904	0.260	0.813		GCR: I_{sp} = 1800 sec N : 850 sec
# of Stages	T	T	1	1		
# or Thrust of Engine(s)	1	1	1	2		GCR: F = 750k N 50k/eng.
Λ	0.195	0.0860	0.228	0.555		
D_λ (10^3 lb)	0	100	40	0		
W_A (10^3 lb)	903	720	183	-		
W_λ (10^3 lb)	903	820	223	90		
ΛW_λ (10^3 lb)	-	-	50.9	50		x = 0.946 for Stages "T" (Method No. 5)
$W_p = \frac{\Lambda W_\lambda}{\lambda}$ (10^3 lb)	222	77.6	164	102		
λ (Stage)	-	-	-	-		
λ (Maneuver)	0.794	0.909	0.31	0.492		
λ (Mission)				0.110		
W_{A1} (10^3 lb)	1138					

Tab. 10-4 COMPUTATION FORM APPLYING METHODS NO. 1 AND 5 TO GCR-SCR/N HISV ON VENUS ROUND-TRIP MISSION 1981 WITH TERMINATION IN CIRCULAR NEAR-EARTH ORBIT

Note: Do not form products $\lambda_1\ \lambda_2$ or $\lambda_1\ \lambda_2\ \lambda_3$. They would be misleading, because "T" does not consider the heavy thrust system which, in a tankage modularized vehicle is accounted for always in the last maneuver. If one wanted to know $\lambda_1\ \lambda_2$ one would have to use # of stages = T - 1 for Maneuvers 1 - 2.

CASE NO. Example

MISSION Mars; Circ. Capt.; Very Fast

T = 60/10/120d; Ea Dep -1-80

COMBINATION Sa V - NP - 35k

$W_\lambda = 90 \cdot 10^3$ lb $D_{\lambda 4}$ = - $D_{\lambda 3} = 0$ $D_{\lambda 2} = 100$ $D_{\lambda 1} = 0$

Maneuver	1	2	3	4	5	Remarks
Δv (10^3 ft/sec)	25.9	37.6	46.0	35.7		
τ / I_{sp}	0.322	0.467	0.571	0.444		I_{sp} = 2500 sec
# of Stages	T	T	T	1		
# or Thrust of Engine(s)	1	1	1	1		F = 750k
Λ	0.275	0.375	0.435	0.36		
D_λ (10^3 lb)	0	100	0	-		
W_A (10^3 lb)	1629	880	474	-		
W_λ (10^3 lb)	1629	980	474	90		
ΛW_λ (10^3 lb)	-	-	-	-		x = 0.944 for all Stages "T". For M-1:
$W_p = \dfrac{\Lambda W_\lambda}{\lambda}$ (10^3 lb)	633	610	383	171		$x = 1.06 + \dfrac{200,000}{W_p} - 1$
λ (Stage)	-	-	-	-		
λ (Maneuver)	0.708	0.602	0.539	0.19		
λ (Mission)				0.0436		See Note on top of page
W_{A1} (10^3 lb)	2300					

Tab. 10-5 COMPUTATION FORM APPLYING METHOD NO. 5 TO NP HISV ON VERY FAST MARS ROUND-TRIP MISSION 1980 WITH TERMINATION IN ELLIPTIC EARTH ORBIT

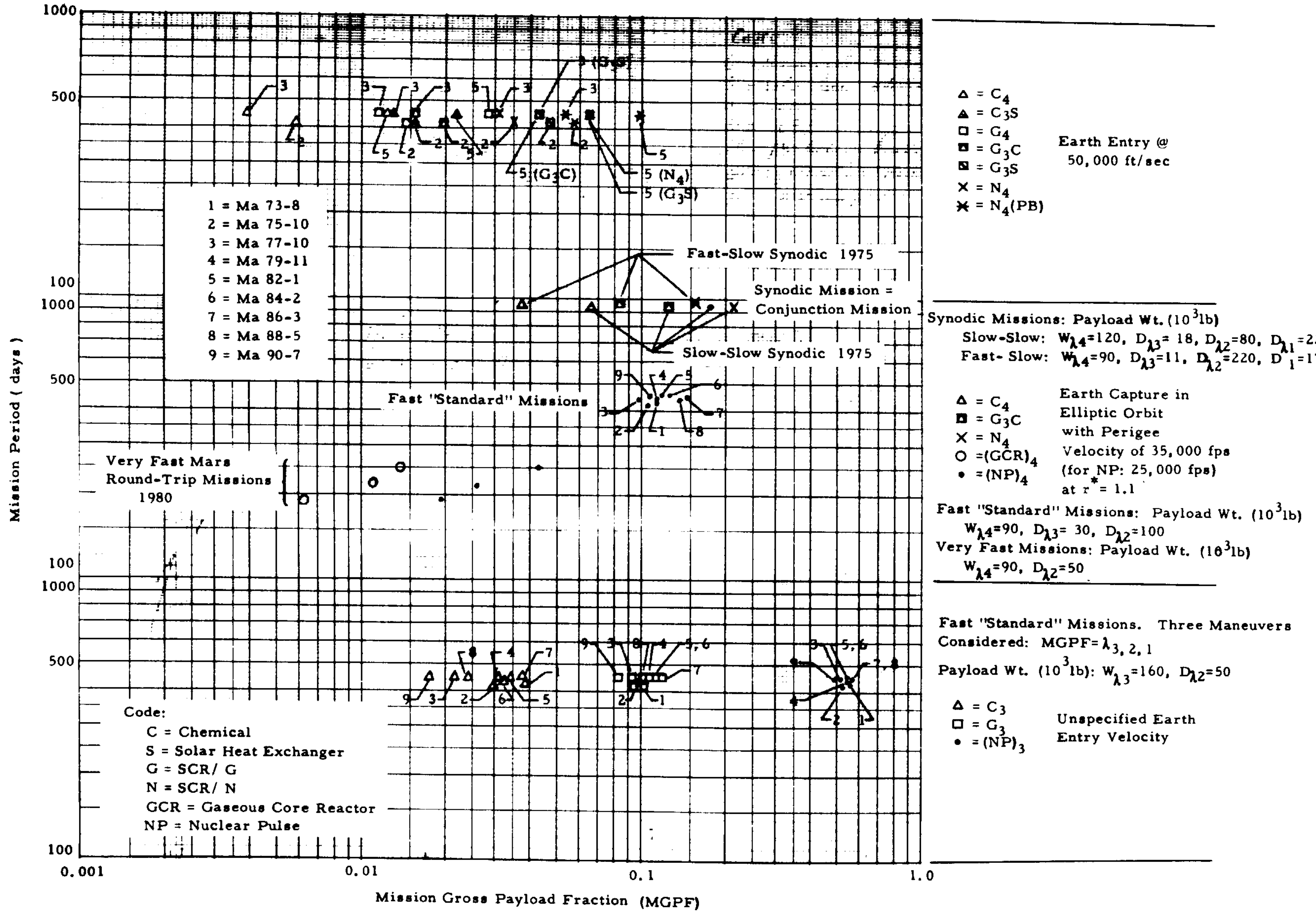

FIG. 10-2 SURVEY OF SOME MISSION GROSS PAYLOAD FRACTIONS FOR ROUND-TRIP MISSIONS TO MARS.

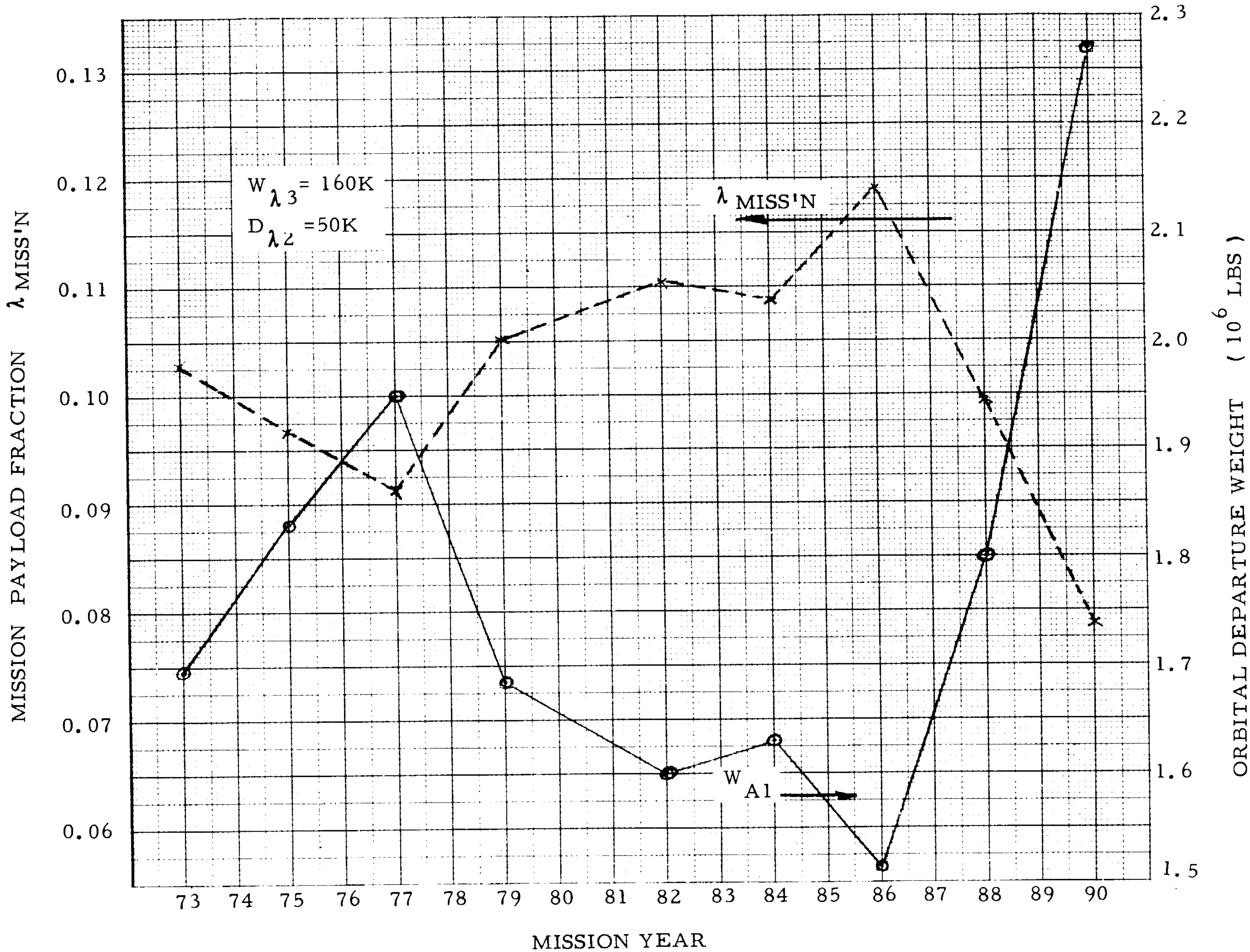

FIG. 10-3 MARS MISSION - PAYLOAD FRACTION AND WEIGHT — SCR/G VEHICLE

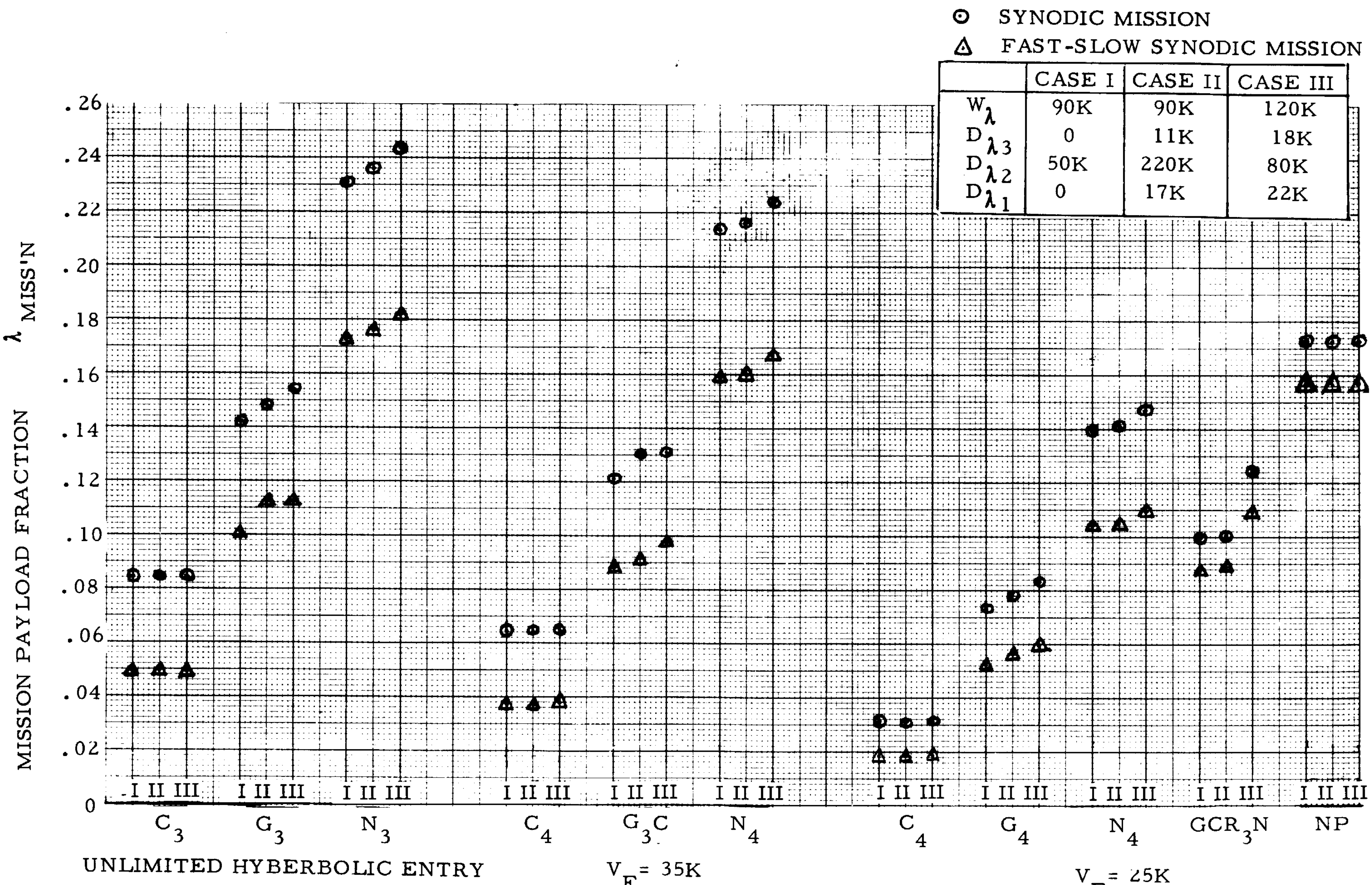

FIG. 10-4 MARS SYNODIC MISSIONS - 1975 - PAYLOAD FRACTIONS

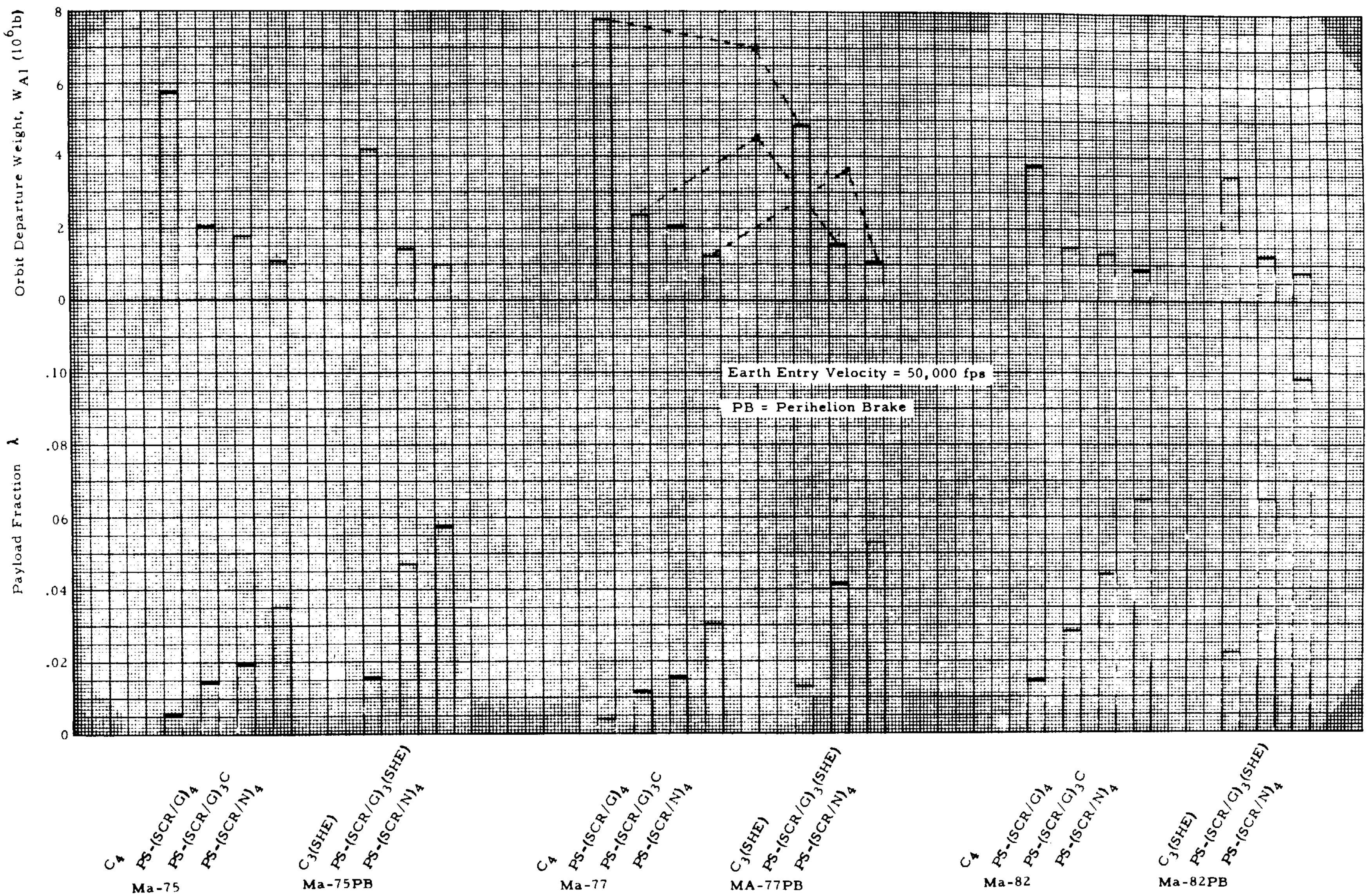

FIG. 10-5 COMPARISON OF PAYLOAD FRACTION AND ORBIT DEPARTURE WEIGHT FOR MARS MISSIONS USING VARIOUS TYPES OF PROPULSION SYSTEMS.

FIG. 10-6 WEIGHT SUMMARY MARS MISSIONS

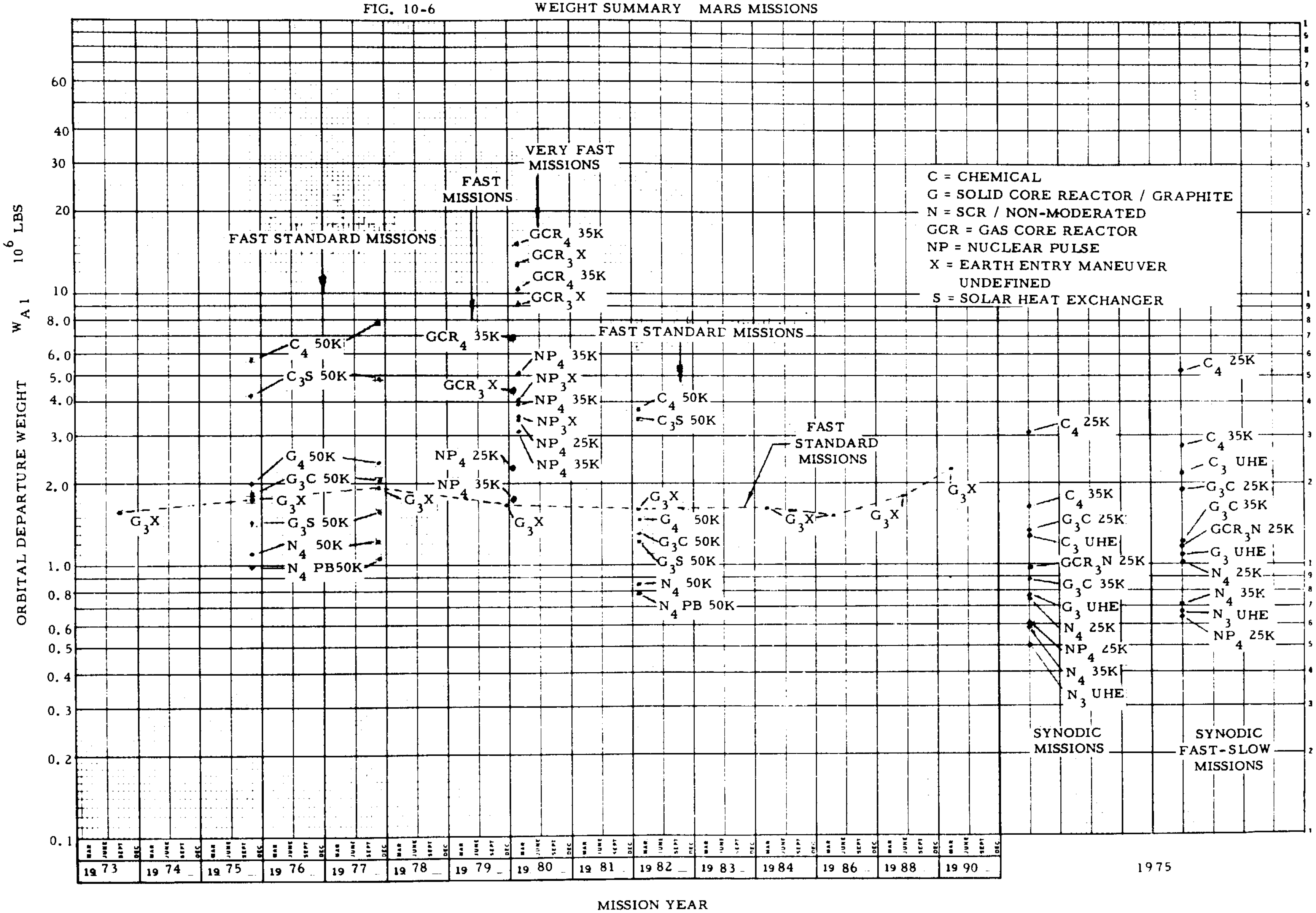

Fig. 10-6

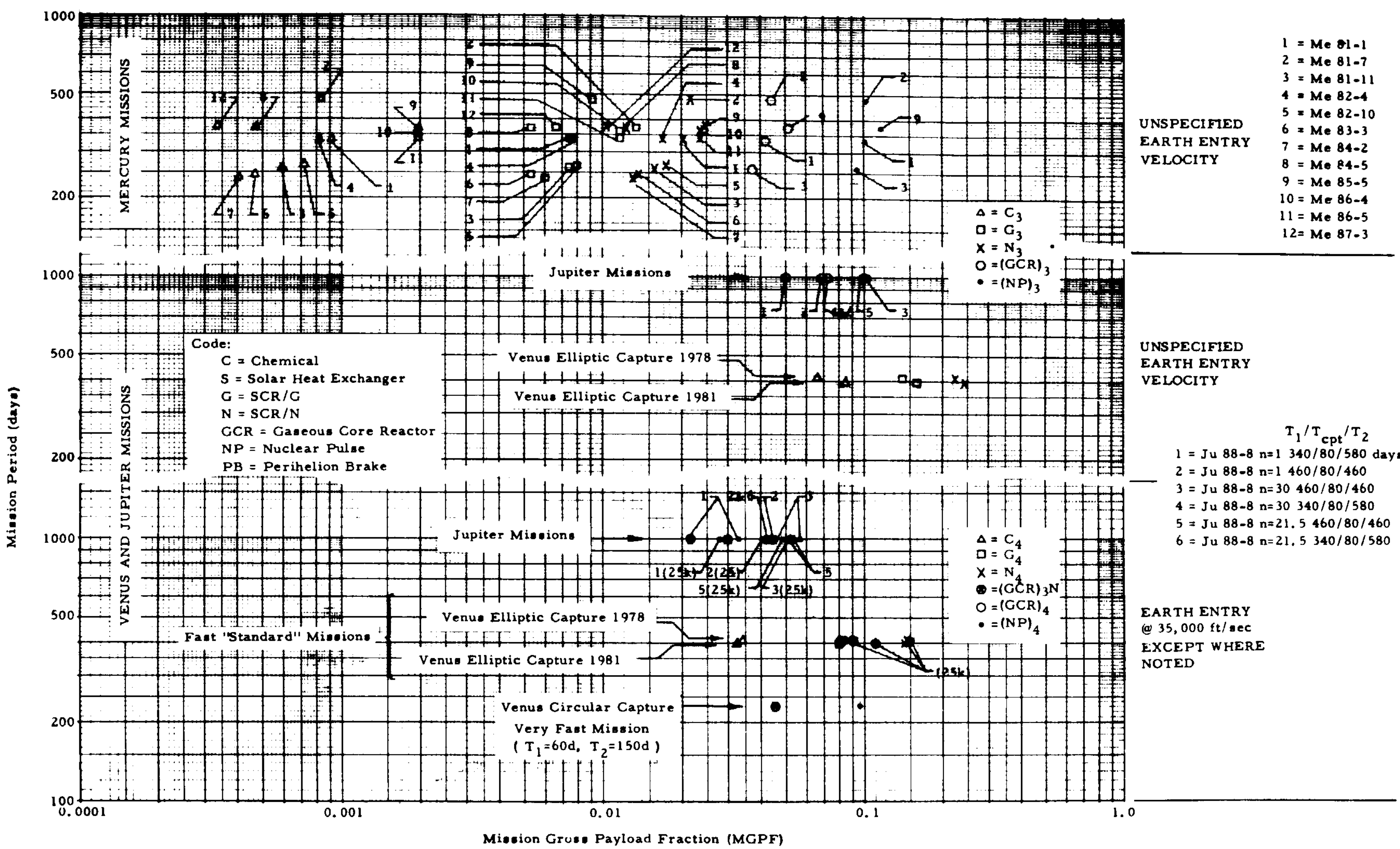

FIG. 10-7 SURVEY OF SOME MISSION GROSS PAYLOAD FRACTIONS FOR ROUND-TRIP MISSIONS. MERCURY, VENUS, AND JUPITER.

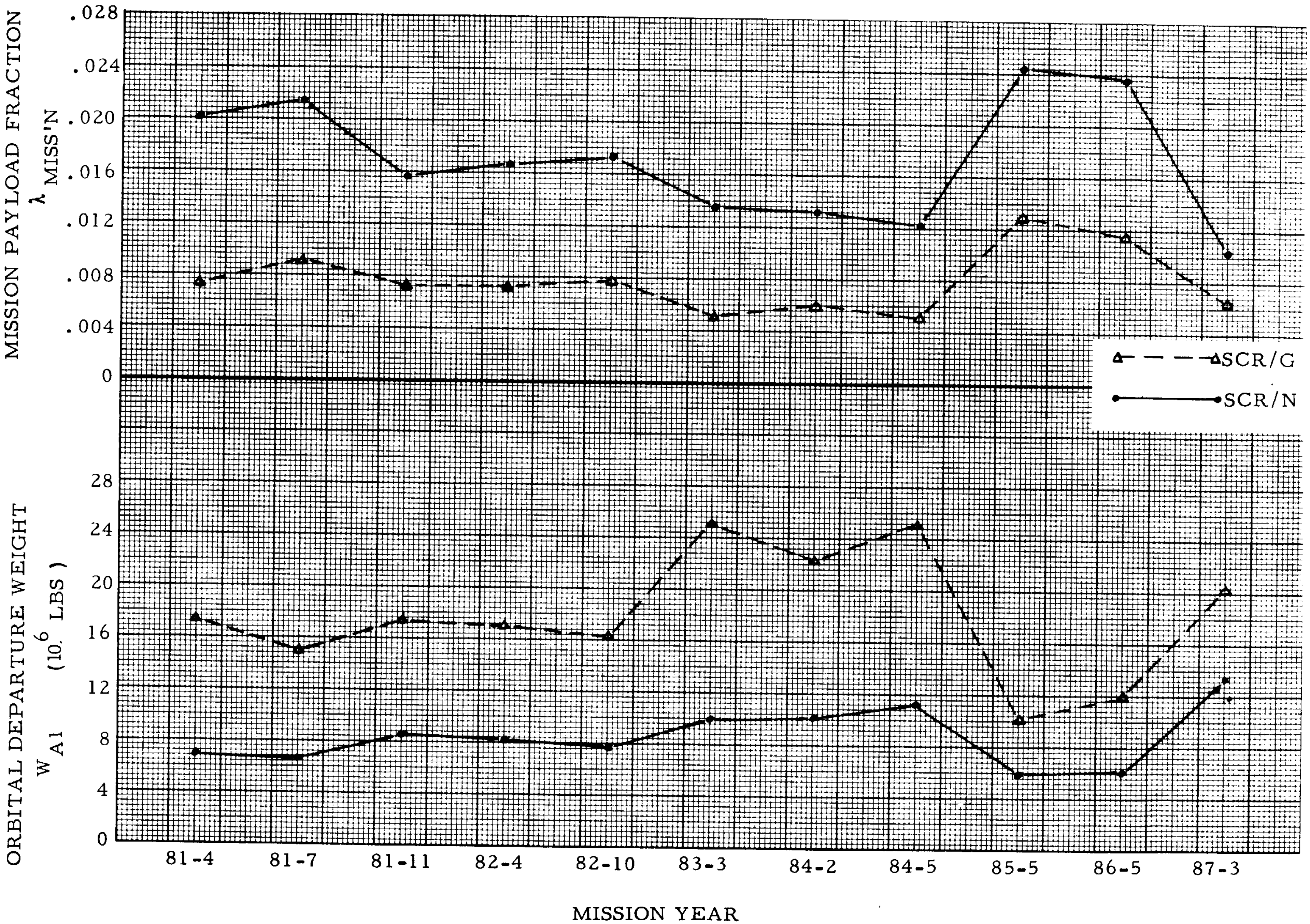

FIG. 10-8 MERCURY MISSIONS

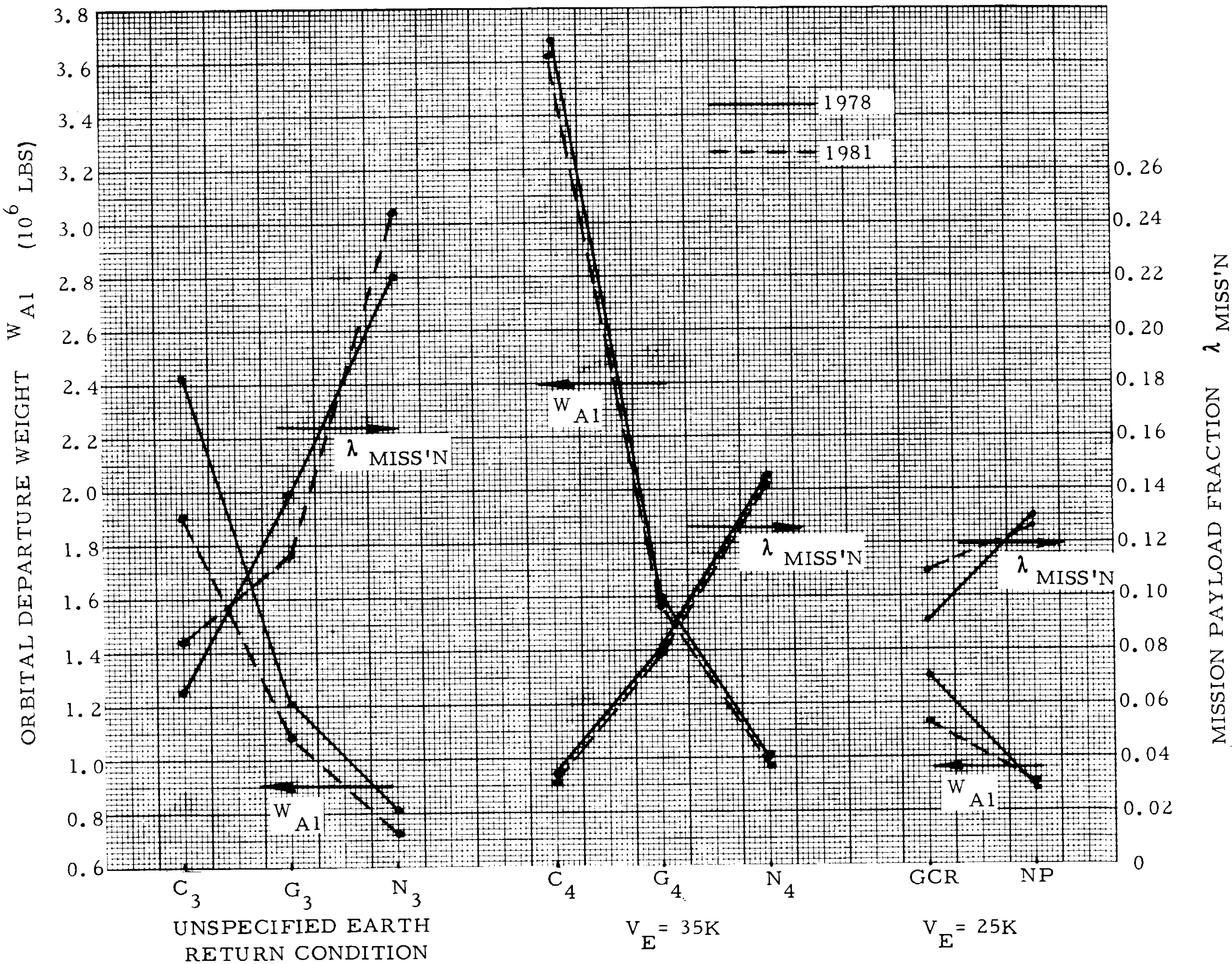

FIG. 10-9 VENUS MISSIONS - ELLIPTIC CAPTURE

FIG. 10-10 WEIGHT SUMMARY FOR MERCURY VENUS AND JUPITER MISSIONS

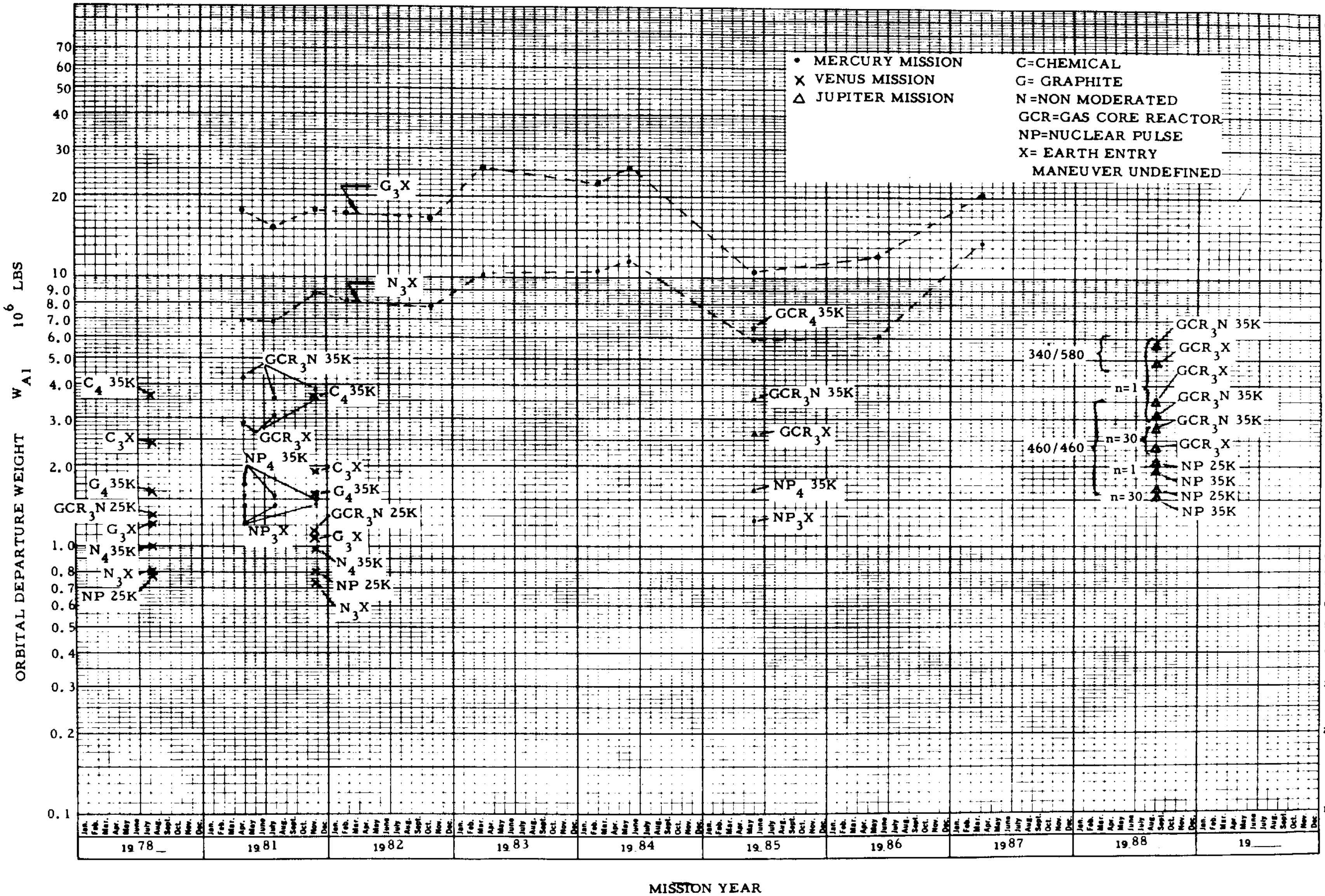

missions whose overall velocity requirement is very low (about 32, 500 for the mission with slow outbound and slow return transfer; about 40, 000 ft/sec for the fast-slow mission) the NP vehicle does not seem to show a superiority in MGPF compared to the SCR/N system (characterized by very low engine weight). However, it should be noted that the terminal condition for the NP vehicle is in a circular orbit (25, 000 ft/sec), as compared to an elliptical orbit (35, 000 ft/sec at perigee) for the SCR/N vehicle. Furthermore, even then the propellant consumption of the NP vehicle is only 50 to 55% of that of the SCR/N vehicle. This advantage of course could be utilized only if the vehicles were reusable. Fig. 10-4 shows MGPF's for the two types of synodic missions in greater detail.

The upper band of Fig. 10-2 shows the MGPF at 4 maneuvers for Earth entry velocity of 50, 000 ft/sec applying a variety of propulsion systems. The hollow squares for missions 2, 3 and 5 should be compared with the corresponding squares in the lower band. They show the reduction in MGPF due to a fourth maneuver in which the gross payload is 16, 500 lb. The fact that the MGPF is lower in the upper band indicates that in those mission years a gross payload of 160, 000 lb at Mars departure would not suffice to reduce a gross payload of 16, 500 lb to 50, 000 ft/sec entry velocity. A survey of the cases considered in the upper band is shown in Tab. 10-6. Their MGPF's and ODW's are compared in Fig. 10-5 in greater detail. The performance improvement due to application of the perihelion brake (PB), especially in the less favorable years 1975 and 1977 is clearly indicated especially for chemical vehicles, but also for SCR/G and SCR/N powered vehicles. In the first two instances a SHE drive is employed, because of the large mass of chemical and SCR/G propulsion systems. In the latter case, however, this is not required, because of the low mass anticipated for the small SCR/N engine. In the latter case, the Ma77 mission indicates a reduction by some 130, 000 lb, compared to the much larger differences for the other drives. It is of importance to note, however, that the improvements in MGPF due to PB application suggest a much larger reuction in ODW than is actually attained. For instance, for the Ma77 mission with the chemical drive, an improvement in MGPF by a factor of better than 3 is obtained. The ODW, however, is not reduced to one third but only to about 70%. The reason for this is, of course, that a larger payload is decelerated at the prihelion than during the geocentric Earth retro-maneuver. Another case which should be noted is the comparison between the second and third columns in the missions without PB. They indicate that use of a chemical drive for the Earth retro-maneuver results in a better payload transport efficiency (higher MGPF), hence a lower ODW, than the use of an SCR/G engine. None of these results offers anything new or unexpected. These cases are shown here, in order to demonstrate the comparatively high accuracy and resolution of the gross payload fraction method of comparison if based on fairly accurate data for scaling coefficients and/or mass fractions.

Mission	Maneuvers (impulsive) (10^3 ft)				Loads (10^3 lb)				Combinations					
					$W_{\lambda 4}$	$D_{\lambda 3}$	$D_{\lambda 2}$	$D_{\lambda 1}$	C_3S 50k	C_4 50k	PS G_4 50k	PS G_3S 50k	PS G_3C 50k	PS N_4 50k
Ma 75	14.3	12.8	19.9	20.3	16.5	75.5	50	0		*	*		*	*
Ma 75 PB	14.3	12.8	19.9	11.0	22	70	50	0	*			*		*
Ma 77	13.3	16.3	18.9	22.2	16.5	75.5	50	0		*	*		*	*
Ma 77 PB	13.3	16.3	18.9	12.0	22	20	50	0	*			*		*
Ma 82	12.0	12.4	20.8	9.3	16.5	75.5	50	0		*	*		*	*
Ma 82 PB	12.0	12.4	20.8	5.9	22	70	50	0	*			*		*

Tab. 10-6 CASES CONSIDERED IN UPPER BAND OF Fig. 10-2

In summary, Fig. 10-2 shows and/or implies that for "standard" fast mono-elliptic round-trip missions to Mars with terminal condition of 50,000 ft/sec hyperbolic entry, only the NP and the GCR drives offer MGPF's above 10%. For the same missions with minimum Earth capture conditions (35k) the implication of Fig. 10-2 is that only the NP offers MGPF's of 10 to 15 percent. Furthermore, the following can be concluded:

1. In the case of unspecified Earth entry velocity (3-maneuver case, lower band in Fig. 10-2) which is also typical for return via Venus with UHE at 45,000 ft/sec or less, the MGPF values obtained with the NP vehicle are 5 times as high as those attained by the chemical (O_2/H_2) vehicle. The impulsive mission velocities involved here lie between 43,000 and 53,000 ft/sec (1986 and 1990 mission, respectively).

2. For a terminal condition of hyperbolic entry a 50,000 ft/sec in unfavorable mission years, the MGPF values for chemical vehicles range from 0.4% without PB maneuver to slightly better than 2% with PB maneuver. The MGPF values of chemo-nculear SCR/G vehicles (G_3C) range from 1.5% to slightly over 4% which is a very significant improvement. If PB maneuvers are applied (G_3S) the MGPF is increased to range from slightly over 4% to about 6.5%. The MGPF of nuclear SCR/N vehicles (N_4) ranges from slightly above 3% to 6.5%; or, with PB maneuver (N_4(PB)), from slightly over 5% to 10%. It should not be forgotten, however, that the PB maneuver, while distinctly reducing the ODW, does not produce as large a reduction as the improvement in MGPF suggests. The GCR drive (not shown) would yield MGPF values between 15 and 20 percent. The NP drive (also not shown) would yield MGPF values between 35 and 40 percent.

3. For a minimum Earth capture terminal condition (35k), the MGPF values of chemical vehicles become prohibitively low. Those of SCR/G and SCR/N vehicles fall under 1% and into the 1 to 2 percent bracket, respectively. Those for the NP lie between 10 and 15%.

4. Only for very fast Mars round-trip missions with a mission period of 190 to 250 days (at 10 days capture period) do the MGPF values for the NP vehicle fall as low as 2 to 5 percent.

5. In conjunction (synodic) missions with minimum Earth capture conditions MGPF values between about 4 and 7 percent are indicated for chemical vehicles (about 8.5% for UHE as terminal condition); between 8 and 13 percent for SCR/G vehicles (G_3/C); and between 15

to 24 percent for SCR/N vehicles (N_4). The NP shows no particular advantage in this low mission energy range. Its MGPF values are comparable to that of the SCR/N vehicles. However, the propellant consumption of the NP is lower than that of the SCR/N vehicle. With increasing payload, therefore, the MGPF of the NP vehicle would grow faster than that of the SCR/N vehicle. In the case of repeated use, the supply requirements for the NP vehicle would be 45 to 50 percent lower.

Fig. 10-6 shows the orbital departure weights (ODW) which correspond to the mission gross payload fractions surveyed in Fig. 10-2.

Fig. 10-7 compares MGPF values for missions to Mercury (cf. Tab. 2-3), to Venus (Tab. 2-5) and to Jupiter. Details regarding the latter mission group are shown in Tab. 10-7. Fig. 10-8 shows MGPF and ODW for the SCR/G and SCR/N vehicles (3 maneuvers; unspecified Earth return conditions) as function of mission years for the Mercury mission group. Fig. 10-9 shows details regarding the fast "standard" Venus missions with three different terminal conditions, for the chemical, the SCR/G and the SCR/N vehicles. The two Venus mission years of 1981 and 1978 were selected, because 1981 is typical for a favorable mission years, 1978 for an unfavorable mission year. The spread is far smaller than for Mars missions reflects about the maximum variation for the same mission with the same load conditions, namely, for the 3-maneuver case (unspecified Earth return conditions): $W_{\lambda 3}$ = 130,000 lb, $D_{\lambda 2}$ = 100,000 lb, $D_{\lambda 1}$ = 0 and for the 4-maneuver cases (35k and 25k terminal capture velocity) $W_{\lambda 4}$ = 90,000 lb, $D_{\lambda 3}$ = 40,000 lb, $D_{\lambda 2}$ = 100,000 lb, $D_{\lambda 1}$ = 0.

In addition, Fig. 10-7 shows the MGPF for a very fast Venus mission flown by a Saturn V compatible NP vehicle and a vehicle using a GCR drive for the first three maneuvers and an SCR/N drive for the Earth capture maneuver. The load conditions for this mission are $W_{\lambda 4}$ = 90,000 lb, $W_{\lambda 2}$ = 100,000 lb, all others zero.

The Mercury mission group was used to compare the various drives within the framework of an advanced high-energy mission. The superiority of the NP drive and, to a lesser degree, of the GCR drive,[1] is manifested

---

1) The "inferiority" of the GCR drive in the context of the comparison in Fig. 10-7 is due primarily to the lower specific impulse of 1800 sec versus 2500 sec for the NP. The most optimistic estimates for the GCR do not exceed 2000 sec. On the basis of available information the estimate of 1800 sec for GCR is as "optimistic", if not more so, as the estimate of 2500 sec for the NP drive.

T (days)		Δv_1	r*	10^3 (ft/sec)		r_P^*	n	Velocities (10^3 ft/sec)						Mission Number Given in Fig. 10-7
T_1	T_2	(10^3 fps)	(Ju Radii)	Δv_2	Δv_3	(Ju Radii)	$= r_A/r_P$	Δv_{P2}	Δv_A	Δv_3	Δv_A	Δv_{P3}	v_E	
460	460	24.7	50	33.1	37.0	-	-	-	-	-	-	-	53.5	2
460	460	24.7	-	-	-	1.1	30	8.3	18	-	18	9.2	53.5	3
460	460	24.7	-	-	-	1.1	21.5 (JIV)	9.4	18.8	-	18.8	10.5	53.5	4
340	580	35.4	50	54.1	24.0	-	-	-	-	-	-	-	54.3	1
340	580	35.4	-	-	-	1.1	30	15.0	18	-	-	23.6	54.3	4
340	580	35.4	-	-	-	1.1	21.5 (JIV)	16.0	18.8	-	-	24.0	54.3	5

Note: Capture periods are about 80 days. Total mission period, 1000 days

Three maneuvers: $W_{\lambda 3} = 220$, $D_{\lambda 3} = N/A$, $D_{\lambda 2} = 100$, $D_{\lambda 1} = 20$

Four maneuvers: $W_{\lambda 4} = 50$ 170 100 20

Note: All weights in 10^3 lb

Tab. 10-7 DETAILS REGARDING JUPITER MISSION GROUP OF Fig. 10-7 in their high MGPF values as well as in the relatively small scatter of these values with varying overall mission velocity.

The fast "standard" Venus mission (elliptic capture) of about 400 days duration is the example of a relatively low energy mission. Relative to this mission with a minimum terminal capture condition (35k), except for GCR/N and NP for which the terminal condition is circular capture (25k), the chemical and all nuclear types of propulsion systems are compared. The superiority of the NP is, in this case, expressed not in a high MGPF, but in a mission profile of higher "quality".

The 3-maneuver Jupiter mission is represented by the GCR powered vehicle, yielding MGPF values in the range of 5 to 10 percent. This implies that for the NP the MGPF would lie between approximately 8 and 16 percent. For the 4-maneuver Jupiter mission the NP vehicle returning into a circular Earth capture orbit (25k) shows still a superior MGPF to the GCR vehicle returning into a minimum Earth capture orbit (35k).

Fig. 10-10, finally shows the ODW values associated with the missions, combinations and their mission gross payload fractions shown in Fig. 10-7.

In the following Section the results of the numerical applications are tabulated and evaluated.

11. EVALUATION

11.1 Results of Special Gross Payload Fraction Analysis

The principal results of the numerical computations presented in Sect. 10 plus a number of Earth orbital injection and lunar delivery missions are presented in Tabs. 11-1 through 11-6. In each set of data, the top line designates the target.

The second line designates the mission. Where the term "standard" is used here, it refers to fast (420-450) round-trip missions to Mars with 30 to 50 days capture period and mono-elliptic transfer orbits out and back. The term "CC" stands for circular capture. A synodic (or conjunction) mission describes a mission (in this case to Mars) in which the outbound and return transfer orbits are flown at the optimum window for the respective transfer condition. These windows recur in the average every 27 months, the average synodic period in which Earth and Mars occupy the same angular position with respect to each other. Among these transfer orbits, those which are slow, requiring 240 to 270 days transfer time, demand a particularly low velocity change at departure and arrival. The missions which follow slow transfer orbits along the outbound and the return transfer were referred to in the preceding section as "slow-slow synodic". Another type of synodic mission, requiring a 3000 to 5000 ft/sec higher overall mission velocity consists of a fast (140 to 180 days) outbound transfer orbit to Mars at the time when the velocity requirement for this transfer orbit is a minimum, followed by a capture period until the minimum velocity window for a slow transfer back to Earth occurs. This mission which involves a 50 to 100 day longer capture period at Mars is referred to as "fast-slow synodic" mission. The velocity requirements for either type of synodic mission do not vary appreciably over the years. Therefore, a 1975 mission was used as characteristic example. The Mars mission designated as "fast" involves an outbound transfer time of 90 days, a 10-day capture period at circular orbit capture and a 150-day return flight period. The Mars missions designated as "very fast" have outbound transfer times of 60 days and return flight times of 120 and 150 days, respectively, at 10-day capture periods. The missions to Mercury, Venus, and Jupiter are explained in Sect. 10.

The third line specifies the Earth launch vehicle (ELV) assumed. They are specified in Tab. 1-1. Where no ELV is given, the design assumed was not dependent on the characteristics of any one particular ELV. This is usually true for the chemical vehicles. However, the mass fractions on which the gross payload fractions are based do not vary very much with the ELV. Especially, the modified Saturn V (Sa V M) could be substituted for the post-Saturn (PS) or vice versa, within small limits of error.

PLANET	Near Parab.				Near Parab.	Moon	Moon	Moon	Moon	Moon	Moon	Moon
MISSION	Injection				Injection	Surface	Surface	Circular	CC	CC	CC	Free Fall
	Reuse OLV				Reusable OLV	Landing	Landing	Capture	48+48 hrs.	12+12 hrs	12+12 hrs.	Deliver 48+48
ELV	Sa V	PS	Sa V M	Sa V M	Sa V	Sa V	PS	Sa V	PS	PS/Sa V M	Sa V	Sa V
ISV	C	SCR/N	SCR/G	GCR	NP	C	SCR/N	C	SCR/N	GCR	NP	NP
ERC	25^K	25^K	25^K	25^K	25^K	25^K	25^K	25^K	25^K	25^K	25^K	25^K
$\lambda_{mission}$	0.062	0.0665	0.0536	0.0098	0.0386	0.025	0.0485	0.08	0.1585	0.0116	0.0332	0.0555
W_{A1}	598	431	457	1690	1323	1010	486	930	545	2400	1045	692
ΣW_p	347	169	196	437	226	839	309	629	254	1938	571	236
ΣW_b	25	36	35	367	205	50	56	59	49	462	232	214
W_λ	6	6	6	6	12	11	11	22	22	22	22	22
$D_{\lambda 4}$	-	-	-	-	-	110	110	0	0	0	0	0
$D_{\lambda 3}$	0	0	0	0	0	0	0	0	0	0	0	0
$D_{\lambda 2}$	0	0	0	0	0	0	0	220	220	220	220	220
$D_{\lambda 1}$	220	220	220	880	880	0	0	0	0	0	0	0

ALL WEIGHTS ARE GIVEN IN 10^3 LBS.

Tab. 11-1 MISSION PAYLOAD FRACTIONS AND VEHICLE WEIGHT DATA FOR NEAR-PARABOLIC INJECTION MISSIONS WITH REUSABLE OLV INJECTING A LOAD $D_{\lambda 1}$ AND FOR CISLUNAR MISSIONS WITH REUSABLE SHUTTLE VEHICLE, DELIVERING LOAD $D_{\lambda 2}$ INTO A LUNAR CIRCULAR ORBIT.

Table 11-2 MISSION PAYLOAD FRACTIONS AND VEHICLE WEIGHT DATA FOR MARS FAST STANDARD MISSIONS

PLANET	MARS										MARS											MARS
MISSION	STANDARD								STANDARD					STANDARD								STANDARD
	1973	1975	1977	1979	1982	1984	1986	1988	1990	1975	1975	1975	1975	1975	1975	1975	1977	1977	1977	1977	1977	1977
ELV	PS	PS	PS	PS	PS	PS	PS	PS	PS	–	–	PS	PS	PS	PS	PS	–	–	PS	PS	PS	PS
ISV	$(SCR/G)_3$								$(SCR/G)_3$	C_4	C_3S	$(SCR/G)_3C$	$(SCR/G)_3S$	$(SCR/G)_4$	$(SCR/H)_4$	$(SCR/H)_4Pb$	C_4	C_3S	$(SCR/G)_3C$	$(SCR/G)_3S$	$(SCR/G)_4$	$(SCR/H)_4$
ERC	–	–	–	–	–	–	–	–	–	50K	50K	50K	50K	50K	50K	50K	50K	50K	50K	50K	50K	50K
$\lambda_{mission}$	0.1111	0.0967	0.0912	0.1052	0.1105	0.1088	0.1190	0.0995	0.0788	0.0058	0.0155	0.0193	0.0472	0.0145	0.035	0.0576	0.0039	0.013	0.0155	0.0416	0.0117	0.0302
W_{A_1}	1568	1831	1950	1685	1600	1630	1515	1800	2270	5750	4200	1790	1435	2040	1110	990	7800	4820	2065	1570	2390	1230
ΣW_P	1155	1404	1520	1278	1225	1221	1108	1367	1809	5392	3890	1439	1104	1634	899	782	7396	4500	1686	1229	1951	1015
ΣW_b	203	217	220	197	165	199	197	223	251	216	168	209	189	264	69	66	262	178	237	199	297	73
W_λ	160	160	160	160	160	160	160	160	160	16.5	22	16.5	22	16.5	16.5	22	16.5	22	16.5	22	16.5	16.5
D_{λ_4}	–	–	–	–	–	–	–	–	–	–	–	–	–	–	–	–	–	–	–	–	–	–
D_{λ_3}	–	–	–	–	–	–	–	–	–	75.5	70	75.5	70	75.5	75.5	70	75.5	70	75.5	70	75.5	75.5
D_{λ_2}	50	50	50	50	50	50	50	50	50	50	50	50	50	50	50	50	50	50	50	50	50	50
D_{λ_1}	–	–	–	–	–	–	–	–	–	–	–	–	–	–	–	–	–	–	–	–	–	–

PLANET	MARS										MARS											MARS
MISSION	STANDARD							STANDARD	VERY FAST		60-10-120			VERY FAST		60-10-150		VERY FAST	FAST	90-10-150		FAST
	1977	1982	1982	1982	1982	1982	1982	1982	1980	1980	1980	1980	1980	1980	1980	1980	1980	1980	1980	1980	1980	1980
ELV	PS	–	–	PS	PS	PS	PS	PS	PS/SaVM	PS/SaVM	SAT V	SAT V	SAT V	SAT V	PS/SaVM	PS/SaVM	SAT V	SAT V	PS/SaVM	PS/SaVM	SAT V	SAT V
ISV	$(SCR/H)_4$	C_4	C_3S	$(SCR/G)_3C$	$(SCR/G)_3S$	$(SCR/G)_4$	$(SCR/H)_4$	$(SCR/H)_4Pb$	$(GCR)_4$	$(GCR)_3$	$(NP)_4$	$(NP)_3$	$(NP)_4$	$(NP)_4$	$(GCR)_4$	$(GCR)_3$	$(NP)_4$	$(NP)_3$	$(GCR)_4$	$(GCR)_3$	$(NP)_4$	$(NP)_3$
ERC	50K	50K	50K	50K	50K	50K	50K	50K	35K	–	35K	–	25K	35K	35K	–	35K	–	35K	–	35K	–
$\lambda_{mission}$	0.0531	0.0144	0.0221	0.044	0.0649	0.0283	0.0648	0.0981	0.0062	0.013	0.0197	0.045	0.0289	0.0326	0.0089	0.0172	0.0256	0.0529	0.0136	0.040	0.0436	0.1045
W_{A_1}	1062	3760	3480	1300	1245	1490	854	784	15,100	12,750	5040	4040	3470	3120	11,000	10155	3970	3490	6940	4320	2300	1767
ΣW_P	584	3472	3179	991	934	1133	657	599	13,863	11,570	4380	3380	2905	2595	9995	9053	3382	2853	6063	3505	1797	1250
ΣW_b	336	146	159	167	169	215	55	43	1007	1040	470	400	375	335	815	842	398	377	687	555	313	257
W_λ	22	16.5	22	16.5	22	16.5	16.5	22	90	160	90	160	90	90	90	160	90	160	90	160	90	160
D_{λ_4}	–	–	–	–	–	–	–	–	–	–	–	–	–	–	–	–	–	–	–	–	–	–
D_{λ_3}	70	75.5	70	75.5	70	75.5	75.5	70	–	–	–	–	–	–	–	–	–	–	–	–	–	–
D_{λ_2}	50	50	50	50	50	50	50	50	50	50	100	100	100	100	100	100	100	100	100	100	100	100
D_{λ_1}	–	–	–	–	–	–	–	–	–	–	–	–	–	–	–	–	–	–	–	–	–	–

ALL WEIGHTS ARE GIVEN IN 10^3 LBS

PLANET	MARS	MARS	MARS	MARS	MARS	MARS	MARS	MARS	MARS
MISSION	STANDARD	STANDARD	STANDARD	STANDARD	STANDARD	STANDARD	STANDARD	STANDARD	STANDARD
	1973	1975	1977	1979	1982	1984	1986	1988	1990
ELV	SA V	SA V	SA V	SA V	SA V	SA V	SA V	SA V	SA V
ISV	NP	NP	NP	NP	NP	NP	NP	NP	NP
ERC	35^K	35^K	35^K	35^K	35^K	35^K	35^K	35^K	35^K
$\lambda_{MISSION}$	0.1125	0.104	0.097	0.112	0.117	0.138	0.1435	0.126	0.105
W_{A1}	985	1070	1130	1000	964	848	815	915	1075
ΣW_P	531.5	612	664	548.5	502	405	366	464	620
ΣW_b	233.5	238	246	232.5	242	223	229	231	235
W_λ	90	90	90	90	90	90	90	90	90
$D_{\lambda 4}$	-	-	-	-	-	-	-	-	-
$D_{\lambda 3}$	30	30	30	30	30	30	30	30	30
$D_{\lambda 2}$	100	100	100	100	100	100	100	100	100
$D_{\lambda 1}$	0	0	0	0	0	0	0	0	0

ALL WEIGHTS ARE GIVEN IN 10^3 LBS

TABLE 11-3 MISSION PAYLOAD FRACTIONS AND VEHICLE WEIGHT DATA FOR MARS FAST STANDARD MISSIONS USING NUCLEAR PULSE VEHICLES

PLANET	MARS	MARS	MARS	MARS	MARS	MARS	MARS	MARS	MARS	MARS	MARS	MARS	MARS	MARS	MARS	MARS	MARS	MARS	MARS	MARS	MARS	MARS
MISSION	SYNODIC	SYNODIC	SYNODIC	SYNODIC	SYNODIC	SYNODIC	SYNODIC	SYNODIC	SYNODIC	SYNODIC	SYNODIC	SYNODIC	SYNODIC	SYNODIC	SYNODIC	SYNODIC	SYNODIC	SYNODIC	SYNODIC	SYNODIC	SYNODIC	SYNODIC
	'75	'75	'75	'75	'75	'75	'75	'75	'75	'75	'75	'75	'75	'75	'75	'75	'75	'75	'75	'75	'75	'75
ELV	—	—	—	SA V M	SA V M	SA V M	PS	PS	PS	PS	SAT V	—	—	—	SA V M	SA V M	SA V M	PS	PS	PS	PS	SAT V
ISV	C_3	C_4	C_4	SCR/G_3	$(SCR/G)_3C$	$(SCR/G)_3C$	$(SCR/N)_3$	$(SCR/N)_4$	$(SCR/N)_4$	$(GCR)_3N$	NP	C_3	C_4	C_4	$(SCR/G)_3$	$(SCR/G)_3C$	$(SCR/G)_3C$	$(SCR/N)_3$	$(SCR/N)_4$	$(SCR/N)_4$	$(GCR)_3N$	NP
ERC	UHE	35K	25K	UHE	35K	25K	UHE	35K	25K	25K	25K	UHE	35K	25K	UHE	35K	25K	UHE	35K	25K	25K	25K
$\lambda_{mission}$	0.0845	0.0642	0.0313	0.1420	0.121	0.0734	0.231	0.189	0.139	0.100	0.173	0.0845	0.0642	0.0313	0.1484	0.1305	0.0783	0.236	0.216	0.141	0.102	0.173
W_{A_1}	1290	1640	3100	775	880	1360	502	590	756	970	600	2080	2550	4050	1240	1360	1800	889	961	1180	1280	850
ΣW_p	1086	1368	2734	489	584	983	320	390	561	468	240	1674	2090	3495	729	841	1211	512	575	779	560	294
ΣW_b	64	132	226	146	156	237	42	60	55	362	220	68	122	217	173	181	251	39	48	63	382	218
W_λ	90	90	90	90	90	90	90	90	90	90	90	90	90	90	90	90	90	90	90	90	90	90
D_{λ_4}	-	-	-	-	-	-	-	-	-	-	-	-	-	-	-	-	-	-	-	-	-	-
D_{λ_3}	-	-	-	-	-	-	-	-	-	-	-	11	11	11	11	11	11	11	11	11	11	11
D_{λ_2}	50	50	50	50	50	50	50	50	50	50	50	220	220	220	220	220	220	220	220	220	220	220
D_{λ_1}	-	-	-	-	-	-	-	-	-	-	-	17	17	17	17	17	17	17	17	17	17	17

PLANET	MARS	MARS	MARS	MARS	MARS	MARS	MARS	MARS	MARS	MARS	MARS	MARS	MARS	MARS	MARS	MARS	MARS	MARS	MARS	MARS	MARS	MARS
MISSION	SYNODIC	SYNODIC	SYNODIC	SYNODIC	SYNODIC	SYNODIC	SYNODIC	SYNODIC	SYNODIC	SYNODIC	SYNODIC	SYNODIC	SYNODIC	SYNODIC	SYNODIC	SYNODIC	SYNODIC	SYNODIC	SYNODIC	SYNODIC	SYNODIC	SYNODIC
	'75	'75	'75	'75	'75	'75	'75	'75	'75	'75	'75	FAST-SLOW	FAST-SLOW	FAST-SLO	FAST-SLO	FAST-SLO	FAST-SLO	FAST-SLO	FAST-SLO	FAST-SLO	FAST-SLO	FAST-SLO
ELV	—	—	—	SA V M	SA V M	SA V M	PS	PS	PS	PS	SAT V	—	—	—	SA V M	SA V M	SA V M	PS	PS	PS	PS	SAT V
ISV	C_3	C_4	C_4	$(SCR/G)_3$	$(SCR/G)_3C$	$(SCR/G)_3C$	$(SCR/N)_3$	$(SCR/N)_4$	$(SCR/N)_4$	$(GCR)_3N$	NP	C_3	C_4	C_4	$(SCR/G)_3$	$(SCR/G)_3C$	$(SCR/G)_3C$	$(SCR/N)_3$	$(SCR/N)_4$	$(SCR/N)_4$	$(GCR)_3N$	NP
ERC	UHE	35K	25K	UHE	35K	25K	UHE	35K	25K	25K	25K	UHE	35K	25K	UHE	35K	25K	UHE	35K	25K	25K	25K
$\lambda_{mission}$	0.0845	0.065	0.0316	0.154	0.1310	0.0835	0.244	0.224	0.147	0.125	0.173	0.0495	0.0377	0.0183	0.1010	0.0885	0.053	0.173	0.159	0.104	0.0875	0.157
W_{A_1}	1830	2480	4420	1040	1280	1770	703	819	1090	1182	828	2190	2770	5200	1090	1200	1890	668	713	1010	1178	659
ΣW_p	1516	2082	3927	647	836	1267	436	529	787	634	326	1964	2526	4869	767	883	1442	479	525	804	627	297
ΣW_b	74	158	253	153	204	263	27	50	63	308	262	86	104	191	183	177	308	49	48	66	411	222
W_λ	120	120	126	120	120	120	120	120	120	120	120	90	90	90	90	90	90	90	90	90	90	90
D_{λ_4}	-	-	-	-	-	-	-	-	-	-	-	-	-	-	-	-	-	-	-	-	-	-
D_{λ_3}	18	18	18	18	18	18	18	18	18	18	18	-	-	-	-	-	-	-	-	-	-	-
D_{λ_2}	80	80	80	80	80	80	80	80	80	80	80	50	50	50	50	50	50	50	50	50	50	50
D_{λ_1}	22	22	22	22	22	22	22	22	22	22	22	-	-	-	-	-	-	-	-	-	-	-

PLANET	MARS	MARS	MARS	MARS	MARS	MARS	MARS	MARS	MARS	MARS	MARS	MARS	MARS	MARS	MARS	MARS	MARS	MARS	MARS	MARS	MARS	MARS
MISSION	SYNODIC	SYNODIC	SYNODIC	SYNODIC	SYNODIC	SYNODIC	SYNODIC	SYNODIC	SYNODIC	SYNODIC	SYNODIC	SYNODIC	SYNODIC	SYNODIC	SYNODIC	SYNODIC	SYNODIC	SYNODIC	SYNODIC	SYNODIC	SYNODIC	SYNODIC
	FAST-SLO	FAST-SLO	FAST-SLO	FAST-SLO	FAST-SLO	FAST-SLO	FAST-SLO	FAST-SLO	FAST-SLO	FAST-SLO	FAST-SLO	FAST-SLO	FAST-SLO	FAST-SLO	FAST-SLO	FAST-SLO	FAST-SLO	FAST-SLO	FAST-SLO	FAST-SLO	FAST-SLO	FAST-SLO
ELV	—	—	—	SA V M	SA V M	SA V M	PS	PS	PS	PS	SAT V	—	—	—	SA V M	SA V M	SA V M	PS	PS	PS	PS	SAT V
ISV	C_3	C_4	C_4	$(SCR/G)_3$	$(SCR/G)_3C$	$(SCR/G)_3C$	$(SCR/N)_3$	$(SCR/N)_4$	$(SCR/N)_4$	$(GCR)_3N$	NP	C_3	C_4	C_4	$(SCR/G)_3$	$(SCR/G)_3C$	$(SCR/G)_3C$	$(SCR/N)_3$	$(SCR/N)_4$	$(SCR/N)_4$	$(GCR)_3N$	NP
ERC	UHE	35K	25K	UHE	35K	25K	UHE	35K	25K	25K	25K	UHE	35K	25K	UHE	35K	25K	UHE	35K	25K	25K	25K
$\lambda_{mission}$	0.0495	0.0377	0.0183	0.1125	0.0920	0.0562	0.176	0.160	0.105	0.0891	0.157	0.0495	0.038	0.0186	0.1125	0.0975	0.0597	0.182	0.167	0.1095	0.109	0.157
W_{A_1}	3500	4300	6650	1620	1920	2510	1188	1286	1580	1460	936	3450	4160	7150	1410	1675	2460	933	1082	1450	1352	939
ΣW_p	3049	3792	6085	1103	1324	1831	796	881	1161	733	375	2976	3724	6760	991	1151	1883	655	786	1133	706	409
ΣW_b	113	170	227	179	258	341	54	67	81	389	223	234	196	150	179	284	337	38	56	77	406	290
W_λ	90	90	90	90	90	90	90	90	90	90	90	120	120	120	120	120	120	120	120	120	120	120
D_{λ_4}	-	-	-	-	-	-	-	-	-	-	-	-	-	-	-	-	-	-	-	-	-	-
D_{λ_3}	11	11	11	11	11	11	11	11	11	11	11	18	18	18	18	18	18	18	18	18	18	18
D_{λ_2}	220	220	220	220	220	220	220	220	220	220	220	80	80	80	80	80	80	80	80	80	80	80
D_{λ_1}	17	17	17	17	17	17	17	17	17	17	17	22	22	22	22	22	22	22	22	22	22	22

ALL WEIGHTS ARE GIVEN IN 10^3 LBS.

TABLE 11-4 MISSION PAYLOAD FRACTIONS AND VEHICLE WEIGHT DATA FOR MARS SYNODIC AND MARS SYNODIC FAST-SLOW MISSIONS

PLANET	Mercury										MERCURY											MERCURY
MISSION	Standard										STANDARD											STANDARD
	81-4	81-7	81-11	82-4	82-10	83-3	84-2	84-5	85-5	86-5	87-3	81-4	81-7	81-11	82-4	82-10	83-3	84-2	84-5	85-5	86-5	87-3
ELV	PS	PS	PS	PS	PS	PS	PS	PS	PS	PS	PS	PS	PS	PS	PS	PS	PS	PS	PS	PS	PS	PS
ISV	$(SCR/G)_3$										$(SCR/G)_3$	$(SCR/N)_3$										$(SCR/N)_3$
ERC	—										—	—										—
$\lambda_{payload}$	0.0075	0.00914	0.0074	0.0076	0.0079	0.0053	0.006	0.0053	0.0132	0.0116	0.0066	0.0201	0.0216	0.0157	0.0167	0.0173	0.0136	0.0131	0.0122	0.0243	0.0235	0.0103
W_{A_1}	17,700	15200	17750	17350	16570	25200	22,200	25200	10500	12000	20550	6906	6853	8770	8190	7885	10,135	10,600	11,400	5920	6120	13570
ΣW_p	15518	13470	15780	15500	14597	22203	19752	22203	9240	10670	18690	6534	6472	8066	7508	7409	9783	9795	10,535	5289	5559	12130
ΣW_b	1962	1510	1750	1630	1753	2777	2228	2777	1040	1110	1640	152	161	484	462	256	132	585	645	411	361	1220
W_λ	120	120	120	120	120	120	120	120	120	120	120	120	120	120	120	120	120	120	120	120	120	120
D_{λ_4}	-	-	-	-	-	-	-	-	-	-	-	-	-	-	-	-	-	-	-	-	-	-
D_{λ_3}	-	-	-	-	-	-	-	-	-	-	-	-	-	-	-	-	-	-	-	-	-	-
D_{λ_2}	100	100	100	100	100	100	100	100	100	100	100	100	100	100	100	100	100	100	100	100	100	100
D_{λ_1}	-	-	-	-	-	-	-	-	-	-	-	-	-	-	-	-	-	-	-	-	-	-

PLANET	Mercury																	MERCURY
MISSION	Standard																	STANDARD
	81-4	81-4	81-4	81-7	81-7	81-11	81-11	85-5	85-5	85-5	81-4	81-4	81-7	81-7	81-11	81-11	85-5	85-5
ELV	PS/S.VM									PS/S.VM	Sn-V							Sn-V
ISV	$(GCR)_3N$	$(GCR)_2$	$(GCR)_4$	$(GCR)_3N$	$(GCR)_3$	$(GCR)_3N$	$(GCR)_3$	$(GCR)_3N$	$(GCR)_3$	$(GCR)_4$	$(NP)_4$	$(NP)_3$	$(NP)_4$	$(NP)_3$	$(NP)_4$	$(NP)_3$	$(NP)_4$	$(NP)_3$
ERC	35K	—	35K	35K	—	35K	—	35K	—	35K	35K	—	35K	—	35K	—	35K	-
$\lambda_{mission}$	0.023	0.0415	0.0227	0.028	0.0441	0.0255	0.0373	0.0277	0.0512	0.045	0.0608	0.101	0.0662	0.1019	0.0619	0.0942	0.0665	0.116
W_{A_1}	4220	2890	4270	3570	3060	3815	3530	3540	2630	6550	1700	1410	1540	1422	1575	1500	1625	1247
ΣW_p	3454	2372	3560	2865	2379	3081	2788	3051	1955	5660	1233	933	1118	954	1158	1008	1172	782
ΣW_b	576	298	520	515	461	544	522	299	455	700	277	257	232	248	227	272	263	245
W_λ	90	120	90	90	120	90	120	90	120	90	90	120	90	120	90	120	90	120
D_{λ_4}	-	-	-	-	-	-	-	-	-	-	-	-	-	-	-	-	-	-
D_{λ_3}	-	-	-	-	-	-	-	-	-	-	-	-	-	-	-	-	-	-
D_{λ_2}	100	100	100	100	100	100	100	100	100	100	100	100	100	100	100	100	100	100
D_{λ_1}	-	-	-	-	-	-	-	-	-	-	-	-	-	-	-	-	-	-

ALL WEIGHTS ARE GIVEN IN 10^3 LBS

TABLE 11-5 MISSION PAYLOAD FRACTIONS AND VEHICLE WEIGHT DATA FOR MERCURY MISSIONS

PLANET	VENUS	←														→	VENUS		
MISSION	ELL. CAPT.	←				→	ELL. CAPT.	ELL. CAPT.	←					→	ELL. CAPT.	CIRC. CAPT.	CIRC. CAPT.		
	78	←				→	78	81	←					→	81	60/150	60/150		
ELV	–	–	Sa V M	Sa V M	PS	PS	PS	Sat V	–	–	Sa V M	Sa V M	PS	PS	PS	Sat V	PS/Sa V M	Sat V		
ISV	C_4	C_3	$(SCR/G)_4$	$(SCR/G)_3$	$(SCR/N)_4$	$(SCR/N)_3$	$(GCR)_3N$	$(NP)_4$	C_4	C_3	$(SCR/G)_4$	$(SCR/G)_3$	$(SCR/N)_4$	$(SCR/N)_3$	$(GCR)_3N$	$(NP)_4$	$(GCR)_3N$	$(NP)_4$		
ERC	35^K	–	35^K	–	35^K	–	25^K	25^K	35^K	–	35^K	–	35^K	–	25^K	25^K	35^K	35^K		
$\lambda_{MISSION}$	0.034	0.066	0.082	0.139	0.145	0.222	0.0905	0.151	0.0324	0.0844	0.08	0.157	0.142	0.244	0.110	0.147	0.0457	0.097		
W_{A_1}	3680	2430	1600	1210	1000	805	1310	794	3630	1910	1575	1078	980	734	1138	805	2170	1110		
ΣW_P	3260	2063	1119	779	711	527	690	336	3233	1607	1097	670	696	459	566	348	1542	666		
ΣW_b	190	137	251	201	59	48	396	228	167	73	248	178	54	45	342	227	438	254		
W_λ	90	130	90	130	90	130	90	90	90	130	90	130	90	130	90	90	90	90		
D_{λ_4}	–	–	–	–	–	–	–	–	–	–	–	–	–	–	–	–	–	–		
D_{λ_3}	40	–	40	–	40	–	40	40	40	–	40	–	40	–	40	40	0	0		
D_{λ_2}	100	100	100	100	100	100	100	100	100	100	100	100	100	100	100	100	100	100		
D_{λ_1}	0	0	0	–	0	–	0	0	0	–	0	–	0	–	0	0	0	0		

PLANET	JUPITER																		JUPITER
MISSION	88-8	88-8/n=1	88-8/n=1	88-8/n=1	88-8/n=30	88-8/n=30	88-8/n=30	88-8/n=30	88-8/n=21.5	88-8/n=21.5	88-8/n=21.5	88-8/n=21.5	88-8/n=1	88-8/n=1	88-8/n=1	88-8/n=1	88-8/n=30	88-8/n=30	88-8/n=21.5	88-8/n=21.5
	n=1 340/580	340/580	460/460	460/460	460/460	460/460	340/580	340/580	460/460	460/460	340/580	340/580	340/580	340/580	460/460	460/460	460/460	460/460	460/460	460/460
ELV	PS	PS	PS	PS	PS	PS	PS	PS	PS	PS	PS	PS	Sa V	Sa V	Sa V	Sa V	Sa V	Sa V	Sa V	Sa V
ISV	$(GCR)_3N$	$(GCR)_3$	$(GCR)_3N$	$(GCR)_3$	$(GCR)_3N$	$(GCR)_3$	$(GCR)_3N$	$(GCR)_3$	$(GCR)_3N$	$(GCR)_3$	$(GCR)_3N$	$(GCR)_3$	NP	NP	NP	NP	NP	NP	NP	NP
ERC	35^K	–	35^K	–	35^K	–	35^K	–	35^K	–	35^K	–	35^K	25^K	35^K	25^K	35^K	25^K	35^K	25^K
$\lambda_{MISSION}$	0.0214	0.0504	0.0424	0.0687	0.0451	0.1016	0.0297	0.0730	0.0523	0.0993	0.0432	0.0735	0.0333	0.0281	0.045	0.0405	0.0566	0.051	0.054	0.0486
W_{A_1}	5834	4951	3185	3525	2822	2374	4000	3320	2810	2520	3660	3410	2675	2950	1962	2100	1550	1645	1660	1760
ΣW_P	4889	3821	2424	2698	2018	1638	3103	2496	2080	1809	2840	2613	2007	2255	1349	1550	956	1177	1061	1162
ΣW_b	605	620	421	317	464	226	557	314	390	201	480	287	328	355	273	210	254	128	259	258
W_λ	50	220	50	220	50	220	50	220	50	220	50	220	50	50	50	50	50	50	50	50
D_{λ_4}	–	–	–	–	–	–	–	–	–	–	–	–	–	–	–	–	–	–	–	–
D_{λ_3}	170	170	170	170	170	170	170	170	170	170	170	170	170	170	170	170	170	170	170	170
D_{λ_2}	100	100	100	100	100	100	100	100	100	100	100	100	100	100	100	100	100	100	100	100
D_{λ_1}	20	20	20	20	20	20	20	20	20	20	20	20	20	20	20	20	20	20	20	20

ALL WEIGHTS ARE GIVEN IN 10^3 LBS

TABLE 11-6 MISSION PAYLOAD FRACTIONS AND VEHICLE WEIGHT DATA FOR VENUS AND JUPITER MISSIONS

The fourth line designates the interorbital space vehicle (ISV) by propulsion system. This ISV is either a reusable orbit launch vehicle (OLV) which returns into a circular near-Earth satellite orbit, a cislunar vehicle (CISV), or a heliocentric vehicle (HISV). Subscripts specify the number of maneuvers in a given mission, to which the particular propulsion system is applied. In the case of the reusable OLV all propulsion systems are assumed to be reused during the mission. In the case of lunar missions, chemical, SCR/N, GCR, and NP drives are assumed to be equipped with reusable engines, whereas the SCR/G drive reuses a given engine only for the lunar capture and departure maneuver and a new engine each, for the Earth departure and the Earth arrival maneuver. In the case of heliocentric missions only the SCR/N, GCR, and NP engines are assumed reusable. For chemical vehicles the masses involved are so large that either assumption causes only very slight changes in gross payload fractions which are within the limits of accuracy of the chemical vehicle design assumptions.

The fifth line specifies the Earth return conditions (ERC). A dash in this line means that the return conditions are unspecified, i.e., that only three mission maneuvers were considered, the last one leaving the target planet for Earth with a payload which contains at least an Earth entry module (EEM) for unretarded hyperbolic entry or possibly a propulsion system for an Earth approach retro-maneuver to retard the hyperbolic entry velocity. The term "UHE" stands for unretarded hyperbolic entry. In this case no maneuver 4 (M-4) is involved, as in the preceding case, but the payload at target planet departure is more precisely defined as the sum of life support section mission modules required for the return flight plus EEM for the return velocities involved. The term "50 k" stands for reduction to a hyperbolic entry velocity of 50,000 ft/sec at Earth return. The term "35 k" specifies near-minimum Earth capture conditions at return, assuming that the velocity relative to Earth is reduced from hyperbolic to 35,000 ft/sec at a perigee distance of 1.1 Earth radii, resulting in a highly eccentric capture ellipse as terminal mission condition. Finally, "25K" means capture in a near-circular orbit near Earth, i.e., a terminal condition which is similar to the condition prior to Earth departure.

The five lines explained above define all essential conditions on which the computation of the MGPF ($\lambda_{mission}$) is based. The subsequent lines state the MGPF (either λ_{321} or λ_{4321}, depending upon whether 3 or 4 maneuvers were considered), the Earth orbital departure weight (ODW), the sum of all propellant weights expended during the mission for the principal maneuvers, the sum of all wet inert weights (tanks, engines, thrust structure, etc.), the GPF (W_λ) at the last maneuver and the weight differences (if any) eliminated between the fourth and fifth maneuver ($D_{\lambda 4}$), between the third and fourth maneuver ($D_{\lambda 3}$), between the second and third maneuver ($D_{\lambda 2}$), and between the first and second maneuver ($D_{\lambda 1}$).

11.2 General Discussion of Evaluation Criteria

The criteria which are useful and relevant in the evaluation of various propulsion systems for interorbital space vehicles (ISV's) are listed in Fig. 1-5 of Sect. 1. They are applied in the subsequent discussion.

The PAYLOAD FRACTION determines orbital departure weight and payload efficiency. The graphs shown in Sect. 10 and Tabs. 11-1 through 11-6 demonstrate the superiority of the NP drive in this respect. The cause of this superiority is the high specific impulse. The mass fraction of the NP drive tends to be poor, unless the propellant fraction is high, due to the large mass of the pusher plate. Therefore, low energy missions without involvement of large payloads tend to penalize the payload fraction of the NP in comparison to propulsion systems of lower specific impulse but higher mass, because the rapidly deteriorating mass fraction overcomes the otherwise so powerful effect of the high specific impulse. Missions which show this effect are, for example, the synodic Mars missions where the mission gross payload fraction (MGPF) for the NP is comparable to that formed for the SCR/N powered HISV whose specific impulse is only one third of that of the NP; and the near-parabolic injection missions with the reusable OLV (Tab. 11-1) where the MGPF ($\lambda_{mission}$) of the NP is lower than that of the SCR/G, the SCR/N and even of the chemical vehicles, in spite of the fact that a four times heavier destination payload was assigned to the NP vehicle than to the others. For the GCR vehicle the conditions are analogous, but numerically worse, since the engine weight is even higher, while the specific impulse is lower.

However, even though the MGPF of the NP is poor in missions of this kind, its propellant consumption is either comparable or lower than that of the other vehicle types. For repeated use, the PROPELLANT CONSUMPTION FACTOR becomes an important evaluation criterion. A high payload fraction automatically means a low propellant consumption factor; whereas a low payload fraction does not necessarily signify a high propellant consumption factor. The latter is consistently low in the case of NP.

The effect on the ORBITAL DEPARTURE WEIGHT of high MGPF and low propellant consumption factor is clearly apparent from the numerical data presented, resulting in the NP having the lowest ODW in almost all cases, the more so the higher the mission energy. Therefore, the thrust of the Saturn V compatible NP vehicle is adequate for a wide variety of missions to Mars, to Venus, to Mercury via Venus fly-by, and even to some Jupiter missions. This means, of course that Saturn V can be used as ELV for the orbital preparation of manned planetary missions more extensively in combination with the NP drive than with any other propulsion system, except the very low thrust nuclear-electric and plasma drives whose specific impulse exceeds that assumed for the NP vehicle. However, the preceding volumes of the final report show that the I_{sp}- values used in the calculations of this report are not the upper limit and that growth into the range which characterizes the low-thrust drives may be feasible. Beyond these values the specific impulse is no longer a critical factor, unless one considers flights to the Jovian planets in a matter of weeks, or one contemplates interstellar missions. Continued use of Saturn V is a factor of great economic significance, because it does not impose an early need for the development of a post-Saturn ELV. The absence of reusability of Saturn V is, of course, not an economical proposition. Therefore, if one contemplates the size of a reusable post-Saturn, rather than the question of whether or not a post-Saturn ELV should be developed, it is clearly apparent that this size will be influenced by the principal ISV with which it will be combined for future lunar and planetary missions.* If combined with a nuclear pulse driven ISV the reusable post-Saturn can be comparatively smaller, in a payload range of 550,000 to 10^6 lb (250 to 450 metric tons) into Earth orbit. This size would, at the same time, be adequate for nuclear-electric and CTR driven ISV's, reaching operational state presumably after the nuclear pulse vehicle can attain operational state. If, on the other hand, the post-Saturn is to be combined with a nuclear heat exchanger drive, such as the SCR/G or the SCR/N, then (cf. the charts in Sect. 10) a post-Saturn ELV of 600 to 800 tons (1.3 to 2 million lb) payload weight into orbit appears more adequate. The development of such very large ELV not only is more expensive, more importantly, it can be rendered obsolescent more readily, in the sense that its payload capability is too large by future improvements in ISV propulsion technology which will not stagnate forever. This sensitivity to advancements in ISV propulsion technology is a more serious threat to the continued economic use of a post-Saturn, which should have a service life in excess of a quarter century in order to justify the high cost of its development, than would be the under-sizing of the post-Saturn ELV.

Another, more immediate effect of the low ODW of the NP vehicle is on the ETO logistic requirements to prepare a mission in orbit or to refuel a cislunar or heliocentric shuttle vehicle. The logistic requirements are a function of ODW and of propellant density, because of limitations in payload weight, as well as in payload section volume of the ELV. If the propellant is sufficiently dense, the ISV is small. It may be possible to transport it into orbit fully assembled (but not fully fueled) or at least in a few large sections, minimizing expensive and time consuming module mating in orbit and replacing it by orbital fueling which appears to be a relatively simpler and potentially less expensive process. This is true especially if the propellant is solid as in the case of the NP (and certain nuclear-electric drives), rather than LH_2.

*No need of a post-Saturn larger than Saturn V is apparent for orbital operations in the foreseeable future.

Because of these reasons, namely, low ODW, small ISV size, and solid state of the propellant, the orbital operations requirements for the NP are lower than those for any other drive for the same mission, not excepting in this case the nuclear-electric ISV's whose mean density for packaging in the payload section of an ELV is low due to the large radiation cooling surfaces required.

The MISSION VERSATILITY is a function of specific impulse, propellant density, thrust, and reusability:

- High I_{sp} yields low values of $\tau_{mission}/I_{sp}$ (ratio of mission velocity divided by g*, to specific impulse) over a wide range of mission velocities. The wider this range, the more missions are covered. A low value of $\tau_{mission}/I_{sp}$ requires fewer or no stagings at all. Simplicity, reliability, and reusability prospects improve if no or only inconsequential stagings (e.g., jettisoning of propellant containers) are required.

- High propellant density minimizes the enclosing area which has to be protected against meteoritic damage and which has to be heat controlled if propellant is liquid. Solid propellants, as in the case of the NP vehicle, are far less sensitive to environmental conditions than liquids, minimizing or eliminating protection requirements and rendering that part of the vehicle rather insensitive to flight distances close to or very far from the Sun. Solid propellants also are better qualified for use in hostile planetary environments, such as the atmosphere of Venus.

- The importance of the thrust level diminishes with increasing specific impulse and increasing mission distances involved. But a higher thrust level will always contribute to greater mission versatility, because a high-thrust vehicle retains the capability of landing on the surface of other bodies, whereas nuclear-electric vehicles do not have sufficient thrust power. This does not only refer to Moon or Mars where one might not want to land with a nuclear pulse vehicle anyway; but it also refers to the major asteroids. The surface acceleration on Ceres, Pallas, Juno, Vesta, and Eros, assuming their mean density to be 0.6 of the Earth is 8.6, 5.7, 2.1, 4.2, and $2.8 \cdot 10^{-2}$ g, respectively, exceeding, for lift-off from the surface, the thrust capability of nuclear-electric systems by a factor of about 100. But even if compared with other high-thrust systems, the ruggedness and insensitivity to environmental conditions of the NP vehicle is unmatched by any of the other propulsion systems. If it is ever intended to land on Venus or enter the atmospheric region of Venus, Jupiter, or Saturn, the NP vehicle alone would have the performance capability and ruggedness required for such endeavor. In this connection another remarkable characteristic of the Orion type ("outside detonation") drive should be noted here which appears to be unique with this particular NP design. In contrast to theadiabatic expansion type rocket, the outside detonation NP operates even more efficiently inside than outside an atmosphere.

- Reusability is dependent for its economic significance primarily upon reusability of engines and life support section, because these are by far the most expensive items; and on a low propellant consumption factor, because this factor determines the cost of the logistic supply operation. For these reasons, a reusable cislunar or heliocentric vehicle should retain its engines in reusable condition, i.e., it should be tankage modularized or outright I-stage design; it should be capable of returning its operational payload (primarily the life support section) intact into a terminal geocentric orbit which requires, for heliocentric vehicles, a high performance level; and it should have a low propellant consumption factor. The nuclear pulse vehicle qualifies in all these respects more than any other advanced propulsion system which offers hope of being technologically realizable during the first half of the eighties. The only exception is possibly the nuclear-electric HISV on the condition that the radiators are not unduly damaged by micrometeorites after an extended heliocentric mission. Despite the fact that the NP vehicle ranks highest, at least among the high-thrust vehicles, for the entire mission spectrum from reusable OLV to planetary missions, nuclear heat exchanger systems with reusable engines can be a close second for near-parabolic injection and cislunar shuttle missions, unless very heavy payloads are involved. This is shown in a series of charts later in this section.

The <u>COST EFFECTIVENESS</u> depends on a number of attributes listed in Fig. 1-5. Cost effectiveness must be defined carefully, to make it a meaningful criterion. Cost effectiveness, as used here, applies to transportation cost only, i.e. to the indirect and direct operating costs of all transportation vehicles involved. Development and manufacturing cost of payloads (operational, destination payloads etc.) is not considered, since this would be approximately the same in all cases.

- Development Cost. Economic considerations discourage heavy initial investment without fair assurance of proper amortization in subsequent operations. For transportation vehicles this amortization is possible only if a sufficiently large number of missions is assured. If only one or a limited number of missions is to be considered, the development of a new vehicle is not likely to pay off and a less efficient, but already operational vehicle type will show higher cost effectiveness in terms of both, development and operational cost.

Fig. 11-1 defines 15 combinations of transportation systems, consisting of ELV, OLV, HISV and EEM. The OLV serves as the Earth departure module of the interplanetary vehicle. This distinction is made here, because the OLV may or may not be reusable. Reusability of the OLV is not a major consideration in determining the development cost of advanced vehicles. It does play a role in the determination of the direct operating cost. In that case, the OLV is treated as a separate vehicle if it is reusable; whereas it is treated as part of the HISV or CISV if it is not reusable.

The largest development cost items, in terms of dollars and years from go-ahead of the program definition phase, are, for purposes of this study, estimated to be:

Post-Saturn (O_2/H_2; 2-stage 10^6 lb payload)	\$5 B	8-9 years
Nuclear Electric System for SV (Saturn V)	\$4.5 B	12-14 years
Nuclear Pulse System for SV	\$4 B	10-12 years
Nuclear Electric System for Post-Saturn	\$7 B	13-16 years
Nuclear Pulse System for Post-Saturn	\$4.7B	12-14 years

Considering that the error margins of these cost estimates are of the order of - 10% and + 50%, one can say that the development costs for the first three

	ELV	OLV	HISV	EEM
(1)	SATURN V	C	C	36k
(2)	SATURN VM	C	C/SHE	36k
(3)	SATURN V	C	C	65k
(4)	SATURN V	SCR	C	65k
(5)	SATURN V	SCR	C/SHE	50k
(6)	SATURN VM	SCR	SCR/SHE	50k
(7)	SATURN VM	SCR	SCR/SHE	65k
(8)	SATURN V	C	NE	36k
(9)	SATURN V	NP	NP	36k
(10)	POST-SATURN	C	C/SHE	50k
(11)	POST-SATURN	C	C/SHE	36k
(12)	POST-SATURN	SCR	C/SHE	36k
(13)	POST-SATURN	SCR	C/SHE	50k
(14)	POST-SATURN	C	NE	36k
(15)	POST-SATURN	NP	NP	36k

The dark areas indicate the largest development steps. The hatched areas indicate intermediate developments and the unmarked areas, developments on the comparatively smallest level.

ELV = Earth Launch Vehicle
OLV = Orbit Launch Vehicle
HISV = Heliocentric Interorbital Space Vehicle
EEM = Earth Entry Module

Fig. 11-1 COMBINATIONS OF TRANSPORTATION SYSTEMS FOR PLANETARY MISSIONS vehicles is practically the same. The development cost for the post-Saturn compatible nuclear-electric (NE) and NP vehicles is based on the assumption that their development is an alternative to the development of the Saturn V based ISV's, rather than that it follows the development of the Saturn V based ISV's.

The lower cost groups comprises:

Solid Core Reactor Engine (SCR/G or SCR/N) Powered Modules	\$2.6 B	6 years
Earth Entry Modules (EEM) for Entry Velocity of 65,000 ft/sec	\$2.7 B	7 years
50,000 ft/sec	\$2.5 B	6 years
Venus Excursion Module	\$2.0 B (not counting cost and time for instrumented probes)	7 years
Mars Excursion Module	\$1.0 B (not counting cost and time for instrumented probes)	5 years
Chemical Modules	\$1.5 B	5 years
Solar Heat Exchanger (SHE) Driven Module	\$0.1 B (not counting test flights, since these would be part of the cost of the chemical or nuclear module in connection with which the SHE drive is developed)	5 years
EEM (Modif. Apollo) for Entry Velocity of 40-44,000 ft/sec	\$0.3 B	4 years

No distinction was made at this point in the development cost between the SCR/G and the SCR/N powered module.

Tab. 11-7 compares the development cost for a wide mission spectrum to which a variety of combinations is applied. The numbers in the mission

Tab. 11-7. MISSION SPECTURM AND DEVELOPMENT COST FOR VARIOUS COMBINATIONS OF ELV, (OLV-HISV), EEM, AND FOR VENUS AND MARS SURFACE EXCURSION MODULES

Ve PFB		75[1]	75	77	80	80	83	83	85	85	81	81	83	83	85	85
Ma PFB			75	77	79	79	82	82	84	84	82	82	82	82	84	84
Ma SM [14]				77	79	79	81	81	83	83	81	81	81	81	86	83
Ve EC					80	80	83	83	85	85	81	81	83	83	85	85
Ma CC } Ve PFB }					79	79	82	82	84	84	82	82	82	82	84	84
Ma CC (PB)							82	82		84	82	82	82	82		84
Ve CC									85	85	81	81	83	83	85	85
Ma CC (Mono-Elliptic)									84	84	82	82	82	82	84	84
Ma CC } Ve CC }								84	84	84			82	82	84	84
Ma SE } Ve PFB }					(79)	(79)		82	84	84	82		82	82	84	84
Ma SE (Mono-Elliptic)								82	84	84	84		82	82	84	84
Ma SB								86		84	84	84	84	84	84	84
Ma LTB										84	84	84	84	84	84	84
Ve SE										85				85	85	85
Me PFB									85	85	85[10]	84[10]	85[10]	85	85	85
Me CC									85	85				85[10]	85	85
Me SE										85				85[10]	85	85
Ju PFB															86	86
Ju EC															86	86
Ju Moon															86	86
ELV		SV[2]	SVM[4]	SV	SV	SV	SVM	SVM	SV	SV	PS[5]	PS	PS	PS	PS	PS
OLV		C[3]	C	C	SCR[6]	SCR	SCR	SCR	C	NP	C	C	SCR	SCR	C	NP
HISV		C	C/SHE[5]	C	C	C/SHE[7]	SCR/SHE	SCR/SHE	NE[8]	NP	C/SHE	C/SHE	C/SHE	C/SHE	NE	NP
EEM		36[9]	36	≤65	≤65	≤50	≤50	≤65	36	36	≤50	36	36	≤50	36	36
SEM[11]		-	-	-	(MEM)	(MEM)	-	MEM	MEM	MEM[12] VEM	MEM	-	MEM	MEM VEM	MEM VEM	MEM VEM
Development Cost (B$)	ELV	.2	1.0	.2	.2	.2	1.0	1.0	.2	.2	5.0	5.0	5.0	5.0	5.0	5.0
	OLV	.5	.5	.5	1.5	1.5	1.5	1.5	.5	} 4.0	.7	.7	2.0	2.0	.7	} 7.0
	HISV	1.5	1.6	1.5	1.5	1.6	2.6	2.6	4.5		1.8	1.8	1.8	1.8	7.0	
	EEM	.3	.3	2.7	2.7	2.5	2.5	2.7	.3	.3	2.5	.3	.3	2.5	.3	.3
	MEM	-	-	-	-	-	-	1.0	1.0	1.0	1.0	-	1.0	1.0	1.0	1.0
	VEM	-	-	-	-	-	-	-	-	2.0	-	-	-	2.0	2.0	2.0
Dev. Total[13]		2.5	3.4	4.9	5.9 (6.9)	5.8 (6.8)	7.6	8.9	6.5	7.5	11.0	7.9	10.1	14.3	16.0	15.3

1) Numbers in mission section represent years
2) Saturn V
3) Chemical (O_2/H_2)
4) Saturn V Modified
5) Post Saturn
6) Solid Core Reactor (Engine)
7) Solar Heat Exchanger (Engine)
8) Nuclear-Electric (Drive)
9) Numbers designated entry velocity in 10^3 ft/sec
10) Via Venus Powered Fly-by on Outbound Transfer
11) SEM = Surface Excursion Module
12) MEM = Mars Excursion Module
VEM = Venus Excursion Module
13) Development is assumed to start in no case earlier than FY 1970
14) SM - Synodic (Conjunction) Mission

section represent the years in which the particular transportation system combination is estimated to be able to carry out the particular mission for the first time, taking into account the lead times not only for the development period, but also for the preceding conceptual phase, the precursory instrumented probe program, the orbital test program and the cislunar and heliocentric flight test program to the extent to which it can be considered to be part of the mission preparation program rather than the development program.

Considering the development costs of ELV, OLV, HISV, SEM (surface excursion module) and EEM, the development costs compare as indicated. The NP system shows up to be comparatively most economical, followed by the NE system. The development cost for the NE system is reduced if its power supply system can be laid out for operation in the heliocentric rather than in the geocentric field of force at Earth departure when the vehicle mass is a maximum. This requires a high-thrust booster to accelerate the NE vehicle to higher elliptic (near parabolic) velocity. While the development cost for this combination appears to be less expensive than for an NE vehicle capable of escaping Earth from parking orbit in 90 days or less under its own power, the development cost of this OLV-HISV combination nevertheless appears to be higher than that of the NP system. The development cost of combinations involving post-Saturn, but not NP or NE, is higher than either of the preceding combinations. The development cost of both, post-Saturn and either NP or NE is, of course, highest. But this development appears to become necessary only where missions into the outer solar system are concerned.

The results shown in Tab. 11-7 are presented in Fig. 11-2 for better clarification, correlating the number of missions of which each combination is capable versus the development total shown in Tab. 11-7 (the term "total" referring to the summation of the table; in reality the overall development funding is greater, involving ecological and other systems. Since these apply to all alternatives they are, in the first approximation, taken as cancelling each other out).

The chart clearly shows the gap which exists between Saturn V ELV with chemical and solid core reactor driven OLV and HISV on the one hand and Saturn V with NE or NP driven HISV's, or post-Saturn based OLV and HISV on the other. Within the upper group (No. 14 and 15), the combinations[4] using NP are again superior, though to a lesser extent than in the Saturn V compatible group (No. 8 and 9).

The conclusion is that combinations using the nuclear pulse system

---

4) A "combination" is taken as an integral transportation system, consisting of ELV, OLV and HISV, or ELV and I/V (= OLV + HISV integrated).

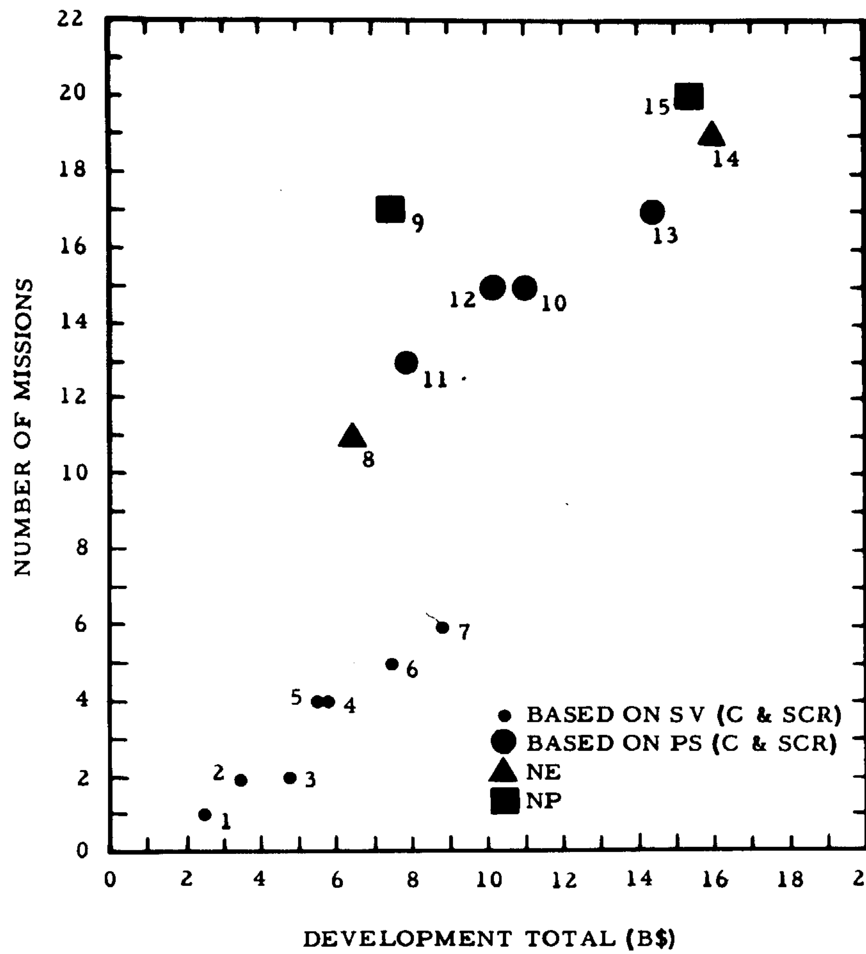

	ELV	OLV	HISV	EEM	SEM
1	SV	C	C	36	—
2	SVM	C	C/SHE	36	—
3	SV	C	C	65	—
4	SV	SCR	C	65	—
5	SV	SCR	C/SHE	50	—
6	SVM	SCR	SCR/SHE	50	—
7	SVM	SCR	SCR/SHE	65	MEM
8	SV	C	NE	36	MEM
9	SV	NP	NP	36	MEM/VEM
10	PS	C	C/SHE	50	MEM
11	PS	C	C/SHE	36	—
12	PS	SCR	C/SHE	36	MEM
13	PS	SCR	C/SHE	50	MEM/VEM
14	PS	C	NE	36	MEM/VEM
15	PS	NP	NP	36	MEM/VEM

SV = Saturn V
PS = Post-Saturn
C = Chemical
NP = Nuclear Pulse
NE = Nuclear Electric
EEM = Earth Entry Module
HISV = Heliocentric Interorbital Space Vehicle

OLV = Orbit Launch Vehicle
ELV = Earth Launch Vehicle
SCR = Solid Core Reactor
MEM = Mars Excursion Module
VEN = Venus Excursion Module
VEM = Venus Excursion Module
SEM = Surface Excursion Module

Fig. 11-2 MISSION VERSATILITY OF EACH COMBINATION VERSUS DEVELOPMENT COST are more promising than any other combination.

The mission matrix in Tab. 11-7 shows the mission versatility; i.e. the number of missions available to a given combination. The associated mission profiles are not necessarily all of the same type. For example round-trip missions to Mercury are listed as available for the Saturn V-NP combination as well as for the post-Saturn-C or post-Saturn-SCR combinations. However, for the latter two the mission profile is restricted to reaching Mercury via Venus powered fly-by (VePFB); whereas the first combination can also be applied to a mono-elliptic round-trip mission to Mercury. Neglecting these smaller differences, Fig. 11-3 shows the results of Tab. 11-7 in the form of a plot of number of missions capable of being flown versus the earliest year in which this appears possible in the 1975-1986 time period. It should be pointed out here that the years have not been checked out with respect to the constellational requirements in the case of missions involving more than one other planet. For example, the implication in Tab. 11-7 is that a capability for a MeCC mission exists in 1985 for PS-SCR-C/SHE-50k combination. This refers to the technological capability only. Tab. 2-39 does indicate a window for a flight to Mercury via VePFB in 1985, but this has not been verified by specific computations, as pointed out in Sect. 2.

In considering the development cost figures shown above, it should be kept in mind that they refer to the propulsion module only. The cost of preparing the first mission in the respective year given in Tab. 11-7 is between 80% and 160% higher. It includes development cost of the operational payload, of the destination payload, crew training and a large variety of test operations in Earth orbit, and the mission preparation test flights of the integrated vehicle or convoy. But most of these cost items are common to all propulsion systems and therefore cancel out in the comparison. If anything, this assumption is conservative. For example, for a test flight of a chemical HISV the ETO logistics requirements would be larger, hence more expensive, than for a nuclear pulse HISV.

- Manufacturing Cost. A comparison on the basis of manufacturing cost is difficult, because none of the propulsion systems compared here, except the chemical vehicles, have reached manufacturing stage yet. Cost estimates for the nuclear pulse vehicle are presented in Vol. II (SECRET) of the final report. On the basis of general considerations, however, it is possible to grade the individual propulsion systems with a high degree of accuracy. Again, it should be remembered that only propulsion module hardware without payload and without propellants are compared here. Electronic and electrical equipment cost are highest, ranging from 200 to 2000 $/lb.

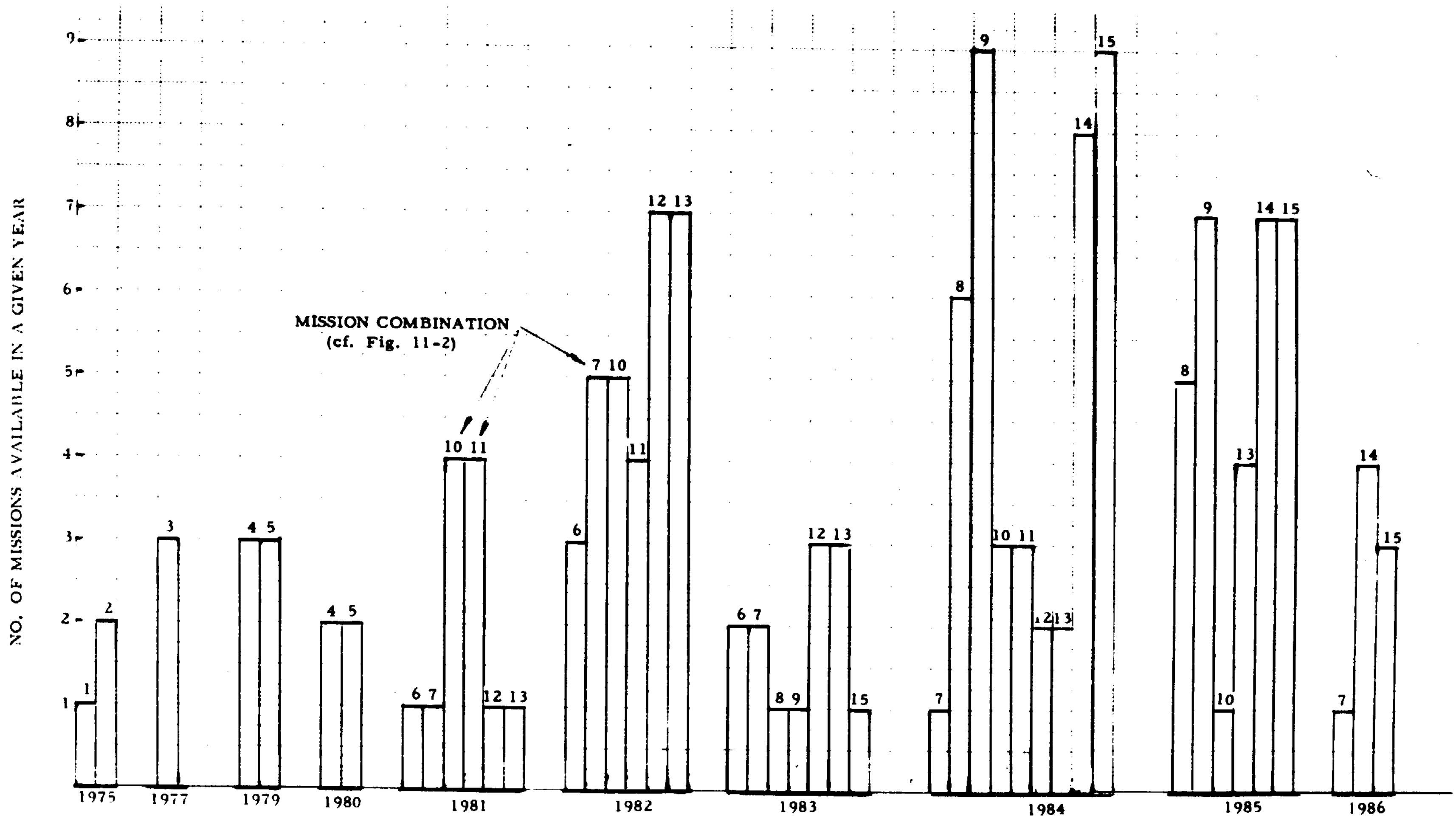

FIG. 11-3 VARIATION OF THE NUMBER OF AVAILABLE MISSIONS VERSUS TIME

Mechanisms and other complex mechanical hardware costs range from 100 to 500 \$/lb. The cost per pound of thrust (\$/lb F) of chemical, SCR (G or N) and GCR engines is shown in Fig. 11-4. The cost of non-complex hardware ranges from 20 to 100 \$/lb.

The bulk of the NE propulsion hardware (which includes power generation and conversion) is electrical, mechanisms and complex mechanical (radiators), resulting in a hardware cost of the order of 700 \$/lb.

The bulk of the GCR hardware is the engine. In the 750 k to 1000 k thrust range a mean cost value of the order of 33 \$/lb F is indicated. At an engine thrust/weight ratio of 2.5 to 3 in this thrust range, the engine cost is of the order of 85 to 100 \$/lb for the first ten operational engines. The uncertainty regarding the manufacturing cost of GCR engines is very high, however, because several candidates are in the picture at this time, ranging from the more complex vortex generating types to the glo-plug types which contain the fissionable material and to the relatively simple open coaxial flow type. The cost figures are meant to apply to the coaxial flow type which is likely to be the least expensive version. Assuming the manufacturing cost of the propellant dependent hardware to be of the order of 50 \$/lb, using titanium tanks, assuming further that the propellant dependent hardware weight is 10% of the LH_2 weight and that maximum propellant load for the engine thrust range in question is $4 \cdot 10^6$ lb, it follows that the average manufacturing cost of the GCR propulsion module (tankage modularized) is not less than about 65 \$/lb.

In the NP propulsion module, the bulk mass is moderately complex hardware, namely, the pusher plate. Shock absorbers, propellant feed system and associated mechanisms represent complex hardware. Comparison with the other propulsion systems indicates a manufacturing cost range for the engine system of 50 to 70 \$/lb for the Saturn V and Saturn V M compatible versions. The manufacturing cost of the expendable propellant magazines, including the ejection mechanism should be higher than the cost of propellant dependent hardware in LH_2 vehicles and probably lies in the range of 60 to 80 \$/lb. Assuming 70 \$/lb, it follows that the cost of the propellant magazines is comparable to that of the engine system and that, therefore, the average cost is not a function of the propellant load. It is further indicated that the manufacturing cost of the Saturn compatible NP versions is about the same as that of the GCR propulsion modules using the coaxial flow engine.

The manufacturing cost of an SCR engine in the 250 k thrust range is indicated in Fig. 11-4 to be approximately 7.5 \$/lb F, or about 70 \$/lb. With propellant dependent hardware cost of 50 \$/lb the manufacturing cost on the per pound basis is comparable to that of the NP system. The conditions

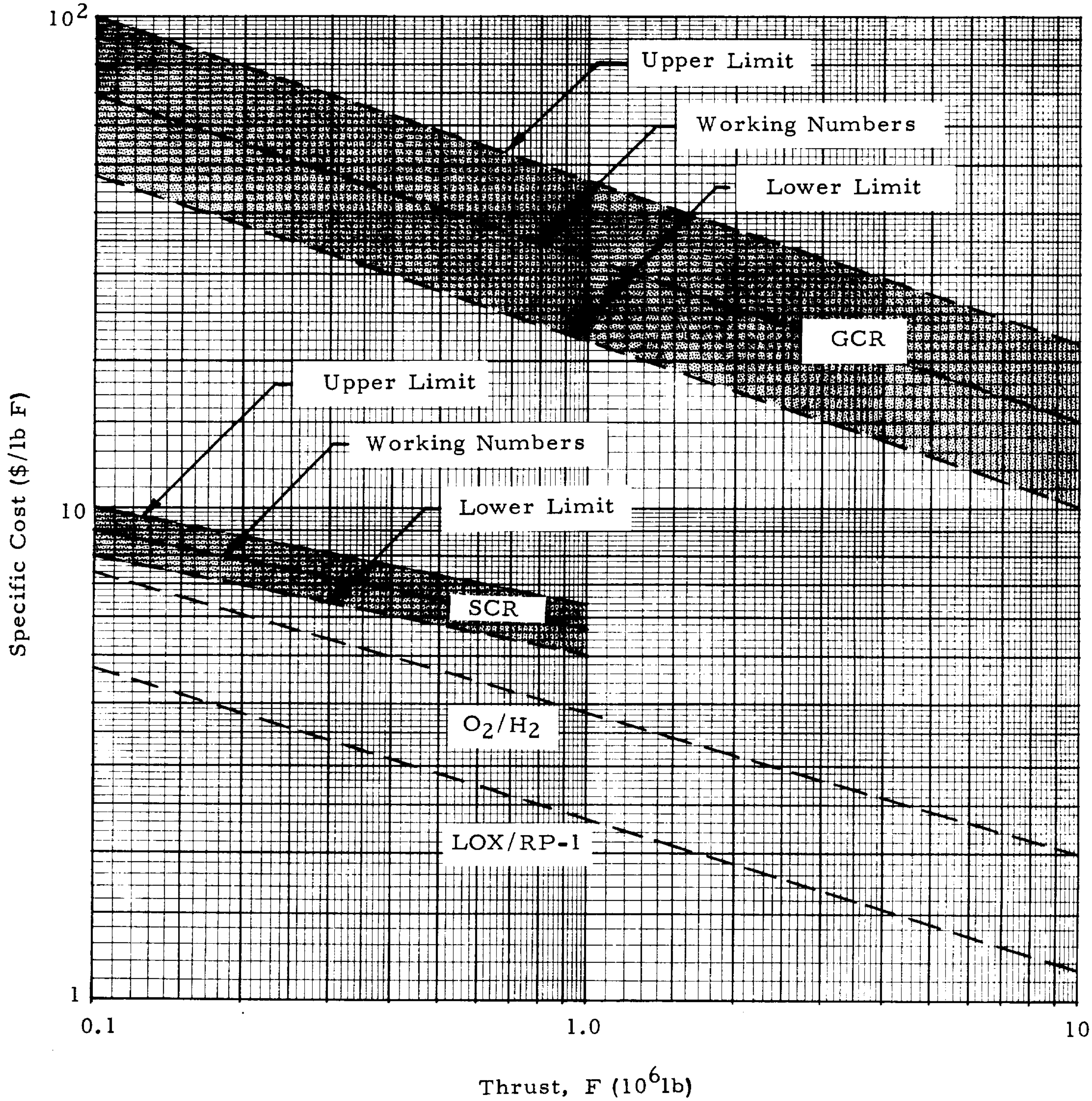

FIG. 11-4 APPROXIMATE THRUST - SPECIFIC PRODUCTION COST OF FIRST 10 OPERATIONAL ENGINES.

are probably similar for the SCR/N powered modules.

The bulk of chemical ISV's is propellant dependent hardware weight. Since, for oxygen storage, tanks made of aluminum or stainless steel would be used, while for LH_2 titanium tanks are assumed as before, an average manufacturing cost of 40 \$/lb is assumed for the propellant dependend hardware of O_2/H_2 vehicles. Fig. 11-4 indicates a cost of 4.70 \$/lbF for engines of 500k thrust and of 3.80 \$/lbF for 1000k thrust. Since these engines weigh about 4% of their thrust, their cost is about 120 \$/lb and 95 \$/lb, respectively. Considering, however that these engines are likely to be produced in greater numbers than those of the nuclear systems, the cost is probably of the order of 100 \$/lb to 80 \$/lb in the thrust range considered. Since the bulk of the hardware weight is in the propellant dependent category, the average manufacturing cost of the O_2/H_2 ISV should, therefore, be in the range of 50 to 60 \$/lb.

- Propellant Cost: One of the most expensive and attractive propellants for NE systems is cesium. The cost of cesium varies according to purity, quantity produced (demand) and producer. The estimate cost of cesium of commercial quality is expected to be as low as 15 \$/lb with a demand of 500 tons per year. Cost for the metal of over 99% purity is estimated not lower than 80 to 100 \$/lb at a 500 tons per year demand. At a demand of 2000 tons per year, commercial cesium is expected to cost 4-8 \$/lb and over 99% pure metal, needed for NE propulsion application, 30 to 60 \$/lb. All other potential propellants for NE drives, such as mercury, are less expensive. At an Earth-to-orbit (ETO) transportation cost of about 300 \$/lb, the manufacturing cost of the NE propellant is, therefore, likely to lie between 1/3 and 1/10 of its transportation cost into orbit.

  The cost of the NP propellant cannot be discussed in detail, because its composition is classified. Its cost is likely to be higher than that of all the other propulsion systems.

  Compared to these figures, the cost of LH_2 and chemical propellants is a negligible fraction of their transportation cost into orbit.

- ETO Logistic Requirements. At 200 to 400 \$/lb Saturn V and Saturn V M cost effectiveness, the orbital delivery cost is higher than the expected manufacturing cost of all propellants. Therefore, the low propellant consumption factor of the NE and the NP drives is of greater economic significance than the lower production cost of LH_2. The following cost effectiveness values are representative for the ELV's selected in this study and described in Tab. 1-1:

Saturn V	:	310 $/lb
Saturn V M	:	250 $/lb
Post-Saturn	:	55 $/lb

corresponding to a manufacturing cost of

Saturn V	:	$ 77.5 M
Saturn V M	:	$ 87.5 M
Post-Saturn	:	$ 55 M per flight, assuming (during the eighties) an average of 4 flights per vehicle at a vehicle production cost of $160 M per flight for recovery and refurbishing

- Orbital Operations Cost. The orbital operations cost is a function of the number of matings, of fuelings, the time period of orbital operations, size of the orbital crew and supply requirements for sustenance and operation in orbit. For the NP fewer matings are required than for any other propulsion system, with the possible exception of the nuclear-electric system. The propulsion system and the payload section are delivered separately and mated in orbit. In addition, a number of propellant supply flights is required. The number depends on the mission, but is lower than for all other propulsion systems (except nuclear-electric). Therefore, all attributes of the NP system tend to lower orbital operations cost below that for any other propulsion system (except nuclear electric) for the same mission. If a post-Saturn vehicle of $1\text{-}2 \cdot 10^6$ lb payload is available, the position of the NP and NE vehicle systems relative to orbital operations cost is no longer quite so unique for lunar and lower energy planetary missions.

- Gross Payload Fraction. The above cost items are essentially all transportation vehicle (ISV) cost, with the exception only of the cost of orbital delivery of the mission payload. The GPF is a measure of the interorbital transportation cost of the payload, as discussed in Section 6,

$$T_{\lambda}^{**} (\$/\text{lb Pld}) = \frac{K_{TV}^{*}}{W_A} \frac{1}{\lambda} \qquad (11\text{-}1)$$

In Sect. 6, this equation was transformed into expressions which contain the parameters needed to compute the GPF using the special method, the results of which are shown in Tabs. 11-1 through 11-6. Using these results, the cost equation can be used in the form

$$T_{\lambda}^{**} = \frac{K_{TV}}{W} = \frac{K_p + K_b + T_{pld}}{\Sigma W_{\lambda}} \qquad (11\text{-}2)$$

where

K_p = Sum of manufacturing cost and ETO transportation cost of the propellant ΣW_p

K_b = Sum of manufacturing cost and ETO transportation cost of the propulsive (i.e. thrust dependent and propellant dependent) hardware ΣW_b

T_{pld} = ETO transportation cost of the payloads (operational, destination, in-transit and transportation payload)

ΣW_{λ} = $W_{\lambda} + D_{\lambda 1} + D_{\lambda 2} + D_{\lambda 3} + D_{\lambda 4}$

The OPERATING EFFECTIVENESS is defined as being a function of the reliability of the transportation vehicles and the orbital operations, namely, module mating and module fueling. While all ISV propulsion modules would use the same ELV with the same success probability of orbital delivery, those who require more launchings are penalized more. For a given success probability, the numerical difference between procurement required and minimum number without redundancy increases with the minimum number. Therefore, an increase in ETO logistic requirements carries the dual penalty of reducing the cost effectiveness and degrading the operating effectiveness which is lowered not only by the cost of redundant ELV's, but also by the cost of redundant ELV payloads. Unsuccessful orbital mating and orbital fueling increases the minimum number of ETO delivers (at 100% delivery success probability) and this, in turn, raises the number of ELV redundancies (assuming less than 100% delivery success probability).

For these reasons it is apparent that the fewer matings and fuelings in orbit, the better. In this respect the NP and NE vehicles are far superior to the GCR vehicle.

A comparative evaluation of the success probability of the ISV propulsion modules is more difficult to carry out. It certainly is true, as pointed out by P. R. Shipps (ref. 10) that only in a 1-stage (or tankage modularized vehicle) is it possible to exercise all systems in a pre-mission shakedown flight. In this respect the NP, the NE and the GCR vehicles have an important advantage over the multi-stage vehicles of the SCR or chemical class.

Beyond this, there are the reliability aspects based on mean time before failure, where failure is caused by repeated use of components and prolonged exposure to hostile environment. These failures, rather than those which become apparent at the beginning of the mission, are likely to cause the worst surprises to the crew. The probability of such occurrences is minimized by the following factors:

- Vehicle simplicity
- Accuracy and thoroughness of diagnostic methods and procedures
- Accessibility and interchangeability of parts
- Repairability of parts
- Spare carrying capability

Relative to the first point the NP rates highest, the NE system lowest. Relative to the last point the NP and NE system rate higher than the others. Relative to the third point, the NP rates highest, the NE lowest, because of continued reactor operation. As to the second point, all vehicles can most likely be brought to a comparable level. Regarding the fourth point, too little practical experience is available and any comparison here is probably highly conjectural.

It was found, however, that the 1-stage characteristics of the NP system gave it an advantage over multi-stage system throughout the mission. A reliability analysis was carried out by this author (ref. 11) of a large variety of HISV's on a multitude of interplanetary missions. Among other things, the effect of chemical, SCR and NP systems on the overall probability of mission success was determined for a number of fast, standard (450 day) Mars capture missions. Details are given in the above reference. The result is shown in Fig. 11-5. In this comparison it is assumed that the NP system reaches initial operational capability in 1981, the SCR system in 1974, the chemical system in 1972. The reason for the initial decrease in mission success probability is due to the effect that from 1973 to 1975 worsening mission conditions (especially the effect of closer perihelion distance on return flight) degrade the probability more than it could be improved between mission opportunities. Subsequently, improvements just barely outweigh still further worsening mission conditions in 1977. Thereafter, the combined effect of increased success probability and more favorable mission conditions lead to a more rapid climb in mission success probability. However, so many

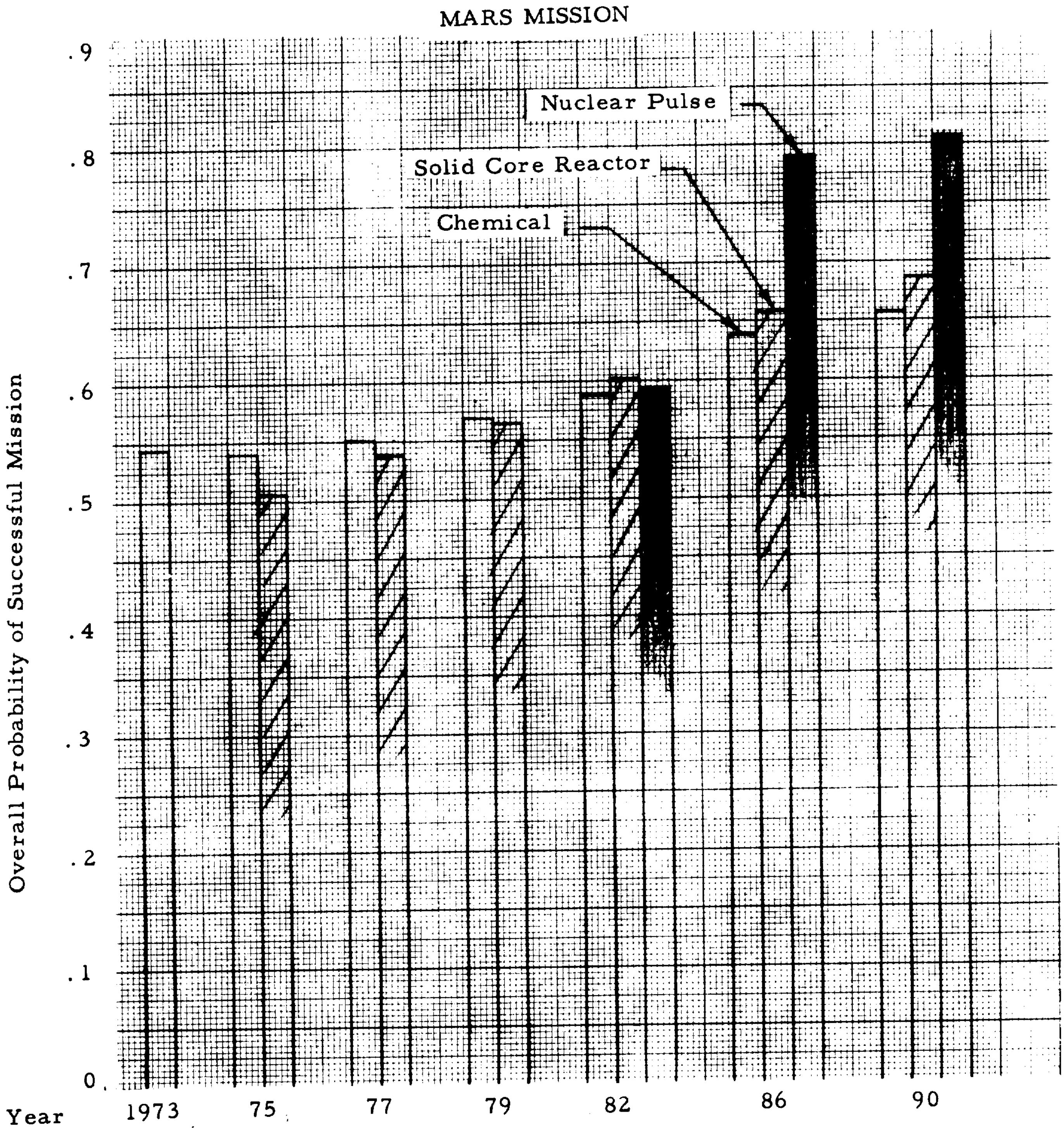

Notes: 1) Orbiting Mission
2) Mono-Elliptic Transfers
3) Earth Retro to 50,000 ft/sec for Chemical and SCR Vehicles. Earth Capture for Nuclear Pulse Vehicle

Fig. 11-5 EFFECT OF PROPULSION SYSTEM TYPES ON OVERALL PROBABILITY OF MISSION SUCCESS systems are involved in the multi-stage vehicles, that even extremely high component reliabilities are unable to raise the mission success probability beyond a certain level which is about 0.67 for the chemical and 0.7 for the SCR vehicles. Further improvements must be accomplished by the crew through proper diagnostic surveillance, preventive maintenance and repair. There is little doubt that the crew, and only the crew, can raise the overall mission success probability considerably above the upper values shown in Fig. 11-5. In fact, the gap between 0.67 or 0.7 and 0.9 to 1.0 is one of the most potent justifications for the existence of the crew during interplanetary transfers.

The overall mission probability of the NP vehicle was estimated to level off at a success probability of about 0.83 to 0.85. Beyond this, the crew must be utilized.

It could be argued that if the crew can raise the overall probability of mission success to 0.9-1.0 in either case, it makes little practical difference where the maximum vehicular success level lies. However, if one considers that it is highly desirable from the standpoint of mission success and crew survival to minimize the probability of "bad surprises" mentioned above, then it does make a difference where the maximum vehicular level lies. The higher this level, the smaller will be the probability of "bad surprises" en route. Thus, as far as ISV operating reliability is concerned, the NP is superior, at least to the chemical and SCR systems. A comparison with the GCR system and the NE drive could not be made within the framework of this study. It appears that the GCR drive should offer a mission success probability which is comparable to that of the NP, but somewhat lower, because of the inherently higher sensitivity of the propellant. The vehicular reliability of the NE drive should be quite a bit lower than that of the NP system, due to the far greater complexity and sensitivity of the system, leaving a much larger gap to fill for the mission crew. Therefore, it is highly probable that the NP system leads all other systems in vehicular mission success probability, hence, safety and survival probability of the crew.

The ninth evaluation criterion is referred to as <u>ABILITY</u> and is defined in Fig. 1-5 as a function of operating effectiveness, mission period and mission safety. It was shown above that the NP system leads in operating effectiveness. Its superior I_{sp} assures a superior capability to attain short mission transfer periods while returning a higher GPF than any of the other vehicles. The GPF of NE systems characteristically falls off rapidly as the mission transfer periods in the inner solar systems approach those attainable by the NP system. In the outer solar system the difference is comparatively smaller. Mission safety must be measured in terms of

11.3 Equivalent Mass Fraction

The equivalent mass fraction of an ISV which is not strictly a 1-stage vehicle is defined by Eq. (4-22a). Using the data in Tabs. 11-1 through 11-6, the equivalent mass fraction was computed, using Eq. (4-22a) in the following form

$$x_{eq} = \frac{\Sigma W_p}{W_{A1} - \text{Terminal Pld.}} \tag{11-4}$$

Applying this equation to the various planetary missions listed in Tabs. 11-1 through 11-6, the value of $W_{\lambda 3}$ or $W_{\lambda 4}$ was used as terminal payload. The results are plotted versus mission velocity in Fig. 11-6. It is seen that the five propulsion systems compared fall into five more or less distinct bands. The GCR and the NP show the poorest equivalent mass fraction due to the heavy mass of their propulsion system; but they also are superior in mission velocity growth potential to the other three systems. For lower mission velocities, their mass fraction can be improved only by carrying a much larger payload than the other three systems. The chemical vehicles show the highest equivalent mass fraction; but they are also less capable of mission velocity growth than any of the other systems. In the 40 to 60 $\cdot$ 10^3 ft/sec mission velocity regime the propellant fraction, Λ_{tot}, ranges from 0.87 to about 0.94, i.e. is approaching the same value as x_{eq} and, since the payload fraction (in this case, the terminal payload fraction) by definition of Eq. (11-4) is equal to $1 - \Lambda_{tot}/x_{eq}$, this means that the payload fraction approaches zero for chemical HISV's in that velocity regime. In practice, the payload fraction at 35 to 40 $\cdot 10^3$ ft/sec is already so small that it exceeds the practical capability of a Saturn V based ETO logistics system.

The solid core reactor systems assume an intermediate position. Their equivalent mass fraction values, especially those of the non-moderated engines, are closer to the chemical than to the very advanced systems. This fact, coupled with their I_{sp} superiority over the chemical vehicles, causes them to be closer to the very advanced systems, as far as performance is concerned, than to the chemical systems.

- Vehicular ruggedness

- Performance for emergency maneuvers

- Vehicular mission reliability

On all three counts the NP system exceeds all other systems, including the NE drive which rates lower in the first and third points; and in the second point as far as long time periods are required for maneuvers, particularly in strong gravitational fields.

GROWTH RATE, finally is primarily a function of the propulsion system's growth capability and the feasibility of follow-on improvements. This feasibility determines the time required to achieve increased performance, hence, the growth rate. Chemical and SCR drives do not have much growth capability and therefore cannot have a significant growth rate. The growth rate of the GCR engine performance is also limited, if for no other reasons than limitations of the material to withstand the rising temperatures which must accompany increasing I_{sp} in any thermal system. A specific impulse of 3000 sec must be considered to be an optimistic upper limit for the GCR engine.

The NP drive, especially the Orion system which is an external thermal system and operates in pulses rather than producing a steady heat flow into the material, does not have these limitations. The NP specific impulse appears to have a growth rate well into the region of NE systems. Specifics on this subject are presented in the classified volumes of this final report.

The NE drive too offers considerable growth potential, both, in terms of lighter power generation equipment and increasing specific impulse.

Both systems may improve so significantly in the late eighties and the nineties that it is difficult at this time to guess which one will advance faster. Therefore both systems are tentatively rated equal as far as growth rate is concerned.

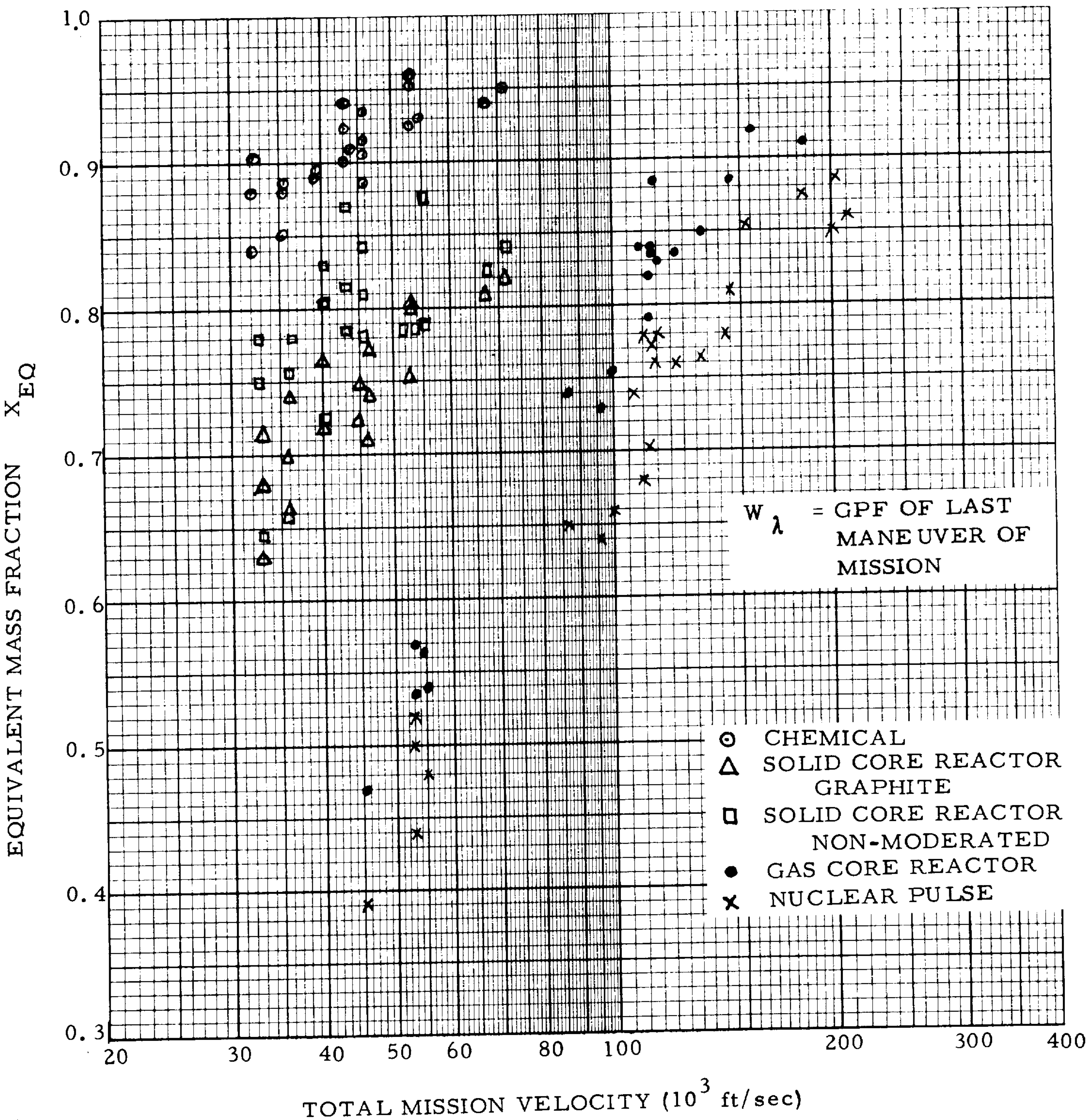

Fig. 11-6 EQUIVALENT MASS FRACTION, BASED ON W_λ VERSUS TOTAL MISSION VELOCITY FOR PLANETARY MISSIONS

11.4 Systems Comparison Synthesis

From the discussions in Par. 11.2 and 11.3, it is possible to extract a group of 16 important, basic attributes. These attributes are listed in Tab. 11-8 and serve as frame of reference by which to grade the propulsion systems under comparison. The NE system is included. Although its characteristics are not discussed in the framework of the methodology applied in this report to the other systems, they are sufficiently well known to permit consideration. of the nuclear-electric system at least on a qualitative basis. Thus, six principal propulsion system types are graded in Tab. 11-8 by 16 principal attributes. Where the propulsion systems are sufficiently different from each other (such as in specific impulse), six grades can easily be applied. Grade 1 is assigned to the system which is most advantageous with respect to the particular attribute. The I_{sp} grading, as well as the grading with respect to all other attributes is based on expected initial capability of man-carrying CISV's or HISV's. Further improvements are covered under growth capability. The initial I_{sp} of NE systems is expected to lie in the 5000 to 10,000 sec regime, that of the NP in the 2500^+ regime, placing, therefore, the NP on the second spot. High mass fractions are advantageous. Therefore, the chemical system leads in this attribute. Likewise, high propellant density and solid state (non-chemical) propellants are desirable. With regard to these attributes, only three brakets exist: very high density, such as for the metals used in the NE and NP systems; densities for chemical propellants ranging from O_2/H_2 to non-cryogenic storables and LH_2 which, in terms of density and state (very low temperature cryogenic fluid) is least desirable. The propellant consumption factor (PCF) should be low. It depends on the GPF and on the propellant fraction; hence, on I_{sp} and mass fraction. Except for small pockets in the mission spectrum, I_{sp} exerts the domineering influence, whence the systems are graded as for the I_{sp}. The same considerations apply to the ODW. Again the I_{sp} exerts the domineering influence most, but not all of the time. The mean packaging density refers to the packaging of the ISV or of its modules in the payload section of the ELV. High packaging density is desirable. The manufacturing cost of the propulsive (thrust and propellant dependent) hardware should be low. A capability for high thrust-to-weight ratio is not always a requirement but, if anything, it upgrades a propulsion system in relation to one incapable of high F/W ratio, simply because a larger number of options and a potentially higher degree of mission versatility. is affected. Vehicular ruggedness, defined as insensitivity to its environment in space or on the surface of other celestial bodies, should be high for reasons of mission versatility and crew safety. The grading relative to mission capability includes not only the bare capability, but also the speed of transfer, hence, the shortness of mission period for a given capture period. In terms of rapidity of transfer, the NP and GCR exceed the NE capability in the inner solar system, but probably not in mission to the outer solar system. NP and NE have the highest growth capability, defined as growth in I_{sp} and perhaps mass fraction. They are followed

Tab. 11-8. GRADING OF PROPULSION SYSTEMS BY THEIR PRINCIPAL ATTRIBUTES

Attribute No.	Grade	1	2	3	4	5	6
1	Specific Impulse	NE	NP	GCR	N	G	C
2	Mass Fraction	C	N	G	GCR	NP	NE
3	Propellant Density	NE; NP	C				GCR; N; G
4	Propellant State	NE; NP	C				GCR; N; G
5	Propellant Cost	C	GCR; N; G			NE	NP
6	Propellant Consumption Factor	NE	NP	GCR	N	G	C
7	Orbital Departure Weight	NE	NP	GCR	N	G	C
8	Mean Packaging Density	NP	C	N	G	GCR	NE
9	Manufacturing Cost of Hardware	C	N	G		NP; GCR	NE
10	High F/W Ratio Capability	C; NP; GCR G; N					NE
11	Vehicular Ruggedness	NP				GCR; N; G C	NE
	Mission Capability						
12	Inner Solar System	NP	GCR	NE	N	G	C
13	Outer Solar System	NE	NP	GCR	N	G	C
14	Growth Capability	NP; NE	GCR		N	G	C
15	Pre-Mission Shake-Down	NP; NE					
	Capability	GCR	N				G; C
16	Vehicular Mission Reliability	NP	GCR; N	G; C			NE

N = SCR/N (solid core reactor, non-moderated)
G = SCR/G (solid core reactor, graphite moderated)
C = Chemical; NP = Nuclear Pulse; GCR = Gaseous Core Reactor; NE = Nuclear-Electric

by the GCR system. The growth capability of SCR/N and SCR/G is very limited (restricted presumably to I_{sp} under 1000 sec); that of the chemical system is virtually negligible. With respect to pre-mission shake-down capability near Earth, NP, NE and GCR are comparable, since they all have clearly one engine which is resued throughout the mission. The same may be true for the SCR/N system, but is not necessarily always the case. The SCR/G (limited operating life engine) system and the chemical system are multistage and clearly have the lowest pre-mission shake-down capability. The vehicular mission reliability is defined (cf. Par. 11-2) as the inherent reliability of the vehicle under "hands-off condition" for the crew. The higher this reliability, the smaller will be the diagnostic, maintenance and repair effort have to be by the crew and the smaller is the probability of sudden critical failures. Thus, the higher the vehicular mission reliability, the higher is the crew survival probability and the smaller is the number of crew members needed to maintain the vehicle.

The results of the grading are presented graphically in Fig. 11-7 NP and NE show the highest accumulation in Grade 1; but the NE, together with C, also shows the highest accumulation in Grade 6. The NP shows 12 out of the 16 attributes in Grades 1 and 2, a larger accumulation than shown by any of the other systems.

The grades of the GCR system are far more diffuse. A maximum accumulation of 4 each is shown in Grades 2 and 3. The SCR/N shows up strong in Grades 2 and 4. The SCR/G displays the strongest single accumulation in Grade 5, smaller ones in Grades 3 and 6. The chemical systems finally show the third largest strength in Grade 1, the fourth in Grade 2 and are represented strongest in Grade 6.

The grading profile in Fig. 11-7 is based on equal weight for all 16 attributes. This condition cannot be maintained if the propulsion systems are rated with respect to certain operational or economic characteristics in which some of the attributes figure more strongly than others. Beyond this, it is probably fair to state that the following attributes can claim general importance, namely, in the appropriate order of their relative importance,

1	Specific Impulse
5	Propellant Cost
16	Vehicular Mission Reliability
12	Mission Capability: Inner Solar System
11	Vehicular Ruggesness
14	Growth Capability

Item No. 13 has been omitted in this "top priority list" simply because a high

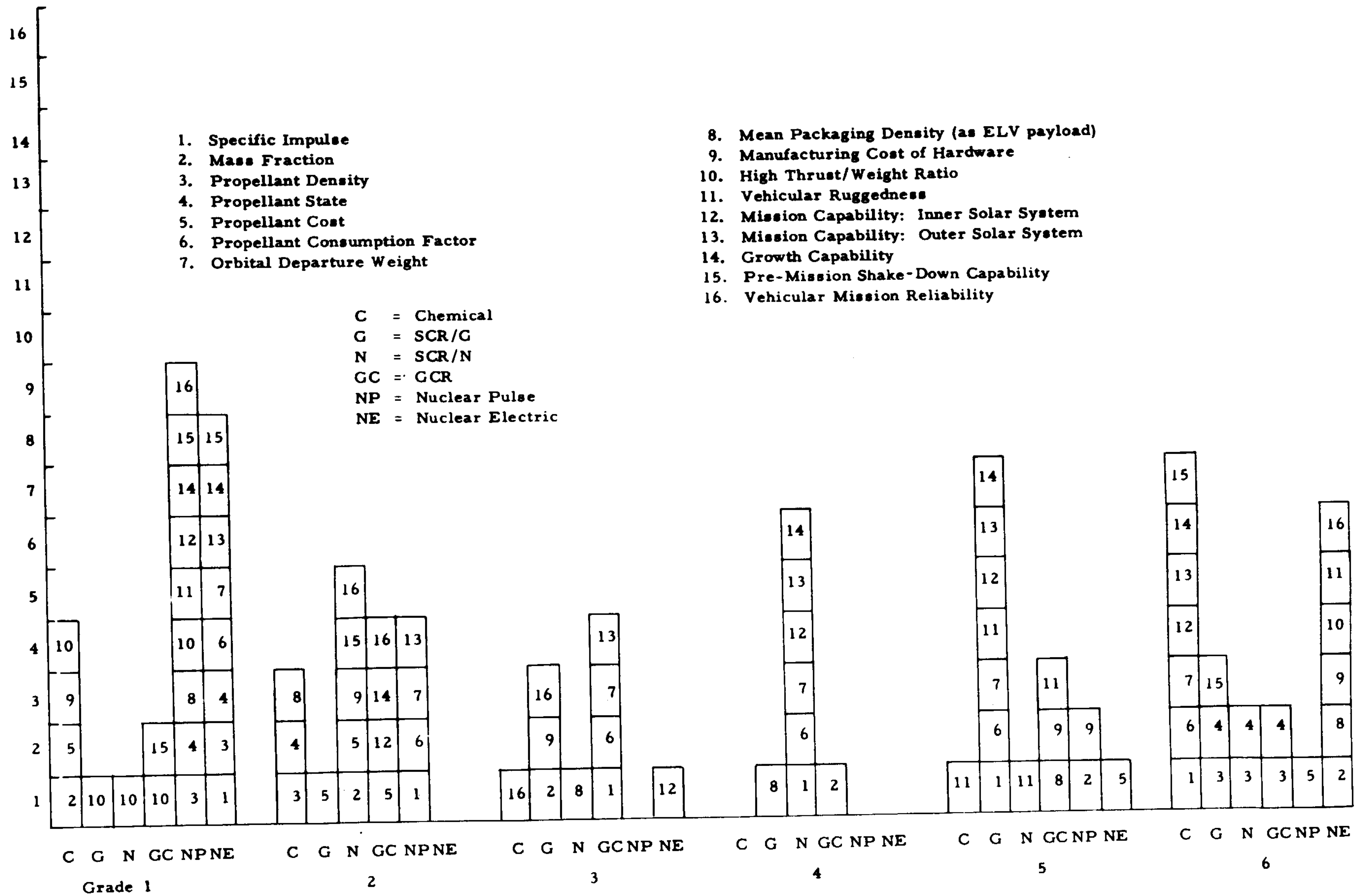

Fig. 11-7 GRADING PROFILE OF PROPULSION SYSTEMS BY THEIR PRINCIPAL ATTRIBUTES ALL GIVEN EQUAL WEIGHT.

Grade in No. 14 includes this capability on the basis that No. 11 must be fulfilled in the first place (and this includes Mercury).

Fig. 11-8 shows the "top priority rating" profile relative to the above listed attributes. The NP maintains its strong lead with 5 out of the 6 attributes in the first two Grades, followed by the GCR with 4 in Grade 2, and NE with 2 in Grade 1. Fourth is SCR/N with 2 attributes in Grade 2 and 3 in Grade 4. Fifth is SCR/G with 4 out of 6 attributes in Grade 5 and lowest rating goes to the chemical with 3 out of 6 in Grade 6.

The "Achilles' heel" of the NP is its low grade in Attribute No. 5, that of the NE is its low grade in No. 11. Thus, in situations where either one of these attributes plays a particularly dominant role, the rating of either system can be degraded seriously. The weak point of the GCR lies in two characteristics not entered in this comparison because of their strong conjectural connotation, namely, that it has potentially the highest development cost and that its eventual operational availability is less certain than that of the other two top contenders, although the latter point has been disputed strongly on occasion.

In comparing the weak points of the three leading contenders, it is fair to state that the one plaguingthe NP system may be overcome comparatively more readily than that of the two other for two reasons:

By properly planning shuttle missions favoring fewer flights with larger loads, the economic superiority of the NP can be maintained, even in cases where it would be lost if its mission schedule and load were made the same as for the lower energy propulsion systems. This was demonstrated in the discussion of the cislunar shuttle operations cost in Para. 11-5. Secondly, the I_{sp} growth potential of the NP is so large that even a partial materialization of this potential should render the NP system economically superior to all other systems for all mission groups considered.

It also should be kept in mind that Attribute No. 5 has a strongly disadvantageous effect only in connection with a low-cost ELV logistic system, such as Post Saturn. But the preceding cost data have also shown that if a Post Saturn of the cost characteristics postulated here is developed, neither the NP (nor, for that matter, the NE) nor the GCR (for most missions), but the SCR/N is the most advantageous ISV. If on the other hand, the ETO system remains based on Sa V or an improved Sa V, such as Sa V M, then the low grading of Attribute No. 5 does not prevent the NP from being the lowest cost means of transportation. This is unlikely to be challenged by the NE due to the high cost of its hardware and the inferior packaging density which appears to require a larger number of Sa V ELV's to deliver the NE than is required by the NP.

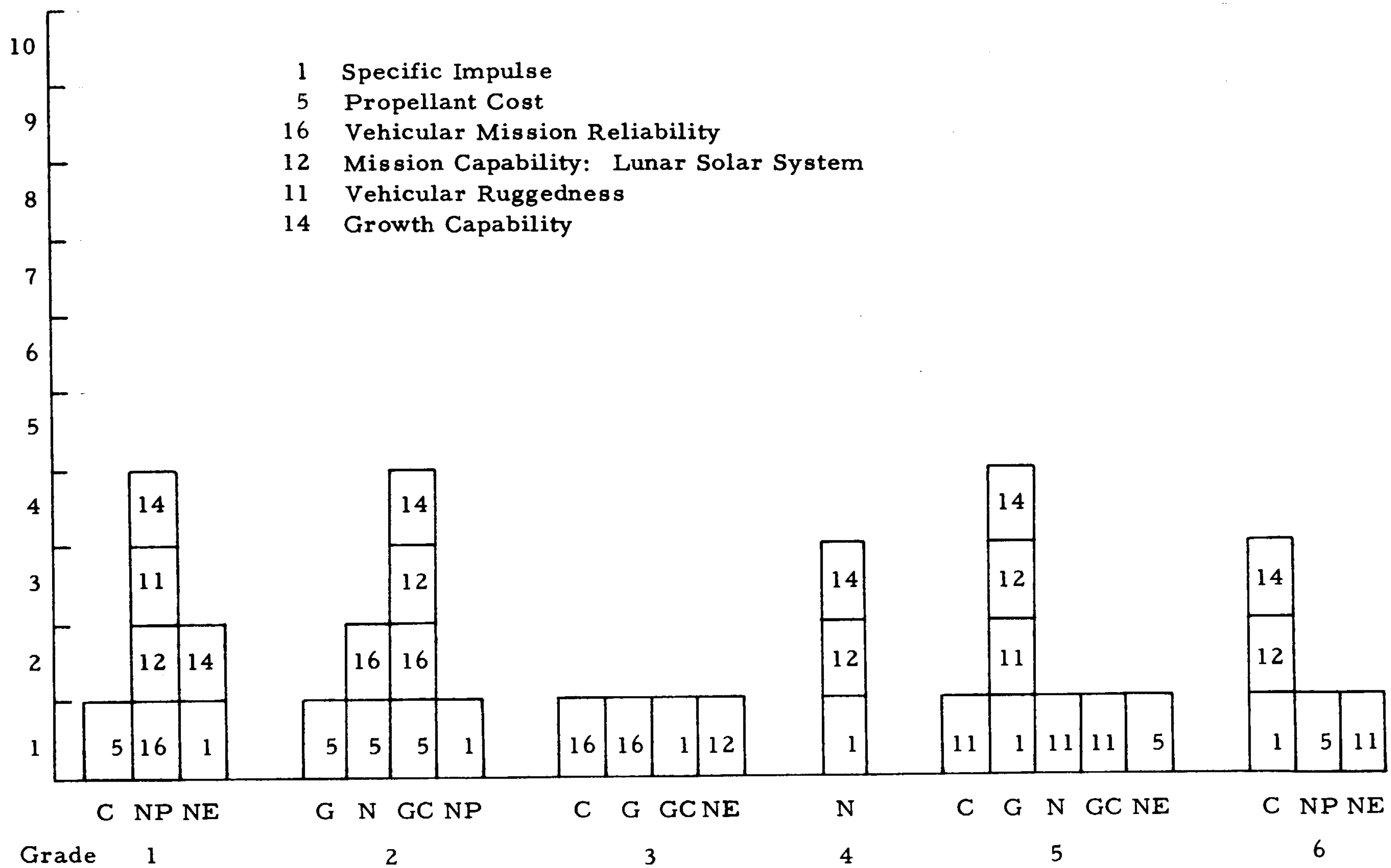

Fig. 11-8 RATING PROFILE OF PROPULSION SYSTEMS WITH RESPECT TO GENERALLY VERY IMPORTANT ATTRIBUTES

A useful method of rating the propulsion systems consists of the following steps:

(A) Define evaluation criteria.

(B) Correlate evaluation criteria with propulsion system attributes.

(C) Grade propulsion systems by attributes.

(D) Establish a qualitative rating profile of each propulsion system with respect to each evaluation criterion.

(E) Weigh the grades and the attributes.

(F) Establish a quantitative rating profile of each propulsion system with respect to each evaluation criterion.

(G) Weigh the evaluation criteria.

(H) Synthesize the quantitative rating profiles into one integral quantitative rating profile.

Steps (A) through (D) are perfectly general. Steps (E) through (F) can, in most cases, be carried out sensibly only with respect to a particular mission project (i.e. group of similar missions; cf. Sect. 1) and in a particular programmatic frame of reference. The need for relation to a particular project becomes apparent if one considers, for example, that the mass fraction plays a greater role, and the specific impulse a comparatively lesser role when comparing systems for near-parabolic injection missions with reusable OLV's than when comparing them for missions to Jupiter. That a programmatic frame of reference must be provided becomes apparent from the following examples:

Depending upon the principal ELV in the ETO logistic system the Attribute "Propellant Cost" must be weighed differently.

Depending upon long range plans in the area of manned lunar and planetary operations, the Attribute "Growth Potential" must be weighed differently.

Depending upon the degree of confidence in using LH_2 in a particular mission project the grading showing LH_2 as inferior to non-chemical solid propellants must be weighed differently. That is to say that, for instance, for missions to Mercury, LH_2 may represent a bigger disadvantage relative to non-chemical solid propellants than for cislunar missions.

Finally, there are, of course many additional imponderables, such as preferences and levels of confidence felt by the person setting the weight figures, which will affect the quantitative rating process.

For these reasons, the subsequent discussion is restricted to steps (A) through (D). The results for a suitable and convenient starting point for the reader who wishes to proceed to quantitative rating for missions or mission projects and programmatic frames of reference of his own choice.

(A) DEFINITION OF EVALUATION CRITERIA. Among several criteria discussed in Par.11-2 the following are selected, listed in the approximate order of decreasing importance:

I Cost Effectiveness. The functional dependency of cost effectiveness is shown in Fig. 1-5. In its present application, cost effectiveness is defined as the ratio of the direct operating cost to overall initial payload.

II Operating Effectiveness. Its functional dependency is shown in Fig. 1-5. Presently, only ISV-related factors are considered, because the comparison is concerned only with ISV's, rather than the overall transportation system, i.e., ELV, ISV and DSV.

III Gross Payload Fraction. The term GPF implies that all payload, rather than any particular payload group (for definitions cf. Sect. 2) is considered. However, instead of the GPF, other payload fractions, for instance the DPF (destination payload fraction), may be used in specific cases.

IV Mission Versatility. This criterion is defined in Fig. 1-5. It is interpreted here in the general sense of the word, namely as its ability to adapt to broad sections of the mission spectrum with more or less large variations in mission velocity, mission time, environmental conditions, payload etc.

V Orbital Operations. This criterion is taken here to include the ETO logistic requirements as well as, mating, fueling, checkout and mission readiness tests (of which pre-mission shake-down is a part).

VI Ability: Ability is defined as the quality of transportation with respect to important systems characteristics, such as their operating effectiveness, capability of fast transfers and mission safety which includes such items as number of emergency options, inherent vehicular reliability, vehicle ruggedness and degree of insensitivity to environmental conditions.

(B) <u>CORRELATION OF EVALUATION CRITERIA WITH PROPULSION SYSTEM ATTRIBUTES.</u> Each of the above evaluation criteria is applied in terms of relevant propulsion system attributes. Sixteen attributes are defined in Tab. 11-23. They are used subsequently.

(C) <u>GRADING OF PROPULSION SYSTEMS BY ATTRIBUTES.</u> See Tab. 11-23.

(D) <u>ESTABLISHMENT OF A QUALITATIVE RATING PROFILE.</u> This is done by applying each evaluation criterion to every propulsion system. The results are shown in Fig. 11-9. They allow a rapid qualitative systems comparison with respect to any of the six evaluation criteria. The qualitative rating of a propulsion system is high if it shows an accumulation of attributes on the left side of its field. Accumulation of attributes on the right hand side indicates poor rating; and a diffuse distribution of the attributes (e.g. the GCR with respect to Operating Effectiveness) indicates an indeterminate or inconclusive image on the qualitative rating plane which needs quantitative rating for further resolution. Some inconclusiveness is indicated also in cases of accumulation of attributes on opposite ends of the rating spectrum. This is most frequently the case with the NE system and indicates that in quantitative rating the system may rate either excellently or very poor.

The individual comparisons relative to particular evaluation criteria can be synthesized to indicate the probability that a system will show up high or low in quantitative rating. The larger the number of evaluation criteria relative to which the system looks good, the higher the probability that it will rate highly in most quantitative ratings. Consistent accumulation of attributes on the right hand side of the grading spectrum implies high <u>probability</u> that the system will come out poorly in most quantitative ratings. Consistent accumulation of attributes on the left hand side of the grading spectrum suggests high probability that the system will rate highly in most quantitative ratings. Fig. 11-9 indicates strongly that the nuclear pulse system occupies a leading position in the great majority of quantitative ratings.

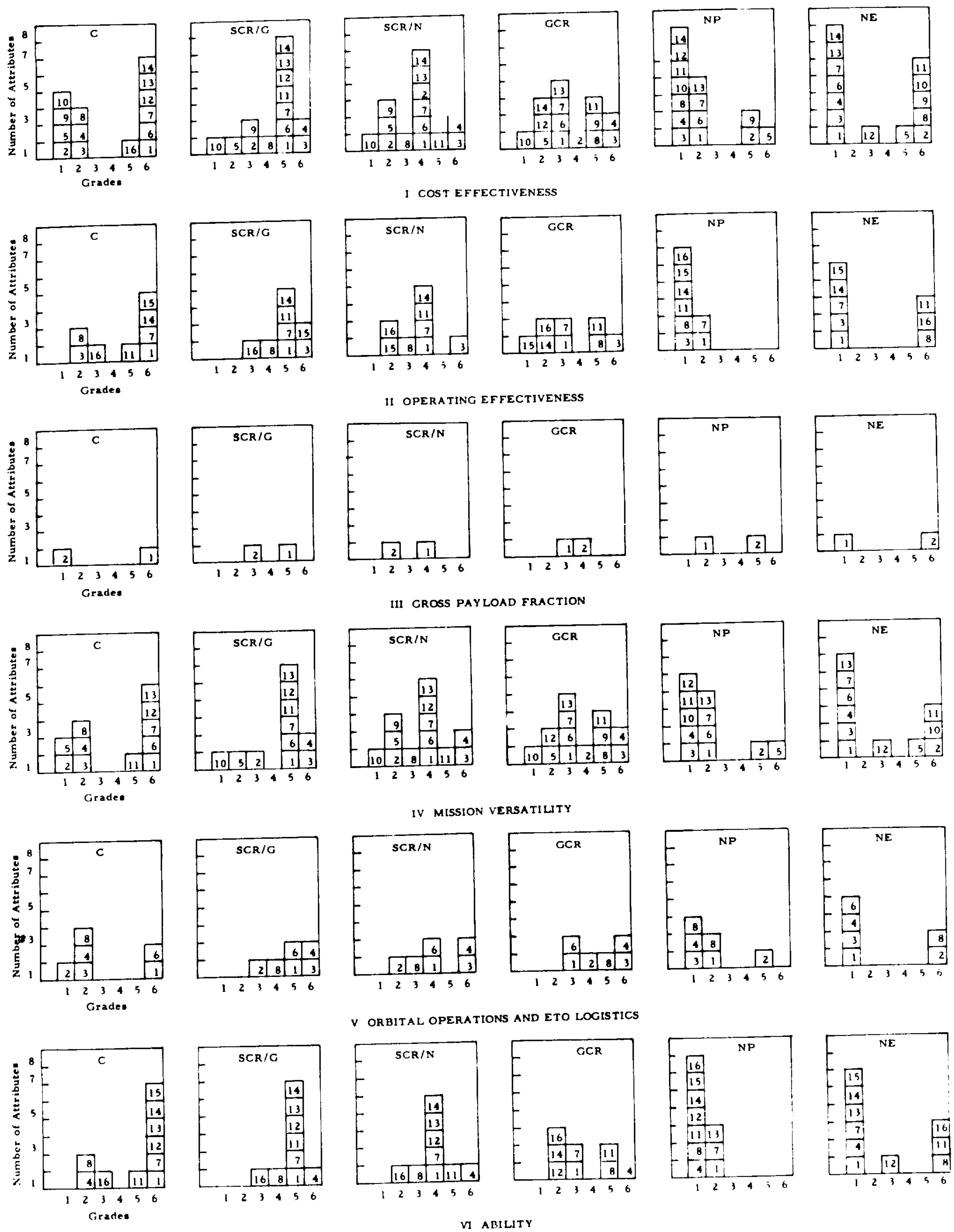

Fig. 11-9 RATING PROFILE OF VARIOUS PROPULSION SYSTEMS WITH RESPECT TO SIX EVALUATION CRITERIA

REFERENCES

1 STAMP (Space Technology Analysis and Mission Planning), General Dynamics/Convair, Reports GD/A AOK 65-001-1 through -4. Prepared by Advanced Studies for George C. Marshall Space Flight Center, Future Projects Office, Huntsville, Alabama., Spring 1965.

2 K. A. Ehricke, Advanced Launch and Carrier Vehicles, Sect. 24.1, Chapter 24 (Space Vehicles), Handbook of Astronautical Engineering, (H. H. Koelle edit.) McGraw-Hill Book Co., Inc., New York, 1961.

3 A Study of Manned Interplanetary Missions, Contract NAS8-5026 (Follow-On), Final Report, Vol. III, Mission Oriented Studies, GD/A AOK 64-006-3, p. 11-67.

4 Manned Mars and Venus Exploration Study, Final Report, Vol. II, Mission Oriented Studies. Contract NAS8-11327, Report No. GD/C AOK 65-002-2, May, 1965.

5 A Study of Interplanetary Missions, by K. A. Ehricke, General Dynamics/Convair, Contract No. NAS8-5026, Presented at the Manned Mars Mission Symposium, NASA/MSFC, 28-30 January, 1964.

6 Space Flight, Vol. II, Dynamics, by K. A. Ehricke, p. 1106 - 1110, D. Van Nostrand Company, Inc., New Jersey, 1962.

7\. A Study of Manned Interplanetary Missions, Contract NAS8-5026, Final Report, Vol. IV Interplanetary Vehicle Design and Propulsion, Par. 20.6, General Dynamics/Convair, Rep. GD/A-AOK-64-006-4, April 1964.

8 Manned Mars and Venus Exploration Study, Final Report, Vol. III, Design Studies, Contract NAS8-11327, Report No. GD/C AOK 65-002-3, March 1965.

9 As ref. 7, Final Report, Vol. V, Crew, Payload, Weights and Parametric Analyses, July 1964.

10 P. R. Shipps, Manned Planetary Exploration Capability Using Nuclear Pulse Propulsion, Second Space Congress Proceedings, Canaveral Council of Technical Societies, Cocoa Beach, 1965.

11 As ref. 4, Sections 13 and 14

DEFINITION OF ABBREVIATIONS AND SYMBOLS

C	Chemical Propulsion
CISV	Cislunar ISV
DPF	Destination payload fraction
DSV	Destination space vehicle
ELV	Earth launch vehicle
ERC	Earth return condition
ETO	Earth-to-orbit
G	SCR/G
GC	GCR
G_3C	4-Maneuver mission, 3 by SCR/G, the 4th by C
GCR	Gaseous core reactor
$(GCR)_4$	4-Maneuver mission, all executed by GCR
$(GCR)_3N$	4-Maneuver mission, 3 by GCR, the 4th by SCR/N
GPF	Gross payload fraction
HISV	Heliocentric ISV
ISV	Interorbital space vehicle
MGPF	Mission gross payload fraction
N	SCR/N
NE	Nuclear electric propulsion system
NP	Nuclear pulse propulsion system
OLV	Orbit launch vehicle
OPF	Operational payload fraction
PCF	Propellant consumption factor
SCR/G	Solid core reactor (engine)/graphite moderated
SCR/N	" " " " /non-moderated
SHE	Solar heat exchanger (engine)
VMR	Vehicular mission reliability

DEFINITIONS OF ABBREVIATIONS AND SYMBOLS

AA	Aphelion acceleration (maneuver)
ABC	Atmospheric braking to (near) circular capture orbit
ABE	Atmospheric braking to elliptic capture orbit
AD	Arrival date
C	Chemical propulsion
CC	Circular orbit capture
DD	Departure date
Ea	Earth
EC	Elliptic orbit capture
EEM	Earth entry module
ELV	Earth launch vehicle
EMOS	Earth mean orbital speed
FB	Fly-by (non-powered)
GEAR	Geocentric Earth approach retro (maneuver)
HEAR	Heliocentric Earth approach retro (maneuver)
HISV	Heliocentric interorbital space vehicle (cf. I/V)
I/V	Interplanetary vehicle (used, in this report, synonymously with HISV)
LSS	Life support section
Ma	Mars
MEM	Mars excursion module
MSP	Mission success probability
M-HEAR	HEAR maneuver
M-PB	Perihelion brake maneuver
M-PFB	Powered fly-by maneuver
M-1	Earth departure maneuver
M-2	Target planet arrival maneuver (capture)
M-3	Target planet departure maneuver
M-4	Earth return maneuver (GEAR)
NP	Nuclear pulse (engine or vehicle)
ODW	Orbital departure weight
PB	Perihelion brake (maneuver)
PFB	Powered fly-by (maneuver executed at periapsis of encounter hyperbola)
PM	Propulsion module
SCR	Solid core reactor (engine)
SCR/G	SCR graphite moderated
SCR/M	SCR metal based (non-moderated)
SE	Surface excursion
SHE	Solar heat exchanger (engine)
Ve	Venus
n	Apsidal ratio of capture ellipse = r_A/r_P
r^*	Distance of circular capture orbit (in planet radii)
r^*_A	Planetocentric apoapsis distance (in planet radii)
r^*_P	Planetocentric periapsis distance (in planet radii)
T	Mission period (overall)
T_{cpt}	Capture period
T_{MAO}	Transfer period in mission abort orbit (between heliocentric mission abort maneuver and Earth)
T_{MaPB}	Transfer period between Mars and perihelion brake maneuver
T_{MaVe}	Transfer period between Mars and Venus
T_1	Earth-to-target planet (or outbound) transfer period
T_2	Target planet to Earth (or return) transfer period; or Mars to Venus transfer period
T_3	Venus to Earth transfer period (at Ma-Ea return via Ve)
W_A	Ignition Weight
W_B	Weight at termination of burning
W_A/W_B	Mass ratio
W_b	Wet inert weight of propulsion module
W_j	Jettisoned weight (subscript 12, 23, or 34 etc., designating weight jettisoned during coast phase between maneuvers 12, 23, or 34 etc., subscript 2, 3, 4, etc., designating weight jettisoned just prior to maneuver 2, 3, 4, etc.)
W_N	Net Weight = $W_b + W_p = W_A - W_\lambda$
W_P	Useful propellant weight of propulsion module
W_λ	Gross payload weight = $W_A - W_N$